Aristotle University of Thessaloniki

DOCTORAL THESIS

Energy markets optimization considering integration of sustainability policies

by

Christos N. Dimitriadis

A thesis submitted in partial fulfilment of the requirements for the degree of Doctor of Philosophy in the

Department of Chemical Engineering

December 2023

Declaration of Authorship

I, Christos Dimitriadis, declare that this thesis titled, “Energy markets optimization considering integration of sustainability policies” and the work presented in it are my own. I confirm that:

- This work was done wholly while in candidature for a research degree at this University.
- Where any part of this thesis has previously been submitted for a degree or any other qualification at this University or any other institution, this has been clearly stated.
- Where I have consulted the published work of others, this is always clearly attributed.
- Where I have quoted from the work of others, the source is always given. Except for such quotations, this thesis is entirely my own work.
- I have acknowledged all main sources of help.
- Where the thesis is based on work done by myself jointly with others, I have made clear exactly what was done by others and what I have contributed myself.

Signed: _____

Date: _____

Energy markets optimization considering integration of sustainability policies

by Christos Dimitriadis

Examination Committee Members

Michael C. Georgiadis
Professor
Supervisor
Dept. of Chemical Engineering
Aristotle University of Thessaloniki

Eustathios Kikkinides
Professor
Advisory Committee Member
Dept. of Chemical Engineering
Aristotle University of Thessaloniki

George Nenes
Professor
Advisory Committee Member
Dept. of Mechanical Engineering
University of Western Macedonia

Spyridon Voutetakis
Director at Chemical Process Engineering and Energy Research Institute
Centre for Research and Technology Hellas

Angelos Sifaleras
Professor
Dept. of Applied Informatics
University of Macedonia

Fotios Stergiopoulos
Associate Professor
Dept. of Industrial Engineering and Management
International Hellenic University

Theodoros Damartzis
Assistant Professor
Dept. of Chemical Engineering
Aristotle University of Thessaloniki

στην οικογένεια μου

ARISTOTLE UNIVERSITY OF THESSALONIKI

Abstract

Faculty of Engineering
Department of Chemical Engineering

Doctor of Philosophy

Energy markets optimization considering integration of sustainability policies

by Christos Dimitriadis

In recent decades, the power industry has experienced remarkable reforms and advances, with the most drastic of these being the deregulation of energy markets from a centralized operational approach to a competitive model. The purpose of this new competitive structure is to eliminate monopolies, enhance the operational efficiency of power systems, ensuring a satisfactory quality of electricity supply and minimize costs for end-users. Furthermore, it seeks to offer improved incentives for capital formation, encourage consumers to abstain from consumption when costs outweigh benefits, and foster incentives for research and development.

The integration of sustainability policies aligns with energy market deregulation by incentivizing environmentally friendly practices. Deregulation allows renewable energy sources and energy storage technologies to compete on a level playing field with traditional forms of energy, encouraging the adoption of sustainable technologies. Governments often use policy instruments like feed-in tariffs or renewable energy certificates to promote the generation and consumption of green energy within a deregulated framework. This approach not only addresses environmental concerns but also aligns with broader societal goals of reducing carbon emissions and achieving a more sustainable energy future. In essence, the combination of energy market deregulation and sustainable policies creates an environment where market forces drive the adoption of cleaner, more efficient energy sources.

This thesis considers the development of optimization frameworks to integrate sustainability policies and investigate the strategic participation of power producers in contemporary energy markets. The proposed methodologies are based on mixed integer linear programming (MILP) modelling and mathematical programs with equilibrium constraints (MPEC). A known issue of these modelling techniques is that the model size increases exponentially with the problem size and can easily become intractable, especially in the case of nonlinear MPECs that must be linearized before being solved. Therefore, decomposition algorithms and linearization techniques have been employed to allow the applicability of the proposed methodologies in real-life cases. The presented solution strategies can address large-scale problems using commercially available MILP solvers, such as CPLEX.

More specifically, at first the strategic participation of a price-maker energy storage agent in pool-based energy and reserve markets, under wind power generation uncertainty is considered. A bi-level model is developed with the upper-level problem aiming to maximize storage agent's expected profits, whereas the lower-level problem represents the two-stage energy market clearing procedure. The first stage refers to a jointly cleared energy and reserve day-ahead market, deriving the optimal quantities for energy dispatch and reserve procurement, while at the second stage, a real-time energy-only market settlement is realized, considering plausible wind power generation scenarios. Real-time decisions include activated upward and downward reserves, already procured in the day-ahead market. The proposed mathematical framework is applied to a 6-bus power grid and investigates the potential arbitrage opportunities for the storage agent, under wind generation increment scenarios and plausible transmission line congestions.

Next, a stochastic mixed-integer linear programming (MILP) optimization framework to investigate the optimal participation and economics of various energy storage technologies, such as pumped-hydro, advanced adiabatic and diabatic compressed air systems and li-ion battery, in a perfectly competitive coupled electricity and natural gas market. The clearing scheme pertains to energy-only markets, aiming to optimize dispatch and maximize social welfare for the integrated energy system, through a two-stage stochastic programming. The first stage presents the day-ahead market clearing procedure, while the second stage illustrates the integrated system operation in the real-time trading floor, through a set of plausible wind power generation realizations.

The two markets mainly interact through the bilateral operation of the diabatic compressed air energy storage system, both as an electricity producer and as natural gas consumer. The proposed algorithm is applied to a real-life modified IEEE 24-bus power grid and a single-node gas network and provides a thorough analysis of the operational characteristics and profitability of each energy storage technology in the integrated energy system.

The strategic participation of a gas-fired power plant, exerting market power in interdependent pool-based electricity and natural gas markets, under a carbon emission trading (CET) scheme, constitutes the third thematic section of this thesis. A novel a bi-level model is developed where the upper-level problem aims at maximizing the profits of the strategic player, while at the lower-level problem, the day-ahead electricity and natural gas markets are cleared sequentially, considering the provision of carbon emission allowances for conventional power producers and high penetration of wind power generation. The proposed algorithm is applied to a Pennsylvania-New Jersey-Maryland (PJM) 5-bus power grid, incurred by transmission constraints and a single node natural gas network. Numerical simulations provide CETS-embedded electricity clearing prices and optimal bidding decisions for the strategic gas-fired power plant, under plausible power transmission congestions and natural gas prices increment scenarios.

The optimal trading strategies for a strategic renewable energy aggregator, exerting market power in a joint auction-based electricity and green certificates market is addressed in the final part of this thesis. In the upper-level problem of the bi-level formulation, the strategic renewable aggregator aims at maximizing its expected profits, while the two lower-level problems represent the sequential day-ahead electricity and green certificates market clearing mechanism, respectively. The proposed approach is first applied to a Pennsylvania-New Jersey-Maryland (PJM) 5-bus transmission constrained power network and then to a modified IEEE 24-bus system to illustrate its computational efficiency and applicability in a real-life case study. Numerical simulations determine electricity and green certificates clearing prices and optimal trading plan for the strategic renewable aggregator, under plausible power network congestion.

Περίληψη

Τις τελευταίες δεκαετίες, ο κλάδος της ηλεκτρικής ενέργειας έχει βιώσει εντυπωσιακές μεταρρυθμίσεις και προόδους, με πιο σημαντική από αυτές να είναι η απελευθέρωση των αγορών ενέργειας από μια κεντρική λειτουργική προσέγγιση σε ένα ανταγωνιστικό μοντέλο. Ο σκοπός αυτής της νέας ανταγωνιστικής δομής είναι η εξάλειψη των μονοπωλίων, η ενίσχυση της λειτουργικής αποτελεσματικότητας των συστημάτων ενέργειας, η εξασφάλιση ικανοποιητικής ποιότητας παροχής ηλεκτρικής ενέργειας και η ελαχιστοποίηση των δαπανών για τους τελικούς χρήστες. Επιπλέον, επιδιώκει να προσφέρει βελτιωμένα κίνητρα για τη συσσώρευση κεφαλαίου, να ενθαρρύνει τους καταναλωτές να απέχουν από την κατανάλωση όταν οι δαπάνες υπερβαίνουν τα οφέλη και να προάγει κίνητρα για έρευνα και ανάπτυξη.

Η ενσωμάτωση πολιτικών βιωσιμότητας συμβαδίζει με την απελευθέρωση των αγορών ενέργειας, παράγοντας κίνητρα για περιβαλλοντικά φιλικές πρακτικές. Η απελευθέρωση επιτρέπει στις ανανεώσιμες πηγές ενέργειας και τεχνολογίες αποθήκευσης ενέργειας να ανταγωνίζονται σε ίση βάση με τις παραδοσιακές μορφές ενέργειας, ενθαρρύνοντας την υιοθέτηση βιώσιμων τεχνολογιών. Οι κυβερνήσεις χρησιμοποιούν συχνά πολιτικές όπως το σύστημα των εγγυημένων σταθερών τιμών (feed-in tariffs) ή τα πιστοποιητικά ανανεώσιμης ενέργειας για την προώθηση της παραγωγής και κατανάλωσης πράσινης ενέργειας εντός ενός απελευθερωμένου πλαισίου αγοράς. Αυτή η προσέγγιση όχι μόνο αντιμετωπίζει περιβαλλοντικά προβλήματα, αλλά συμβαδίζει και με τους ευρύτερους κοινωνικούς στόχους της μείωσης των εκπομπών άνθρακα και της επίτευξης μιας πιο βιώσιμης ενεργειακής μελλοντικής προοπτικής. Ουσιαστικά, ο συνδυασμός της απελευθέρωσης της αγοράς ενέργειας και των πολιτικών βιωσιμότητας δημιουργεί ένα περιβάλλον όπου οι δυνάμεις της αγοράς καθοδηγούν την υιοθέτηση καθαρότερων, πιο αποδοτικών μορφών παραγωγής ενέργειας.

Η παρούσα διατριβή εξετάζει την ανάπτυξη μοντέλων βελτιστοποίησης για την ενσωμάτωση πολιτικών βιωσιμότητας και την εξέταση της στρατηγικής συμμετοχής των παραγωγών ηλεκτρικής ενέργειας στις σύγχρονες αγορές ενέργειας. Οι προτεινόμενες μεθοδολογίες βασίζονται σε μοντέλα μεικτού ακέραιου γραμμικού προγραμματισμού (MILP) και μοντέλα μαθηματικού προγραμματισμού με περιορισμούς εξισορρόπησης (MPEC). Ένα γνωστό πρόβλημα αυτών των τεχνικών μοντελοποίησης

είναι ότι το μέγεθος του μοντέλου αυξάνεται εκθετικά με το μέγεθος του προβλήματος και μπορεί εύκολα να καταστεί μη επιλύσιμο, ειδικά στην περίπτωση των μη γραμμικών MPECs που πρέπει να γραμμικοποιούνται πριν λυθούν. Επομένως, έχουν χρησιμοποιηθεί αλγόριθμοι διάσπασης (decomposition) και τεχνικές γραμμικοποίησης για να επιτραπεί η εφαρμογή των προτεινόμενων μεθοδολογιών σε πραγματικές περιπτώσεις. Οι παρουσιαζόμενες στρατηγικές επίλυσης μπορούν να αντιμετωπίσουν προβλήματα μεγάλης κλίμακας χρησιμοποιώντας εμπορικά διαθέσιμα εργαλεία επίλυσης MILP, όπως ο CPLEX.

Πιο συγκεκριμένα, αρχικά εξετάζεται η στρατηγική συμμετοχή ενός ιδιοκτήτη δύο μονάδων αποθήκευσης στις αγορές ενέργειας και εφεδρειών, υπό αβεβαιότητα στην παραγωγή αιολικής ενέργειας. Ένα διεπίπεδο μοντέλο αναπτύσσεται, με το πρόβλημα του άνω επιπέδου να έχει ως στόχο τη μεγιστοποίηση του κέρδους που αναμένεται για τον ιδιοκτήτη μονάδων αποθήκευσης, ενώ το πρόβλημα του κάτω επιπέδου αντιπροσωπεύει τη διαδικασία εκκαθάρισης της αγοράς σε δύο στάδια. Το πρώτο στάδιο αναφέρεται σε ένα πλαίσιο κοινής εκκαθάρισης των αγορών ενέργειας και εφεδρειών επόμενης ημέρας, προκειμένου να καθοριστούν οι βέλτιστες ποσότητες για την κατανομή ενέργειας και την προμήθεια εφεδρειών, ενώ στο δεύτερο στάδιο, πραγματοποιείται η εκκαθάριση της αγοράς εξισορρόπησης, λαμβάνοντας υπόψη πιθανά σενάρια παραγωγής αιολικής ενέργειας. Οι αποφάσεις στην αγορά εξισορρόπησης περιλαμβάνουν ενεργοποίηση ανοδικών και καθοδικών εφεδρειών, που έχουν ήδη υποβληθεί στην αγορά επόμενης ημέρας. Το προτεινόμενο μαθηματικό πλαίσιο εφαρμόζεται σε ένα ηλεκτρικό δίκτυο 6 κόμβων και εξετάζει τις δυνητικές ευκαιρίες εξισορροπητικής κερδοσκοπίας (arbitrage) για τον ιδιοκτήτη συστημάτων αποθήκευσης, υπό σενάρια αύξησης της παραγωγής αιολικής ενέργειας και πιθανές περιπτώσεις συμφόρησης στις γραμμές μεταφοράς ενέργειας του δικτύου.

Στη συνέχεια, παρουσιάζεται ένα στοχαστικό πλαίσιο βελτιστοποίησης μεικτού ακέραιου γραμμικού προγραμματισμού (MILP) για τη μελέτη της βέλτιστης συμμετοχής και την οικονομική ανάλυση διάφορων τεχνολογιών αποθήκευσης ενέργειας, όπως το συστήματα αντλησιοταμίευσης, προηγμένα αδιαβατικά και διαβατικά συστήματα συμπίεσης αέρα και μπαταρίες ιόντων λιθίου, σε συζευγμένη αγορά ηλεκτρικής ενέργειας και φυσικού αερίου υπό συνθήκες τέλειου ανταγωνισμού (perfect competition). Το πλαίσιο εκκαθάρισης αφορά μόνο αγορές ενέργειας, με στόχο τη βέλτιστη κατανομή και τη μεγιστοποίηση του κοινωνικού πλεονάσματος (social welfare)

για το ενοποιημένο ενεργειακό σύστημα, μέσω ενός μοντέλου στοχαστικού προγραμματισμού δύο σταδίων. Το πρώτο στάδιο παρουσιάζει τη διαδικασία εκκαθάρισης της αγοράς επόμενης ημέρας, ενώ το δεύτερο στάδιο παρουσιάζει την εκκαθάριση και λειτουργία της αγοράς εξισορρόπησης, μέσω ενός συνόλου πιθανών σεναρίων παραγωγής αιολικής ενέργειας. Οι δύο αγορές επικοινωνούν κυρίως μέσω της αμφίπλευρης λειτουργίας του διαβατικού συστήματος αποθήκευσης ενέργειας με συμπίεση αέρα, τόσο ως παραγωγός ηλεκτρικής ενέργειας όσο και ως καταναλωτής φυσικού αερίου. Ο προτεινόμενος αλγόριθμος εφαρμόζεται σε ένα πραγματικό τροποποιημένο δίκτυο ηλεκτρικής ενέργειας IEEE 24 σταθμών και ένα μονοκομβικό δίκτυο φυσικού αερίου και παρέχει μια λεπτομερή ανάλυση των λειτουργικών χαρακτηριστικών και της κερδοφορίας κάθε τεχνολογίας αποθήκευσης ενέργειας στο ενοποιημένο ενεργειακό σύστημα.

Η στρατηγική συμμετοχή μιας μονάδας παραγωγής ηλεκτρικής ενέργειας με χρήση φυσικού αερίου (GFPP), ασκώντας ισχύ (market power) στις συζευγμένες αγορές ηλεκτρικής ενέργειας και φυσικού αερίου που βασίζονται σε ωριαίες δημοπρασίες, με ενσωμάτωση της αγοράς δικαιωμάτων εκπομπών άνθρακα (CETS), αποτελεί τον τρίτο θεματικό τομέα αυτής της διατριβής. Αναπτύσσεται ένα νέο διεπίπεδο μοντέλο όπου το πρόβλημα του άνω επιπέδου στοχεύει στο να μεγιστοποιήσει τα κέρδη του στρατηγικού παίκτη, ενώ στο πρόβλημα του κάτω επιπέδου, οι αγορές ηλεκτρικής ενέργειας και φυσικού αερίου εκκαθαρίζονται διαδοχικά για την υπό εξέταση ημέρα, λαμβάνοντας υπόψη την έκδοση αδειών εκπομπής άνθρακα (emission allowances) για τους συμβατικούς παραγωγούς ηλεκτρικής ενέργειας και την υψηλή διείσδυση της παραγωγής ηλεκτρικής ενέργειας από αιολικά πάρκα. Ο προτεινόμενος αλγόριθμος εφαρμόζεται σε ένα ηλεκτρικό δίκτυο 5 κόμβων σύμφωνα με τα πρότυπα της αγοράς Πενσυλβάνια-Νιου Τζέρσεϊ-Μέριλαντ (PJM), και ένα μονοκομβικό δίκτυο φυσικού αερίου. Τα αποτελέσματα των μελετών παρέχουν τιμές εκκαθάρισης ηλεκτρικής ενέργειας που έχουν ενσωματώσει τις τιμές άνθρακα και τις βέλτιστες προσφορές για το στρατηγικό παίκτη (GFPP), υπό πιθανά προβλήματα συμφόρησης στη μεταφορά ηλεκτρικής ενέργειας και σενάρια αύξησης των τιμών του φυσικού αερίου.

Οι βέλτιστες στρατηγικές συναλλαγών για ένα στρατηγικό φορέα σωρευτικής εκπροσώπησης (ΦοΣΕ, aggregator) ανανεώσιμης ενέργειας, που κατέχει κυρίαρχη θέση στην κοινή αγορά ηλεκτρικής ενέργειας και πράσινων πιστοποιητικών, αντιμετωπίζονται στο τελευταίο μέρος αυτής της διατριβής. Στο πρόβλημα του άνω

επιπέδου της διεπίπεδης μαθηματικής διατύπωσης, ο στρατηγικός ΦοΣΕ ανανεώσιμης ενέργειας στοχεύει στο να μεγιστοποιήσει τα κέρδη του, ενώ τα δύο προβλήματα του κάτω επιπέδου αντιπροσωπεύουν τον διαδοχικό μηχανισμό εκκαθάρισης της αγοράς επόμενης ημέρας ηλεκτρικής ενέργειας και πράσινων πιστοποιητικών αντίστοιχα. Η προτεινόμενη προσέγγιση εφαρμόζεται πρώτα σε ένα ηλεκτρικό δίκτυο 5 κόμβων στην στα πρότυπα της αγοράς PJM και στη συνέχεια σε ένα τροποποιημένο σύστημα IEEE 24 κόμβων για να επιδείξει την υπολογιστική αποδοτικότητα και την εφαρμοσιμότητα της σε ένα ρεαλιστικό πλαίσιο. Οι αριθμητικές προσομοιώσεις που πραγματοποιήθηκαν καθορίζουν τις τιμές εκκαθάρισης ηλεκτρικής ενέργειας και πράσινων πιστοποιητικών και το βέλτιστο σχέδιο συναλλαγών για το στρατηγικό ΦοΣΕ ανανεώσιμης ενέργειας, υπό πιθανές συμφορήσεις στο δίκτυο ηλεκτρικής ενέργειας.

Acknowledgements

When I embarked on my PhD journey four years ago, little did I know about the insightful, yet challenging experiences that would lay before me and that I would have to face. However, it was the moments of reward and happiness that followed each small or large achievement that gave me the extra motivation to keep going and constantly improve. Today, looking back, all these experiences will accompany me for the rest of my life. The following few lines are devoted to the people who encouraged and stood by me during this journey.

First and foremost, I would like to express my gratitude to my supervisor Professor Michael C. Georgiadis for his tangible belief and support throughout the course of these years. His valuable mentorship and consistent guidelines proved decisive in shaping my academic profile and broadening my research horizon. Furthermore, I wish to thank the company HELLENiQ ENERGY for providing me financial support, so that I can undividedly pursue my doctoral studies. Specially, I would also like to thank the members of my academic committee Professor Eustathios Kikkinides and Professor George Nenes for the assistance and feedback they provided.

Throughout the years of my PhD, I had the pleasure of meeting and working with wonderful people. First, I would like to make a special mention to Dr. Evangelos Tsimopoulos. In addition to the scientific guidance that he provided as co-supervisor of my PhD, we developed a close friendship accompanied by deep appreciation. Then, I would like to thank my friends and colleagues in the Process Systems Engineering laboratory of the Chemical Engineering Department, Dr. Georgios Georgiadis, Dr. Apostolos Elekidis and Achilleas Arvanitidis. Our conversations, laughs and mutual support contributed decisively to the formation of a pleasant working environment and made even the most challenging and stressing moments seem like a drop in the ocean.

Last but not least, I would like to express my sincere gratitude and respect to my parents Nikolaos and Thomai, and my long-life “partner in crime”, my brother Iordanis, for their love and support in every aspect of my life. They are the ones to whom I owe everything and dedicate this work.

Contents

Declaration of Authorship iii

Abstract iii

Acknowledgements xii

List of Figures xviii

List of Tables xxi

Abbreviations xxiiiii

1 Introduction 1

1.1 Motivation and objectives 1

1.2 Pool-based energy markets 4

1.2.1 Market structure 4

1.2.2 Merit-order effect – Market clearing price 5

1.2.3 Market power in energy markets 6

1.2.4 Capacity withholding strategies 8

1.3 Derivatives markets 10

1.3.1 Carbon emission trading 10

1.3.2 Green certificates 11

1.4 Literature review 12

1.4.1 Electricity market 12

1.4.1.1 Integration of renewable energy sources 15

1.4.1.2 Integration of energy storage technologies 22

1.4.1.2.1 Pumped-Hydroelectric Storage 22

1.4.1.2.2 Compressed Air Energy Storage 23

1.4.1.2.3 Battery Energy storage 24

1.4.2 Natural gas market 25

1.4.3 Carbon emission trading 29

1.4.4 Green certificates market 30

1.5 Mathematical framework for perfect and imperfect competition 32

1.5.1 Perfect competition – LP 32

1.5.2 Imperfect competition - MPEC 33

1.6 Thesis overview 37

2 Strategic bidding of an energy storage agent in electricity and reserve markets 39
2.1 Introduction 39
2.2 Problem statement 41
2.3 Mathematical Formulation 43
2.3.1 Bi-level model structure 43
2.3.2 Upper-level problem: ESS's expected profit maximization 43
2.3.3 Lower-level problem: Joint energy and reserve day-ahead market 46
2.3.4 Lower-level problem: Real-time market clearing under wind power generation uncertainty 48
2.3.5 Solution Approach 50
2.4 Application study 51
2.4.1 Uncongested network 54
2.4.2 Congested Network 57
2.4.3 Wind power generation increment scenarios 64
2.5 Computational issues 67
2.6 Conclusions 67
3 Analysis of energy storage technologies in electricity and natural gas markets 72
3.1 Introduction 72
3.2 Problem Statement 74
3.3 Mathematical framework 74
3.3.1 General energy storage modelling 74
3.3.2 Pumped-Hydroelectric Storage Modelling 76
3.3.3 Advanced Adiabatic Compressed Air Energy Storage Modelling 77
3.3.4 Diabatic Compressed Air Energy Storage Modelling 78
3.3.5 Battery Energy Storage Modelling 80
3.3.6 Electricity and Natural Gas Market Clearing Modelling 80
3.4 Application study 84
3.4.1 Data 84
3.4.2 Uncongested power network 87
3.4.3 Congested power network 92
3.4.4 Impact of wind power generation volatility 96
3.5 Computational issues 97
3.6 Conclusions 98

4 Strategic bidding of a gas-fired unit in low carbon electricity and natural gas market 103
4.1 Introduction 103
4.2 Problem statement 105
4.3 Mathematical framework 106
4.3.1 Upper-level problem: GFPP's expected profit maximization 107
4.3.2 Lower-level problem: Electricity market clearing 108
4.3.3 Lower-level problem: Natural gas market clearing 109
4.3.4 Solution methodology 110
4.4 Application study 111
4.4.1 Uncongested power network 113
4.4.2 Congested power network 117
4.4.3 Natural gas price increase 119
4.5 Computational issues 121
4.6 Conclusions 122
5 Trading strategy of a renewable energy aggregator in electricity and green certificates markets 155
5.1 Introduction 126
5.2 Problem statement 127
5.3 Bi-level model formulation 129
5.3.1 Upper-level problem: GFPP's expected profit maximization 130
5.3.2 Lower-level problem: Electricity market clearing 130
5.3.3 Lower-level problem: Green certificates market clearing 132
5.3.4 Solution methodology 133
5.4 Application study 134
5.4.1 Uncongested power network 136
5.4.2 Congested power network 142
5.4.3 Modified IEEE-24 bus power network 144
5.5 Computational issues 148
5.6 Conclusions 149
6 Conclusions and Future Research 153
6.1 Conclusions 153
6.2 Main Contributions of this work 156
6.3 Recommendations for future research 157

Bibliography..158

List of Figures

Figure 1.1: Merit-Order effect 5
Figure 1.2: Physical withholding strategy 8
Figure 1.3: Financial withholding strategy 9
Figure 1.4: Market clearing formulation 32
Figure 1.5: Bi-level formulation for strategic participation 33
Figure 1.6: MPEC formulation 35
Figure 2.1: Mathematical structure and function of the bi-level model 43
Figure 2.2: 6-bus power network 53
Figure 2.3: Day-ahead prices and energy (dis)charging quantities for storage systems s1, s2 55
Figure 2.4: Upward and downward day-ahead reserve market prices and procurements for storage system s1. 55
Figure 2.5: State of charge of storage systems, for the uncongested network 57
Figure 2.6: Local marginal prices for the congested network 58
Figure 2.7: Day-ahead (dis)charging energy dispatch and reserve procurements for storage system s1, for the congested network 59
Figure 2.8: State of charge of storage systems, for the congested network 59
Figure 2.9: Energy dispatch and revenue comparison for storage system s1, between uncongested and congested network 63
Figure 2.10: Energy dispatch and revenue comparison for storage system s2, between uncongested and congested network 64
Figure 2.11: Profit comparison between uncongested and congested network 64
Figure 2.12: Overall energy dispatch and reserve procurements of storage system s1, under three wind generation cases 66
Figure 2.13: Profit differentiation for storage systems s1, s2 and ESS agent, under three wind generation cases 66
Figure 3.1: The layout of the advanced adiabatic CAES 77
Figure 3.2: The layout of the diabatic CAES 79
Figure 3.3: Coupled electricity and natural gas market structure 81
Figure 3.4: Total hourly electricity and natural gas load 85
Figure 3.5: Modified 24-bus IEEE Reliability Test System 86

Figure 3.6: Single-node natural gas network 87
Figure 3.7: Day-ahead electricity and gas market clearing prices 88
Figure 3.8: Day-ahead (dis)charging energy dispatch for storage systems 89
Figure 3.9: Real-time electricity market clearing prices 90
Figure 3.10: Real-time gas market clearing prices and D-CAES dispatch 91
Figure 3.11: Day-ahead and overall profits for electricity storage systems 92
Figure 3.12: Day-ahead electricity market clearing price, under network congestion 94
Figure 3.13: Real-time electricity market clearing price, under network congestion 94
Figure 3.14: D-CAES high and low wind real-time electricity dispatch 95
Figure 3.15: Day-ahead and overall profits for electricity storage systems under power network congestion 96
Figure 3.16: Impact of wind generation volatility on storage systems profits and social welfare 97
Figure 4.1: Bi-level structure of the proposed strategic bidding framework 107
Figure 4.2: PJM 5-bus power grid 112
Figure 4.3: Forecasting load and maximum wind power generation 113
Figure 4.4: Comparison of CETS-embedded ELMPs and ELMPs 115
Figure 4.5: Electricity dispatch and strategic bids for the GFPP 116
Figure 4.6: Hourly difference between allocated and actual carbon emission allowances for the strategic GFPP 117
Figure 4.7: CETS-embedded ELMPs for the congested network 118
Figure 4.8: Electricity generation and profits for strategic GFPP under a gas price increase 120
Figure 4.9: CETS-embedded ELMPs under a gas price increase 121
Figure 5.1: Bi-level structure of the proposed strategic bidding framework 129
Figure 5.2: PJM 5-bus power network 135
Figure 5.3: Power producers' dispatch and LSEs' power demand 136
Figure 5.4: Electricity and green certificates clearing prices 138
Figure 5.5: Green certificates trading by strategic renewable aggregator 139
Figure 5.6: Green certificates trading by non-strategic renewable aggregator 139
Figure 5.7: Hourly available tradable green certificates of the strategic renewable aggregator 141

Figure 5.8: Hourly available tradable green certificates of the non-strategic renewable aggregator 141
Figure 5.9: Electricity and green certificates clearing prices under power network congestion 142
Figure 5.10: Modified IEEE 24-bus power network 144
Figure 5.11: Power producers' dispatch and LSEs' power demand in the IEEE 24-bus power network 146
Figure 5.12: Electricity and green certificates clearing prices in the uncongested IEEE 24-bus power network 146
Figure 5.13: Electricity and green certificates clearing prices in the congested IEEE 24-bus power network 147

List of Tables

Table 2.1: Data for ESS's units 53
Table 2.2: Data for conventional and wind generators 53
Table 2.3: Storage system's $s1$ operation in charging mode during time period 7 61
Table 2.4: Storage system's $s1$ operation in discharging mode during time period 14 61
Table 2.5: Storage system's $s2$ operation in charging mode during time period 4 62
Table 2.6: Storage system's $s2$ operation in discharging mode during time period 16 62
Table 3.1: Data for electricity storage technologies 87
Table 4.1: Data for electricity and natural gas producers. 112
Table 4.2: Strategic GFPP's electricity generation and expected profits. 118
Table 4.3: GLMPs under a gas price increase 120
Table 5.1: Data for power producers. 135
Table 5.2: Profits of strategic and non-strategic renewable aggregators 140
Table 5.3: Renewable aggregators' overall electricity generation and certificates trading. 143
Table 5.4: Profits of strategic and non-strategic renewable aggregators under power network congestion 143
Table 5.5:Profits of strategic and non-strategic renewable aggregators in the uncongested IEEE 24-bus power network 147
Table 5.6: Renewable aggregators' overall electricity generation and certificates trading in the IEEE 24-bus power network 148
Table 5.7: Profits of strategic and non-strategic renewable aggregators in the congested IEEE 24-bus power network 148

Table B.1 Marginal energy cost offers for conventional generators 193
Table B.2 Maximum energy capacity for demand loads 194
Table B.3 Maximum upward/downward reserve capacity for demand loads 194
Table B.4 Results for storage system s1, in the joint energy and reserve day-ahead market 195
Table B.5 Results for storage system s1 in the balancing market 196
Table B.6 Results for storage system s2, in the joint energy and reserve day-ahead market 197

Table B.7 Results for storage system s2 in the balancing market 198
Table B.8 Results for conventional generators in the joint energy and reserve day-ahead market 199
Table B.9 Results for conventional generators in the balancing market 200
Table B.10 Results for storage system s1, in the joint energy and reserve day-ahead market under network congestion 201
Table B.11 Results for storage system s1 in the balancing market under network congestion 202
Table B.12 Results for storage system *s*2, in the joint energy and reserve day-ahead market under network congestion 203
Table B.13 Results for storage system *s*2 in the balancing market under network congestion 204
Table B.14 Results for conventional generators in the joint energy and reserve day-ahead market under network congestion 205
Table B.15 Energy dispatch (MWh) and reserve provisions (MW) for conventional generators, under wind generation increment Cases 1,2,3 206
Table B.16 Energy dispatch and reserve procurements of storage system *s*1, during time period 1, under wind generation increment *Cases 1,2,3* 206

Abbreviations

MILP	Mixed Integer Linear Programming
MPEC	Mathematical Program with Equilibrium Constraints
IEEE	Institute of Electrical and Electronics Engineers
PJM	Pennsylvania – New Jersey – Maryland
IRENA	International Renewable Energy Agency
GC	Green Certificate
REC	Renewable Energy Credit
MO	Market Operator
KKT	Karush-Kuhn-Tucker
PX	Power Exchange
LMP	Locational Marginal Price
ISO	Independent System Operator
ETS	Emission Trading System
OTC	Over-The-Counter
RPS	Renewable Portfolio Standards
PTDF	Power Transfer Distribution Factor
VPP	Virtual Power Plant
REM	Regional Electricity Market
SW	Social Welfare
RES	Renewable Energy Sources
DERA	Distributed Energy Resource Aggregator
DA	Day-Ahead
RT	Real-Time
CVaR	Conditional Value at Risk
PV	Photovoltaic
PAB	Pay-As-Bid
WPP	Wind Power Producer

EV	Electric Vehicle
CSP	Concentrating Solar Power
GenCo	Generation Company
RTS	Reliability Test System
PHS	Pumped-Hydro-Storage
MCP	Market Clearing Price
CAES	Compressed Air Energy Storage
LAES	Liquid Air Energy Storage
MINLP	Mixed Integer Non-Linear Programming
BSS	Battery Storage System
GFPP	Gas-Fired Power Plant
IES	Integrated Energy System
ERCOT	Electric Reliability Council of Texas
GHG	Greenhouse Gas
P2G	Power-to-Gas
ED	Economic Dispatch
EPEC	Equilibrium Program with Equilibrium Constraints
ESS	Energy Storage System
SOC	State-of-Charge
GAMS	General Algebraic Modelling System
FERC	Federal Energy Regulatory Commission
NEMO	National Electricity Market Operator
SOAC	State-of-Available-Certificates
ACP	Alternative Compliance Penalty

Chapter 1

Introduction

1.1 Motivation and objectives

In recent years, climate change has emerged as one of the most pressing challenges of our time, with far-reaching consequences for the planet and its inhabitants (Olabi & Abdelkareem, 2022). Rising temperatures, extreme weather events, and disruptions to ecosystems are just a few manifestations of this crisis. One of the primary problems arising from climate change is the overreliance on fossil fuels for energy, leading to a significant increase in greenhouse gas emissions. A shift towards renewable energy sources holds immense potential in addressing these problems and vastly supports the transition towards a low-carbon economy. In particular, renewable energy derived mostly from sources such as solar, wind, hydro, and geothermal power, can contribute to the greenhouse gas emissions mitigation, disengagement from fossil fuels, industrial development, generation portfolio diversification and poverty reduction (Gielen et al., 2019). Global tendencies designate a sound growth in renewables, accounting for the 40% of the global installed power capacity, according to the International Renewable Energy Agency (IRENA, 2021), while by 2050 it is estimated that renewable sources will hold around two-thirds of the total energy supply (Larsson, 2009).

In tandem with the adoption of renewable energy, advancements in energy storage technologies play a crucial role in addressing the intermittent nature of some renewable sources (IRENA, 2017). Energy storage systems, such as advanced batteries, pumped-hydro and compressed air energy storage, enable the capture and efficient utilization of energy generated from renewable sources during peak production times. This stored energy can then be deployed during periods of high demand or when renewable sources are not actively generating power. By overcoming the intermittency challenge, energy storage technologies contribute to the reliability and stability of renewable energy, making it a more viable and consistent option for meeting the world's growing energy needs.

Moreover, sustainability policies play a pivotal role in steering societies towards a greener and more resilient future. Governments, businesses, and communities must collaborate to formulate and implement policies that incentivize the adoption of renewable energy and promote sustainable practices. Carbon emission trading (CET), often referred to as cap-and-trade or carbon pricing, is a market-based mechanism aiming at reducing greenhouse gas emissions by putting a price on carbon (Tang et al., 2020). Integrating carbon emission trading into energy markets is a key strategy for promoting sustainability and incentivizing a shift toward lower-carbon energy sources. In cap-and-trade systems worldwide, governments or regulatory bodies set a limit (cap) on the total amount of emissions allowed within a specific time frame. Emission allowances that represent the right to emit a certain amount of greenhouse gases are issued, often auctioned, and allocated to regulated entities, such as power plants, industrial facilities, and energy producers. Companies that can reduce emissions at a lower cost may sell excess allowances, while those facing challenges may purchase additional allowances. The regulatory cap can be gradually reduced over time to encourage emissions reduction.

Tradable green certificates (GCs), often referred to as renewable energy certificates (RECs) or green energy credits, are a financial instrument used in energy markets to promote and track the production and consumption of renewable energy (Hulshof et al., 2019). RECs play a crucial role in supporting the growth of renewable energy sources and encouraging the transition to a more sustainable and environmentally friendly energy mix. Renewable energy generators, such as wind farms, solar parks, and hydroelectric plants, produce electricity from clean and sustainable sources. For every megawatt-hour (MWh) of electricity generated, a corresponding number of green certificates are issued. The specific details of issuance and the number of certificates per MWh can vary by region and program. RECs are traded in energy markets, either directly between parties or through various platforms and brokers. Buyers purchase RECs to support and claim the environmental attributes of renewable energy. The revenue generated from REC sales can provide an additional source of income for renewable energy projects. This revenue can help make these projects economically viable and encourage further investment in clean energy infrastructure.

Within the above context, our focus is to integrate the above-mentioned sustainability policies in the current energy market framework and study the strategic

participation of power producers that have dominant position and exert market power in such market schemes. The proposed methodologies are based on the assumptions of a Stackelberg single-leader single-follower game. Initially, we develop a stochastic bi-level complementarity model. The upper-level problem seeks to maximize the expected profits of the strategic producer (leader), while the lower-level problems address the markets' clearing procedure managed by Market Operator (MO) as the follower. Assuming continuity and differentiability of the lower-level problem, the latter is replaced by its first-order Karush-Kuhn-Tucker (KKT) reformulation, transforming the bi-level model into a single-level mathematical programming with equilibrium constraints (MPEC). Subsequently, the KKT complementarity conditions are formulated as disjunctive constraints (Fortuny-amat et al., 1981), reshaping the MPEC into a mixed-integer linear programming (MILP) format. This MILP formulation is amenable to solution by commercial solvers and allows for achieving global optimality.

The primary objectives of this thesis are:

i. To develop a novel optimization framework to investigate the optimal bidding and offering strategies of an energy storage agent participating in a jointly cleared energy and reserve day-ahead and balancing market.
ii. To develop a stochastic MILP market-clearing model and analyze the economics of various energy storage technologies in a coupled electricity and natural gas market, under perfect competition.
iii. To propose a novel CET-embedded electricity and natural gas market scheme and determine the optimal bidding decisions and emission allowances manipulation of a strategic gas-fired power plant who acts bilaterally as power producer and natural gas consumer.
iv. To develop a novel auction-based hourly clearing scheme for green certificates market that harmonizes with EnergyTag Initiative standards (EnergyTag, 2021) and verifies the source of electricity.
v. To provide a bi-level mathematical model that ensures optimal trading strategies and management of green certificates for a renewable energy aggregator in an integrated electricity and green certificates market.

1.2 Pool-based energy markets

1.2.1 Market structure

Energy markets nowadays operate in two separate trading arenas to provide a holistic interchange framework and optimally manage transactions between energy generators and consumers i.e., futures and pools. Future markets are managed by for-profit organizations and allow medium- and long-term power trading. While they illustrate significant research and practical interest, a thorough overview of their operational structure and function is beyond the realm of this work. Instead, a meticulous analysis on pool-based energy markets' design and agents' interactions, is the fundamental purpose of this thesis.

A power exchange (PX), also called market operator (MO), is the independent nonprofit entity that operates pool-based energy markets and handles short-term transactions i.e., couples generation and demand quotes and settles market prices (Conejo et al., 2010). Day-ahead market (also referred as spot markets in Europe) is predominantly characterized as the main marketplace for energy transactions and is organized as a two-sided auction, where market participants (producers, consumers, retailers) submit their corresponding energy and demand blocks, as well as their price offers/bids, one day in advance. Adjustment (intraday) and balancing (real-time) markets successively, constitute the necessary actions to prevent unwanted deviations and balance power system's operation (Morales et al., 2014). In particular, balancing markets deal with last minute energy schedule clutters and cover dispatched power, that due to equipment failures and the stochastic nature of renewable energy sources does not materialize. Transmission congestions and load deviations also constitute key factors that justify the crucial contribution of balancing stage to well-regulated energy markets' operation.

Apart from energy markets, some countries have established reserve capacity markets to further guarantee the sufficient supply of balancing power throughout the power system's real-time operation. Reserve capacity provision can be determined by two means i.e., sequentially, in a series of auctions subsequent to the day-ahead energy market clearing, so that unsuccessfully placed capacity, to be offered in the following auctions and simultaneously, in a single coupled auction by employing co-optimizing

algorithms. Producers participating in that type of markets, are compensated according to the available capacity. It is worth noting that the majority of market frameworks also provide long-term clearing services through financial contracts, such as options, forwards and derivatives. However, an extended examination on these terms is beyond the purview of this work.

1.2.2 Merit-order effect – Market clearing price

In organized pool-based power markets two principal mechanisms for the determination of wholesale prices are embraced. In the absence of transmission congestion, the resulting power price is identical for all locations and set by the marginal cost offer of the most expensive generating asset. On the contrary, when power network congestion takes place, various locational marginal prices (LMPs) for each system's node emerge, due to line losses, and nodal pricing is adopted (Gan et al., 2013). Significant benefits, such as several operational characteristics and explicit price signals and incentives for the establishment of new investments and demand response, render LMP-based markets the preferred approach for the majority of well-regulated energy pools. While alternative approaches exist -with the principal one dictating a single price across the network and the handling of congestion cost as a separate uplift charge- their application is considered insufficient, due to their inefficiency in hedging long-term contracts and their unpredictable nature (Sioshansi, 2008).

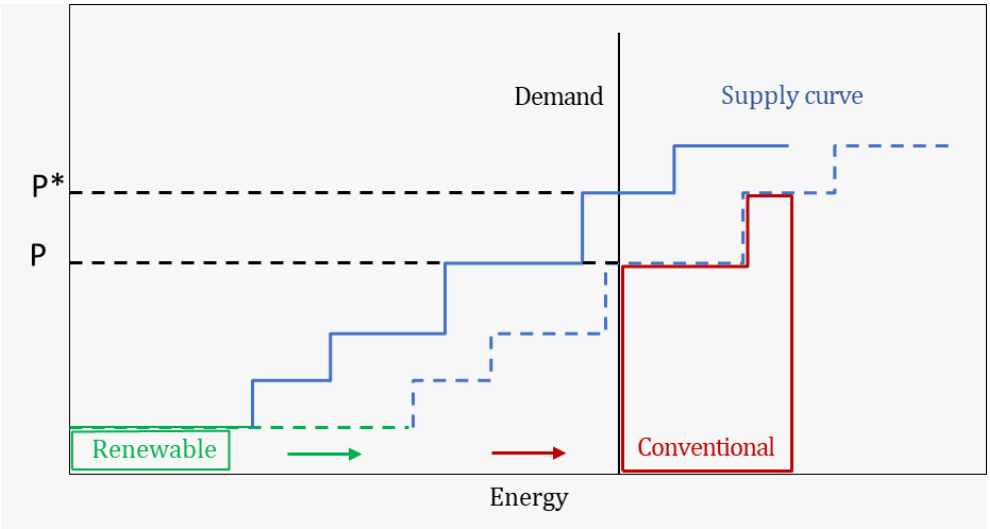

Figure 1.1: Merit-order effect

The endorsement of the appropriate auction design in electricity spot markets constitutes a fundamental decision for the constitution of a well-configurated market framework and depends on several factors. Sealed-bid auction format, where each buyer/seller submits its offers/bids anonymously and without having knowledge of the rest of the agents' offering strategies, comprises two primary pricing mechanism approaches i.e., uniform and pay-as-bid (or discriminatory). Uniform pricing rule entails that all generators receive an identical market clearing price, set by the highest priced resource nominated to provide supply and is particularly popular in the US ISO markets. Conversely, in a pay-as-bid auction setup, prices paid to the dispatching generators are based on their actual offers, rather than the offer of the most expensive supplier selected for energy provision. As a result of paying winning suppliers in a distinct price, depending on their individual bids, pay-as-bid auctions are also called discriminatory auctions, while energy markets of England and Wales constitute nowadays the main ground of their application.

As supported by numerous analyses, while small deviations may emerge due to market design, organization, and setting factors, market prices are unlikely to substantially differ between these auction formats, while the literature cannot audaciously support a verdict that a pay-as-bid auction will generate lower overall prices in competitive energy markets (Tierney et al., 2007).

1.2.3 Market power in energy markets

The main objective of electricity market deregulation/liberalisation is to motivate electricity producers to reduce their expenses, promote innovation, and maintain competitive market prices, ultimately delivering high-quality services and affordable electricity to consumers. Nevertheless, it's not always assured that deregulation alone will automatically create competitive conditions and outcomes. Factors such as pricing strategies, industry-specific characteristics, and the inherent properties of electrical energy can leave the market susceptible to the exercise of market power. To begin with, the absence of large-scale energy storage options means that real-time electricity production is necessary to meet demand, and this can lead to supply shortages because power generators may face technical limitations in providing short-term reserve power (Borenstein, 2000). Secondly, the physical laws governing power flow make the

scheduled operation of the grid complex and any network stability failure can have significant financial consequences. Thirdly, the power generation industry often exhibits a concentration of firms, coupled with relatively inelastic demand for electricity and its limited supply, which provides an incentive for incumbent companies to boost their profits by stifling competition and raising market prices.

In the realm of economic theory, the concept of market power is defined as "the capacity to adjust prices in a way that is profitable when compared to competitive pricing" (Kirschen & Strbac, 2005), (Twomey et al., 2005). The United States Department of Justice offers a similar definition, stating that market power is "the ability of a supplier to raise prices above competitive levels and sustain those prices over a significant period." Each term in these definitions carries significant weight and is chosen thoughtfully. The term "ability" is crucial because it enables regulators to differentiate between merely "possessing" market power and actively "utilizing" it, as the latter isn't inherently illegal. However, a firm with market power typically has a rational incentive to exercise it. This distinction becomes meaningful when examining market power through either an ex-post (post-exercise) or ex-ante (pre-exercise) analysis.

The term "profitably" in the definition signifies that market power exertion should be carried out in a way that generates profits. Therefore, actions like reducing production or shutting down units can only be considered as instances of market power exertion if they meet profitability criteria. The phrase "maintain prices above" excludes situations where an established firm sets prices lower than competitive levels to discourage new competitors (known as predatory pricing). Moreover, Hansen and Percebois (2019) suggest that a dominant firm might have incentives to allow new entrants, benefiting from short-term price increases while attracting less attention from regulatory authorities. This is why the definition of market power indirectly alludes to an increase in market prices.

Finally, the phrase "above competitive levels" is the most crucial aspect of the market power definition, even though it can be contentious because there are situations where it may result in higher market prices. For instance, this can occur when demand outstrips supply, and consumers are willing to pay more than the cost of supply or when high demand allows more expensive units to operate and cover their fixed costs. In these cases, market power isn't exercised, as market equilibrium is based on the system's

marginal cost, even if prices are high. Hence, a firm is considered to exercise market power when it raises market prices above the system's marginal cost.

1.2.4 Capacity withholding strategies

In the context of energy markets, the literature acknowledges the existence of two distinct forms of market power: vertical and horizontal. Vertical market power pertains to companies that engage in multiple aspects of the downstream process, such as both energy generation and transmission. In such instances, a company leverages its dominant position in one of these activities to gain a competitive advantage and boost its overall earnings. On the other hand, horizontal market power pertains to companies that wield their market influence at one stage of the production process, affecting outcomes and prices at another stage. In our specific study, which focuses solely on electricity generation and energy-only markets, our attention is directed toward examining horizontal market power. The primary means by which a power producer exercises this type of market power typically involves strategies like capacity withholdings.

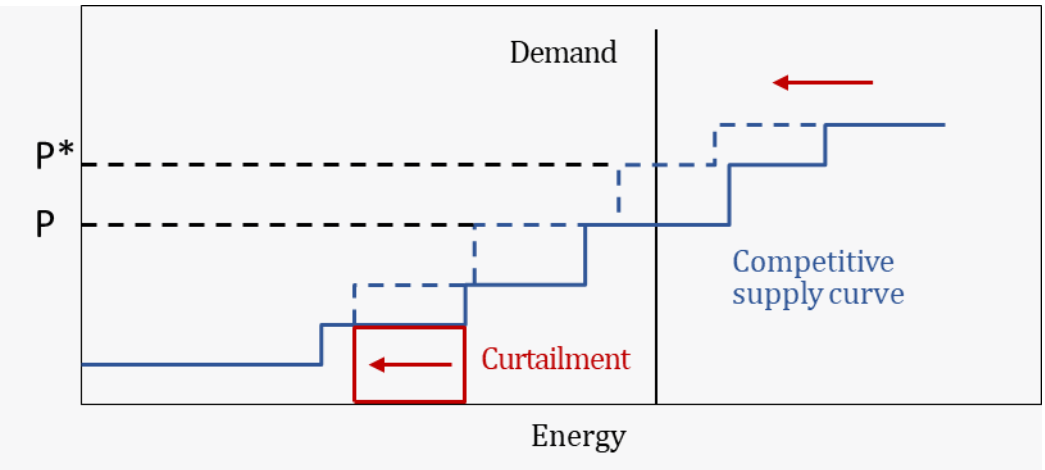

Figure 1.2: Physical withholding strategy

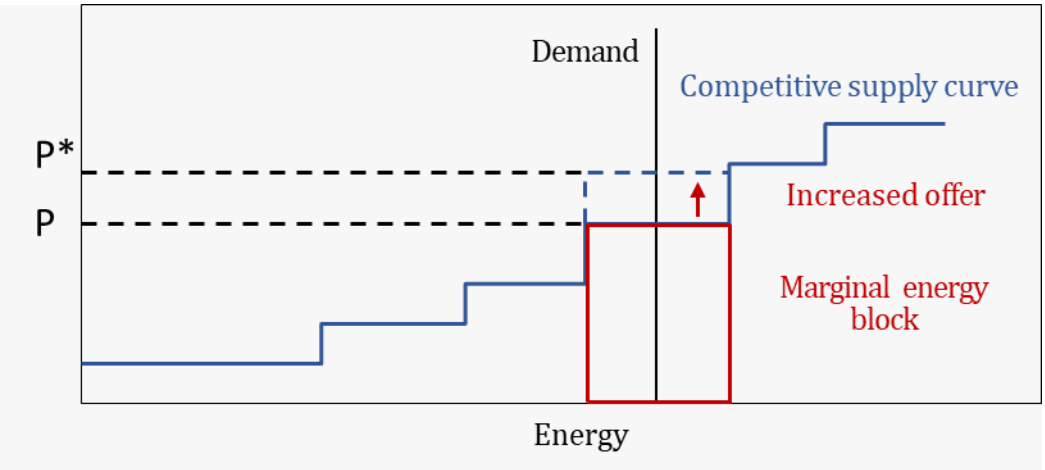

Figure 1.3: Financial withholding strategy

The term "withholding" refers to tactics that have two main components: physical or quantity withholding and financial or economic withholding. The former involves situations where a producer uses their market influence to reduce production intentionally. As illustrated in *Figure 1.2*, when production is deliberately reduced (shown in red), it shifts the competitive supply curve to the left, resulting in a higher market price. In the case of financial withholding, strategic producers achieve the same outcome by making higher offers. As depicted in *Figure 1.3*, the marginal energy block (in red), which dictates the market price, bids higher, causing the competitive supply curve to move upward. When examining markets, we observe the effects of capacity withholding, but it can be challenging to discern which strategy the producer is employing. Lastly, in a network-constrained market, a producer with a diversified generation portfolio may use a third method to exert market power: manipulating the mix of production. By doing so, based on transmission line constraints, the producer can create areas of monopoly, driving up Locational Marginal Prices (LMPs) and increasing their profits.

The exertion of market power has two primary social implications. Firstly, it leads to a wealth shift from consumers to producers, which can be calculated as the difference in price ($P^* - P$) multiplied by the total energy production, resulting in price distortion. Secondly, the enhanced profits resulting from market power exertion are not exclusive to the specific producer wielding this power; they benefit all producers since everyone is paid the same price. In reality, in many instances, the entity exerting market power may find it less profitable due to the associated exercise costs.

1.3 Derivatives markets

1.3.1 Carbon emission trading

Carbon markets are structured systems designed to regulate and incentivize the reduction of greenhouse gas emissions. They typically operate through one of two main mechanisms: cap and trade schemes (also known as emissions trading schemes or ETS) and baseline-and-credit mechanisms (carbon credit schemes). These markets aim to encourage emissions reductions by assigning a financial value to carbon emissions and allowing companies to trade emissions allowances or carbon credits.

Cap and trade schemes are typically regulated and enforced by government agencies or regulatory bodies and place a cap on the total allowable emissions of greenhouse gases within a specific jurisdiction or industry sector. Emissions allowances or permits are allocated to participating companies, often based on historical emissions or other criteria. Companies can buy, sell, or trade these allowances among themselves in a secondary market. This trading allows entities that can reduce emissions more cost-effectively to sell excess allowances to those facing greater challenges in reducing emissions. Companies must also provide enough allowances at the end of a compliance period to cover their actual emissions. If they exceed their allocated allowances, they may face financial penalties.

On the other hand, baseline-and-credit mechanisms operate in a more decentralized manner. Organizations, projects, or individuals implement activities that reduce or remove greenhouse gas emissions. These activities are assessed and verified to determine the number of carbon credits they generate. Carbon credits represent a quantifiable reduction in emissions or removal of carbon from the atmosphere (e.g., 1 tonne of CO_2 equivalent). These credits can be bought and sold on voluntary carbon markets. Participation in carbon credit schemes is usually voluntary, and organizations may purchase credits to offset their own emissions voluntarily or as part of corporate sustainability initiatives.

Carbon markets involve a range of participants, including emitters, project developers, carbon credit brokers, and investors and most of them are influenced by international agreements and protocols, such as the Kyoto Protocol or the Paris Agreement, which set global emission reduction targets and mechanisms for carbon

trading on an international scale. Overall, carbon markets aim to create economic incentives for reducing greenhouse gas emissions and promoting sustainable practices while providing a flexible approach to achieving emission reduction goals. The structure and regulation of these markets can vary significantly between jurisdictions and market types.

1.3.2 Green certificates

Green certificates, often referred to as renewable energy certificates (RECs) or renewable energy credits (RECs), are market-based instruments designed to promote the production and use of renewable energy sources. They are an important component of renewable energy policy and sustainability efforts in many countries.

Green certificates are created when renewable energy is generated. For each megawatt-hour (MWh) of electricity produced from a renewable source, one green certificate is typically issued. These certificates represent the environmental attributes of the renewable electricity and can be bought, sold, or traded independently of the electricity itself. The entity that owns the certificate is considered the "owner" of the renewable energy attributes. To ensure transparency and avoid double counting, green certificates are tracked in a centralized registry or database. This tracking system records the issuance, transfer, and retirement of certificates. Green certificates usually have an expiration date to encourage timely use and retirement. If a certificate is not retired by the deadline, it may become invalid.

Most regions or countries have specific legislation or regulations that govern the creation, trading, and use of green certificates. These regulations define the eligibility criteria for renewable energy sources, the structure of the certificate market, and compliance obligations for market participants. Common sources include wind, solar, hydroelectric, biomass, and geothermal energy. Regulatory authorities, such as energy agencies or commissions, oversee the green certificate market. They ensure compliance with the rules and monitor trading activities.

Green certificates can be traded on various platforms, including over-the-counter (OTC) markets and organized exchanges. Many regions require electricity suppliers or utilities to obtain a certain number of green certificates to demonstrate their commitment

to renewable energy. These obligations are often referred to as renewable portfolio standards (RPS) or similar mandates. Non-compliance can result in penalties.

When a certificate is used to make a renewable energy claim, it is retired, indicating that the associated environmental benefits have been accounted for. Verification processes ensure that certificates are legitimate and represent genuine renewable energy generation. It's important to note that the specific structure and regulations governing green certificates can vary significantly from place to place, reflecting the unique energy policy goals and priorities of each jurisdiction.

1.4 Literature review

1.4.1 Electricity market

Electricity market clearing and the determination of the optimal offering strategies for participating agents are considered areas of particular interest in the scientific community and have drawn a lot of attention in recent years. Ruiz and Conejo (2009) are considered some of the first to propose a non-linear bi-level optimization mathematical framework to derive the optimal strategic decisions of a power generator, participating in a pool-based electricity market and a network-constrained six-bus test system. The upper-level objective aims at maximizing the strategic producer's profit, while the lower-level problem represents the market clearing procedure, deriving the local marginal prices (LMPs) endogenously, with respect to social welfare maximization. The algorithm is reduced to a mixed-integer linear programming (MILP) problem using well established mathematical techniques such as, the strong duality theorem, Karush-Kuhn-Tucker optimality conditions and Fortuny-Amat and McCarl linearization approach. The computational analysis demonstrated the capability of the proposed model to generate optimal multiple-block offers for the strategic producer and the fact that network congestion can be highlighted as profit-increasing factor. Gabriel and Leuthold (2010) presented a novel linear bi-level model to capture the behavior of a strategic player, acting as a Stackelberg leader and exercising market power in a network-constrained electricity market, where ISO acts a follower, considering offering decisions of competitive firms. As Stackelberg leaders are considered large-scale electricity generation companies, such as EDF, Electrabel, EON and RWE. The approach is

implemented into two different power networks i.e., a 3-bus test system and a 15-bus representation of the Western European grid. A thorough comparison between perfect and imperfect competition market setups is conducted, and the effects of network congestion are analyzed. Results indicate that the proposed mathematical approach is promising in addressing realistic problems and that when these firms act strategically (particularly EDF), acquire great profit increase.

Although binary variables constitute fundamental elements to model non-convexities, such as electricity generators' minimum power outputs and start-up costs, they prevent MILP models to obtain market clearing prices as dual variables of the energy balance equations. Ruiz et al. (2012) addressed this problematic situation, by proposing a novel primal-dual multi-block formation that ensures well approximated social welfare comparing to the original clearing problem. The suggested approach provides LMPs for a single-shot pool-based market and guarantees generators' revenue adequacy, without incorporating additional uplift charges. A base-demand and a peak-demand case study concerning an IEEE 24-bus Reliability Test System was used to demonstrate the efficiency of the proposed methodology. Simulation analysis illustrates that both market prices and total profits are higher in the relaxed duality approach, when compared to the equivalent conventional one.

Ruiz et al. (2013) extended their research scope considering a strategic electricity producer participating in an electricity market regime, similar to the ISO New England and PJM, interested in revealing its rival producers' offering decisions, via inverse optimization. The market clearing procedure conducted by the Independent System Operator (ISO) is expressed by a primal linear optimization problem formulation, aiming at social welfare maximization and its equivalent dual formulation. The solution of these problems provides the main market outcomes, such as power produced by block for each generator and local marginal prices for each electric network bus. Consequently, considering the results arisen from the above procedure, the inverse problem is developed and solved by the strategic producer, in order to identify rival stepwise offer prices setting the market clearing price. The mathematical framework considers a 24-period electricity pool for a 30-days duration and is applied to a 24-bus test system. The results indicate that network congestion stimulates offer price revealing process on account of strategic generator.

Kardakos et al. (2014) introduced a bi-level mathematical model to derive optimal offering strategies for a strategic producer, owning multiple generating units, under a day-ahead transmission-constrained electricity market setup. The upper-level represents producer's detailed unit commitment problem aiming at maximizing its expected profit, whereas the lower-level illustrates ISO's hourly market clearing mechanism, under the Nodal and the Power Transfer Distribution Factor (PTDF) formulation. The particular methodology is implemented on a modified IEEE 118-bus power test system, to examine its applicability and efficiency, in a realistic pool-based market environment. The authors (Kardakos et al., 2016) extended their research on optimal bidding in electricity markets, considering a price-maker virtual power plant (VPP), which consists of wind farms, battery storage systems and residential/commercial electricity consumers. More specifically, a stochastic bi-level mathematical model is formed, the upper-level of which, aims at maximizing VPP's expected profits, while the lower-level represents ISO's day-ahead market clearing procedure. Uncertainty is introduced into the problem, via unpredictable market measures, such as RESs' generation, demands' consumption, rivals' offering curves and real-time prices. A series of case studies applied to the Greek power system are examined. Numerical results demonstrate that the coordinated operation of VPP elements leads to a significant profit increase by 4.7%, compared to the uncoordinated operation scenario, and that when VPP acts as a price-maker agent, acquires higher profits in comparison to the price-taker or non-strategic case.

Several European electricity markets nowadays, such as Germany and Italy, have adopted a pay-as-bid pricing scheme in the balancing stage. While these markets' trading problem is typically addressed though non-linear optimization approaches, Mazzi et al. (2018) proposed a leading-edge linear formulation to bypass possible computational challenges, instigated by these nonlinearities. More specifically, authors considered a two-stage stochastic MILP model to derive optimal offering strategies for a price-taker conventional generator, under a simultaneous clearing of a two-settlement electricity market i.e., the day-ahead stage, characterized by a uniform pricing scheme, and the balancing stage, based on a pay-as-bid pricing scheme. Results underline the efficiency of the linear formulation, as it fairly approximates the non-linear one, and demonstrate that the simultaneous market clearing, provides a better performance in view of generator's profitability, compared to the sequential market clearing case. However, the application

of the model to a multi-bus electric network could provide better insights about its efficiency in large-scale problems.

Lastly, Porras-Ortiz et al. (2020) introduced an inspired bi-level mathematical approach, for a strategic zonal operator in a regional electricity market (REM) setup. In the upper-level optimization problem, strategic operator seeks to maximize zonal social welfare (SW), by managing zonal generators' strategic day-ahead energy and reserve offers, whereas the objective function of the lower-level problem aims at maximizing regional social welfare and generating market equilibrium prices and dispatches. Results emphasized that strategic behavior on behalf of zonal operator can negatively affect regional social welfare and induce crucial alterations in congestion rents.

1.4.1.1 Integration of renewable energy sources

Climate change and security of energy supply constitute two increasingly critical challenges affecting markets, regulations, policies and investments at a global level (Olabi & Abdelkareem, 2022). Renewable energy (RE) plays a significant role in the transition towards a low-carbon economy and contributes to the mitigation of greenhouse gas emissions, disengagement from fossil fuels, industrial development, generation portfolio diversification and poverty reduction (Gielen et al., 2019). Global trends indicate a substantial increase in renewable energy, comprising 40% of the worldwide installed power capacity, as reported by the International Renewable Energy Agency (IRENA, 2021). Projections suggest that by 2050, renewable sources are expected to constitute approximately two-thirds of the overall energy supply (Larsson, 2009). Thus, the analysis of the participation and operation of renewables assets in modern energy and derivatives markets constitutes a fundamental field of research.

De la Nieta et al. (2013) proposed a mathematical framework to derive the optimal bidding strategy of a power producer with a mixed wind-hydro generation portfolio in the Iberian pool-based day-ahead market. The authors investigated the synergies arising from the combined operation of these two technologies. Results show that a single joint offer with physical connection between the two units ensures the highest profit for the producer. Sheikhahmadi and Bahramara (2020) considered a bi-level optimization approach to study the strategic participation of a distributed energy resource aggregator (DERA) with RE assets in the real time (RT) energy market. The risk level of the

aggregator due to the uncertain nature of RE is managed by employing Conditional Value at Risk (CVaR) and the outcomes confirm that the presence of the DERA leads to an increase in social welfare of the RT market. Sun et al. (2022) formulated a bi-level model to determine the optimal bidding strategies of a prosumer aggregator with renewable energy production (photovoltaic, PV) in day-ahead energy and reserve markets. The upper-level problem maximizes the prosumer's profits, while the lower-level problem describes the market clearing procedure.

Afshar et al. (2018) developed a bi-level mathematical framework to derive the strategic bidding of the wind power producers exercising market power in the day-ahead market and matching its actual and predicted production in the balancing market. Since the producers' compensation mechanism is pay-as-bid (PAB), the authors employ particle sward optimization (PSO) to solve the problem at both levels. Hosseini et al. (2020) introduced a bi-objective two-stage change-constrained model to examine the optimal bidding strategy of a wind power producer (WPP) participating in a day-ahead joint electricity and reserve market. Results show that compared to alternative models, the proposed methodology ensures the availability of the offered bid and enhances WPP's revenues. Zhang et al. (2023) proposed a bi-level market model based on a Nash-Stackelberg game to determine the strategic participation of a WPP and large-scale electric vehicles (EV) in day-ahead energy and frequency regulation market. Numerical simulations illustrate that the suggested method can achieve accurate and more consistent solution, compared to price taker or collaborative bidding modes, with reasonable computational requirements.

Laia et al. (2016) presented a stochastic mixed-integer linear program (MILP) to examine the bidding strategies of a price-taker joint wind and thermal power producer in a pool-based electricity market setup. A series of different scenarios is considered to model the uncertainty on wind generation and electricity price. Li et al. (2023) developed a MILP model to determine the offering strategy of a RE and energy storage aggregator in mid-to-long-term and spot electricity markets. To deal with the uncertainty of RE output the authors solve the problem by employing distributionally robust optimization (DRO). Fang and Zhao (2020) developed a MILP look-ahead technique to derive the optimal bidding for a joint system of concentrating solar power (CSP) plant with wind farms in the day-ahead and ancillary services markets. Numerical simulations show that

the joint bidding approach enhances the coordination of the system and improves its profitability.

Gomes et al. (2023) formulated a MILP framework to optimize the operation and maximize revenue for an integrated system comprising a wind farm, a solar PV and an electrical battery participating in the Italian and Iberian day-ahead electricity markets. Results verify the superiority of the proposed methodology in terms of revenue, compared to the non-optimized bidding strategy case. Khaloie et al. (2020) examined the optimal bidding problem of a strategic wind producer in the spot electricity market through a bi-level stochastic optimization model. Wind power generation and demand uncertainties are represented by multiple plausible scenarios. Tsimopoulos and Georgiadis (2020), (2019a) developed a bi-level complementarity model to derive optimal withholding strategies for a producer with mixed conventional and wind power generation portfolio participating in energy and reserve markets. Khaloie et al. (2020) formulated a stochastic multi-objective MILP to derive the determine the optimal offering strategy for a wind-thermal-energy storage generation company (GenCo) in the energy and reserve markets. The proposed algorithm simultaneously maximizes company's profits and minimizes carbon emissions, while the uncertainty that originates from wind power generation is modeled through a set of plausible scenarios.

Morales et al. (2010) were among the firsts to propose a mathematical framework that delves into wind power generator's actions. They formulated a multi-stage stochastic LP problem to generate optimal offering strategies and maximize expected profits for a wind power generator, in a joint day-ahead, adjustment and balancing market settlement. Uncertainty induced by wind availability and hourly market clearing prices at different trading stages, is modelled through the realization of weighted plausible scenarios, the higher quality of which leads to more reliable and representative results. Consequently, the authors (Morales et al., 2012) developed a fundamental two-stage stochastic electricity pool-based market clearing approach, including a substantial number of WPPs. The first stage represents the day-ahead market clearing procedure, while the second stage presents the balancing system operation, under a set of plausible wind generation realizations. Co-optimization of both electricity and reserves, endogenously provides pool (day-ahead) and real-time energy prices, as dual variables of the equivalent energy equilibriums. The proposed algorithm is studied in a 24-bus transmission-constrained

single-area IEEE Reliability Test System (RTS) (Grigg & Wong, 1999) and ensures producers' cost recovery and revenue reconciliation in expectation.

Baringo and Conejo (2011) on the other hand, introduced a stochastic mathematical programming with equilibrium constraints (MPEC) model, to identify the profit margin for a wind power investor willing to implement a wind investment and participating in an electricity pool. The upper-level problem accounts for the optimal investment and operation decisions of the wind investor, considering different plausible load and wind generation scenarios. Concerning the lower-level problem, due to the fact that demand loads are considered to be inelastic, the social welfare maximization and cost minimization problems can be equivalently formulated by the system operator. The proposed algorithm is applied to a 118-bus case study to illustrate the applicability of the model to real-world energy systems. The solution strategy of this problem considers linearization of the MPEC formulation to an MILP through the aforementioned mathematical techniques. The results showed that overestimating the number of plausible scenarios needed, does not negatively affect the resulting investment decisions, while their underestimation leads to a suboptimal investment evaluation.

Baringo et al. (2013) proceed with their research formulating an inspired stochastic bi-level mathematical model, to derive optimal offering strategies for a wind power generator, exercising its market power by participating as price-maker in the day-ahead stage, while acting as a deviator in the real-time stage. A set of weighted scenarios is employed, to imprint the uncertainty, induced by wind production and real-time market price. The upper-level problem, seek to maximize the wind producer's expected profit, whereas the lower-level objective function represents the day-ahead market clearing process, in terms of maximizing social welfare. Case studies performed, indicate a sound escalation of wind producer's expected profits and market prices, when adopting strategic behavior, compared to the non-strategic state, and a parallel decrease of social welfare. The considerable size of test systems (up to 118-buses), combined with their negligible temporal computational requirements, highlight the applicability of the proposed model in real-world power networks.

Zugno et al. (2013) investigated the optimal offering strategies of a wind power generator by acting as a price-taker in the day-ahead market and as a price-maker in balancing market. The uncertainty inserted in the system concerns the day-ahead market price, wind generation and residual system deviation and is modelled though the

weighted probabilistic realization of different scenarios. At the upper-level problem, wind power generator seeks to maximize its profit from its involvement in both markets, while the lower-level problem pertains to the balancing market clearing for each plausible scenario. The case study simulated, considered the Scandinavian electricity market framework and an one price balancing market settlement, with one of the critical findings of this work reporting that the optimal offer for the wind producer in day-ahead market, increases analogously to its market penetration. Pandžić et al. (2013) considered a virtual power plant (VPP) with a mixed generation portfolio (conventional (CPP), wind (WPP) and pumped hydro storage (PHS) power plants), purchasing and selling electricity, in a joint day-ahead and real-time market setup. A two-stage stochastic MILP framework is designed, in order to maximize VPP's expected profits, which acts as a price-taker in the day-ahead market and as a passive agent in the balancing market. Uncertainty-related parameters, such as non-dispatchable power output and market prices, are modelled through a set of plausible scenarios realization, based on historical data. Numerical analysis illustrates that the majority of energy is traded in the day-ahead floor, while the balancing market revenue constitutes less than 2% of the overall earnings.

Delikaraoglou et al. (2015) introduced a bi-level mathematical configuration based on Stackelberg hypothesis' game, where wind power generator acts as a leader (price-maker) in both day-ahead and balancing market, while system operator, as a follower. The stochastic nature of the power production of non-dispatchable agents, is inserted into the problem via 50 different plausible wind generation scenarios using a Beta distribution. At the upper-level problem strategic wind power producer seeks to maximize its expected profit from its participation in both electricity markets, while the lower-level objective presents the simultaneous day-ahead and balancing market clearing procedure conducted by ISO. A case study concerning an IEEE Reliability Test System showed, that the strategic wind producer improves its expected profits by regulating its day-ahead quantity offers and avoiding severe up regulation costs.

Dai and Qiao (2015) proposed a bi-level stochastic mathematical model to derive the optimal offering strategy for a wind power generator acting strategically in a pool-based electricity market. The upper-level problem maximizes the total profit of the strategic producer, while at the lower-level one a sequential clearing procedure of the day-ahead and balancing market takes place. The risk induced by the uncertainty in

demand power consumption, wind power production and offering strategies of power producers is managed by including the conditional value at risk of the worst-case scenarios in the objective function. The above methodology is applied to the IEEE Reliability Test System and features significant results such as: the day-ahead and balancing LMPs decrease as the market share of wind power generation amplifies, the network congestion can be exploited by the wind power producer to further arbitrage and increase its expected profits. Reddy et al. (2015) recommended a novel electricity and spinning reserves market clearing mechanism for a power system, comprised of conventional and wind generators, under wind power generation uncertainty. More specifically, authors calculated a real-time adjustment cost, deploying data from day-ahead schedule and plausible balancing operating scenarios, and incorporated it in the day-ahead problem, to address the uncertainties emerged. The mathematical approach consists of two discrete models, with the first one accounting for spinning reserve deployment exclusively by thermal generators, whereas the second one, also allowing the participation of demand-side offers in reserve market setup. The proposed technique is tested on an IEEE 30-bus system, while the results validation is realized through Monte Carlo Simulation method.

Exizidis et al. (2016) proposed a stochastic bi-level mathematical model to analyze the impact of rival wind generators, on the optimal bidding strategy of a WPP, exercising market power in a deregulated electricity market settlement. At the upper-level, the WPP's profit maximization problem is represented, while in the lower-level a joint day-ahead and balancing market clearing takes place. Power generation of both strategic and non-strategic WPPs is considered problem's uncertainty source and is modelled through a set of foreseen balancing scenarios. The algorithm is applied to an IEEE one-area RTS, while numerical analysis reveals that strategic WPP further exerts market power, when having a mid- or low-mean forecast distribution and that its bidding strategies firmly depends on rival's wind power production. Soares et al. (2017) developed an optimization framework to derive optimal bidding strategies for a wind power producer, participating in an electricity and primary reserve market setup. Authors considered two different reserve offering strategies i.e., proportional and constant, the discretization of which lies on the allocation of wind power generation in energy and reserve markets. Despite their divergent characteristics, quantitative analysis shown that both approaches ensure critical profit increase for the wind plant owner, especially in comparison to an

energy-only bid case and are firmly affected by market prices and penalties from being insufficient to meet market requirements. Finally, a central conclusion of this work states that, even though the provision of market services by a wind power plant is technically feasible, it is not a common tactic in current market environments.

Tsimopoulos and Georgiadis (2019b) presented a bi-level optimization model to derive optimal hourly offering strategies for a conventional power producer possessing a dominant position in pool-based electricity market, under high penetration of non-dispatchable generation. The upper-level problem demonstrates the expected profit maximization of the strategic dispatchable producer, whereas at the lower-level materializes the simultaneous clearing of day-ahead and balancing markets. The case study pertains to a network constrained 2-bus system, while network congestions outcomes are also investigated, as capacity decrement of the transmission line constitutes a possible contingency. Additionally, a thorough comparison is carried out regarding the market price scheme and the electricity dispatch, when the conventional generator under study, acts strategically versus as a price-taker. Tsimopoulos and Georgiadis (2019a) extended their work to incorporate the stepwise offering strategy for the dispatched energy production and consumption blocks, introduced by Ruiz and Conejo (2009). This offering structure requires, accepted energy blocks to be offered at their marginal cost, whereas marginal blocks at the equivalent market price, to avoid multiple solutions and degeneracy. The mathematical programming with equilibrium constraints model is recast into a MILP to investigate optimal offering decisions of a conventional producer, under wind generation uncertainty and is applied to a 6-bus network constrained system and consequently to the IEEE RTS. Results reinforced findings from previous contributions on this topic and shown that expected profits of strategic agent decrease, while wind generation market's share increases.

Tsimopoulos and Georgiadis (2020) examined the optimal withholding strategies for an agent with a mixed conventional and wind production portfolio, participating in a pool-based energy and reserve market. The upper-level of the proposed mathematical framework guarantees profit maximization for the market agent under study, whereas at the lower level the simultaneous day-ahead and balancing market clearing process is modelled, through a two-stage stochastic programming. Aftermath established the generic perception that the strategic agent can financially benefit by network congestion, by charging the production blend and exploiting transmission line capacities. Finally,

Rintamäki et al. (2020) recently proposed a bi-level optimization model to study the optimal offering decisions of a flexible generator in day-ahead and intraday markets. The upper-level problem's objective concerns the profit maximization of the generator, while the lower-level one represents the sequential market clearing procedure of the markets. At first the authors, considered a three-node transmission constrained network and demonstrated that the flexible generator can increase its expected profits by regulating its offers in order to cause transmission congestion or shortage on price-takers generators' capacity. Furthermore, authors applied their optimization model in a Nordic 5-node test network and confirmed that flexible benefit at a greater extent when acting strategically under imperfect forecasts, compared to a perfect competition setup.

1.4.1.2 Integration of energy storage technologies

Given the strong penetration and the growing market share of renewable energy sources, as well as their stochastic nature regarding electricity generation, the role of electricity storage in mitigating potential market imbalances becomes particularly important. For this reason, a plethora of research publications have emerged in recent years, to evaluate the strategic and non-strategic market behavior of various storage technologies.

1.4.1.2.1 Pumped-Hydroelectric Storage

According to the U.S. Department of Energy (DOE), pumped-hydro storage (PHS) is eminently the most popular form, accounting for 95% of the total utility-scale energy storage in the United States (Uria-Martinez et al., 2021). Despite the fact that PHS facilities are large-scale plants that provide long-duration energy storage (LDES), their operation requires unique topographic characteristics that do not allow their ubiquitous utilization. Lu et al. (2004) developed a mathematical framework to derive the optimal offering strategies for a PHS unit and maximize its profit under a competitive electricity market scheme. The optimization performed entails the precise knowledge of the weekly market clearing price curve and is compared to a fixed-schedule bidding strategy, based on the profit each one ensures for the storage agent.

Kazempour et al. (2008) formulated a mixed-integer non-linear program (MINLP) to investigate the shelf-scheduling problem of an individual PHS agent, participating in the day-ahead (DA) energy and regulation markets. The proposed algorithm guarantees

to attain the maximum expected profits, while the agent is considered a price-taker, with no capability of acting strategically and influencing market clearing prices (MCPs). Kanakasabapathy et al. (2010) proposed a multistage-looping algorithm to determine optimal bidding strategies for a PHS plant and maximize its expected profits in a coupled day-ahead electricity and ancillary services market. Aburub et al. (2019) developed an optimization framework to model the operation of adjustable-speed PHS systems in the day-ahead U.S electricity market, considering both networks constraints in a 240-bus system and the effects of the ramping rate. Akbari-Dibavar et al. (2020) presented a bilevel mathematical framework, where the upper-level provides optimal offering strategies and maximizes profit for PHS systems, while the lower-level illustrates the pay-as-bid electricity market clearing, under wind power generation uncertainty.

1.4.1.2.2 Compressed Air Energy Storage

Compressed air energy storage (CAES) is an additional LDES technology that seems to lead to significant economic potential. Depending on its' operational characteristics it is further divided into diabatic (D-CAES) and the more recently developed advanced adiabatic (AA-CAES) systems (Cavallo, 2007). Liquid air energy storage (LAES), is also a developed concept over the CAES systems (Babaei et al., 2021). Budt et al. (2016) presented a comprehensive review on the fundamental concepts and principles of these storage systems, and also provided a thorough classification and evaluation of different CAES types.

Drury et al. (2011) introduced a mixed integer linear program (MILP) to simulate the optimal energy dispatch of diabatic and adiabatic CAES units, under a day-ahead energy and reserves market setup. Results show that the provision of operating reserves is considered essential for the CAES investment to become economically viable. Madlener and Latz (2013) introduced a mathematical model to investigate the economic feasibility of three different CAES concepts for improved wind power integration. In particular, the authors analyzed the economics of a wind power plant with centralized or integrated CAES in diabatic or adiabatic operation and the corresponding results without any storage system. Simulations demonstrated that the centralized and diabatic CAES case proves to be the most economically viable one.

Rahimi et al. (2022) introduced an MILP approach to study the scheduling of a virtual power plant (VPP) containing a compressed air energy storage wind turbine (CA-WT), in the day-ahead and real-time (RT) market. Results demonstrated that the integration of the CA-WT significantly increases VPP's profitability in both trading floors, while also effectively handles stochastic generation uncertainty. Arabkoohsar et al. (2020) proposed a thermodynamic model and conducted a comprehensive analysis of a low-temperature AA-CAES, to determine at which demanded or surplus power levels, it is economically viable for the system to (dis)charge electricity in real-life energy markets. Khatami et al. (2020) presented a novel look-ahead approach for the optimal participation of a CAES unit in the day-ahead and real-time energy and ancillary services market. Chen et al. (2020) performed a thorough energy, economic and environmental analysis of an integrated biomass-driven combined heat and power plant with a CAES system. Lastly, Bafrani et al. (2021) developed a two-stage stochastic MINLP model to determine the optimal operation of CAESs in a unit-commitment based joint energy and reserve market. Numerical analysis indicated that the consideration of restrictions on reserve deliverability resulted in lower total reserves and higher operation cost.

1.4.1.2.3 Battery Energy storage

Battery storage systems (BSSs) also constitute a popular and viable energy storage technology that has received a great deal of research interest, mainly due to a wide range of advantages they offer compared to other energy storage technologies. Especially with the rapid evolution and utilization of electric vehicles (EV) (Baherifard et al., 2022), (Ahmad et al., 2022) by numerous manufacturers in recent years, special emphasis has been placed on the technological development of various battery types with distinct characteristics. However, the effort to increase storage duration as well as their maximum capacity is considered crucial, in order to play a dominant role in contemporary energy markets. Lithium-ion (Li-ion) batteries constitute the most established type of battery storage and represent nearly 90% of the total installed capacity, while sodium sulphur and lead acid batteries are secondary alternatives for the provision of grid applications (IRENA, 2019b).

Akhavan-Hejazi et al. (2015) proposed an optimization framework for the optimal offering and operation strategy of a battery storage agent, willing to maximize its expected revenues in the day-ahead and real-time market. The authors deploy the

Markowitz portfolio selection theory to efficiently control financial risk and a real-time receding horizon algorithm, to update profit and financial value-at-risk (VAR) predictions. He et al. (2016) examined the optimal bidding and operating strategies for a large-scale battery storage system seeking to increase its profitability. The authors also incorporated a novel mathematical approach to account for battery life drop, due to frequent charging and discharging cycling operation. Mohsenian-Rad (2016) formulated a nonlinear mathematical model to optimally coordinate the operation of independently-operated price-maker battery storage systems which are seeking to maximize their revenues, under a nodal transmission-constrained electricity market scheme.

Khojasteh et al. (2022) provided a security-constrained linear mathematical model for the optimal scheduling of BSSs in a joint energy and reserve market, based on the limitations of primary and secondary frequency services. Results show that the increased battery capacity reduces total frequency reserves and total system's cost. Lastly, Arteaga and Zareipour (2019) developed a mixed-integer nonlinear algorithm to model the participation of a shelf standing Li-ion battery storage facility, participating as a price-taker in the energy and ancillary services markets.

1.4.2 Natural gas market

The coupled operation of electricity and natural gas markets is considered to provide significant benefits as it allows better coordination and information exchange between the two systems and also reduces the overall cost. In recent years, there seems to be a particular shift towards this operation, with more and more organizations worldwide choosing to adopt it.

Duenas et al. (2015) were some of the first to study the market coupling and develop a mixed integer programming problem to simulate the optimal long- and medium- term operation of a power generation company (Genco), owning a group of gas-fired power plants (GFPPs), under a coordinated competitive electricity and gas market settlement. The model also accounts for the simultaneous optimization of natural gas purchases in a zonal gas spot market and minimization of long-term natural gas pipeline capacity contracting costs under renewable energy sources' (RES) power generation uncertainty.

As interactions between electricity and natural gas markets are increasing, a plethora of companies appear to act simultaneously as major players in both markets, by

operating a decision-making department for each market. Gil et al. (2016) developed two mathematical approaches to simulate each's departments optimization actions. The "electricity-perspective" approach accounts for the maximization of the electricity market profit, after generating equivalent natural gas contracts via the implementation of the gas market algorithm. On the other hand, "gas-perspective" method aims at minimizing natural gas operation costs, in the aftermath of acquiring the correlation between marginal revenue and gas consumption by the electricity market equilibrium problem. Results display, that both methodologies produce identical optimal solutions and are characterized by sufficient adaptability.

Ordoudis et al. (2017) proposed an insightful price-based stochastic bi-level approach, considering a coupled electricity and natural gas market, where gas consumption and price offered by NGFPPs, constitute the coordination parameters between the two market setups. The upper-level problem minimizes total operation cost of the integrated energy system, by optimally determining the gas price adjustment variable. In turn, lower-level problems account for the sequential clearing of the electricity and natural gas coupled market. The recommended optimization mechanism ensures that ISO will form a financial day-ahead equilibrium, whereas may encounter an implicit real-time shortage or surplus. Numerical analysis reveals a substantial market efficiency increase, due to a significant reduction in the overall system cost, through an enhanced unit dispatch, that successfully addresses stochastic generation. The authors extended their research approach to examine the coordination of electricity and natural gas markets, in view of their mutual interactions and time intersection of day-ahead/real-time trading floors (Ordoudis et al., 2019). More specifically, three mixed-integer linear programming (MILP) approaches are presented accounting for the linepack of the natural gas network i.e., a coupled and a decoupled deterministic sequential and a coupled stochastic market clearing procedure. A modified IEEE RTS and a 12-node natural gas network are employed to compose the integrated power system, while wind power generation uncertainty is modelled, via the realization of 25 equally probable scenarios. Results demonstrated that although all three models adequately capture gas system operation, coupled stochastic scheme, ensures the lowest expected costs and incorporates uncertainty induced by significant amounts of wind energy in a preferable manner, compared to the remaining two methodologies.

Ordoudis et al. (2020) depending on their previously developed PB method, established a novel volume-based coordination approach, to reduce the expected cost of an integrated electricity and natural gas system, by optimally defining gas availability for power generation by GFPPs, under high shares of renewable energy. The presented bi-level mathematical formulation seeks to improve day-ahead and real-time stage coordination, while conforming to the sequential market clearing settlement, which constitutes the current market design. A realistic analysis is conducted to evaluate the proposed model's performance and compare it with the price-based method; thus, an identical integrated power and gas system setup is employed. Results revealed that, an efficient adjustment of natural gas quantities or price, can critically enhance the performance of the sequential market clearing model, in terms of minimizing system cost, so as to resemble the ideal condition of stochastic modelling.

Chen et al. (2018) recommended a non-deterministic scenario-based mathematical model for the day-ahead market clearing, under a coordinated electricity and natural gas market setup. This approach achieves a direct link between the flexible resources and the system uncertainties arisen by RESs' (wind and solar) unpredictable power production, thus enhancing economic efficiency. Case studies indicate a more suitable allocation of available resources, such as gas transmission capacity, as joint market curtails (with the analogous compensation) low-priority gas demand loads, in order to meet electricity demand and ensure the power system's stability. Solution time ranges at reasonable levels, considering the substantial size and complexity of the proposed algorithm. However, the general assumptions and compromises made to reduce computational requirements render the proposed model inadequate to be implemented in current market designs.

Zhao et al. (2019) developed two independent optimization frameworks for the day-ahead market clearing of power and natural gas systems. The coordination between these two systems is implemented via an iterative heuristic algorithm, which is based on Lagrangian Relaxation, which allows the exchange of fundamental information such as fuel price, supply and demand and aims at maximizing social welfare. The purpose of such a coordination lies on ensuring that, natural gas supplied to power system to meet electricity demands, does not result in gas loads' curtailment. Results for a case study concerning a 24-bus IEEE RTS and a 25-node gas system, revealed that gas curtailments may lead to unserved energy in the electricity system, which can cause a great social

welfare reduction and in parallel electricity prices increase. Yan et al. (2019) considered an Integrated Energy System (IES) with multi-type energy units and storage systems, integrated in a coupled simultaneous day-ahead electricity and natural gas market, including carbon emission market. Gaussian Copula method is adopted to form the joint probability distribution of market prices and develop an optimal low-carbon offering strategy. A sensitivity analysis of emission prices is conducted, to assess the impact of the carbon emission trading mechanism in the IES operation, considering a Henry Hub natural gas and ERCOT electricity market settlement. Simulation results illustrated that the proposed approach can efficiently address possible price fluctuation uncertainties and that carbon emission trading, could stimulate wind penetration level in the IES.

Nasiri et al. (2020) introduced a stochastic bi-level optimization approach to analyze the impact of ESSs on a regional-local coupled electricity and natural gas market clearing. More specifically, the upper-level problem presents energy hub operator's optimal scheduling, with the aim of minimizing purchasing costs of electricity and natural gas, whereas the objective function of the lower-level one, aims at clearing the coordinated electricity and natural gas market, considering wind power generation and the integration of linepack flexibility. The proposed algorithm is simulated on an IEEE 6-bus power system and a 6-node natural gas network and three case studies to analyze MES's operation at local-regional level, are formulated. Numerical analysis demonstrated that the adaptation of the multi-carrier ESS can entail a significant drop of 7.01% and 1.7%, on the daily operational cost of local and regional level, equivalently.

Finally, Baziar et al. (2021) proposed a two-stage algorithm to derive optimal offering strategies for electricity and gas generators, under a coupled power and gas, day-ahead energy and reserve market settlement. At the first stage, a bi-level formulation is presented, pertaining to the minimization of strategic electricity producers' expected cost-revenue difference and the electricity market clearing problem, whereas at the second stage, the equivalent bi-level model for strategic gas producers and natural gas market, is implemented. Demand and RESs' power uncertainty is modelled by stochastic programming, through a set of probability weighted scenarios. Two case studies with different networks topologies were considered, with the second one consisting of an IEEE 24-bus power network and a 7-node gas network. Numerical analysis emphasizes the computational efficiency of the proposed model and reports that, assets with low operation costs, tend to participate in the day-ahead energy market, while strategic

electricity and gas producers achieve a profit of 37.5% and 13.6%, correspondingly, in their operational cost. However, the case of network congestion, which could offer a more in-depth analysis, has not been studied.

1.4.3 Carbon emission trading

Global warming caused by greenhouse gas (GHG) emissions, constitutes one of the predominant international concerns during the last decades and the establishment of a low-carbon economy is crucial (R. Zhang et al., 2020). Power industry is one of the major emission sources, mainly due to the large amounts of CO_2 generated by fossil fuel-fired power plants (Reddy et al., 2013). Emission trading system (ETS) is considered a particularly promising market-based instrument that creates incentives to mitigate GHG emissions and save significant natural gas reserves (Labay et al., 2019), by exposing emitters to the external emission costs in the most versatile and least costly way (Wei et al., 2022).

Chen et al. (2006) formulated a mathematical program with equilibrium constraints (MPEC) based on Stackelberg hypothesis, to investigate the strategic participation of a price-maker power producer and its ability to manipulate Pennsylvania-New Jersey-Maryland (PJM) electricity and emission market. The analysis indicated that the leader could gain significant economic profits by withholding emission permits and thus increasing NO_x permit costs for rival producers. Tanaka and Chen (2012) developed a general mathematical model, in which Cournot firms are able to manipulate permit and electricity prices in the California energy market, through fringe firms in order to maximize their profits. Simulation results illustrated that the firms substantially raise power and CO_2 permit prices, resulting in a significant loss in social welfare.

Akbari-Dibavar et al. (2021) introduced a multi-objective mixed-integer non-linear program (MINLP) to model the economic-emission dispatch problem including wind farms and carbon capture power plants. The model is implemented in a modified IEEE 24-bus reliability test system (RTS), while stochastic programming is deployed to model wind generation and demand uncertainty. Zhang et al. (2023) considered a Stackelberg-based game to study the participation and derive the optimal bidding of renewable energy power producers in an integrated day-ahead electricity and CET market. Feng et al. (2020) developed a multi-objective bi-level model to derive the optimal carbon price

and achieve revenue maximization and minimization of carbon intensity in the electricity supply sector. Corchero et al. (2012) proposed a novel stochastic mathematical model to derive the optimal unit commitment and bidding strategy of a Genco for the day-ahead Iberian electricity market, considering SO_2, CO_2 and NO_x emissions.

Lu et al. (2022) formulated a bi-level model for a multi-leader multi-follower game based on Stackelberg hypothesis, to analyze the impact of carbon emission trading (CET) market on the bidding strategy of the leader Gencos, participating in the day-ahead and real-time electricity market. The authors employed a real 2778-bus system to show the applicability of the model. Zhang et al. (2021) presented a novel bi-level algorithm to determine optimal bidding approach for a power-to-gas (P2G) facility in the PJM electricity market, considering carbon emission trading. The upper-level objective function aims at maximizing P2G facility's expected profit, while the lower-level model represents market clearing through a low-carbon ED under wind power uncertainty.

1.4.4 Green certificates market

Tradable green certificates, also known as renewable energy certificates/credits (REC) (Nguyen & Felder, 2020), is a market-based policy instrument established to provide incentives for further investments in the renewable energy sector and mitigate greenhouse gas (GHG) emissions in a global level (Narula, 2013). In particular, green certificates mechanism has been designed to deal with the mismatch between the potential renewable electricity generation and the renewable purchase obligations of the load-serving entities (Gupta & Purohit, 2013). A plethora of articles have been published to investigate and assess the performance of green certificates market in either a group of nations, such as the European countries (Hulshof et al., 2019) and BRICS (Z. Chen et al., 2023), or in individual states such as USA (Joshi, 2021).

Irfan (2021) conducted an empirical analysis employing an econometric approach to examine the relationship between electricity and REC markets in India, using monthly data. The strong correlation between traded volume/wholesale price of electricity and traded volume of solar and non-solar RECs are some of the main findings of this research. Helgesen et al. (2018) investigated the economic impact of integrating green certificates trading to enhance the renewable assets' generation. In particular, the authors developed a mixed complementarity partial equilibrium model to simulate the joint clearing of

electricity and green certificates market under Nash-Cournot competition. Results showed that the integration of tradable green certificates can affect to a different extent each marker participant, with existing participants, however, bearing most of the losses.

Hustveit et al. (2017) extended the work of Coulon et al. (2015) and developed a dynamic programming-based stochastic model to analyze the operation of the Swedish-Norwegian electricity and green certificates market. Numerical simulations highlighted that electricity generation/consumption and over-investment can increase certificates' price volatility and significantly affect market stability, respectively. Pineda et al. (2016) proposed a class of generation expansion model regarding a joint electricity and green certificates market, to examine to what extent renewable-based generation investment is affected by quota obligations and non-compliance penalty. Safarzadeh et al. (2022) proposed a novel leader-follower mathematical framework to maximize energy market performance integrating tradable white certificates and green certificates, as effective financial instruments. In this game, the government plays the role of the leader, while the energy suppliers act as followers in a duopolistic competition scheme.

An et al. (2019) proposed an equilibrium problem with equilibrium constraints (EPEC) to investigate the power generation firms' strategic behavior in an imperfect wholesale electricity tradable green certificates market. Results showed that renewable power producers can exercise market power both by withholding green certificates and by cutting back their electricity dispatch depending on the renewable portfolio standards (RPS) value. Hui et al. (2021) examined the financialization of green certificates and investigated market participants' optimal strategies in green certificates market both in a theoretical and a methodological level. Results indicated that the strategic behavior of the market participants can critically affect the stability of green certificates price and convergence rate to the equilibrium price. Guo et al. (2020) developed a nonlinear bi-level model to study the strategic behavior of renewable energy sources in day-ahead and real-time joint electricity and green certificates market. The authors transformed their problem into a single-level linear model and applied it into a modified IEEE 30-bus system.

1.5 Mathematical framework for perfect and imperfect competition

Modelling electricity markets has received considerable attention over the past few years. A plethora of mathematical approaches has been proposed to address several problems in energy markets, such as the market-clearing process and games of single or multiple leaders.

1.5.1 Perfect competition – LP

Perfect competition in energy markets refers to a theoretical scenario where numerous small firms produce an identical product with easy market entry. No single firm can influence prices, and buyers and sellers have perfect information. This model rarely applies to real-world energy markets, where various factors lead to imperfect competition. This type of competition in electricity markets is usually formulated as single-level two-stage stochastic programming, with the first stage involving day-ahead optimal energy dispatch and generating LMPs as dual variables. Equivalently, the second stage derives real-time market dispatch and prices, while the various sources of uncertainty are handled through the realization of multiple plausible scenarios. The objective function of the energy market clearing problem aims at the maximization of social welfare, as depicted in *Figure 1.4*. The addition of binary variables that capture specific market operations or agents' decisions, such as (dis)charging function for energy storage systems (ESSs), transforms the existing problem into a mixed-integer program (MIP).

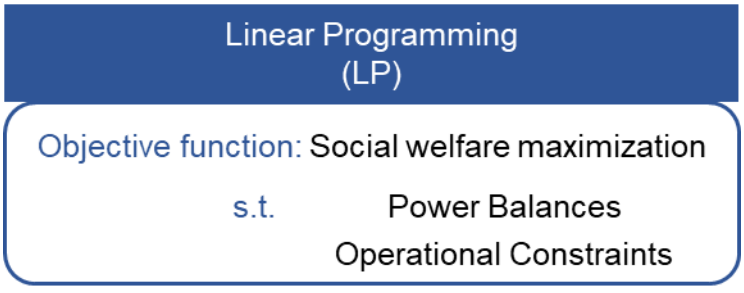

Figure 1.4: Market clearing formulation.

1.5.2 Imperfect competition - MPEC

Imperfect competition in energy markets refers to a situation where market conditions fall between the extremes of perfect competition and monopoly. Factors such as differentiated products, barriers to entry, and limited supplier options create an environment where an individual strategic market participant has some degree of market power, influencing prices and outcomes. This type of competition, following the Stackelberg hypothesis, is described as a single-leader single-follower game, in which the strategic participant, referred to as the leader, makes the initial decision regarding its output, while the ISO (Independent System Operator), acting as the follower, subsequently makes its optimal choice (*Figure 1.5*). A strategic participant is mainly considered a producer holding a dominant position in the market due to their ownership of a substantial number of generation units. In the case of a two-stage market structure, where both day-ahead and balancing market are investigated, two distinct clearing mechanisms can be employed, that is, simultaneous and sequential. While electricity markets are currently organized sequentially, both approaches have drawn significant attention in the recent literature.

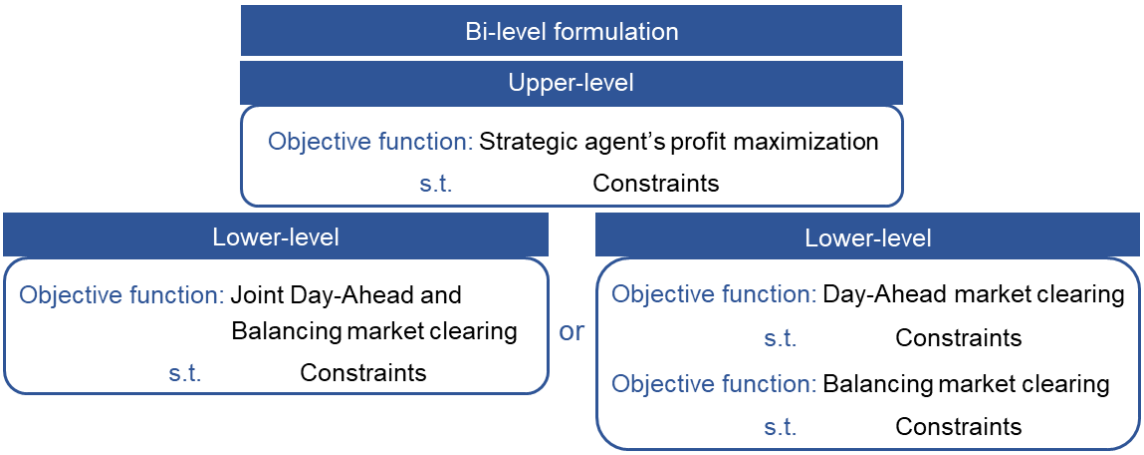

Figure 1.5: Bi-level formulation for strategic participation.

A Stackelberg game can be mathematically captured through bi-level modelling. In this context, the upper-level problem (1.1) – (1.3) allows the strategic agent to optimally determine its profit-maximizing offering/bidding strategy, while the lower-level problem (1.4) – (1.6) represents ISO's market-clearing procedure and yields pool prices as dual variables, as illustrated in *Figure 1.5.*

The two optimization problems have distinctive objective functions and constraints, denoted by the superscripts U and L, respectively. Consequently, there also exist two sets of decision variables, namely x^U and x^L. Given that the lower-level problem imposes constraints on the upper-level problem, the primary variable vector x^L, along with the dual variable vectors λ and μ, from the former, is also included in the variable vector set of the latter. Therefore, the primary variable set for the upper-level problem (1.1) - (1.3) is denoted as $\Xi^U = \{ x^U, x^L; \lambda, \mu\}$.

Upper-level problem

$$\underset{\Xi^U}{minimize} \quad f^U(x^U, x^L, \lambda, \mu) \tag{1.1}$$

$$s.t. \quad h^U(x^U, x^L, \lambda, \mu) = 0 \tag{1.2}$$

$$g^U(x^U, x^L, \lambda, \mu) \leq 0 \tag{1.3}$$

Lower-level problem

$$\underset{x^L}{minimize} \quad f^L(x^U, x^L) \tag{1.4}$$

$$s.t. \quad h^L(x^U, x^L) = 0 \quad : \lambda \tag{1.5}$$

$$g^L(x^U, x^L) \leq 0 \quad : \mu \tag{1.6}$$

To efficiently generate solutions though, bi-level model is recast into a mathematical program with equilibrium constraints (MPEC). MPECs are complementarity hierarchical problems, that are extensively used in modelling a broad range of market-based scopes. Investment and sizing models for market agents, as well as the demand-side strategic bidding, are well-established examples of the MPECs' applicability. The MPEC models' structure consists of the upper-level's objective function and the Karush–Kuhn–Tucker (KKT) optimality conditions of the lower level, as depicted in *Figure 1.6*.

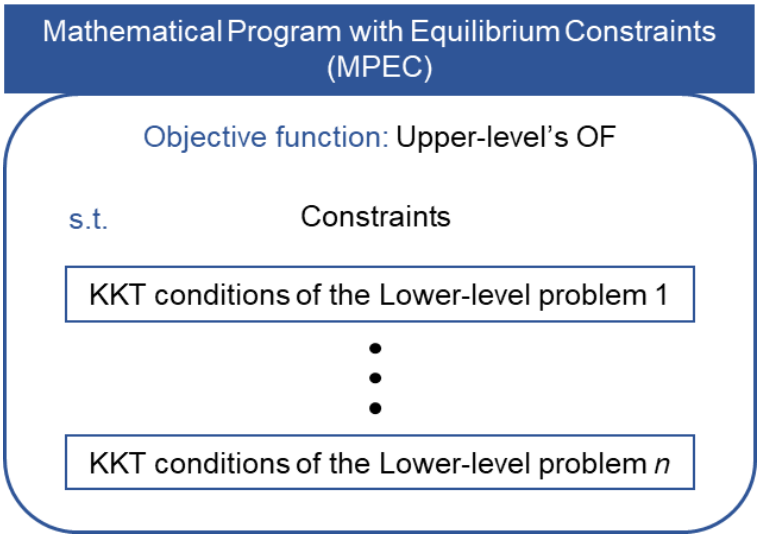

Figure 1.6: MPEC formulation

Karush–Kuhn–Tucker conditions are characterized as first-order conditions, as they are formulated through first derivative vectors and Jacobian matrices, and their implementation constitutes an essential requirement for the solution of various non-linear bi-level optimization problems. The substitution of the lower-level problem (1.4) – (1.6) occurs through the introduction of a series of equality constraints (1.11), which are obtained from the partial derivatives of the corresponding Lagrangian function (1.10) concerning each primary variable. Additionally, a set of complementarity conditions (1.12) is incorporated, articulating the orthogonal relationship between the lower-level problem's inequality constraints and the corresponding dual variables. Finally, the condition (1.13) ensured that the dual variable related to the equality (1.5) is free.

$$minimize \quad f^U(x^U, x^L, \lambda, \mu) \tag{1.7}$$

$$s.t. \quad h^U(x^U, x^L, \lambda, \mu) = 0 \tag{1.8}$$

$$g^U(x^U, x^L, \lambda, \mu) \leq 0 \tag{1.9}$$

$$\nabla_{x^L} f^U(x^U, x^L) + \lambda^T \nabla_{x^L} h^L(x^U, x^L) + \mu^T \nabla_{x^L} h^L(x^U, x^L) = 0 \tag{1.10}$$

$$h^L(x^U, x^L) = 0 \tag{1.11}$$

$$0 \leq -g^L(x^U, x^L) \perp \mu \geq 0 \tag{1.12}$$

$$\lambda: free \tag{1.13}$$

Given that the lower-level problem (1.4) - (1.6) is regarded as linear, it can be reformulated in a linear form. The dual variable vectors are then denoted by a colon alongside the corresponding constraints.

Primal lower-level problem

$$minimize \quad c(x^U)^T x^L \tag{1.14}$$

$$s.t. \quad A(x^U)x^L = b(x^U) \quad : \lambda \tag{1.15}$$

$$B(x^U)x^L \leq d(x^U) \quad : \mu \tag{1.16}$$

$$x^L \geq 0 \quad : \zeta \tag{1.17}$$

The cost vector is denoted as $c(x^U)$, while $A(x^U)$ and $B(x^U)$ represent the constraint matrices. The right-hand-side vectors are $b(x^U)$ and $d(x^U)$. Additionally, the dual variable vectors λ and μ correspond to the constraints (1.15) and (1.16), similar to those in the bi-level model's constraints (1.5) and (1.6). Finally, the dual variable vector ζ is associated with the non-negativity of the lower-level prime variable vector x^L. The Lagrangian dual problem for the primal problem (1.14) - (1.17) is as follows:

Dual lower-level problem

$$maximize \quad b(x^U)^T\lambda + d(x^U)^T\mu \tag{1.18}$$

$$s.t. \quad A(x^U)^T\lambda + B(x^U)^T\mu + \zeta = c(x^U) \tag{1.19}$$

$$\mu \geq 0, \zeta \geq 0 \tag{1.20}$$

$$\lambda: free \tag{1.21}$$

The following are the optimality conditions linked to the lower-level problem (1.14) - (1.17), originating from the primal-dual formulation:

$$A(x^U)x^L = b(x^U) \tag{1.22}$$

$$B(x^U)x^L \leq d(x^U) \tag{1.23}$$

$$A(x^U)^T\lambda + B(x^U)^T\mu + \zeta = c(x^U) \tag{1.24}$$

$$c(x^u)^T x^L = b(x^U)^T\lambda + d(x^U)^T\mu \tag{1.25}$$

$$x^L \geq 0, \mu \geq 0, \zeta \geq 0 \tag{1.26}$$

$$\lambda: free \tag{1.27}$$

The primal problem (1.14) - (1.17) incorporates constraints $A(x^U)x^L = b(x^U)$, $B(x^U)x^L \leq d(xU)$, and $xL \geq 0$. In the dual problem (1.18) - (1.21), constraint $A(x^U)^T \lambda + B(x^U)^T \mu + \zeta = c(x^U)$ is included, where λ is unrestricted, $\mu \geq 0$, and $\zeta \geq 0$. The strong duality constraint $c(x^U)^T x^L = b(x^U)^T \lambda + d(x^U)^T \mu$ ensures equality between the primal optimal objective function (1.14) and the dual optimal objective function (1.18). The resulting MPEC model, formulated with a primal-dual approach equivalent to the bi-level model (1.1) - (1.6), is as follows:

$$minimize \quad f^U(x^U, x^L, \lambda, \mu) \tag{1.28}$$

$$s.t. \quad h^U(x^U, x^L, \lambda, \mu) = 0 \tag{1.29}$$

$$g^U(x^U, x^L, \lambda, \mu) \leq 0 \tag{1.30}$$

$$A(x^U)x^L = b(x^U) \tag{1.31}$$

$$B(x^U)x^L \leq d(x^U) \tag{1.32}$$

$$A(x^U)^T\lambda + B(x^U)^T\mu + \zeta = c(x^U) \tag{1.33}$$

$$c(x^U)^T x^L = b(x^U)^T\lambda + d(x^U)^T\mu \tag{1.34}$$

$$x^L \geq 0 \tag{1.35}$$

$$\mu \geq 0 \tag{1.36}$$

$$\zeta \geq 0 \tag{1.37}$$

1.6 Thesis overview

This thesis is organized as follows:

Chapter 2 addresses the strategic bidding problem of an energy storage agent in joint electricity and reserve markets. A bi-level modelling approach is presented, where the upper-level problem ensures the strategic agent's profit maximization, while the two lower-levels mimic the clearing of the day-ahead and balancing market. The model is formulated as a MPEC problem and is further recast into a MILP using a series of mathematical transformations. Numerical simulations provide the optimal dispatch and bidding strategies for the strategic agent under the assumption of a congested and an uncongested power network.

Chapter 3 presents an optimization-based economic analysis of various electricity storage technologies participating as standalone entities in a fully coupled electricity and natural gas market. More specifically, a MILP model is formulated to represent the simultaneous clearing procedure of the day-ahead and balancing market. The power generation uncertainty introduced by the nature of the wind energy is modelled through a set of plausible wind power generation scenarios. The analysis reveals the profitability and optimal power dispatch of each storage technology in the market under power network congestion and natural gas price increase scenarios.

Chapter 4 studies the optimal participation of a strategic GFPP in a low-carbon integrated pool-based electricity and natural gas market. In particular, the upper-level of the proposed bi-level formulation ensures profit maximization of the strategic producer, while the lower-level mimics the sequential clearing of the two markets incorporating a cap-and-trade program for carbon emissions. The model is applied in a modified PJM 5-bus system and derives the optimal bidding and management of carbon emission allowances for the strategic player under plausible power transmission congestions and natural gas prices increment scenarios.

Chapter 5 investigates the optimal trading strategies of a renewable aggregator in electricity and green certificates markets. A novel bi-level model is developed to address this problem. The upper-level problem focuses on maximizing the strategic player's profits, while the two lower-level problems represent the sequential clearing mechanism of the two markets conducted by the same Market Operator and aim at minimizing overall operating market cost. The proposed model is initially applied to a PJM 5-bus and then to a modified IEEE 24-bus system to showcase its effectiveness in a real-life case.

Chapter 6 provides a synopsis of the research outcomes of this thesis and proposes possible future research directions.

Chapter 2

Strategic bidding of an energy storage agent in electricity and reserve markets

In this Chapter, a bi-level model is proposed, based on a single-leader single-follower Stackelberg game, to derive the optimal bidding strategies for an energy storage agent participating in electricity and reserve markets. The upper-level problem maximizes the expected profits of the strategic storage agent, while the two lower-level problems mimic the day-ahead and balancing market clearing procedure conducted by the MO (follower). The bi-level problem is recast into an MPEC, which is further reformulated into a MILP, using the KKT first-order conditions, strong duality theory and binary expansion. The model provides the clearing prices, the optimal bids and electricity dispatch for the strategic agent under network congestion and different wind power generation scenarios.

2.1 Introduction

The ever-increasing necessity for assertive penetration of non-dispatchable energy sources, such as wind, due to their beneficial financial and environmental impact, has contributed to the critical deployment of the role, Energy Storage Systems (ESS) own in electricity markets' contemporary scheme. An increased contribution of renewable energy sources' (RES) share into the electricity grid's mixture, can provide a decisive prospect for suppressing wholesale energy prices, through outplacing high-cost generators from the merit-order. Furthermore, this RES contribution can lead to downscaling dependence on dispatchable generation (fossil fuels) and confining greenhouse gas emissions (Green & Vasilakos, 2010). Their erratic and fluctuating nature

regarding their generation levels though, can originate concerns about the reliability of the power grid comprised in great measure of these sources (Denholm et al., 2011).

The significant progress that has been achieved in energy storage technologies and their applications can address the aforementioned issues, leading to a rapid decarbonization, while providing ancillary services such as reserves, to guarantee the stability of supply and demand equilibrium in power systems (International Renewable Energy Agency (IRENA), 2017). Apart from the implicitly advantageous contribution to the electrical grid, nowadays a large-scale privately owned ESS can enable significant economic opportunities for an investor who seeks to maximize his expected profit, participating in a liberalized energy market environment (Shafiee et al., 2016). In particular, storage systems can act strategically and capitalize their (dis)charging decisions by arbitraging; procuring and storing electricity when off-peak electricity prices occur and trade it back in the market when electricity prices rise (R. Sioshansi et al., 2009). A case study conducted by McConnell et al. (2015) demonstrated that the above ESS's operation can stimulate a significant competitive advantage over other involved generators in Australian National Electricity Market, an especially well designed and regulated energy-only market, that is characterized by high wind power generation insertion (Sioshansi, 2008).

Inspired by the market clearing optimization algorithm presented in (Nasrolahpour et al., 2018), this Chapter proposes an MPEC approach, to derive optimal offering strategies for a strategic ESS operator, participating in a sequential joint energy and reserve day-ahead and real-time market clearing settlement. While a common assumption suggests that ESS agents act as price-takers, large-scale investor-owned storage systems can offer/bid strategically in electricity markets, especially as wind power generation uncertainty increases (Mohsenian-Rad, 2016). Electricity market of California constitutes a great example of such a market environment, as California Public Utilities Commission has called the three large independently-operated utility companies to install a capacity of 1325 MW of energy storage by 2020 (California Public Utility Commission). Therefore, examining and analyzing the optimal strategic behavior of large-scale investor-owned energy storage systems appears to attract significant interest in recent years. Other types of renewable energy sources could also be considered in the mathematical framework, but this will inevitably lead to computationally intractable

problems. It is important to emphasize that ESS agent is considered as profit-making agent and its detailed operational scheduling is beyond the scope of this work.

In the above context, the main objectives and contributions of this Chapter are as follows:

i. A novel bi-level complementarity model to analyze the inter-relationships between the ESS's optimal bidding and offering strategies, participating in a jointly cleared energy and reserve day-ahead pool, as well as in real-time pool, under network transmission constraints.
ii. Transformation of the bi-level model into an MPEC and further reduce it to the equivalent MILP model, by deploying KKT optimality conditions, strong duality theorem and a binary expansion method.
iii. A systematic methodology, in order to generate day-ahead, upward/downward reserve and real-time market prices, as dual variables of the corresponding energy balance constraints.
iv. Introduce a comprehensive market operations structure and a thorough mathematical framework for the integration of ESS in a transmission constrained multi-bus network, under wind power generation uncertainty.
v. Analyse the market outcomes of transmission lines congestions and variable levels of wind power generation insertion and the measure of their influence on ESS agent's (dis)charging decision strategies.

2.2 Problem statement

The proposed bi-level programming problem is formulated on the basis of a single leader-follower Stackelberg hypothesis' game (Vega-Redondo, 2003) and considers the optimal offering/bidding strategies and (dis)charging decisions for a price-maker ESS operator, while competing conventional and wind generation agents, which act as price-takers in energy and reserve pools. The adopted market setup is aligned with the Pennsylvania-New Jersey-Maryland (PJM) market's structure, where wind power generation uncertainty is addressed through the real-time realization of ancillary services' operations.

The upper level of the proposed mathematical framework contains strategic generator's expected profit maximization problem and relies on the marginal prices, intrinsically provided by the lower-level problem's implementation. The lower-level problem on the other hand, represents the market clearing mechanism conducted by the ISO (*Figure 2.1*). It also determines the optimal generators' energy dispatch and reserve procurement, for the purpose of maximizing social welfare, by virtue of a two-stage stochastic program (Morales et al., 2014). The first stage pertains to the optimization of a jointly encountered energy and upward/downward reserve day-ahead pool, deriving the optimal amounts of scheduled generation and reserve procurement, as well as their reciprocal clearing prices. At the second stage, the ISO's real-time market clearing procedure is presented, determining the deployment levels of the reserves -formerly procured in the day-ahead clearance phase- and generating the RT market prices (Stoft, 2003). Wind power generation uncertainty is modelled through the establishment of conceivable wind generation scenarios (Conejo et al., 2010). Considering the lower problem satisfies continuity and convexity prerequisites, the proposed bi-level problem can be reformulated to an MPEC, on the strength of the KKT optimality conditions' application. Consequently, applying Fortuny-Amat and McCarl linearization approach (Fortuny-Amat & McCarl, 1981), strong duality theorem and a binary expansion method (Pereira et al., 2005), the mathematical model is further reduced into an equivalent MILP, which entails reasonable computational requirements by commercial solvers such as GAMS/CPLEX (Brook et al., 1988).

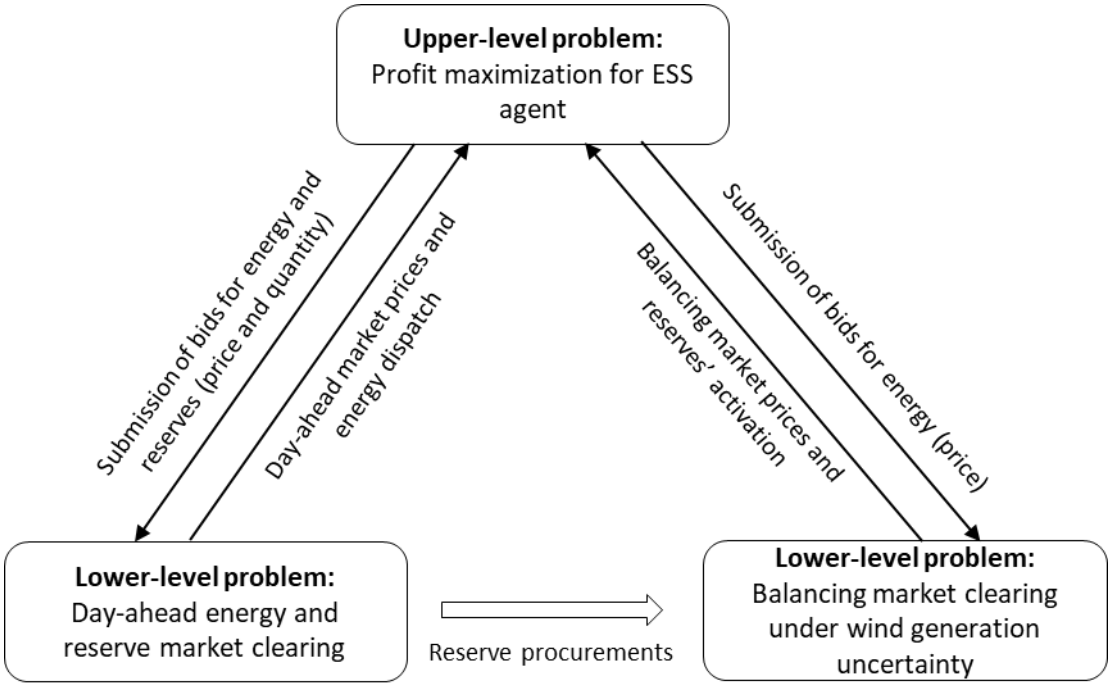

Figure 2.1: Mathematical structure and function of the bi-level model

2.3 Mathematical Formulation

2.3.1 Bi-level model structure

The following bi-level mathematical model is formulated to determine optimal offering and (dis)charging strategies for an ESS agent, in a joint energy and reserve market settlement, in order to counteract occasional system imbalances, imposed by wind power generation deviations and plausible network congestions.

2.3.2 Upper-level problem: ESS's expected profit maximization

The upper-level problem maximizes the expected profit for the ESS operator, stemming from its involvement in all different types of markets, and is described below by constraints (2.1) - (2.18):

$$\textbf{Maximize} \quad \sum_t \sum_s \Bigg[-\left(\lambda_{n,t}^{DA} + c_s^{ch}\right) \cdot G_{s,t}^{DA,ch} + \left(\lambda_{n,t}^{DA} - c_s^{dis}\right) \cdot G_{s,t}^{DA,dis} + \left[\lambda_t^{\uparrow} \cdot \left(rp_{s,t}^{ch,\uparrow} + rp_{s,t}^{dis,\uparrow}\right) + \lambda_t^{\downarrow} \cdot \left(rp_{s,t}^{ch,\downarrow} + rp_{s,t}^{dis,\downarrow}\right)\right] + \sum_{\omega} \pi_{\omega} \cdot \left[\left(\lambda_{n,t,\omega}^{RT} + c_s^{ch}\right) \cdot \left(ra_{s,t,\omega}^{ch,\uparrow} - ra_{s,t,\omega}^{ch,\downarrow}\right) + \left(\lambda_{n,t,\omega}^{RT} - c_s^{dis}\right) \cdot \left(ra_{s,t,\omega}^{dis,\uparrow} - ra_{s,t,\omega}^{dis,\downarrow}\right)\right] \Bigg] \tag{2.1}$$

s.t.

$$x_{s,t}^{ch}, x_{s,t}^{dis} \in \{0,1\} \quad \forall s, \forall t \tag{2.2}$$

$$x_{s,t}^{ch} + x_{s,t}^{dis} \leq 1 \quad \forall s, \forall t \tag{2.3}$$

$$0 \leq \bar{G}_{s,t}^{dis} \leq x_{s,t}^{dis} \cdot G_s^{dis,max} \quad \forall s, \forall t \tag{2.4}$$

$$0 \leq \bar{rc}_{s,t}^{dis,\uparrow} \leq x_{s,t}^{dis} \cdot RC_s^{dis,\uparrow,max} \quad \forall s, \forall t \tag{2.5}$$

$$0 \leq \bar{rc}_{s,t}^{dis,\downarrow} \leq x_{s,t}^{dis} \cdot RC_s^{dis,\downarrow,max} \quad \forall s, \forall t \tag{2.6}$$

$$\bar{G}_{s,t}^{dis} + \bar{rc}_{s,t}^{dis,\uparrow} \leq x_{s,t}^{dis} \cdot G_s^{dis,max} \quad \forall s, \forall t \tag{2.7}$$

$$\bar{rc}_{s,t}^{dis,\downarrow} - \bar{G}_{s,t}^{dis} \leq 0 \quad \forall s, \forall t \tag{2.8}$$

$$0 \leq \bar{G}_{s,t}^{ch} \leq x_{s,t}^{ch} \cdot G_s^{ch,max} \quad \forall s, \forall t \tag{2.9}$$

$$0 \leq \bar{rc}_{s,t}^{ch,\uparrow} \leq x_{s,t}^{ch} \cdot RC_s^{ch,\uparrow,max} \quad \forall s, \forall t \tag{2.10}$$

$$0 \leq \bar{rc}_{s,t}^{ch,\downarrow} \leq x_{s,t}^{ch} \cdot RC_s^{ch,\downarrow,max} \quad \forall s, \forall t \tag{2.11}$$

$$\bar{G}_{s,t}^{ch} + \bar{rc}_{s,t}^{ch,\downarrow} \leq x_{s,t}^{ch} \cdot G_s^{ch,max} \quad \forall s, \forall t \tag{2.12}$$

$$\bar{rc}_{s,t}^{ch,\uparrow} - \bar{G}_{s,t}^{ch} \leq 0 \quad \forall s, \forall t \tag{2.13}$$

$$O_{s,t}^{ch},\ O_{s,t}^{ch,\uparrow},\ O_{s,t}^{ch,\downarrow} \geq 0 \quad \forall s, \forall t \tag{2.14}$$

$$O_{s,t}^{dis},\ O_{s,t}^{dis,\uparrow},\ O_{s,t}^{dis,\downarrow} \geq 0 \quad \forall s, \forall t \tag{2.15}$$

$$0 \leq soc \leq SOC_s^{max} \quad \forall s, \forall t \tag{2.16}$$

$$soc_{s,t} = SOC_s^{ini} \quad \forall s, t = N_t \tag{2.17}$$

$$soc_{s,t} = SOC_s^{ini} + \sum_k \eta^{ch} \cdot \left[G_{s,t}^{DA,ch} + \sum_{\omega} \pi_{\omega} \cdot \left(-ra_{s,t,\omega}^{ch,\uparrow} + ra_{s,t,\omega}^{ch,\downarrow}\right)\right] - \sum_k \frac{1}{\eta^{dis}} \cdot \left[G_{s,t}^{DA,dis} + \sum_{\omega} \pi_{\omega} \cdot \left(ra_{s,t,\omega}^{dis,\uparrow} - ra_{s,t,\omega}^{dis,\downarrow}\right)\right] \quad \forall s, \forall t \tag{2.18}$$

Objective function (2.1) includes all ESS operator's revenue and cost terms, generated from its participation in the day-ahead, reserve and balancing pool. More specifically, the first line corresponds to the day-ahead market profit, derived from the energy discharged income, $\lambda_{n,t}^{DA} \cdot G_{s,t}^{DA,dis}$, operational charging/discharging costs, $c_s^{ch} \cdot G_{s,t}^{DA,ch} / c_s^{dis} \cdot G_{s,t}^{DA,dis}$, as well as the cost for purchasing energy during charging periods, $\lambda_{n,t}^{DA} \cdot G_{s,t}^{DA,ch}$. The second line, refers to the ESS's income, originating from the upward and downward reserve procurement, in the course of day-ahead market clearing. The remaining lines, correlate with the ESS's profit in the balancing market. The upward charging reserve activation, $ra_{s,t,\omega}^{ch,\uparrow}$ constitutes an income factor for the storage system agent, as it is compensated from the market at real-time price, $\lambda_{n,t,\omega}^{RT}$, for its charging power curtailment and is exempt from the corresponding operational charging cost, c_s^{ch}. Regarding downward charging reserve activation, the storage system disburses funds to purchase the additional charging power, $\lambda_{n,t,\omega}^{RT} \cdot ra_{s,t,\omega}^{ch,\downarrow}$, and to cover the necessary operational costs, $c_s^{ch} \cdot ra_{s,t,\omega}^{ch,\downarrow}$. In the upward discharging reserve activation mode, the energy storage agent provides power to the market, acquiring earnings based on the real-time price, $\lambda_{n,t,\omega}^{RT} \cdot ra_{s,t,\omega}^{dis,\uparrow}$ and bearing the cost of discharging function, $c_s^{dis} \cdot ra_{s,t,\omega}^{dis,\uparrow}$. Conclusively, in the downward discharging reserve activation mode, ESS agent compensates market for the energy not dispatched $\lambda_{n,t,\omega}^{RT} \cdot ra_{s,t,\omega}^{dis,\downarrow}$, while freed from discharging operational expenses, $c_s^{dis} \cdot ra_{s,t,\omega}^{dis,\downarrow}$.

Constraints (2.2) and (2.3) declare the binary nature and ensure the mutually exclusive function of the charging/discharging decision variables. Constraints (2.4)-(2.6) and (2.9)-(2.11) limit the energy and reserve capacity offers/bids of the ESS, in discharging and charging mode correspondingly. Constraints (2.7), (2.8) and (2.12), (2.13) ensure that the summation of energy and reserve quantity offers/bids, cannot exceed the discharging/charging maximum capacity of the storage system. Furthermore, constraints (2.14), (2.15) guarantee the non-negative interpretation of energy and reserve bidding/offering prices, whereas constraints (2.16) and (2.17) enforce that the state of charge at the end of the planning horizon harmonizes with the initial one. Constraints (2.18) represent the ESS's hourly state of charge fluctuations, depending on the ESS's optimal operational decisions, with η^{ch}, η^{dis} denoting charging and discharging efficiencies, respectively. The analyzed upper-level problem is constrained by the two-

stage lower-level problem (2.19)-(2.44) and (2.45)-(2.59), described in the following sections.

2.3.3 Lower-level problem: Joint energy and reserve day-ahead market clearing

The lower-level problem thoroughly investigates a two-stage sequentially cleared day-ahead and real-time market structure, providing the optimal energy dispatch and reserve procurement, as well as deriving marginal prices, as dual variables of the energy and reserve equilibriums analogously. It is critical to mention that ESS agent's offering/bidding decisions $O_{s,t}^{ch}$, $O_{s,t}^{ch,\uparrow}$, $O_{s,t}^{ch,\downarrow}$, $O_{s,t}^{dis}$, $O_{s,t}^{dis,\uparrow}$, $O_{s,t}^{dis,\downarrow}$ are treated as variables in the profit maximization upper-level problem, while in the lower-level problem are encountered by ISO as parameters. Hence, the mathematical framework presented in *Section 2.3.2* and *2.3.3* is classified as linear and convex (Steven A. Gabriel et al., 2013).

$$\begin{aligned}\textbf{\textit{Maximize}} \quad & \sum_{s}\left(O_{s,t}^{ch}\cdot G_{s,t}^{DA,ch}-O_{s,t}^{dis}\cdot G_{s,t}^{DA,dis}\right)+\sum_{d}u_{d,t}\cdot L_{d,t}^{DA}\\ & -\sum_{i}c_{i,t}\cdot P_{i,t}^{DA}-\sum_{j}c_{j,t}^{w}\cdot W_{j,t}^{DA}\\ & -\sum_{s}\left(O_{s,t}^{ch,\uparrow}\cdot rp_{s,t}^{ch,\uparrow}+O_{s,t}^{ch,\downarrow}\cdot rp_{s,t}^{ch,\downarrow}+O_{s,t}^{dis,\uparrow}\cdot rp_{s,t}^{dis,\uparrow}+O_{s,t}^{dis,\downarrow}\right.\\ & \left.\cdot rp_{s,t}^{dis,\downarrow}\right)-\sum_{i}c_{i,t}^{res}\cdot\left(rpc_{i,t}^{\uparrow}+rpc_{i,t}^{\downarrow}\right)\\ & -\sum_{d}u_{d,t}^{res}\cdot\left(rpd_{d,t}^{\uparrow}+rpd_{d,t}^{\downarrow}\right)\qquad\forall t\end{aligned}\tag{2.19}$$

s.t.

$$\begin{aligned}&\sum_{d\in DaN}L_{d,t}^{DA}-\sum_{s\in SaN}\left(G_{s,t}^{DA,dis}-G_{s,t}^{DA,ch}\right)-\sum_{i\in IaN}P_{i,t}^{DA}-\sum_{j\in JaN}W_{j,t}^{DA}\\ &\qquad+\sum_{m\in NaM}B_{n,m}\cdot\left(\delta_{n,t}^{\circ}-\delta_{m,t}^{\circ}\right)=0\quad:\left[\lambda_{n,t}^{DA}\right]\quad\forall n,\forall t\end{aligned}\tag{2.20}$$

$$\sum_{s}\left(rp_{s,t}^{ch,\uparrow}+rp_{s,t}^{dis,\uparrow}\right)+\sum_{i}rpc_{i,t}^{\uparrow}+\sum_{d}rpd_{d,t}^{\uparrow}=R_{t}^{\uparrow}\quad:\left[\lambda_{t}^{\uparrow}\right]\quad\forall t\tag{2.21}$$

$$\sum_{s}\left(rp_{s,t}^{ch,\downarrow}+rp_{s,t}^{dis,\downarrow}\right)+\sum_{i}rpc_{i,t}^{\downarrow}+\sum_{d}rpd_{d,t}^{\downarrow}=R_{t}^{\downarrow}\quad:\left[\lambda_{t}^{\downarrow}\right]\quad\forall t \tag{2.22}$$

$$0\leq P_{i,t}^{DA}\leq P_{i}^{max}\quad:\left[a_{i,t}^{min},a_{i,t}^{max}\right]\quad\forall i,\forall t \tag{2.23}$$

$$0\leq L_{d,t}^{DA}\leq L_{d,t}^{max}\quad:\left[\beta_{d,t}^{min},\beta_{d,t}^{max}\right]\quad\forall d,\forall t \tag{2.24}$$

$$0\leq G_{s,t}^{DA,ch}\leq\bar{G}_{s,t}^{ch}\quad:\left[\gamma_{s,t}^{ch,min},\gamma_{s,t}^{ch,max}\right]\quad\forall s,\forall t \tag{2.25}$$

$$0\leq G_{s,t}^{DA,dis}\leq\bar{G}_{s,t}^{dis}\quad:\left[\gamma_{s,t}^{dis,min},\gamma_{s,t}^{dis,max}\right]\quad\forall s,\forall t \tag{2.26}$$

$$0\leq rp_{s,t}^{ch,\uparrow}\leq\bar{rc}_{s,t}^{ch,\uparrow}\quad:\left[\gamma_{s,t}^{ch,\uparrow,min},\gamma_{s,t}^{ch,\uparrow,max}\right]\quad\forall s,\forall t \tag{2.27}$$

$$0\leq rp_{s,t}^{ch,\downarrow}\leq\bar{rc}_{s,t}^{ch,\downarrow}\quad:\left[\gamma_{s,t}^{ch,\downarrow,min},\gamma_{s,t}^{ch,\downarrow,max}\right]\quad\forall s,\forall t \tag{2.28}$$

$$0\leq rp_{s,t}^{dis,\uparrow}\leq\bar{rc}_{s,t}^{dis,\uparrow}\quad:\left[\gamma_{s,t}^{dis,\uparrow,min},\gamma_{s,t}^{dis,\uparrow,max}\right]\quad\forall s,\forall t \tag{2.29}$$

$$0\leq rp_{s,t}^{dis,\downarrow}\leq\bar{rc}_{s,t}^{dis,\downarrow}\quad:\left[\gamma_{s,t}^{dis,\downarrow,min},\gamma_{s,t}^{dis,\downarrow,max}\right]\quad\forall s,\forall t \tag{2.30}$$

$$rp_{s,t}^{ch,\uparrow}\leq G_{s,t}^{DA,ch}\quad:\left[\gamma_{s,t}^{ch,\uparrow}\right]\quad\forall s,\forall t \tag{2.31}$$

$$rp_{s,t}^{dis,\downarrow}\leq G_{s,t}^{DA,dis}\quad:\left[\gamma_{s,t}^{dis,\downarrow}\right]\quad\forall s,\forall t \tag{2.32}$$

$$0\leq rpc_{i,t}^{\uparrow}\leq RCc_{i}^{\uparrow,max}\quad:\left[a_{i,t}^{\uparrow,min},a_{i,t}^{\uparrow,max}\right]\quad\forall i,\forall t \tag{2.33}$$

$$0\leq rpc_{i,t}^{\downarrow}\leq RCc_{i}^{\downarrow,max}\quad:\left[a_{i,t}^{\downarrow,min},a_{i,t}^{\downarrow,max}\right]\quad\forall i,\forall t \tag{2.34}$$

$$P_{i,t}^{DA}+rpc_{i,t}^{\uparrow}\leq P_{i}^{max}\quad:\left[a_{i,t}^{\uparrow}\right]\quad\forall i,\forall t \tag{2.35}$$

$$rpc_{i,t}^{\downarrow}-P_{i,t}^{DA}\leq 0\quad:\left[a_{i,t}^{\downarrow}\right]\quad\forall i,\forall t \tag{2.36}$$

$$0\leq rpd_{d,t}^{\uparrow}\leq RCd_{d,t}^{\uparrow,max}\quad:\left[\beta_{d,t}^{\uparrow,min},\beta_{d,t}^{\uparrow,max}\right]\quad\forall d,\forall t \tag{2.37}$$

$$0\leq rpd_{d,t}^{\downarrow}\leq RCd_{d,t}^{\downarrow,max}\quad:[\beta_{d,t}^{\downarrow,min},\beta_{d,t}^{\downarrow,max}]\quad\forall d,\forall t \tag{2.38}$$

$$L_{d,t}^{DA}+rpd_{d,t}^{\downarrow}\leq L_{d,t}^{max}\quad:\left[\beta_{i,t}^{\downarrow}\right]\quad\forall d,\forall t \tag{2.39}$$

$$rpd_{d,t}^{\uparrow}-L_{d,t}^{DA}\leq 0\quad:\left[\beta_{i,t}^{\uparrow}\right]\quad\forall d,\forall t \tag{2.40}$$

$$0\leq W_{j,t}^{DA}\leq W_{j,t}^{max}\quad:\left[\varepsilon_{j,t}^{min},\varepsilon_{j,t}^{max}\right]\quad\forall j,\forall t \tag{2.41}$$

$$-T_{n,m}^{max}\leq B_{n,m}\cdot\left(\delta_{n,t}^{\circ}-\delta_{m,t}^{\circ}\right)\leq T_{n,m}^{max}\quad:\left[\zeta_{n,m,t}^{min},\zeta_{n,m,t}^{max}\right]\quad\forall n,\forall m\in NaM,\forall t \tag{2.42}$$

$$-\pi\leq\delta_{n,t}^{\circ}\leq\pi\quad:\left[\tilde{\zeta}_{n,t}^{min},\tilde{\zeta}_{n,t}^{max}\right]\quad\forall n,\forall t \tag{2.43}$$

$$\delta_{n_1,t}^{\circ}=0\quad:\left[\zeta_{n,t}^{\circ}\right]\quad\forall n=n_1,\forall t \tag{2.44}$$

Objective function (2.19) constitutes the basis for the first stage optimization and represents the joint day-ahead and reserve market clearing, maximizing total social welfare. Alternative definitions for the objective function can be considered the economic dispatch or total social cost minimization, given the inelasticity of electricity demand. It is

worth mentioning that conventional generators, energy storage systems and demands are capable of procuring both upward and downward reserves, in order to contribute to market's function stability, in contrast to wind power generation systems, whose erratic nature excludes equivalent potential. Constraints (2.20), (2.21) and (2.22) ensure energy and upward/downward reserve procurement equilibriums, deriving day-ahead market's energy and reserve prices, as their corresponding dual variables. Constraints (2.23) and (2.24) limit conventional generators' production and demands' consumption level, respectively. Constraints (2.25) and (2.26) restrict ESS's charging/discharging energy levels, while (2.27)-(2.32) restrain upward/downward (dis)charging reserve provision. Equally, constraints (2.33)-(2.36) and (2.37)-(2.40) limit conventional generators' and demand's reserve procurements, respectively. Constraints (2.41) on the other hand, circumscribe the wind power dispatch levels in the day-ahead market. Finally, constraints (2.42) enforce capacity limits for network transmission lines, while constraints (2.43), (2.44) limit each bus's voltage angle range and define $n1$ as power grid's slack bus, at the day-ahead market.

2.3.4 Lower-level problem: Real-time market clearing under wind power generation uncertainty

The second stage of the lower-level problem represents real-time market clearing under stochastic wind power generation. The participation of non-dispatchable generators, such as wind, into the power grid can evoke imbalances into the final supply-demand equilibrium, due to their volatile electricity provision. Thus, the existence of the balancing market accounting for these supply deviations can contribute establishing an auxiliary stability tier.

$$\begin{aligned}\textbf{\textit{Minimize}}\quad & \sum_{d} VOLL_{d,t}\cdot L^{sh}_{d,t,\omega} + \sum_{j} c^{w}_{j,t}\cdot\left(W^{RT}_{j,t,\omega} - W^{DA}_{j,t} - W^{SP}_{j,t,\omega}\right)\\ & + \sum_{i} c_{i,t}\cdot\left(rac^{\uparrow}_{i,t,\omega} - rac^{\downarrow}_{i,t,\omega}\right) + \sum_{s} O^{dis}_{s,t}\cdot\left(ra^{dis,\uparrow}_{s,t,\omega} - ra^{dis,\downarrow}_{s,t,\omega}\right)\\ & + \sum_{s} O^{ch}_{s,t}\cdot\left(ra^{ch,\uparrow}_{s,t,\omega} - ra^{ch,\downarrow}_{s,t,\omega}\right)\\ & + \sum_{d} u_{d,t}\cdot\left(rad^{\uparrow}_{d,t,\omega} - rad^{\downarrow}_{d,t,\omega}\right) \qquad \forall t,\omega\end{aligned} \tag{2.45}$$

s.t.

$$\begin{aligned}&\sum_{d\in DaN} L^{sh}_{d,t,\omega} + \sum_{s\in SaN}\left(ra^{ch,\uparrow}_{s,t,\omega} - ra^{ch,\downarrow}_{s,t,\omega}\right) + \sum_{s\in SaN}\left(ra^{dis,\uparrow}_{s,t,\omega} - ra^{dis,\downarrow}_{s,t,\omega}\right)\\ &\quad + \sum_{i\in IaN}\left(rac^{\uparrow}_{i,t,\omega} - rac^{\downarrow}_{i,t,\omega}\right) + \sum_{d\in DaN}\left(rad^{\uparrow}_{d,t,\omega} - rad^{\downarrow}_{d,t,\omega}\right)\\ &\quad + \sum_{j\in JaN}\left(W^{RT}_{j,t,\omega} - W^{DA}_{j,t} - W^{SP}_{j,t,\omega}\right)\\ &\quad - \sum_{m\in NaM} B_{n,m}\cdot\left(\delta_{n,t,\omega} - \delta^{\circ}_{n,t} + \delta^{\circ}_{m,t} - \delta_{m,t,\omega}\right) = 0\\ &\quad : \left[\lambda^{RT}_{n,t,\omega}\right] \qquad \forall n,\forall t,\forall\omega\end{aligned} \tag{2.46}$$

$$0 \le rac^{\uparrow}_{i,t,\omega} \le rpc^{\uparrow}_{i,t} \quad : \left[\theta^{\uparrow,min}_{i,t,\omega}, \theta^{\uparrow,max}_{i,t,\omega}\right] \qquad \forall i,\forall t,\forall\omega \tag{2.47}$$

$$0 \le rac^{\downarrow}_{i,t,\omega} \le rpc^{\downarrow}_{i,t} \quad : \left[\theta^{\downarrow,min}_{i,t,\omega}, \theta^{\downarrow,max}_{i,t,\omega}\right] \qquad \forall i,\forall t,\forall\omega \tag{2.48}$$

$$0 \le rad^{\uparrow}_{d,t,\omega} \le rpd^{\uparrow}_{d,t} \quad : \left[\mu^{\uparrow,min}_{d,t,\omega}, \mu^{\uparrow,max}_{d,t,\omega}\right] \qquad \forall d,\forall t,\forall\omega \tag{2.49}$$

$$0 \le rad^{\downarrow}_{d,t,\omega} \le rpd^{\downarrow}_{d,t} \quad : \left[\mu^{\downarrow,min}_{d,t,\omega}, \mu^{\downarrow,max}_{d,t,\omega}\right] \qquad \forall d,\forall t,\forall\omega \tag{2.50}$$

$$0 \le ra^{dis,\uparrow}_{s,t,\omega} \le rp^{dis,\uparrow}_{s,t} \quad : \left[\nu^{dis,\uparrow,min}_{s,t,\omega}, \nu^{dis,\uparrow,max}_{s,t,\omega}\right] \qquad \forall s,\forall t,\forall\omega \tag{2.51}$$

$$0 \le ra^{dis,\downarrow}_{s,t,\omega} \le rp^{dis,\downarrow}_{s,t} \quad : \left[\nu^{dis,\downarrow,min}_{s,t,\omega}, \nu^{dis,\downarrow,max}_{s,t,\omega}\right] \qquad \forall s,\forall t,\forall\omega \tag{2.52}$$

$$0 \le ra^{ch,\uparrow}_{s,t,\omega} \le rp^{ch,\uparrow}_{s,t} \quad : \left[\nu^{ch,\uparrow,min}_{s,t,\omega}, \nu^{ch,\uparrow,max}_{s,t,\omega}\right] \qquad \forall s,\forall t,\forall\omega \tag{2.53}$$

$$0 \le ra^{ch,\downarrow}_{s,t,\omega} \le rp^{ch,\downarrow}_{s,t} \quad : \left[\nu^{ch,\downarrow,min}_{s,t,\omega}, \nu^{ch,\downarrow,max}_{s,t,\omega}\right] \qquad \forall s,\forall t,\forall\omega \tag{2.54}$$

$$0 \le L^{sh}_{d,t,\omega} \le L^{DA}_{d,t} \quad : \left[\mu^{min}_{d,t,\omega}, \mu^{max}_{d,t,\omega}\right] \quad \forall d,\forall t,\forall\omega \tag{2.55}$$

$$0 \le W^{sp}_{j,t,\omega} \le W^{RT}_{j,t,\omega} \quad : \left[\xi^{min}_{j,t,\omega}, \xi^{max}_{j,t,\omega}\right] \quad \forall j,\forall t,\forall\omega \tag{2.56}$$

$$-T^{max}_{n,m} \le B_{n,m}\cdot\left(\delta_{n,t,\omega} - \delta_{m,t,\omega}\right) \le T^{max}_{n,m} \quad : \left[\varphi^{min}_{n,m,t,\omega}, \varphi^{max}_{n,m,t,\omega}\right] \quad \forall n,\forall m \in NaM,\forall t,\forall\omega \tag{2.57}$$

$$-\pi \le \delta_{n,t,\omega} \le \pi \quad : \left[\tilde{\varphi}^{min}_{n,t,\omega}, \tilde{\varphi}^{max}_{n,t,\omega}\right] \quad \forall n,\forall t,\forall\omega \tag{2.58}$$

$$\delta_{n_1,t,\omega} = 0 \quad : [\varphi^{\circ}_{n,t,\omega}] \quad \forall n = n_1, \forall t, \forall \omega \tag{2.59}$$

Objective function (2.45) portrays the minimization of the expected social imbalance cost of the system, conducted by ISO and contains the following terms: i) load shedding cost, ii) wind power spillage cost iii) conventional generators' upward/downward reserve activation savings/cost iv) ESS's upward/downward (dis)charging reserve activation savings/cost, v) demands' upward/downward reserve activation savings/cost. Constraints (2.46) on the other hand, constitute the real-time energy balances and counteract the supply-demand equilibrium's asymmetries, posed by wind production discontinuities in the multi-bus network. Constraints (2.47)-(2.54) regulate activated energy's levels, with respect to the equivalent amounts, already procured in the day-ahead market. Concerning constraints (2.55) and (2.56), they ensure that both curtailed load and wind spillage cannot exceed day-ahead energy consumption and real-time wind production correspondingly. Conclusively, constraints (2.57)-(2.59) apply limits to the network's transmission lines capacity and buses' voltage angle, while establishing $n1$ as the real-time market slack bus.

2.3.5 Solution Approach

The solution approach aims at reformulating the above analyzed bi-level model, into a computationally solvable single-level model, while simultaneously eradicating any inherent non-linearities. Given the linear and continuous nature of lower-level problems *2.3.2* and *2.3.3*, KKT first order optimality conditions (Gabriel et al., 2013) can be applied, thus recasting the bi-level optimization problem, into a single level MPEC. Due to manuscript space limitations, the KKT optimality conditions of the lower-level problems and all the necessary mathematical reformulations, are detailed in the Appendix A.

The resulted non-linear complementarity conditions (A.15)-(A.50) and (A.62)-(A.85) of the form $0 \leq g(x) \perp \mu \geq 0$, are replaced by equations (A.86)-(A.158) and (A.159)-(A.206) respectively, using the Fortuny-Amat and McCarl big-M linearization technique (Fortuny-Amat & McCarl, 1981). The determination of big-Ms comprises a significant challenge, as both the over- and underestimation of their value can lead to an unrestricted or computationally and numerically inadequate problem, respectively. While many algorithmic approaches have been developed for this determination, in this chapter

the value of Ms was established at 10^4, after implementing a series of trials, aiming at achieving an optimal solution time and results' robustness equilibrium. Strong duality theorem is applied to the day-ahead and real-time ISO's optimization problems, in order to incorporate dual variables and generate a linear equivalent for the objective functions (2.19) and (2.45) respectively. Combining these formulations, objective function (2.1) can be recast into the following expression:

$$\begin{aligned}
\textbf{\textit{Minimize}} \quad & \sum_t \sum_s \Bigg[\left(c_s^{ch} \cdot G_{s,t}^{DA,ch} + c_s^{dis} \cdot G_{s,t}^{DA,dis} \right) - \sum_d u_{d,t} \cdot L_{d,t}^{DA} \\
& + \sum_i c_{i,t} \cdot P_{i,t}^{DA} + \sum_i c_{i,t}^{res} \cdot \left(rpc_{i,t}^{\uparrow} + rpc_{i,t}^{\downarrow} \right) \\
& + \sum_d u_{d,t}^{res} \cdot \left(rpd_{d,t}^{\uparrow} + rpd_{d,t}^{\downarrow} \right) - \Omega_t^{DA} \\
& + \sum_\omega \pi_\omega \\
& \cdot \Bigg[-c_s^{ch} \cdot \left(ra_{s,t,\omega}^{ch,\uparrow} - ra_{s,t,\omega}^{ch,\downarrow} \right) + c_s^{dis} \cdot \left(ra_{s,t,\omega}^{dis,\uparrow} - ra_{s,t,\omega}^{dis,\downarrow} \right) \\
& + \sum_d VOLL_{d,t} \cdot L_{d,t,\omega}^{sh} + \sum_i c_{i,t} \cdot \left(rac_{i,t,\omega}^{\uparrow} - rac_{i,t,\omega}^{\downarrow} \right) \\
& + \sum_d u_{d,t} \cdot \left(rad_{d,t,\omega}^{\uparrow} - rad_{d,t,\omega}^{\downarrow} \right) - \Omega_{t,\omega}^{RT} \Bigg] \Bigg]
\end{aligned} \tag{A.247}$$

The remaining non-linearities in the objective function (A.247), are due to the term $\Omega_{t,\omega}^{RT}$ (A.232), which consists of bilinear terms i.e., the product of a primal day-ahead and a dual real-time variable $\{\theta_{i,t,\omega}^{\uparrow,max} \cdot rpc_{i,t}^{\uparrow}, \theta_{i,t,\omega}^{\downarrow,max} \cdot rpc_{i,t}^{\downarrow}, \mu_{d,t,\omega}^{\uparrow,max} \cdot rpd_{d,t}^{\uparrow}, \mu_{d,t,\omega}^{\downarrow,max} \cdot rpd_{d,t}^{\downarrow}, \mu_{d,t,\omega}^{max} \cdot L_{d,t}^{DA}, \lambda_{n,t,\omega}^{RT} \cdot W_{j,t}^{DA}, \lambda_{n,t,\omega}^{RT} \cdot \delta_{n,t}^{\circ}\}$. The linearization process of these terms originates from a binary expansion method (Nasrolahpour et al., 2018),(Pereira et al., 2005), as illustrated in the Appendix A.

2.4 Application study

The proposed bi-level model is implemented into a 6-bus transmission constrained network and consists of two main areas, interrelated through the transmission lines that

connect buses n2-n4 and n3-n6, as illustrated by *Figure 2.2.* The left area, which consists of buses n1, n2 and n3 is characterized by augmented generation and limited consumption levels, while in the right area (buses n4, n5, n6) a diametrically opposed scheme is adopted. The reason for this network separation lies in investigating the behavior of the ESS agent and the rest of the market participants in case of network congestion. Strategic ESS agent owns storage units $s1, s2$, each one established at different area and incurred by unique (dis)charging costs and installed energy and reserve capacity tiers, as shown in *Table 2.1*. Unit $s1$ is characterized by greater energy-reserve capacities and reduced marginal costs comparing to $s2$, therefore being more flexible and inexpensive for the ESS operator. The capacity and cost offer of each storage unit is chosen to be slightly different, considering that their installation on different buses can affect these parameters, since each bus is governed by different conditions.

Conventional units $i1 - i6$ and wind power generator $j1$, represent a non-strategic producer apiece and their technical data are given in *Table 2.2*. Conventional generators $i4 - i6$ are associated with greater flexibility, as they can provide higher reserve provisions, while generators $i2, i6$ claim extended upward and downward reserve procurements, due to their inexpensive reserve offers. Wind power generation uncertainty is captured through a dual-scenario approximation i.e., a high wind generation scenario $\omega 1$ and a low wind generation scenario $\omega 2$, with occurrence probability 0.7 and 0.3 respectively. Conventional generators' cost offers for dispatching energy are summarized in *Table B.1* in the Appendix B, in the interest of presentation purposes. It is necessary to mention that all Table numbers starting with an B are available in the Appendix B. From this table, it can be seen that conventional producers $i1, i4, i6$ offer their energy provision at lower prices than the rest of the producers, increasing their possibility of being chosen by ISO, for dispatching energy in the day-ahead and balancing pool. The value of lost load $VOLL_{d,t}$ equals to 200 €/MWh for all the demand loads. Furthermore, the (dis)charging efficiencies η^{ch}, η^{dis} equal to 1 for both storage units $s1, s2$, while maximum capacity and susceptance for each grid's transmission line $T_{n,m}^{max}$, $B_{n,m}$, equal to 200 MW and 12.412, respectively.

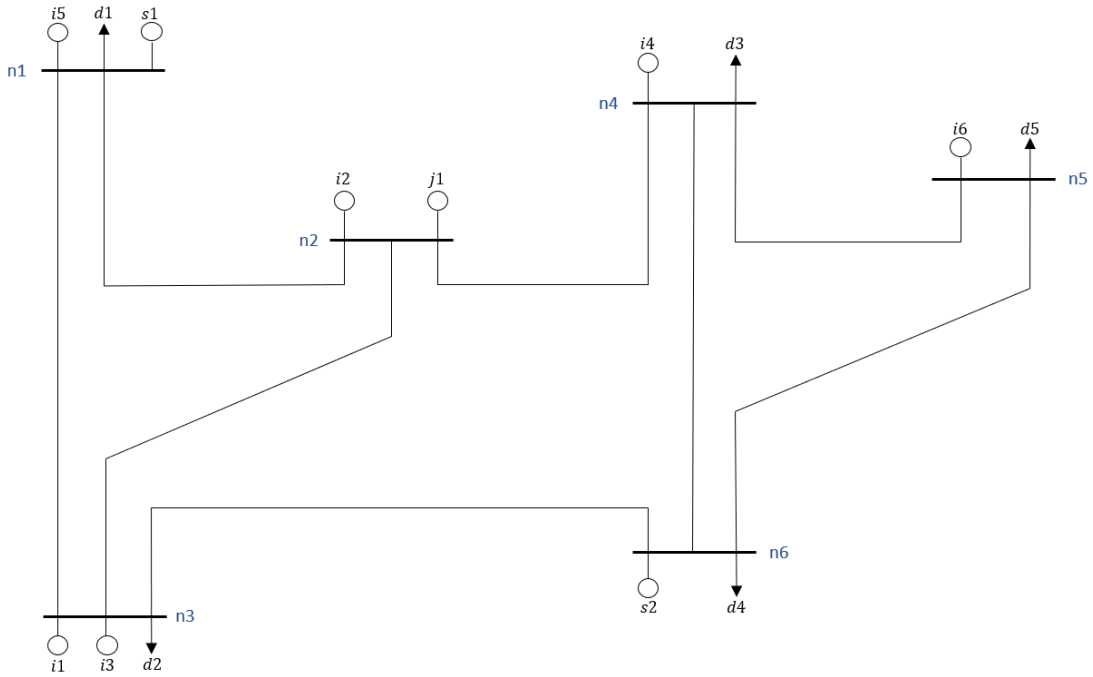

Figure 2.2: 6-bus network.

Units	$G_s^{ch,max}$ (MW)	c_s^{ch} $(€/MWh)$	$G_s^{dis,max}$ (MW)	c_s^{dis} $(€/MWh)$	$RC_s^{ch,\uparrow,max}$ $RC_s^{ch,\downarrow,max}$ (MW)	$RC_s^{dis,\uparrow,max}$ $RC_s^{dis,\downarrow,max}$ (MW)	SOC_s^{max} (MW)	SOC_s^{ini} (MW)
$s1$	50	4	50	24	12	12	120	0
$s2$	40	5	40	25	10	10	100	0

Table 2.1: Data for ESS's units.

Units	P_i^{max} (MW)	$W_{j,t}^{max}$ (MW)	$RCc_i^{\uparrow,max}, RCc_i^{\downarrow,max}$ (MW)	$c_{i,t}^{res}$ $(€/MWh)$	$W_{j,t,\omega1}^{RT}, W_{j,t,\omega2}^{RT}$ (MWh)	$c_{j,t}^{w}$ $(€/MWh)$
$i1$	80	-	8,8	7	-	-
$i2$	80	-	7,7	5.5	-	-
$i3$	100	-	6,6	7	-	-
$i4$	75	-	10,10	6	-	-
$i5$	70	-	9,9	5	-	-
$i6$	100	-	9,9	7	-	-
$j1$	-	70	-	-	70,12	0

Table 2.2: Data for conventional and wind generators.

2.4.1 Uncongested network

The proposed optimization framework is solved for this case, assuming an uncongested network, using the GAMS/CPLEX solver (Brook et al., 1988). The strategic ESS operator participates in the day-ahead market -designated as a joint energy and reserve establishment- and real-time market, through two individually operating electricity storage units $s1, s2$, on a 24-hours horizon basis. Storage systems behave strategically by charging, when the day-ahead prices range at low levels and discharging at time periods, identified by high prices. More specifically, as shown in *Table B.4,* unit $s1$ strategically bids at 200 €/MWh during charging time periods (i.e., 1,3,7,11,13,18-20,23-24) to ensure it is being supplied, as the day-ahead prices are low. On the other hand, the same unit discharges at time periods 9, 14-17, 21-22, exploiting the elevated energy prices, and maximizing its profit share. An equivalent bidding/offering arbitrage approach is adopted by storage unit $s2$. The results are presented in *Table B.6*.

It is important to emphasize that ESS's strategic decisions dictate low price offers, to ensure that the storage systems are being selected from ISO to dispatch energy in the day-ahead market, displacing the non-strategic producers from the merit-order. Concerning the reserve market realization, storage systems offer their upward and downward reserve provisions at a low price, in order to assure their robust presence in this type of market and capitalize this advantageous position in the real-time market, where the clearing prices can approximate 200 €/MWh. To ratify the above policy, *Table B.5* and *Table B.7* reveal that the storage systems $s1$ and $s2$, are actively involved in the balancing market and increase their revenues mostly by deploying upward charging and discharging reserves in the low wind generation scenario $\omega 2$.

Intending to thoroughly investigate the storage system's $s1$ operation, its behavior is analyzed in time period 14. At this time interval, it can be noticed from *Figure 2.3* that the day-ahead price increases up to 35 €/MWh (due to the cost offer of marginal producer $i3$) and therefore the storage system $s1$ decides to discharge 8.3 MWh of energy. In parallel, system $s1$ strategically procures 8.3 MW of downward and 3.7 MW of upward reserve in discharging mode. As illustrated by *Figure 2.4*, the upward and downward reserve prices are 5 €/MWh and 7 €/MWh respectively and are defined by the participation of marginal conventional generators, $i5, i6$, in the reserve market. Conclusively, as demonstrated in *Table B.5*, unit $s1$ activates the entire amount of the

already engaged upward and downward reserves, depending on the real-time wind generation scenario $\omega 1, \omega 2$, and is compensated in the corresponding premium balancing price i.e., 41 €/MWh and 200 €/MWh.

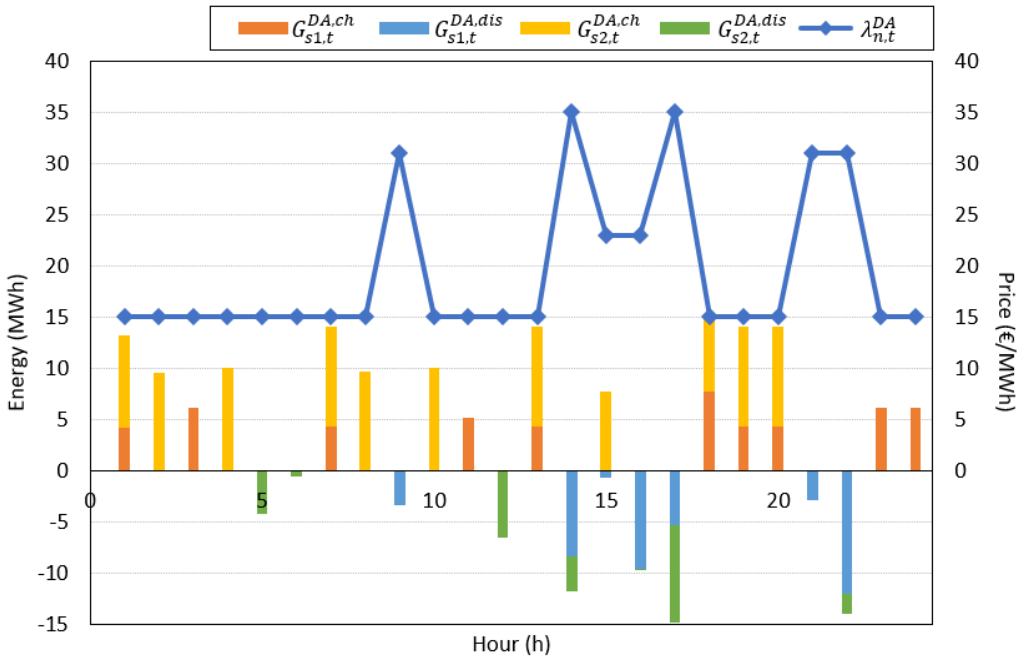

Figure 2.3: Day-ahead prices and energy (dis)charging quantities for storage systems $s1, s2$.

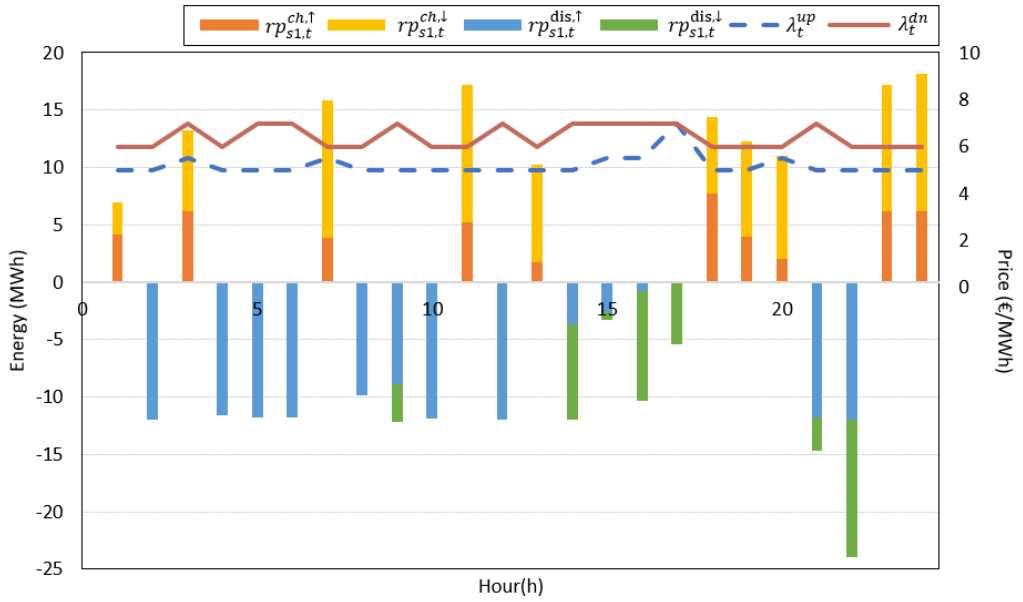

Figure 2.4: Upward and downward day-ahead reserve market prices and procurements for storage system $s1$.

Another, significant observation derived from *Table B.5* is related to the amount of activated upward reserves in discharging mode, for the real-time scenario $\omega 2$. Due to the curtailed wind power generation (i.e.,12 MWh) comparing to scenario $\omega 1$ (70 MWh), the storage system $s1$ is deployed by the Independent System Operator, for the purpose of providing additional energy and balancing the supply-demand equilibrium. Indisputably, this contribution of the storage system $s1$ in the balancing market is associated with significant income sources, as formerly mentioned. *Table B.7* demonstrates an homologous demeanor pursued by the energy storage system $s2$.

Apropos of the price-taker agents' involvement in the market, wind generator $j1$ is nominated by ISO to dispatch the entire amount of its electricity production in the day-ahead pool (70 MWh), for each time period, as a result of its zero cost offers' contribution to the market prices suppression. Analogous results are realized in the real-time market framework, with wind generator $j1$ dispatching his whole electricity production. As for the balancing market prices, as shown in *Table B.5*, low wind power generation in real-time scenario $\omega 2$ (i.e.,12 MWh) stimulates explicit escalation of the market price up to 200 €/MWh, comparing to the equivalent market price generated from the high wind generation scenario $\omega 1$, which ranges between 16 €/MWh and 41€/MWh. On the other hand, conventional generators' day-ahead dispatch and reserve procurement, are determined in respect of their equivalent energy and upward/downward reserve cost offers. Specifically, as depicted in *Table B.8*, producers $i1, i3, i4, i6$ are characterized by relatively low generation marginal costs, therefore generating energy for the whole 24-hours planning horizon. Furthermore, unit $i5$ occasionally dispatch energy to the day-ahead pool, while unit $i2$ is constantly eliminated by the ISO clearing, due to its higher-priced offers. On the contrary, units $i1, i2, i5$ dominate the upward and downward reserve provision settlement -and consequently the balancing market- overthrowing the remaining conventional generators, since their correlated offering is summarized in 5.5 €/MWh, 6 €/MWh and 5 €/MWh respectively, as presented in *Table 2.2 and Table B.8.* It is also worth mentioning that, equally to the ESSs' operation, dispatchable generators preeminently deploy their procured reserves in the low wind generation balancing scenario $\omega 2$, to offset possible system supply imbalances, as *Table B.9* renders.

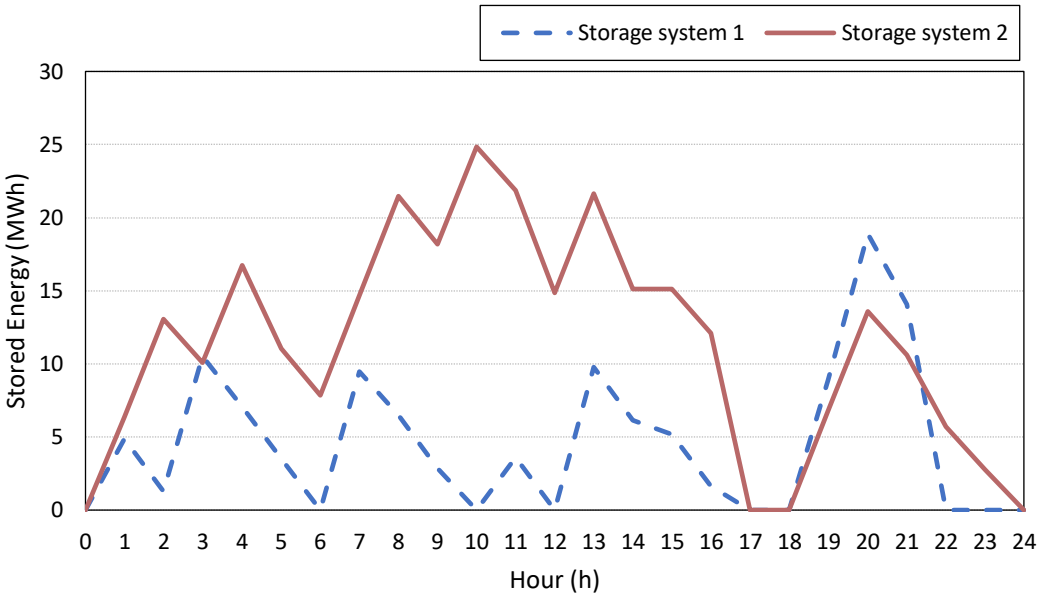

Figure 2.5: State of charge of storage systems, for the uncongested network.

Figure 2.5 illustrates the storage systems' $s1, s2$ state of charge for a 24-hours horizon. More specifically, unit's $s2$ state of charge varies at higher levels than the equivalent of the unit $s1$ and this policy can be justified by their different marginal costs in discharging mode, 24 €/MWh and 25 €/MWh, respectively. Due to this operating cost distinction, storage unit $s1$ is favored by the ESS agent, to discharge higher amounts of energy in the day-ahead market (42.19 MWh), comparing to the corresponding from the unit $s2$ (26.25 MWh), thus leading to higher energy accumulation for storage unit $s2$.

2.4.2 Congested Network

In this case study, power systems congestions are considered for the 6-bus network, as a result of a capacity decrement for the transmission line 3-6. More precisely, while the maximum power flow between buses $n3 - n6$ for the uncongested network reaches up to 30.33 MW, the system's response during the same 24-hours horizon when line capacity is reduced to 15 MW is studied. A substantial differentiation occurred, pertains to the existence of different local marginal prices (LMPs) in the day-ahead market, due to the impeded energy transfer among buses, as shown in *Figure 2.6*.

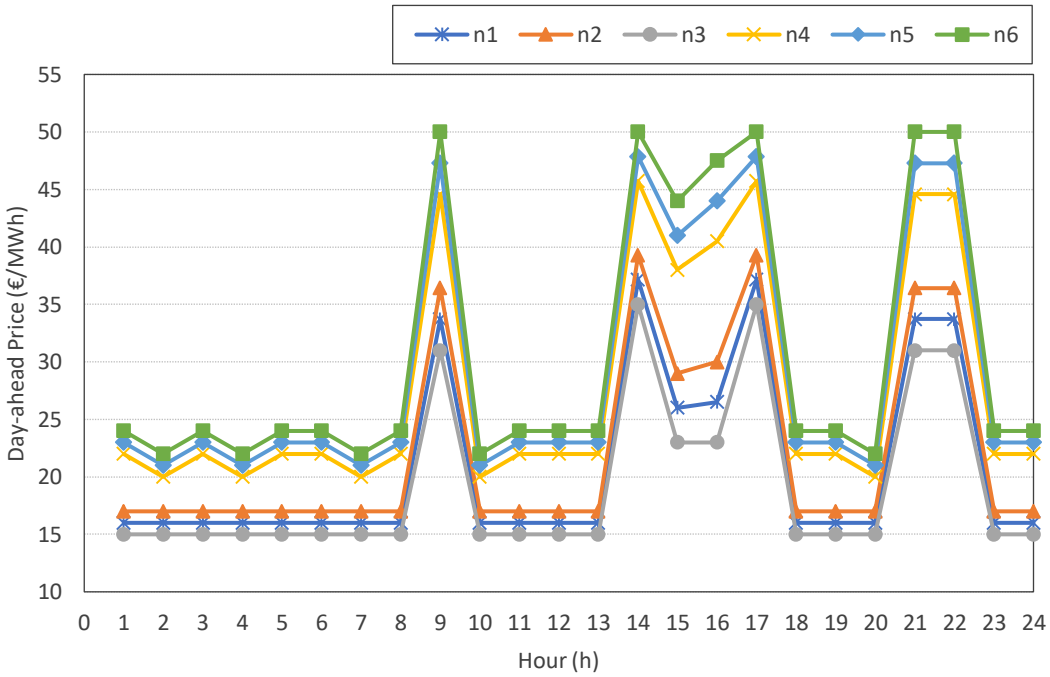

Figure 2.6: Local marginal prices for the congested network.

Despite these design modifications, the main ESS agent's offering/bidding and (dis)charging principles comply with the overall strategic behavior, adopted at the uncongested network case. As *Figure 2.7* indicates, storage system $s1$ discharges at time periods when the day-ahead price for the bus $n1$ fluctuates at high levels, such as 33.7 €/MWh and 37 €/MWh for time periods 9,21,22 and 14,17, respectively. Equivalently, unit $s1$ charges when the price levels are reduced i.e., time periods 1-4,6-8,10-13,15-16,18,20,23. *Figure 2.7*, also illustrates the upward and downward reserve procurements in the dis(charging) mode, which constitute a precursor of storage system's $s1$ involvement in the real-time market.

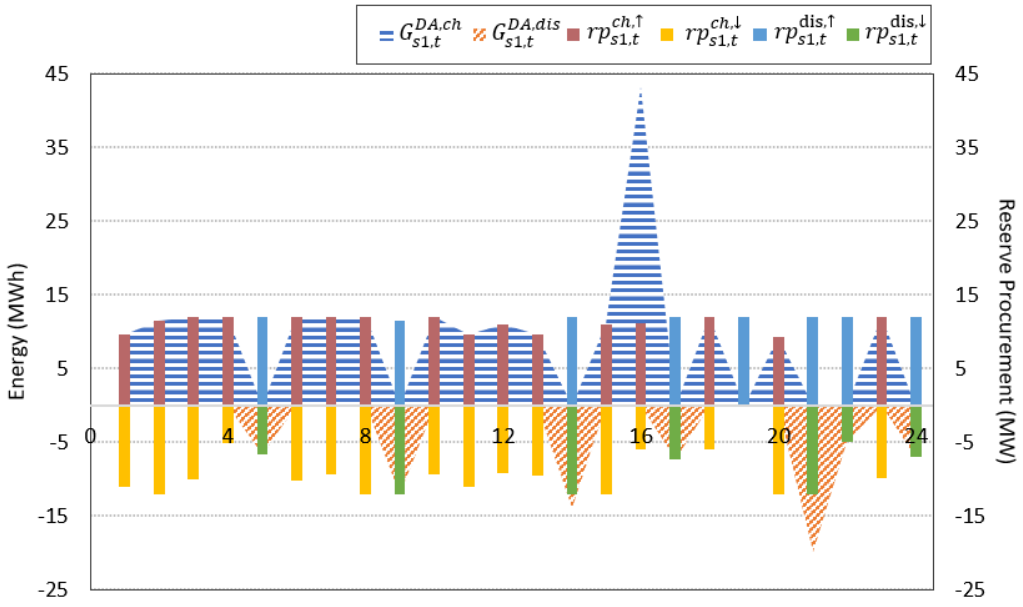

Figure 2.7: Day-ahead (dis)charging energy dispatch and reserve procurements for storage system $s1$, for the congested network.

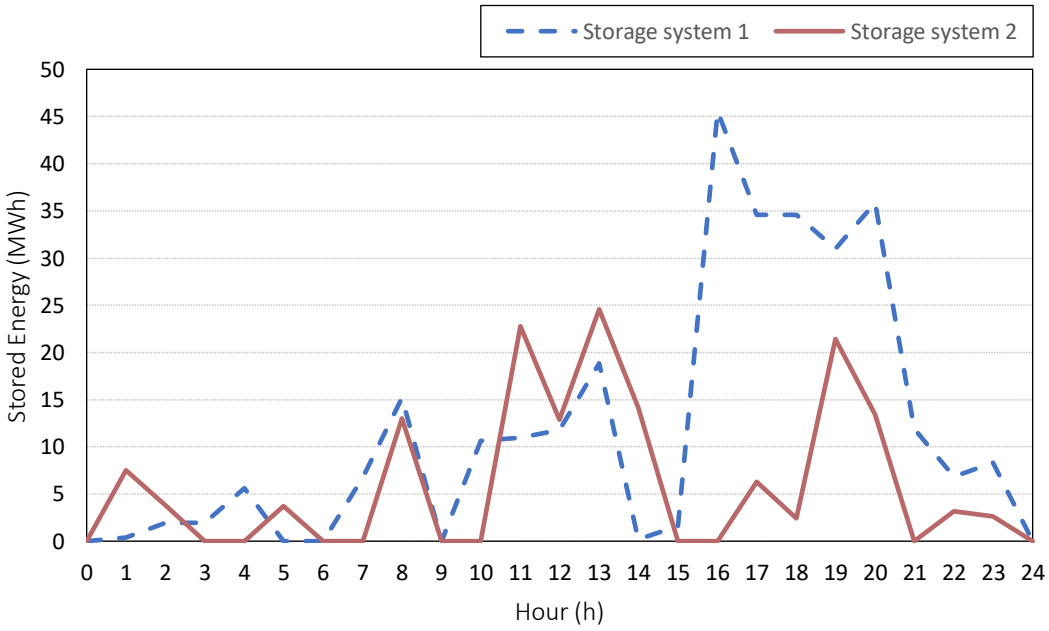

Figure 2.8: State of charge of storage systems, for the congested network.

As already mentioned in *Section 2.4*, the network is discretized into two subareas i.e., the left one where the installed capacity outblanaces demand loads and the right one, where the potential power generation yields at the demand's higher quantity levels. Due to the congested transmission line 3-6, energy tranfer between these areas becomes

extremely limited, thus leading to two discretized network settlements and resulting in different outcomes for the ESS agent, comparing to the uncongested network case. More specifically, storage system $s1$ located at bus $n1$ exploits this generation surplus occurred in the left area, by receiving more profitable (dis)charging decisions in order to maximize its revenues. These optimal strategies culminate in increased state-of-charge levels, as displayed in *Figure 2.8*, in comparison to the equivalent quantities presented in *Figure 2.5*. On the contrary, storage system $s2$ located in the low power generation subarea (bus $n6$), is qualified for managing restricted amount of energy comparing to the uncongested network case, which negatively affects its profit share, as it is analyzed below.

Table 2.3 to *Table 2.4* and *Table 2.5* to *Table 2.6* summarize a comparison between the ESS agent's function in these two different networks. *Table 2.3* presents the charging operation of storage system $s1$ for time period 7. More specifically, given the higher amounts of the energy charged and the increased day-ahead pool price, system $s1$ appears at first to experience profit losses under the congested network conditions. Analyzing the results further, the increase of upward reserve deployments at scenario $\omega 2$ (which are compensated at 200 €/MWh) with the parallel elimination of downward reserve deployments (which constitute a cost factor) seem to recast this conviction and crucially contribute to the $s1's$ revenue increment in the congested network.

An equivalent attribute by $s1$ is noticed in *Table 2.4*, regarding time period 14. Storage system $s1$ under congested power grid conditions, dispatches higher energy amounts in the day-ahead and real-time market, escalating the corresponding incomes and nullifies expenses originating from downward reserve activation in discharging mode, in comparison to the uncongested network. A reverse settlement is portrayed in *Table 2.5* and *Table 2.6*, regarding the strategies of storage system $s2$. System $s2$ charges less energy in the congested day-ahead market during time period 4, avoiding operational and purchasing expenses. Its insignificant participation in the real-time market though and particularly in activating upward reserves in the low wind generation scenario $\omega 2$, leads to profit depletion in comparison to $s2's$ profit generated in the uncongested network. Ultimately, during time period 16 and under congested network conditions, storage system $s2$ experiences zero revenues in the day-ahead and real-time energy market, in contradiction to the uncongested power grid case, where $s2$ increase its profit by activating upward reserves in discharging mode.

	$G_{s1,t7}^{DA,ch}$ (MWh)	$rp_{s1,t7}^{ch,\downarrow}$ (MW)	$rp_{s1,t7}^{ch,\uparrow}$ (MW)	$ra_{s1,t7,\omega1}^{ch,\downarrow}$ (MWh)	$ra_{s1,t7,\omega2}^{ch,\downarrow}$ (MWh)	$ra_{s1,t7,\omega1}^{ch,\uparrow}$ (MWh)	$ra_{s1,t7,\omega2}^{ch,\uparrow}$ (MWh)	$\lambda_{n1,t7}^{DA}$ $(€/MWh)$	$\lambda_{n1,t7,\omega1}^{RT}$ $(€/MWh)$	$\lambda_{n1,t1,\omega2}^{RT}$ $(€/MWh)$
Uncongested network	4.3	12	3.83	12	-	-	3.83	15	16	200
Congested network	12	9.35	12	-	-	2.36	12	16	16	200

Table 2.3: Storage system's $s1$ operation in charging mode during time period 7.

	$G_{s1,t14}^{DA,dis}$ (MWh)	$rp_{s1,t14}^{dis,\downarrow}$ (MW)	$rp_{s1,t14}^{dis,\uparrow}$ (MW)	$ra_{s1,t14,\omega1}^{dis,\downarrow}$ (MWh)	$ra_{s1,t14,\omega2}^{dis,\downarrow}$ (MWh)	$ra_{s1,t14,\omega1}^{dis,\uparrow}$ (MWh)	$ra_{s1,t14,\omega2}^{dis,\uparrow}$ (MWh)	$\lambda_{n1,t14}^{DA}$ $(€/MWh)$	$\lambda_{n1,t14,\omega1}^{RT}$ $(€/MWh)$	$\lambda_{n1,t14,\omega2}^{RT}$ $(€/MWh)$
Uncongested network	8.3	8.3	3.7	8.3	-	-	3.7	35	41	41
Congested network	14	12	12	-	-	1.6	12	37.14	41	41

Table 2.4: Storage system's $s1$ operation in discharging mode during time period 14.

	$G_{s2,t4}^{DA,ch}$ (MWh)	$rp_{s2,t4}^{ch,\downarrow}$ (MW)	$rp_{s2,t4}^{ch,\uparrow}$ (MW)	$ra_{s2,t4,\omega1}^{ch,\downarrow}$ (MWh)	$ra_{s2,t4,\omega2}^{ch,\downarrow}$ (MWh)	$ra_{s2,t4,\omega1}^{ch,\uparrow}$ (MWh)	$ra_{s2,t4,\omega2}^{ch,\uparrow}$ (MWh)	$\lambda_{n6,t4}^{DA}$ $(€/MWh)$	$\lambda_{n6,t4,\omega1}^{RT}$ $(€/MWh)$	$\lambda_{n6,t4,\omega2}^{RT}$ $(€/MWh)$
Uncongested network	10	10	10	-	-	0.5	10	15	16	200
Congested network	-	7.8	-	-	-	-	-	22	16	200

Table 2.5: Storage system's $s2$ operation in charging mode during time period 4.

	$G_{s2,t16}^{DA,dis}$ (MWh)	$rp_{s2,t16}^{dis,\downarrow}$ (MW)	$rp_{s2,t16}^{dis,\uparrow}$ (MW)	$ra_{s2,t16,\omega1}^{dis,\downarrow}$ (MWh)	$ra_{s2,t16,\omega2}^{dis,\downarrow}$ (MWh)	$ra_{s2,t16,\omega1}^{dis,\uparrow}$ (MWh)	$ra_{s2,t16,\omega2}^{dis,\uparrow}$ (MWh)	$\lambda_{n6,t16}^{DA}$ $(€/MWh)$	$\lambda_{n6,t16,\omega1}^{RT}$ $(€/MWh)$	$\lambda_{n6,t16,\omega2}^{RT}$ $(€/MWh)$
Uncongested network	-	0.03	10	-	-	-	10	24	26	26
Congested network	-	-	-	-	-	-	-	47.5	26	26

Table 2.6: Storage system's $s2$ operation in discharging mode during time period 16.

Figure 2.9, through the triangular points on the green line, illustrates the positive or negative differentiations occurred in revenue for storage system $s1$, between the uncongested and congested network cases for an 24-hours planning horizon and are measured in the right y-axis. On the other hand, the bars shown in the figure, correspond to energy amounts and are measured in MWh. Storage system $s1$ under congested network conditions, experiences losses due to an increase of day-ahead charging energy $G_{s1,t}^{DA,ch}$ and decrease of upward discharging reserve activation for low wind generation scenario $ra_{s1,t,\omega2}^{dis,\uparrow}$, comparing to the uncongested network case. However, the quantitative increase of the remaining income increasing terms, such as $G_{s2,t1}^{DA,dis}$, $ra_{s1,t,\omega1}^{ch,\uparrow}$, $ra_{s1,t,\omega2}^{ch,\uparrow}$, contribute to a total profit increase by 6,206 € in the congested network, as presented in *Figure 2.11*. On the other hand, as demonstrated in *Figure 2.10*, storage system $s2$, mainly due to the curtailed real-time upward charging and discharging reserve activation in scenario $\omega2$ ($ra_{s2,t,\omega2}^{ch,\uparrow}$, $ra_{s2,t,\omega2}^{dis,\uparrow}$), generates significant profit losses up to 3,406.6 €, comparing to the uncongested network settlement. In conclusion, despite the deficit of storage system $s2$, ESS agent, from the joint operation of storage systems s1 and s2, benefits from network congestions and experiences an overall profit increase by 2,799.4 € compared to the uncongested case, as depicted in *Figure 2.11*.

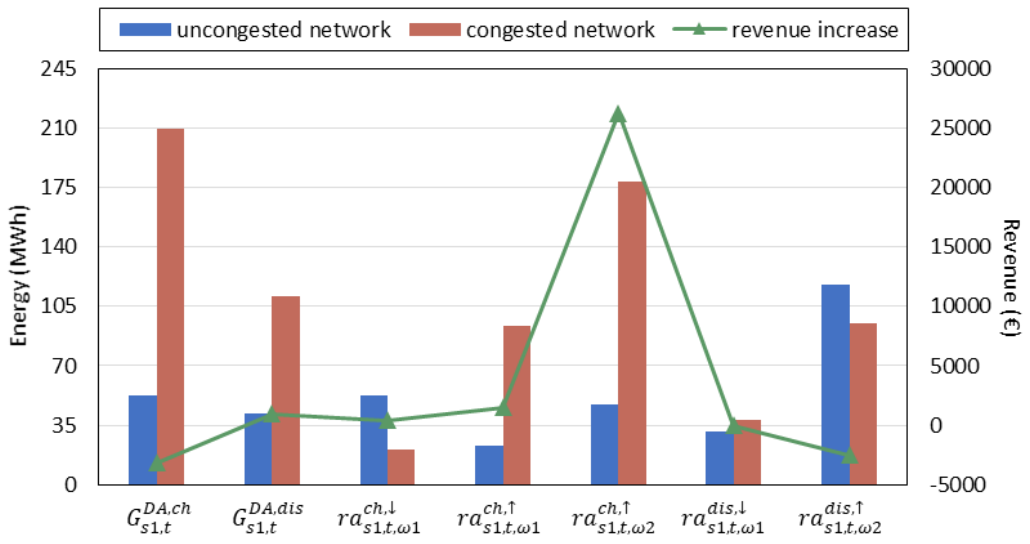

Figure 2.9: Energy dispatch and revenue comparison for storage system $s1$, between uncongested and congested network.

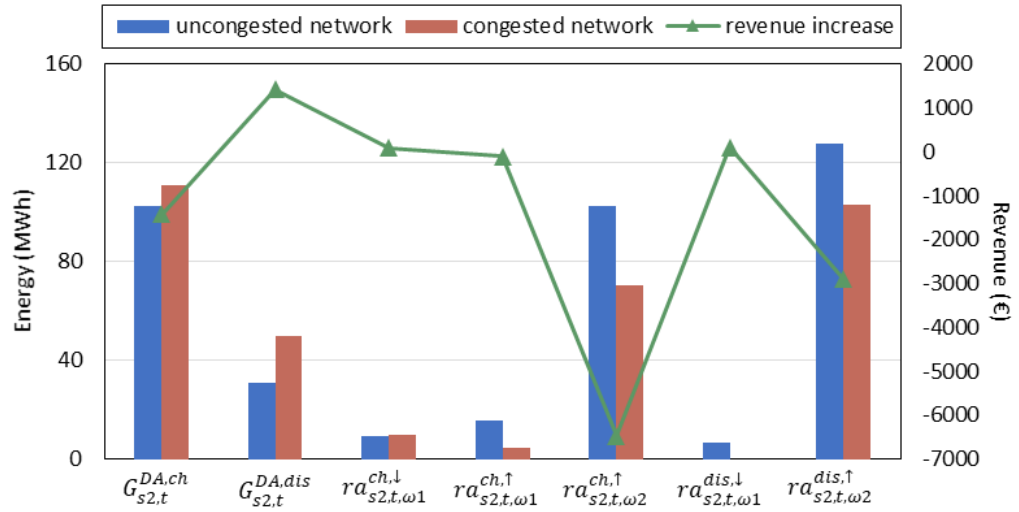

Figure 2.10: Energy dispatch and revenue comparison for storage system $s2$, between uncongested and congested network.

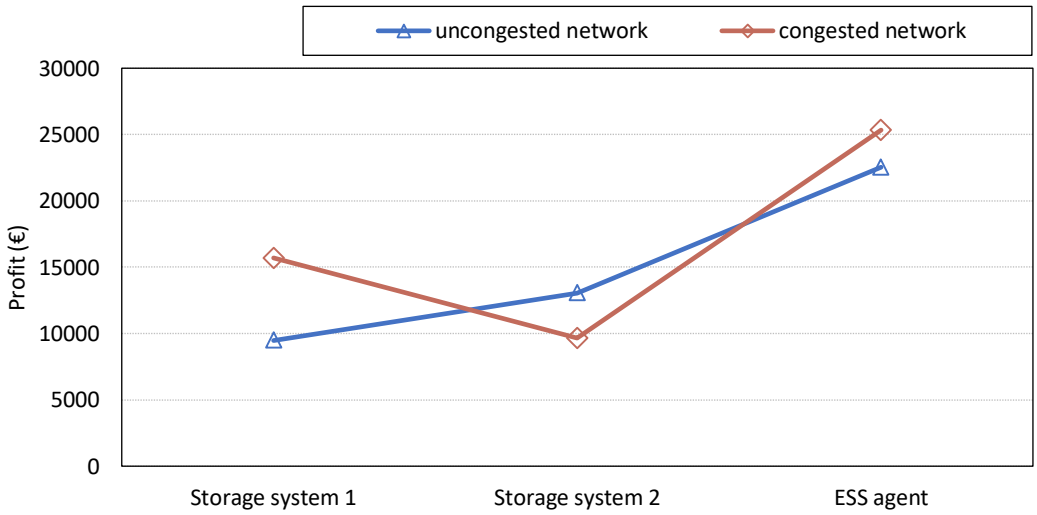

Figure 2.11: Profit comparison between uncongested and congested network.

2.4.3 Wind power generation increment scenarios

Two additional cases of wind power generation increment are investigated, under uncongested network conditions, with Case 1 representing the base case with zero wind generation increase. Particularly, in *Case 2*, production of unit $j1$ rises from 70 MWh - which constitute the 12.17% of the grid's installed capacity- to 100 MWh in the high wind scenario $\omega1$, thus increasing wind generation's share up to 16.53%, in the examined

power system. As for the low wind scenario $\omega 2$, wind penetration increases to 20 MWh. These alterations result to less generation of expensive conventional units, as ISO favors the augmented energy provision by unit $j1$, due to its zero marginal cost offers. Specifically, unit's $i3$ and $i4$ dispatch in the day-ahead market is reduced by 56.2% and 15.1% respectively, due to their increased cost offers during the 24-hours horizon, as shown in *Table B.1*. Concerning *Case 3*, wind power provision reaches up to 19.2% of network's installed capacity, by dispatching 120 MWh and 20 MWh in the high and low wind scenario correlatively and de novo restricts conventional generators' participation in the energy day-ahead and real-time market.

Table B.16 depicts storage system's $s1$ response in the above analyzed wind increment cases, during time period 1. While additional energy originated from non-dispatchable producers accesses the power system, storage system $s1$, acting as a demand load, charges higher amounts of energy in the day-ahead and activates increased quantities of upward reserves in the real-time pool, as the market prices de-escalate, due to the zero marginal cost offers by $j1$. Characteristically, day-ahead price $\lambda_{n,t1}^{DA}$ is reduced from 15 €/MWh to 14 €/MWh, while the balancing price $\lambda_{n,t1,\omega 1}^{RT}$ for the high wind generation scenario $\omega 1$ decreases from 16 €/MWh to 14 €/MWh. *Figure 2.12* illustrates the differentiations in storage system's $s1$ energy dispatch and reserve procurements, occurred by the different wind generation increment cases. In *Case 2* and *Case 3*, a parallel increase of energy charged, and a decrease of energy discharged in the day-ahead market appear. At first, this realization could lead to the conclusion that $s1$ suffers significant profit losses while wind penetration intensifies, as $G_{s1,t}^{DA,ch}$ and $G_{s1,t}^{DA,dis}$ correspond to an expense and revenue factor apiece. However, the assertive involvement of $s1$ in balancing market and especially by activating upward reserves in charging mode, compensated by market prices up to 200 €/MWh, leads to a critical source of income, which dominates any potential losses.

This claim is unambiguously justified in *Figure 2.13*, as storage system's $s1$ profits systematically rise up to 15,792 € and 16,734 € in *Case 2* and *Case 3* equivalently. On the other hand, profit of storage system $s2$ is not considerably affected by the level of wind penetration. As for the ESS agent in total, mainly due to the unit's $s1$ optimal operation, experiences profit surplus by 6,293 € in *Case 2* and 7,004 € in *Case 3*, in comparison to *Case 1*.

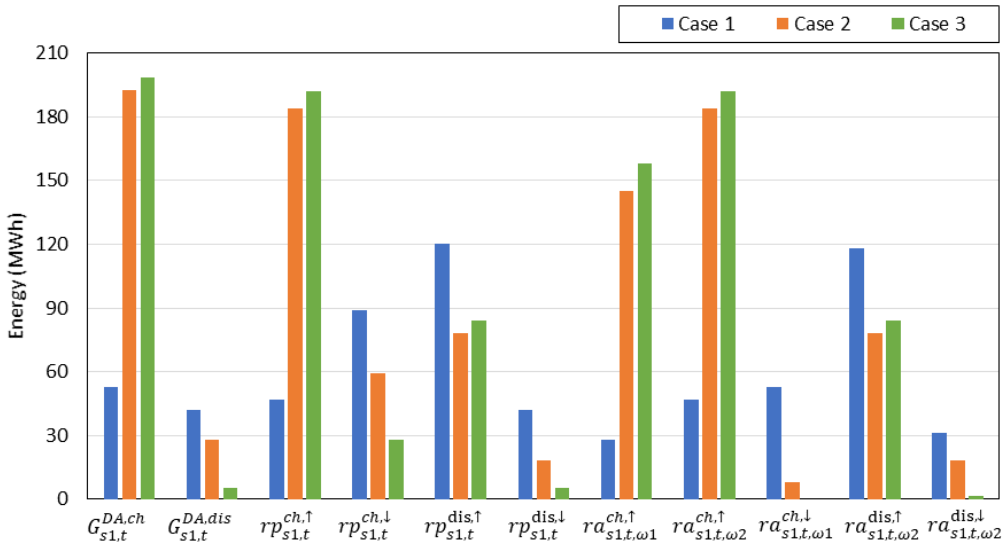

Figure 2.12: Overall energy dispatch and reserve procurements of storage system $s1$, under three wind generation cases.

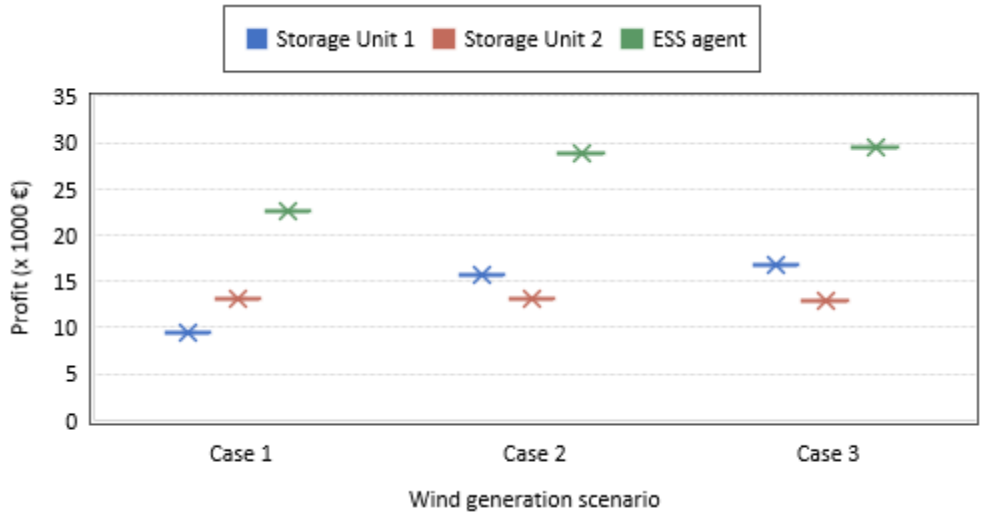

Figure 2.13: Profit differentiation for storage systems $s1$, $s2$ and ESS agent, under three wind generation cases.

2.5 Computational issues

The resulting MILP has been solved using CPLEX/GAMS 32.1.0, on an Intel Core i7-9700 processor at 3.00 GHz, with 32 GB RAM. The average CPU time for solving the Uncongested network case is 1150 seconds, while for the Congested network case, 1640 seconds. Computational time increases in accordance with the network sophistication, examined wind power generation scenarios and transmission lines congestions. Binary expansion approach provides an additional critically challenging factor, regarding the computational requirements of the model, as each bilinear term is substituted by a set of multiple parameters. Finally, as already mentioned the determination of big-Ms' value is firmly associated with the efficiency of the computation procedure.

2.6 Conclusions

This chapter, based on a single leader-follower Stackelberg hypothesis' game, illustrates a bi-level mathematical framework to generate optimal offering/bidding strategies for a strategic ESS agent in a pool-based market settlement. The model considers a sequential clearing mechanism of a joint energy and reserve day-ahead market and an energy-only real-time market, conducted by ISO. Uncertainty is introduced in the balancing stage through the realization of plausible wind power generation scenarios. The application of the proposed modelling approach on a 6-bus transmission constrained network, derives local marginal prices as dual variables of the lower-level problems and generates optimal dis(charging) energy dispatch and upward/downward reserve provisions for the ESS operator. The algorithm leads to an increase in clearing prices compared to cost optimization. Furthermore, the effects on ESS's functioning and expected profit inflow caused by potential network transmission congestions, are investigated. More specifically, the ESS agent benefits from line congestions and experiences significant profit increase, compared to the uncongested case. Conclusively, the model provides significant insights into designing policies that the energy storage agents should adopt, in order to capitalize a possible rise in the wind generation installed capacity and achieve an attractive profit increase.

Nomenclature

Indices and sets

i	Index of conventional generating units
j	Index of wind generating units
d	Index of demands
s	Index of storage systems
t, k	Indices of time periods
n, m	Indices for system buses
ω	Index of scenarios
$I\alpha N$	Set of indices of conventional generating units located at bus n
JaN	Set of indices of wind generating units located at bus n
DaN	Set of indices of demands located at bus n
SaN	Set of indices of storage systems located at bus n
NaM	Set of buses n connected with bus m

Superscripts

ch	Charging mode of storage system s
dis	Discharging mode of storage system s
↑	Upward reserve
↓	Downward reserve

Parameters

c_s	Marginal cost of storage system s at (dis)charging mode (€/MWh)
G_s^{max}	Maximum (dis)charging capacity of storage system s (MW)
RC_s^{max}	Maximum upward/downward reserve capacity of storage system s at (dis)charging mode (MW)
SOC_s^{max}	Maximum storage capacity of storage system s (MW)
SOC_s^{ini}	Initial reserved energy of storage system s (MW)
η	(Dis)charging efficiency of storage system s

$B_{n,m}$	Susceptance of line *n-m*
R_t	Upward/downward reserve requirements of the market at time interval *t* (MW)
P_i^{max}	Maximum capacity at conventional generating unit *i* (MW)
$L_{d,t}^{max}$	Maximum load of demand d at time *t* (MW)
RCc_i^{max}	Maximum upward/downward reserve capacity of conventional generating unit *i* (MW)
$RCd_{d,t}^{max}$	Maximum upward/downward reserve capacity load of demand *d* (MW) at time *t*
$W_{j,t}^{max}$	Available generation of wind unit *j* at time *t* (MW)
$T_{n,m}^{max}$	Transmission capacity of circuit line *n-m*
π_ω	Occurrence probability of scenarios ω
$VOLL_{d,t}$	Value of lost load d at time *t* (€/MWh)
$W_{j,t,\omega}^{RT}$	Scenario dependent generation of wind unit *j* at time *t* (MWh)
$c_{i,t}$	Cost offer for dispatched energy of conventional unit *i* at time *t* (€/MWh)
$c_{i,t}^{res}$	Cost offer for procured reserves of conventional unit i at time *t* (€/MWh)
$c_{j,t}^{w}$	Cost offer for dispatched energy of wind generator *j* at time *t* (€/MWh)
$u_{d,t}$	Utility cost for consumed energy of demand *d* at time *t* (€/MWh)
$u_{d,t}^{res}$	Utility cost for procured reserves of demand *d* at time *t* (€/MWh)

Upper-level variables

$soc_{s,t}$	Energy stored for storage system *s* at time *t* (MWh)
$x_{s,t}$	Binary decision variable indicating (dis)charging mode of storage system *s* at time *t*
$\bar{G}_{s,t}$	Energy amount bid by storage system *s* at time *t* in (dis)charging mode (MW)

$\overline{rc}_{s,t}$	Reserve capacity bid by storage system *s* at time *t* in (dis)charging mode (MW)
$O_{s,t}$	Price bid by storage system *s* at time *t* in (dis)charging mode (€/MWh)

Lower-level variables

$P_{i,t}^{DA}$	Scheduled production of conventional generating unit *i* at time *t* in DA market (MWh)
$rp_{s,t}$	Upward/downward reserve procurement from storage unit *s* in time *t* in (dis)charging mode in DA market (MW)
$L_{d,t}^{DA}$	Energy consumed by load *d* at time *t* in DA market (MWh)
$rpd_{d,t}$	Reserve procurement from demand *d* at time *t* in DA market (MW)
$G_{s,t}^{DA}$	Scheduled energy consumption of storage system *s* at time *t* in (dis)charging mode in DA market (MWh)
$rpc_{i,t}$	Reserve procurement from conventional generating unit *i* at time *t* in DA market (MW)
$W_{j,t}^{DA}$	Scheduled energy production of wind generating unit *j* at time *t* in DA market (MWh)
$\lambda_{n,t}^{DA}$	Clearing price in DA market at bus *n* at time *t* (€/MWh)
$\delta_{n,t}^{\circ}$	Voltage angle at bus *n* in DA market
$\lambda_t^{\uparrow}$	Clearing price for upward reserve procurement at time *t* (€/MWh)
$\lambda_t^{\downarrow}$	Clearing price for downward reserve procurement at time *t* (€/MWh)
$rac_{i,t,\omega}$	Reserve activation from conventional generating unit *i* at time *t* under scenario ω (MWh)
$rad_{d,t,\omega}$	Reserve activation from demand *d* at time *t* under scenario ω (MWh)
$L_{d,t,\omega}^{sh}$	Load shedding of demand *d* at time *t* under scenario ω (MWh)

$ra_{s,t,\omega}$	Reserve activation from storage system *s* at time *t* under scenario ω in (dis)charging mode (MWh)
$\lambda^{RT}_{n,t,\omega}$	Clearing price in RT market at bus *n* at time *t* under scenario ω (€/MWh)
$\delta_{n,t,\omega}$	Voltage angle at bus *n* at time *t* under scenario ω
$W^{sp}_{j,t,\omega}$	Power spillage from wind generating unit *j* at time *t* under scenario ω (MWh)

Dual Variables

α, θ	Dual variables corresponding to conventional generating unit *i* in DA and RT market
β, μ	Dual variables corresponding to demand *d* in DA and RT market
γ, ν	Dual variables corresponding to storage system *s* in DA and RT market
ε, ξ	Dual variables corresponding to wind generating unit *j* in DA and RT market
ζ, φ	Dual variables corresponding to transmission lines of buses *n, m* in DA and RT market

Chapter 3

Analysis of energy storage technologies in electricity and natural gas markets

This chapter introduces a stochastic mixed-integer linear programming (MILP) optimization framework designed to explore the optimal participation and economic aspects of diverse energy storage technologies—such as pumped-hydro, advanced adiabatic and diabatic compressed air systems, and li-ion batteries—in a perfectly competitive interconnected electricity and natural gas market. The clearing mechanism is specific to energy-only markets, with the objective of optimizing dispatch and maximizing social welfare for the integrated energy system. This is achieved through a two-stage stochastic programming approach: the first stage involves the day-ahead market clearing process, while the second stage depicts the real-time operation of the integrated system on the trading floor, considering various plausible wind power generation scenarios. The two markets are primarily interconnected through the bilateral operation of the diabatic compressed air energy storage system, serving both as an electricity producer and a consumer of natural gas. The proposed algorithm is applied to a modified IEEE 24-bus power grid and a single-node gas network, offering a comprehensive analysis of the operational characteristics and profitability of each energy storage technology within the integrated energy system.

3.1 Introduction

In the wake of climate change, the adoption of a green agenda that will establish the increase of renewable energy sources' (RES) percentage into the global energy mix, seems to be the only solution. However, the verdicts that emerge from both international literature and real facts prove that a disproportionate integration of RESs into the energy markets can give rise to significant stability problems, due to their inherent uncertain

nature. Energy storage systems (ESSs) on the other hand seem to provide a solution to this problem. Among the numerous advantages they offer, they seem to constitute one of the main pillars of reliability for the optimal operation of contemporary energy markets, thus experiencing a sound appeal in the global re-search community. In particular, the Market Operator (MO) can optimally adjust the (dis)charging energy dispatch of the energy storage systems, to improve the electricity market efficiency and suppress prices.

Up to the present time, a plethora of energy storage technologies have been developed including different types of mechanical, electrochemical and battery, thermal, chemical (Koohi-Fayegh & Rosen, 2020), hydrogen energy storage (Nasiri et al., 2021) and water-energy microgrids (Moazeni & Khazaei, 2020). However, not all technologies have received the same research interest, as some of them seem to unveil comparative disadvantages, or may not be technologically mature enough, to comprise a reliable and sustainable alternative.

This chapter provides a novel stochastic MILP framework to evaluate the financial gains and optimal (dis)charging dispatch of pumped-hydro, advanced adiabatic CAES, diabatic CAES and Li-ion battery systems in a coupled electricity and natural gas market, under perfect competition. The choice of these specific energy storage technologies lies, either on their technological maturity and the large share they hold in the energy mix (PHS, D-CAES), or on their promising evolution (AA-CAES, Li-ion). The coupling of the two markets and the merger of the two MOs (EMO and GMO) to create a common clearing entity is of great importance, as it allows the optimal synchronization and exchange of information between them thus resulting in lower operating costs (Ordoudis et al., 2019). Especially for the investigation of the operation of a diabatic CAES plant, which acts bilaterally as an electricity generator and a natural gas consumer, the market coupling is essential for the simultaneous determination of its optimal (dis)charging decisions, based on the electricity and gas MCPs. To the best of authors' knowledge this is the first time that such an analysis is carried out, since the participation of electricity storage technologies has only been studied in an electricity market settlement (Zou et al., 2016). With this approach, however, the bilateral operation of the D-CAES plant, which naturally affects the operation of the rest of storage systems as well, cannot be captured. Furthermore, contrary to the common practice of treating the natural gas MCPs as fixed values, in the present model, gas prices are generated endogenously, during the gas market clearing process.

The contributions of this Chapter are fourfold:

i. A coupled day-ahead and real-time electricity and natural gas market de-sign, considering the integration of electricity storage technologies and wind power production uncertainty.
ii. Development of a stochastic MILP market-clearing model to determine optimal dispatch and analyze expected profits of PHS, AA-CAES, D-CAES and Li-ion battery systems in a coupled electricity and natural gas market, under perfect competition.
iii. Modelling of the diabatic CAES system operation and its participation in an integrated electricity and natural gas market.
iv. Analysis of the impact of transmission line congestions and increasing levels of wind power generation volatility on the expected profits of the four energy storage technologies.

3.2 Problem Statement

The proposed MILP framework considers the operation of four energy storage technologies (PHS, AA-CAES, D-CAES, Li-ion battery), as well as conventional power plants and demand loads in the electricity and natural gas networks. Both day-ahead and real-time trading floors are taken into account, while wind power production uncertainty is modelled via the realization of two plausible real-time wind generation scenarios.

3.3 Mathematical framework

3.3.1 General energy storage modelling

In this section, a generalized presentation of the operational constraints of an electricity storage system in energy markets, is carried out. Certainly, the set of constraints below does not necessarily govern all storage technologies, since each system has its own peculiarities, however it constitutes a comprehensive guide of the operational limitations faced by the majority of storage systems.

Constraints (3.1), (3.2) limit the electricity dispatch for the day-ahead charging and discharging mode, while constraints (3.3)–(3.6) serve the same purpose for the

charging/discharging upward and downward reserves in the real-time market. It is critical to point out that both the upward charging and discharging reserves constitute an income factor for any storage system, since it is compensated from the MO for its charging power curtailment and the additional electricity discharged, respectively. Contrastingly, downward charging and discharging reserves mean that the storage system has to pay off the MO, either for charging additional power or for failing to dispatch the agreed amount of electricity. Constraints (3.7), (3.9) guarantee that the summation of the day-ahead and real-time electricity dispatch cannot exceed the maximum capacity of the storage system, while constraints (3.8), (3.10) certify that the reserves' provision is lower than the day-ahead electricity dispatch. Constraint (3.11) excludes the simultaneous operation in charging and discharging mode, while constraints (3.12), (3.13) impose that a storage system cannot provide both upward and downward reserves at the same time. Constraints (3.14)–(3.15) pertain to the upper and lower levels of the electricity stored in the system and enforce that the state of charge at the end of the daily horizon is equal to the amount of energy stored in the beginning of the day. Constraint (3.16) represents the storage system's state-of-charge intertemporal fluctuations, depending on its optimal dispatching decisions, as stated in (Nasrolahpour et al., 2018).

$$\underline{G}_s \cdot x_{s,t}^{ch} \leq g_{s,t}^{ch} \leq \overline{G}_s \cdot x_{s,t}^{ch} \qquad \forall s, \forall t \tag{3.1}$$

$$\underline{G}_s \cdot x_{s,t}^{dis} \leq g_{s,t}^{dis} \leq \overline{G}_s \cdot x_{s,t}^{dis} \qquad \forall s, \forall t \tag{3.2}$$

$$\underline{G}_s^{\uparrow} \cdot \hat{x}_{s,\omega,t}^{ch,\uparrow} \leq \hat{g}_{s,\omega,t}^{ch,\uparrow} \leq \overline{G}_s^{\uparrow} \cdot \hat{x}_{s,\omega,t}^{ch,\uparrow} \qquad \forall s, \forall \omega, \forall t \tag{3.3}$$

$$\underline{G}_s^{\downarrow} \cdot \hat{x}_{s,\omega,t}^{ch,\downarrow} \leq \hat{g}_{s,\omega,t}^{ch,\downarrow} \leq \overline{G}_s^{\downarrow} \cdot \hat{x}_{s,\omega,t}^{ch,\downarrow} \qquad \forall s, \forall \omega, \forall t \tag{3.4}$$

$$\underline{G}_s^{\uparrow} \cdot \hat{x}_{s,\omega,t}^{dis,\uparrow} \leq \hat{g}_{s,\omega,t}^{dis,\uparrow} \leq \overline{G}_s^{\uparrow} \cdot \hat{x}_{s,\omega,t}^{dis,\uparrow} \qquad \forall s, \forall \omega, \forall t \tag{3.5}$$

$$\underline{G}_s^{\downarrow} \cdot \hat{x}_{s,\omega,t}^{dis,\downarrow} \leq \hat{g}_{s,\omega,t}^{dis,\downarrow} \leq \overline{G}_s^{\downarrow} \cdot \hat{x}_{s,\omega,t}^{dis,\downarrow} \qquad \forall s, \forall \omega, \forall t \tag{3.6}$$

$$g_{s,t}^{ch} + \hat{g}_{s,\omega,t}^{ch,\downarrow} \leq \overline{G}_s \qquad \forall s, \forall \omega, \forall t \tag{3.7}$$

$$\hat{g}_{s,\omega,t}^{ch,\uparrow} - g_{s,t}^{ch} \leq 0 \qquad \forall s, \forall \omega, \forall t \tag{3.8}$$

$$g_{s,t}^{dis} + \hat{g}_{s,\omega,t}^{dis,\uparrow} \leq \overline{G}_s \qquad \forall s, \forall \omega, \forall t \tag{3.9}$$

$$\hat{g}_{s,\omega,t}^{dis,\downarrow} - g_{s,t}^{dis} \leq 0 \qquad \forall s, \forall \omega, \forall t \tag{3.10}$$

$$x_{s,t}^{ch} + x_{s,t}^{dis} \leq 1 \qquad \forall s, \forall t \tag{3.11}$$

$$\hat{x}_{s,\omega,t}^{ch,\uparrow} + \hat{x}_{s,\omega,t}^{ch,\downarrow} \leq 1 \qquad \forall s, \forall \omega, \forall t \tag{3.12}$$

$$\hat{x}_{s,\omega,t}^{dis,\uparrow} + \hat{x}_{s,\omega,t}^{dis,\downarrow} \leq 1 \qquad \forall s, \forall \omega, \forall t \tag{3.13}$$

$$\underline{SOC_s} \leq soc_{s,t} \leq \overline{SOC_s} \qquad \forall s, \forall t \tag{3.14}$$

$$soc_{s,t} = SOC_s^{ini} \qquad \forall s, t = N_t \tag{3.15}$$

$$\begin{aligned} soc_{s,t} = SOC_s^{ini} &+ \sum_{\theta}^{t} \eta_s^{ch} \left[g_{s,t}^{ch} + \sum_{\omega} \pi_\omega \cdot \left(-\hat{g}_{s,\omega,t}^{ch,\uparrow} + \hat{g}_{s,\omega,t}^{ch,\downarrow} \right) \right] \\ &- \sum_{\theta}^{t} \eta_s^{dis} \left[g_{s,t}^{dis} + \sum_{\omega} \pi_\omega \cdot \left(\hat{g}_{s,\omega,t}^{dis,\uparrow} - \hat{g}_{s,\omega,t}^{dis,\downarrow} \right) \right] \qquad \forall s, \forall t \end{aligned} \tag{3.16}$$

3.3.2 Pumped-Hydroelectric Storage Modelling

The pumped-hydroelectric storage facilities reserve energy in an upper reservoir in the form of water originating from a lower reservoir. During high electricity demand periods, the PHS station discharges (generates) energy, as the stored water is released through turbines to generate electric power. Conversely, when the electricity demand is low, the station operates in charging (pumping) mode as the water is pumped back to the upper reservoir (Arabkoohsar & Namib, 2021). Adopting the principles applied in (Kazempour et al., 2008), the PHS facility has the ability to operate in discharging mode in the real-time market as shown by constraints (3.5), (3.6), but is not qualified for providing up and down regulation in charging mode. Thus, constraints (3.3), (3.4), (3.7), (3.8), (3.12) are not included in the modelling of the PHS's operation, while constraint (3.16) should be reformulated and take the form of constraint (3.19). Constraints (3.17), (3.18) capture the (dis)charging changeover times of the pumped hydro power plant, which correspond to one hour, for an electricity market operated on an hourly basis.

$$x_{h,t-1}^{ch} + x_{h,t}^{dis} \leq 1 \qquad \forall h, \forall t \tag{3.17}$$

$$x_{h,t-1}^{dis} + x_{h,t}^{ch} \leq 1 \qquad \forall h, \forall t \tag{3.18}$$

$$soc_{h,t} = SOC_h^{ini} + \sum_{\theta}^{t} \left[\eta_h^{ch} \cdot g_{h,t}^{ch} \right] \tag{3.19}$$

$$-\sum_{\theta}^{t}\eta_{h}^{dis}\cdot\left[g_{h,t}^{dis}+\sum_{\omega}\pi_{\omega}\cdot\left(\hat{g}_{h,\omega,t}^{dis,\uparrow}-\hat{g}_{h,\omega,t}^{dis,\downarrow}\right)\right]\qquad\forall h,\forall t$$

3.3.3 Advanced Adiabatic Compressed Air Energy Storage Modelling

An AA-CAES system is an energy storage system based on air compression, expansion and storage in geological underground caverns, as shown in *Figure 3.1*. The available electricity from the grid is used to compress air and inject it into the cavern at high pressures up to 100 bar. The thermal energy produced by the compression stage is stored and then re-used for heating the released compressed air before entering suitable turbines for power generation at the expansion stage. Contrary to the PHS, the AA-CAES has no further operational limitations and is capable of providing both charging and discharging balancing services. Thus, all the constraints of *Section 3.3.1*, are employed to model the function of the AA-CAES. Compressor's and expander's efficiencies $\eta_{c_a}^{com}$, $\eta_{c_a}^{exp}$ imposed in constraints (3.20), (3.21) and (3.22)–(3.25) determine the quantitative correspondence between charged/injected energy and discharged/released energy for the day-ahead and real-time market, respectively.

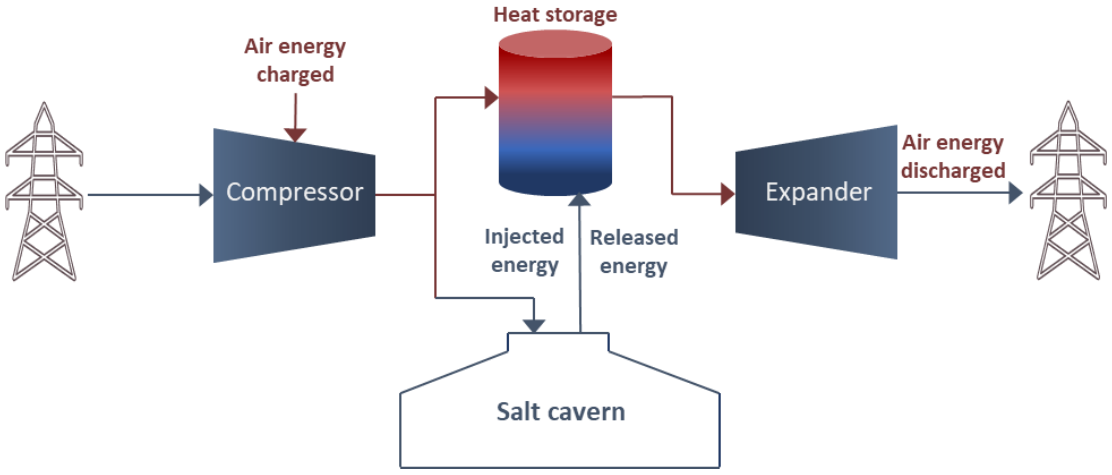

Figure 3.1: The layout of the advanced adiabatic CAES.

$$g_{c_a,t}^{ch}=\frac{g_{c_a,t}^{inj}}{\eta_{c_a}^{com}}\qquad\forall c_a,\forall t \tag{3.20}$$

$$g_{c_a,t}^{dis}=\eta_{c_a}^{exp}\cdot g_{c_a,t}^{rel}\qquad\forall c_a,\forall t \tag{3.21}$$

$$\hat{g}_{c_a,\omega,t}^{ch,\uparrow} = \frac{\hat{g}_{c_a,\omega,t}^{inj,\uparrow}}{\eta_{c_a}^{com}} \qquad \forall c_a, \forall \omega, \forall t \tag{3.22}$$

$$\hat{g}_{c_a,\omega,t}^{ch,\downarrow} = \frac{\hat{g}_{c_a,\omega,t}^{inj,\downarrow}}{\eta_{c_a}^{com}} \qquad \forall c_a, \forall \omega, \forall t \tag{3.23}$$

$$\hat{g}_{c_a,\omega,t}^{dis,\uparrow} = \eta_{c_a}^{exp} \cdot \hat{g}_{c_a,\omega,t}^{rel,\uparrow} \qquad \forall c_a, \forall \omega, \forall t \tag{3.24}$$

$$\hat{g}_{c_a,\omega,t}^{dis,\downarrow} = \eta_{c_a}^{exp} \cdot \hat{g}_{c_a,\omega,t}^{rel,\downarrow} \qquad \forall c_a, \forall \omega, \forall t \tag{3.25}$$

3.3.4 Diabatic Compressed Air Energy Storage Modelling

Diabatic or conventional CAES (D-CAES), is another electricity storage technology, which is governed by the same fundamental operating principles as the adiabatic CAES system, thus the majority of the constraints are common for both systems. The main difference lies on the fact that the thermal energy released during the compression stage of the diabatic system is not stored. Therefore, an exogenous energy source, such as natural gas, is required to heat the released air, in order to drive the turbine and generate electricity, as illustrated by *Figure 3.2*.

As with the adiabatic CAES case, the D-CAES also follows the operational constraints analytically presented in *Section 3.3.1*. In this section only the function mechanism differentiations ruling the diabatic CAES system, are presented. Constraints (3.26), (3.27) and (3.28)–(3.31) serve the same purpose for the D-CAES as the constraints (3.20), (3.21) and (3.22)–(3.25) for the AA-CAES, equivalently. However, the difference with the AA-CAES, lies in the fact that the energy discharged by the D-CAES consists of the summation of the energy equivalent of the air released from the cavern and the natural gas $exp_{c_d,t}$, required for its heating. Constraints (3.32)–(3.35) ensure that the proper ratio between these two energy sources is maintained for both the day-ahead and real-time dispatch. This ratio emerges from the diabatic CAES McIntosh power plant case in Alabama, which requires 0.67 kWh of electricity before the compression stage and 1.17 kWh of natural gas, in order to generate 1 kWh of electricity (Madlener & Latz, 2013), (Greenblatt et al., 2007). Constraints (3.35)–(3.37) impose capacity limits for the required natural gas for both trading floors, while constraint (3.38) excludes the simultaneous natural gas upward and downward provision for the real-time market.

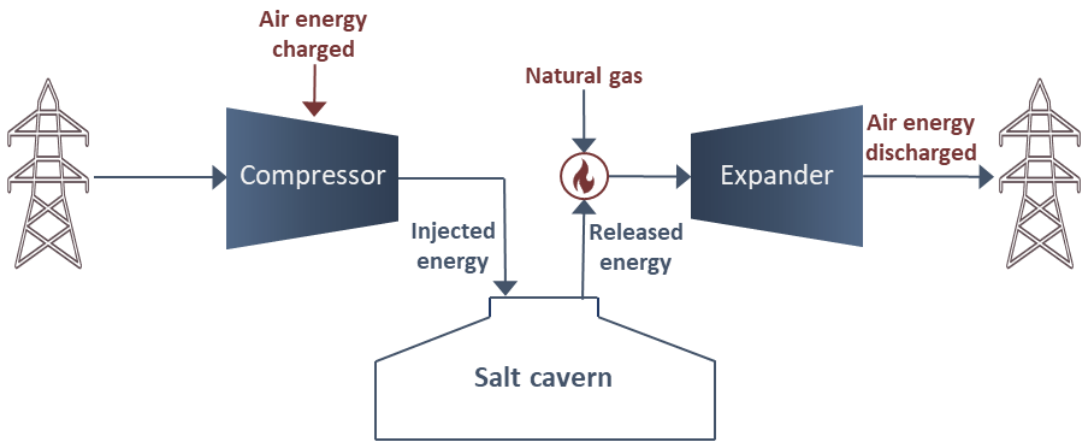

Figure 3.2: The layout of the diabatic CAES.

$$g_{c_d,t}^{ch} = \frac{g_{c_d,t}^{inj}}{\eta_{c_d}^{com}} \qquad \forall c_d, \forall t \tag{3.26}$$

$$g_{c_d,t}^{dis} = \eta_{c_d}^{exp} \cdot \left(g_{c_d,t}^{rel} + exp_{c_d,t}\right) \qquad \forall c_d, \forall t \tag{3.27}$$

$$\hat{g}_{c_d,\omega,t}^{ch,\uparrow} = \frac{\hat{g}_{c_d,\omega,t}^{inj,\uparrow}}{\eta_{c_d}^{com}} \qquad \forall c_d, \forall \omega, \forall t \tag{3.28}$$

$$\hat{g}_{c_d,\omega,t}^{ch,\downarrow} = \frac{\hat{g}_{c_d,\omega,t}^{inj,\downarrow}}{\eta_{c_d}^{com}} \qquad \forall c_d, \forall \omega, \forall t \tag{3.29}$$

$$\hat{g}_{c_d,\omega,t}^{dis,\uparrow} = \eta_{c_d}^{exp} \cdot \left(\hat{g}_{c_d,\omega,t}^{rel,\uparrow} + \widehat{exp}_{c_d,\omega,t}^{\uparrow}\right) \qquad \forall c_d, \forall \omega, \forall t \tag{3.30}$$

$$\hat{g}_{c_d,\omega,t}^{dis,\downarrow} = \eta_{c_d}^{exp} \cdot \left(\hat{g}_{c_d,\omega,t}^{rel,\downarrow} + \widehat{exp}_{c_d,\omega,t}^{\downarrow}\right) \qquad \forall c_d, \forall \omega, \forall t \tag{3.31}$$

$$exp_{c_d,t} = \frac{1.17}{0.402} g_{c_d,t}^{rel} \qquad \forall c_d, \forall t \tag{3.32}$$

$$\widehat{exp}_{c_d,\omega,t}^{\uparrow} = \frac{1.17}{0.402} \hat{g}_{c_d,\omega,t}^{rel,\uparrow} \qquad \forall c_d, \forall \omega, \forall t \tag{3.33}$$

$$\widehat{exp}_{c_d,\omega,t}^{\downarrow} = \frac{1.17}{0.402} \hat{g}_{c_d,\omega,t}^{rel,\downarrow} \qquad \forall c_d, \forall \omega, \forall t \tag{3.34}$$

$$\underline{EXP}_s \cdot x_{c_d,t}^{exp} \leq exp_{c_d,t} \leq \overline{EXP}_s \cdot x_{c_d,t}^{exp} \qquad \forall c_d, \forall t \tag{3.35}$$

$$\underline{EXP}_s^{\uparrow} \cdot \hat{x}_{c_d,\omega,t}^{exp,\uparrow} \leq \widehat{exp}_{c_d,\omega,t}^{\uparrow} \leq \overline{EXP}_s^{\uparrow} \cdot \hat{x}_{c_d,\omega,t}^{exp,\uparrow} \qquad \forall c_d, \forall \omega, \forall t \tag{3.36}$$

$$\underline{EXP}_s^{\downarrow} \cdot \hat{x}_{c_d,\omega,t}^{exp,\downarrow} \leq \widehat{exp}_{c_d,\omega,t}^{\downarrow} \leq \overline{EXP}_s^{\downarrow} \cdot \hat{x}_{c_d,\omega,t}^{exp,\downarrow} \qquad \forall c_d, \forall \omega, \forall t \tag{3.37}$$

$$\hat{x}_{c_b,\omega,t}^{exp,\uparrow} + \hat{x}_{c_b,\omega,t}^{exp,\downarrow} \leq 1 \qquad \forall c_d, \forall \omega, \forall t \tag{3.38}$$

3.3.5 Battery Energy Storage Modelling

As already mentioned, Li-ion batteries constitute the dominant battery technologies nowadays and their market integration does not illustrate any particular modelling eccentricities. In particular, the application of the constraints developed in *Section 3.3.1*, fully describes the operation and participation of a Li-ion battery in energy markets.

3.3.6 Electricity and Natural Gas Market Clearing Modelling

Historically, natural gas markets are developed mainly on long-term contracts with confined short-term variability, while electricity and gas markets are cleared independently. However, a coupled market design allows for increased operational flexibility and improved communication between the two systems, thus it is adopted in this work (*Figure 3.3*). The objective function (3.39) represents a stochastic day-ahead and real-time coupled market clearing procedure (Ordoudis et al., 2019), conducted by the MO. The aim is to determine the optimal energy production and consumption dispatch, with respect to social welfare maximization. Equivalently, the objective function can represent the total market cost minimization (economic dispatch), as both electricity and natural gas demands are assumed to be inelastic (Ordoudis et al., 2019). The stochastic approach is preferred over the sequential one, in order to ensure perfect temporal coordination and lower expected operating costs (Morales et al., 2014).

It is important to emphasize that the D-CAES's power generation cost is not fully included in the objective function, as this would lead to double counting it (Ordoudis et al., 2019), since it operates equivalently to a gas-fired power plant i.e., as a power producer and a natural gas consumer. More specifically, the objective function includes only the D-CAES's generation cost derived from the use of electricity $\eta_{c_d}^{exp} \cdot g_{c_d,t}^{rel}$, while the production cost from natural gas is omitted, so as not to be double-measured. The operating cost of this unit can be explicitly determined through the natural gas balancing constraints (3.41) and (3.43). Constraints (3.40) and (3.41) apply the electric and natural gas balance for each bus/node equivalently, enforcing transmission capacity limits at the day-ahead stage. Similarly, constraints (3.42) and (3.43) offset the imbalances caused by the uncertain wind power generation, activating reserve procurements, and employing wind power spillage and load shedding. Electricity and natural gas prices for the day-

ahead and real-time market are endogenously generated as dual variables from the above analyzed energy balance constraints.

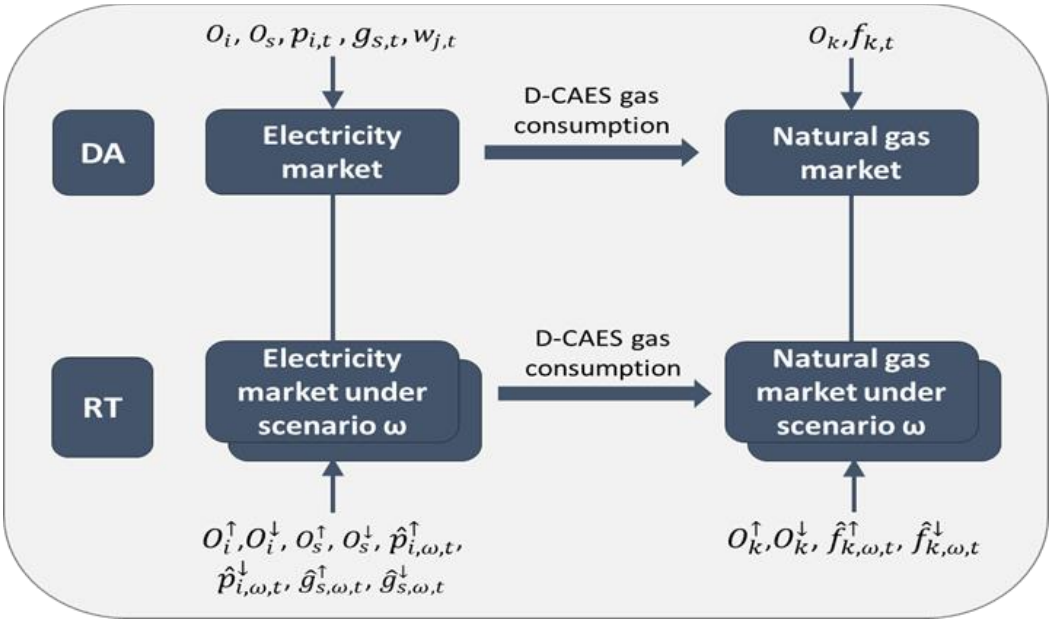

Figure 3.3: Coupled electricity and natural gas market structure.

Constraints (3.44), (3.45), (3.46) define the day-ahead upper and lower capacity limits for conventional power, wind and natural gas generating units, respectively. Constraints (3.47), (3.48) and (3.49), (3.50) define the capacity limits for reserve deployments offered by each conventional power plant and natural gas generating unit. Constraints (3.51), (3.52) and (3.53), (3.54) capture the interdependency between the scheduled energy dispatch and the activated reserves for the above units and ensure that the overall energy production does not exceed maximum capacity. Moreover, constraints (3.55), (3.56) and (3.57) guarantee that the wind power spillage cannot surpass actual wind power generation and that electricity and natural gas load shedding cannot exceed the consumption of these energy sources. Constraints (3.58) and (3.59) apply capacity limits to power network transmission lines, while constraints (3.60) and (3.61) determine the upper and lower bounds of voltage angle at each power bus. Finally, constraints (3.62) and (3.63) dictate *n1* as the slack bus, for both the day-ahead and the real-time market.

$$
\begin{aligned}
\textbf{\textit{maximize}} \quad & \sum_{\boldsymbol{t}} \Bigg\{ - \sum_{i \in IaN} O_i \cdot p_{i,t} - \sum_{k \in KaR} O_k \cdot f_{k,t} + \sum_{h \in SaN} O_h \cdot \left(g_{h,t}^{ch} - g_{h,t}^{dis} \right) \\
& + \sum_{c_a \in SaN} O_{c_a} \cdot \left(g_{c_a,t}^{ch} - g_{c_a,t}^{dis} \right) + \sum_{c_d \in SaN} O_{c_d} \cdot \left(g_{c_d,t}^{ch} - \eta_{c_d}^{exp} \cdot g_{c_d,t}^{rel} \right) \\
& + \sum_{li \in SaN} O_{li} \cdot \left(g_{li,t}^{ch} - g_{li,t}^{dis} \right) + \sum_{d^{EL} \in DaN} U_d^{EL} \cdot \mathrm{L}_{d,t}^{EL} \\
& + \sum_{d^{NG} \in DaR} U_d^{NG} \cdot \mathrm{L}_{d,t}^{NG} \\
& - \sum_{\omega} \pi_\omega \cdot \Bigg[\sum_{i \in IaN} \left(O_i^{\uparrow} \cdot \hat{p}_{i,\omega,t}^{\uparrow} - O_i^{\downarrow} \cdot \hat{p}_{i,\omega,t}^{\downarrow} \right) \\
& + \sum_{k \in KaR} \left(O_k^{\uparrow} \cdot \hat{f}_{k,\omega,t}^{\uparrow} - O_k^{\downarrow} \cdot \hat{f}_{k,\omega,t}^{\downarrow} \right) + \sum_{h \in HaN} \left(O_h^{\uparrow} \cdot \hat{g}_{h,\omega,t}^{\uparrow} - O_h^{\downarrow} \cdot \hat{g}_{h,\omega,t}^{\downarrow} \right) \\
& + \sum_{c_a \in SaN} O_{c_a}^{\uparrow} \cdot \left(\hat{g}_{c_a,\omega,t}^{dis,\uparrow} - \hat{g}_{c_a,\omega,t}^{ch,\uparrow} \right) - \sum_{c_a \in SaN} O_{c_a}^{\downarrow} \cdot \left(\hat{g}_{c_a,\omega,t}^{dis,\downarrow} - \hat{g}_{c_a,\omega,t}^{ch,\downarrow} \right) \\
& + \sum_{c_d \in SaN} O_{c_d}^{\uparrow} \cdot \left(\eta_{c_d}^{exp} \cdot \hat{g}_{c_d,\omega,t}^{rel,\uparrow} - \hat{g}_{c_d,\omega,t}^{ch,\uparrow} \right) \\
& - \sum_{c_d \in SaN} O_{c_d}^{\downarrow} \cdot \left(\eta_{c_d}^{exp} \cdot \hat{g}_{c_d,\omega,t}^{rel,\downarrow} - \hat{g}_{c_d,\omega,t}^{ch,\downarrow} \right) \\
& + \sum_{li \in SaN} O_{li}^{\uparrow} \cdot \left(\hat{g}_{li,\omega,t}^{dis,\uparrow} - \hat{g}_{c_a,\omega,t}^{ch,\uparrow} \right) - \sum_{li \in SaN} O_{li}^{\downarrow} \cdot \left(\hat{g}_{li,\omega,t}^{dis,\downarrow} - \hat{g}_{c_a,\omega,t}^{ch,\downarrow} \right) \\
& + \sum_{d^{EL} \in DaN} VOLL_{d,t}^{EL} \cdot l_{d,\omega,t}^{EL,sh} + \sum_{d^{NG} \in DaR} VOLL_{d,t}^{NG} \cdot l_{d,\omega,t}^{NG,sh} \Bigg] \Bigg\}
\end{aligned}
\tag{3..39}
$$

s.t.

$$
\begin{aligned}
& \sum_{i \in IaN} p_{i,t} + \sum_{j \in JaN} w_{j,t} - \sum_{h \in SaN} \left(g_{h,t}^{ch} - g_{h,t}^{dis} \right) - \sum_{c_a \in SaN} \left(g_{c_a,t}^{ch} - g_{c_a,t}^{dis} \right) \\
& \quad - \sum_{c_d \in SaN} \left(g_{c_d,t}^{ch} - g_{c_d,t}^{dis} \right) - \sum_{li \in SaN} \left(g_{li,t}^{ch} - g_{li,t}^{dis} \right) - \sum_{d^{EL} \in DaN} L_{d,t}^{EL} \\
& \quad - \sum_{m \in NaM} B_{n,m} \cdot \left(\delta_{n,t} - \delta_{m,t} \right) = 0 \qquad : \left[\lambda_{n,t}^{EL} \right] \qquad \forall n, \forall t
\end{aligned}
\tag{3.40}
$$

$$\sum_{k\in KaR} f_{k,t} - \sum_{d^{NG}\in DaR} L_{d,t}^{NG} - \sum_{c_d\in C_d aR} heatrate\cdot exp_{c_d,t} = 0 \quad : \left[\lambda_{r,t}^{NG}\right] \quad \forall n, \forall t \tag{3.41}$$

$$\begin{aligned}
&\sum_{i\in IaN}\left(\hat{p}_{i,\omega,t}^{\uparrow} - \hat{p}_{i,\omega,t}^{\downarrow}\right) + \sum_{h\in SaN}\left(\hat{g}_{h,\omega,t}^{dis,\uparrow} - \hat{g}_{h,\omega,t}^{dis,\downarrow}\right) - \sum_{c_a\in SaN}\left(\hat{g}_{c_a,\omega,t}^{ch,\uparrow} - \hat{g}_{c_a,\omega,t}^{ch,\downarrow}\right) \\
&\quad + \sum_{c_a\in SaN}\left(\hat{g}_{c_a,\omega,t}^{dis,\uparrow} - \hat{g}_{c_a,\omega,t}^{dis,\downarrow}\right) \\
&\quad - \sum_{c_d\in SaN}\left(\hat{g}_{c_d,\omega,t}^{ch,\uparrow} - \hat{g}_{c_d,\omega,t}^{ch,\downarrow}\right) + \sum_{c_d\in SaN}\left(\hat{g}_{c_d,\omega,t}^{dis,\uparrow} - \hat{g}_{c_d,\omega,t}^{dis,\downarrow}\right) \\
&\quad - \sum_{li\in SaN}\left(\hat{g}_{li,\omega,t}^{ch,\uparrow} - \hat{g}_{li,\omega,t}^{ch,\downarrow}\right) \\
&\quad + \sum_{li\in SaN}\left(\hat{g}_{li,\omega,t}^{dis,\uparrow} - \hat{g}_{li,\omega,t}^{dis,\downarrow}\right) + \sum_{j\in JaN}\left(W_{j,\omega,t}^{RT} - w_{j,t} - w_{j,\omega,t}^{sp}\right) \\
&\quad + \sum_{d^{EL}\in DaN} l_{d,\omega,t}^{EL,sh} \\
&\quad - \sum_{m\in NaM} B_{n,m}\cdot\left(\hat{\delta}_{n,\omega,t} - \delta_{n,t} + \delta_{m,t} - \hat{\delta}_{m,\omega,t}\right) \\
&\quad = 0: \quad \left[\hat{\lambda}_{n,\omega,t}^{EL}\right] \quad \forall n, \forall\omega, \forall t
\end{aligned} \tag{3.42}$$

$$\begin{aligned}
&\sum_{k\in KaN}\left(\hat{f}_{k,\omega,t}^{\uparrow} - \hat{f}_{k,\omega,t}^{\downarrow}\right) + \sum_{d^{NG}\in DaR} l_{d,\omega,t}^{NG,sh} \\
&\quad - \sum_{c_d\in C_d aR} heatrate\cdot\left(\widehat{exp}_{c_d,\omega,t}^{\uparrow} - \widehat{exp}_{c_d,\omega,t}^{\downarrow}\right) = 0 \\
&\quad : \left[\hat{\lambda}_{r,\omega,t}^{NG}\right] \quad \forall r, \forall\omega, \forall t
\end{aligned} \tag{3.43}$$

$$0 \le p_{i,t} \le \overline{P}_i \qquad \forall i, \forall t \tag{3.44}$$

$$0 \le w_{j,t} \le \overline{W}_j \qquad \forall j, \forall t \tag{3.45}$$

$$0 \le f_{k,t} \le \overline{F}_k \qquad \forall k, \forall t \tag{3.46}$$

$$0 \le \hat{p}_{i,\omega,t}^{\uparrow} \le \overline{P}_i^{\uparrow} \qquad \forall i, \forall\omega, \forall t \tag{3.47}$$

$$0 \le \hat{p}_{i,\omega,t}^{\downarrow} \le \overline{P}_i^{\downarrow} \qquad \forall i, \forall\omega, \forall t \tag{3.48}$$

$$0 \le \hat{f}_{k,\omega,t}^{\uparrow} \le \overline{F}_k^{\uparrow} \qquad \forall k, \forall\omega, \forall t \tag{3.49}$$

$$0 \le \hat{f}_{k,\omega,t}^{\downarrow} \le \overline{F}_k^{\downarrow} \qquad \forall k, \forall\omega, \forall t \tag{3.50}$$

$$p_{i,t} + \hat{p}_{i,\omega,t}^{\uparrow} \le \overline{P}_i \qquad \forall i, \forall\omega, \forall t \tag{3.51}$$

$$\hat{p}^{\downarrow}_{i,\omega,t} - p_{i,t} \leq 0 \qquad \forall i, \forall \omega, \forall t \tag{3.52}$$

$$f_{k,t} + \hat{f}^{\uparrow}_{k,\omega,t} \leq \overline{F}_k \qquad \forall k, \forall \omega, \forall t \tag{3.53}$$

$$\hat{f}^{\downarrow}_{k,\omega,t} - f_{k,t} \leq 0 \qquad \forall k, \forall \omega, \forall t \tag{3.54}$$

$$0 \leq w^{sp}_{j,\omega,t} \leq W^{RT}_{j,\omega,t} \qquad \forall j, \forall \omega, \forall t \tag{3.55}$$

$$l^{EL,sh}_{d,\omega,t} \leq \mathrm{L}^{EL}_{d,t} \qquad \forall d^{EL}, \forall \omega, \forall t \tag{3.56}$$

$$l^{NG,sh}_{d,\omega,t} \leq \mathrm{L}^{NG}_{d,t} \qquad \forall d^{NG}, \forall \omega, \forall t \tag{3.57}$$

$$-\overline{T}_{n,m} \leq B_{n,m} \cdot \left(\delta_{n,t} - \delta_{m,t}\right) \leq \overline{T}_{n,m} \qquad \forall (n,m) \in NaM, \forall t \tag{3.58}$$

$$-\overline{T}_{n,m} \leq B_{n,m} \cdot \left(\hat{\delta}_{n,\omega,t} - \hat{\delta}_{m,\omega,t}\right) \leq \overline{T}_{n,m} \qquad \forall (n,m) \in NaM, \forall \omega, \forall t \tag{3.59}$$

$$-\pi \leq \delta_{n,t} \leq \pi \qquad \forall n, \forall t \tag{3.60}$$

$$-\pi \leq \hat{\delta}_{n,\omega,t} \leq \pi \qquad \forall n, \forall \omega, \forall t \tag{3.61}$$

$$\delta_{n_1,t} = 0 \qquad \forall n = n_1, \forall t \tag{3.62}$$

$$\hat{\delta}_{n_1,\omega,t} = 0 \qquad \forall n = n_1, \forall \omega, \forall t \tag{3.63}$$

3.4 Application study

3.4.1 Data

The applicability of the proposed MILP optimization framework is illustrated using an integrated energy system, consisting of a modified 24-bus IEEE Reliability Test System and a single-node natural gas network, analytically presented at *Figure 3.5* and *Figure 3.6*, respectively. Apropos of the 24-bus electricity network, considering an imaginary horizontal line between buses $n11$, $n12$, $n24$ and $n3$, $n9$, $n10$, the power grid can be divided into two different areas, the upper and the lower. The difference between these two areas lies in the fact that the upper area is characterized by increased electricity generation and limited consumption, while in the lower area an exact opposite scheme takes place. The reason for this separation pertains to the power network congestion case and will be analyzed in detail in *subsection 3.4.3*.

The integrated system includes 10 conventional power plants, 2 wind farms, 2 gas suppliers, 17 electricity loads, 1 natural gas load and 4 electricity storage facilities (PHS, AA-CAES, D-CAES and Li-ion battery). It is important to emphasize that the diabatic CAES system constitutes the means of interconnection of the two systems, as it acts as

generators in the electricity market and as demand loads in the natural gas market. The total installed capacity of the conventional units accounts for 3,918 MW, while for wind farms this capacity reaches up to 350 MW.

Wind power generation uncertainty is modelled through a dual scenario approach i.e., a high wind generation scenario $\omega 1$, where the two wind farms operate at their maximum capacity and a low wind generation scenario $\omega 2$, where their total power production reaches up to 70 MW. Their occurrence probability is estimated at 0.8 and 0.2, respectively. Total electricity demand fluctuates over the 24-hour horizon between 1,517 MW and 2,989 MW, while the corresponding hourly gas demand remains constant throughout the day and is equal to 1,210 kcf, as shown in *Figure 3.4*. The value of lost load $VOLL_{d,t}^{EL}, VOLL_{d,t}^{NG}$ equals 2,000 \$/MWh and 600 \$/kcf, respectively.

Furthermore, *Table 3.1* shows the electricity storage technologies' quantitative and economic figures, extracted from (Madlener & Latz, 2013), (Jülch, 2016). In particular, (dis)charging energy and reserve capacities, maximum and initial state-of-charge (dis)charging efficiency parameters and cost offers for each storage technology in both the day-ahead and the real-time stage, are presented. It is critical to emphasize that a price premium is applied in the real-time market. In an economic perspective, this means that $O^{\uparrow} > O$ and $O^{\downarrow} < O$, for each electricity and natural gas market agent.

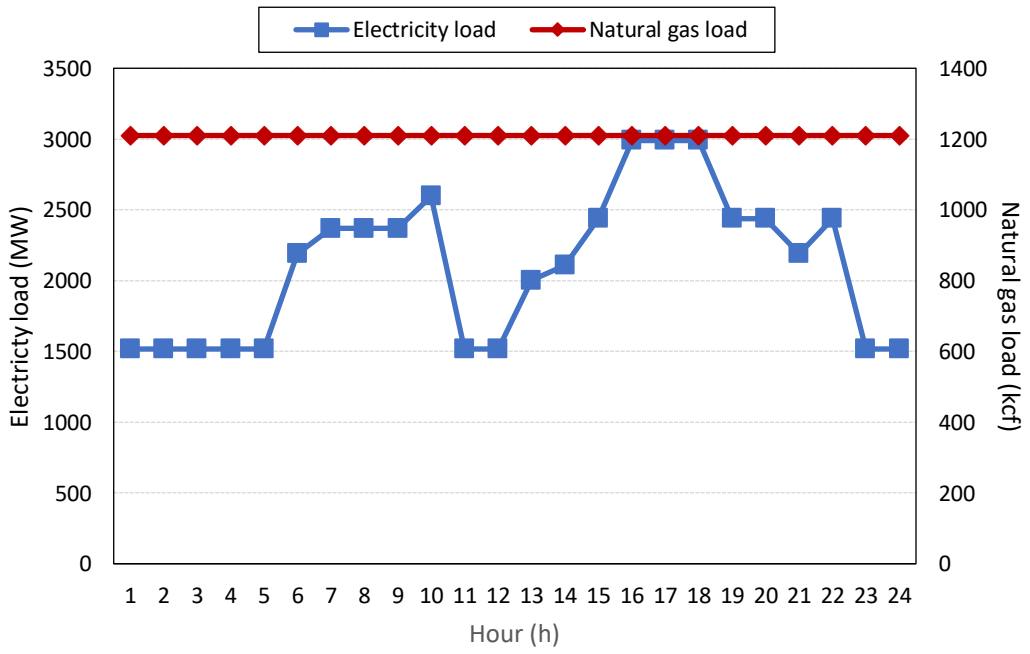

Figure 3.4: Total hourly electricity and natural gas load.

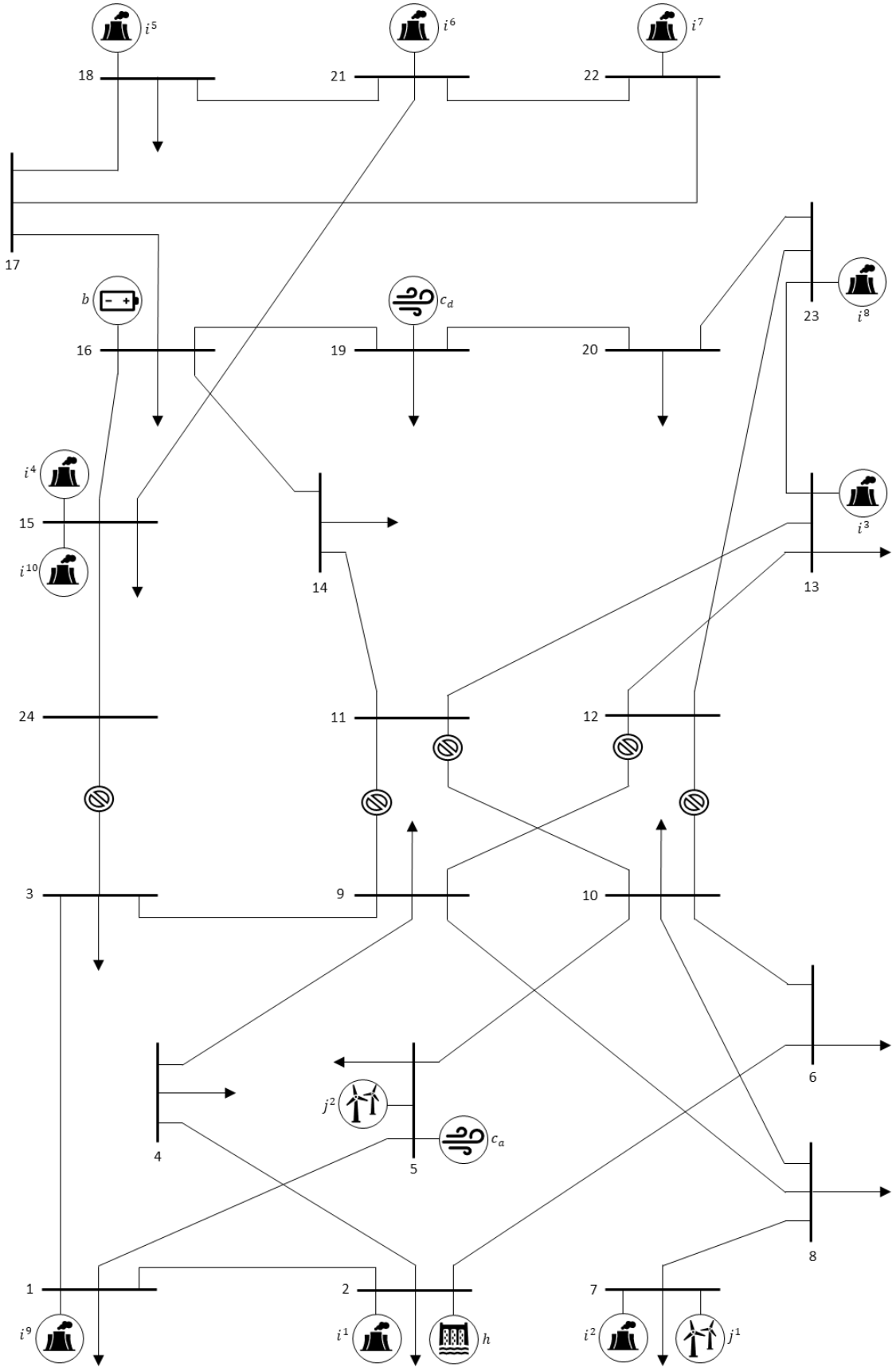

Figure 3.5: Modified 24-bus IEEE Reliability Test System.

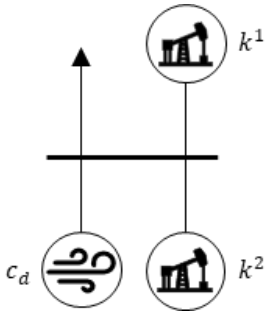

Figure 3.6: Single-node natural gas network.

	$\overline{G_s}$ (MW)	$\overline{G_s^{\uparrow}}$ (MW)	$\overline{G_s^{\downarrow}}$ (MW)	$\overline{SOC_s}$ (MW)	SOC_s^{ini} (MW)	η_s^{ch}	η_s^{dis}	O_s $(\$/MWh)$	$O_s^{\uparrow}$ $(\$/MWh)$	$O_s^{\downarrow}$ $(\$/MWh)$
PHS	*400*	*40*	*40*	*400*	*200*	*0.86*	*0.88*	*5*	*5.5*	*4.5*
AA-CAES	*260*	*26*	*26*	*260*	*100*	*0.81*	*0.86*	*4*	*4.4*	*3.6*
D-CAES	*300*	*80*	*80*	*300*	*100*	*0.6*	*0.63*	*4*	*4.4*	*3.6*
Li-ion	*130*	*13*	*13*	*130*	*100*	*0.98*	*0.98*	*7*	*7.7*	*6.3*

Table 3.1: Data for electricity storage technologies.

3.4.2 Uncongested power network

The proposed MILP framework is applied to the integrated energy system assuming an uncongested power network and solved using GAMS/CPLEX (Brooke et al., 1998). The coupled electricity and natural gas market operates in a perfectly competitive settlement; thus, all market agents offer their generation at marginal cost.

The integration of the pumped-hydro, adiabatic/diabatic CAES and Li-ion battery electricity storage systems in the proposed integrated energy system, proves to be particularly beneficial for the MO, to balance the generation-consumption dipole and optimize economic dispatch. In particular, *Figure 3.7* illustrates the day-ahead electricity locational marginal prices, both when the four storage technologies are active (ELMPs) and when there are no storage (NS) units (ELMPs NS) in the power network. It is obvious that the ELMPs NS are significantly higher compared to the normal ELMPs, since the only units that provide electricity into the mix, besides the wind power plants, are the more expensive conventional power plants. It is important to point out that even at the time periods $t2-t5, t11-t12$, when the ELMPs are higher that the ELMPs NS, it is beneficial for the market. In particular, at these periods, as shown in *Figure 3.8*, the storage units

charge electricity and thus constitute a positive factor for the social welfare maximization. To confirm the economic importance of the establishment of electricity storage facilities, the social welfare in both cases is calculated. In the case where all storage units are present, the social welfare is estimated at 9,134,065.3 $ and it is 6.2% higher compared to the NS case.

By combining *Figure 3.7* and *Figure 3.8,* the operation of storage units can also be analyzed. At time periods $t6 - t10$ and $t16 - t18$, where the day-ahead prices range at high levels (89 $/MWh to 117 $/MWh) due to increased electricity demand, the storage systems operate in discharging mode to ensure energy balance and minimize total cost. For a better understanding of *Figure 3.8*, it is clarified that the negative values of the y-axis correspond to the discharging energy amounts of the aforementioned storage technologies. On the other hand, in the remaining time periods $t1 - t5, t11, t23$ when the requirements for electricity are lower, the storage systems operate in charging mode to take advantage of the low day-ahead prices of 28.22 $/MWh to 52.9 $/MWh. Despite the fact that the natural gas demand is stable during the daily horizon, a GLMP fluctuation is observed, which is due to the power generation by the D-CAES. More specifically, for the time periods $t16 - t18$, the diabatic CAES discharges the highest hourly amount of electricity i.e.,127.1 MWh. As a result, the more expensive natural gas supplier also needs to provide gas to meet the demand, thus increasing the GLMP from 3.5 $/kcf to 4.2 $/kcf.

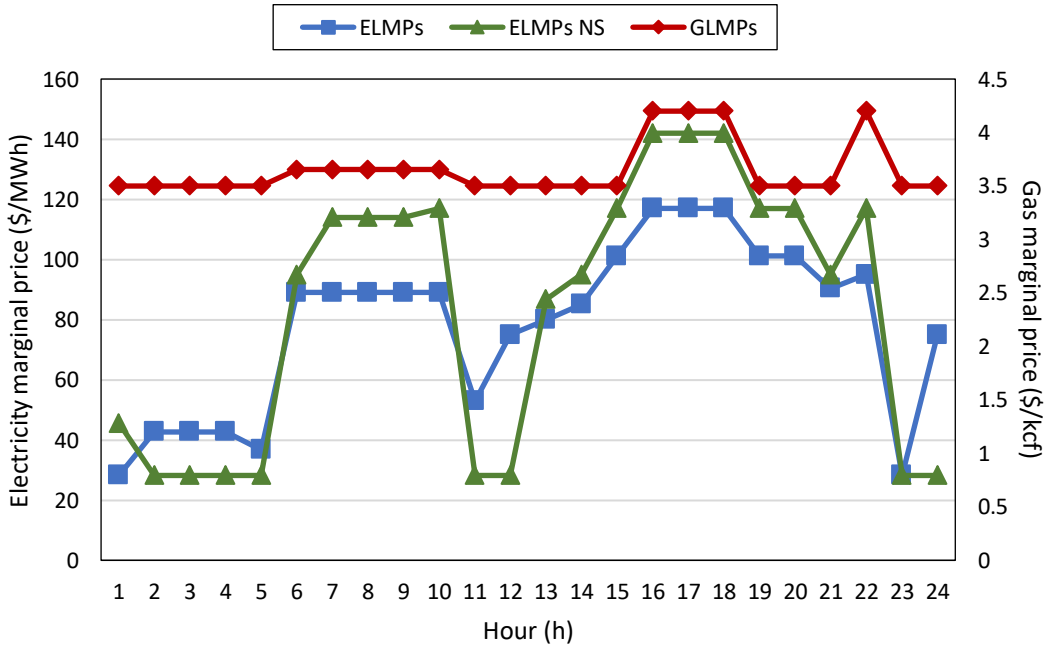

Figure 3.7: Day-ahead electricity and gas market clearing prices.

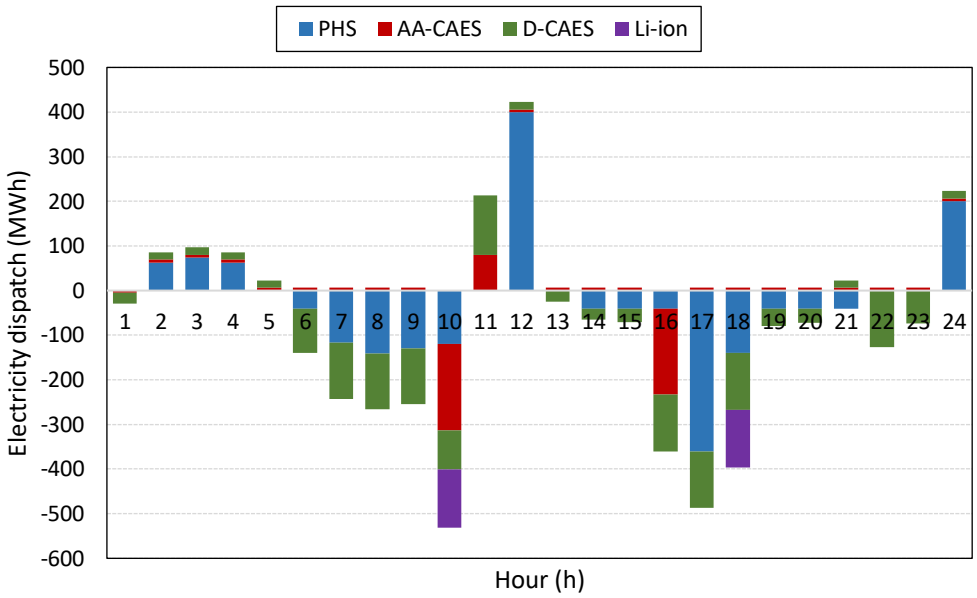

Figure 3.8: Day-ahead (dis)charging energy dispatch for storage systems.

Figure 3.9 shows the real-time ELMPs for two wind power generation scenarios i.e., a high and a low. In the high wind generation scenario $\omega 1$ realization, the RT prices range in lower levels compared those of the DA market with the maximum clearing price reaching up to 95.4 \$/MWh. This happens, since the almost zero cost electricity production from wind farms contributes to a great extent into the system, thus lowering the electricity prices. The exact opposite situation is observed with the low wind generation scenario $\omega 2$, where due to the low production in cheaper energy, generators with higher cost offers enter the energy mix in order to meet the demand. Consequently, the equivalent prices fluctuate at particularly high levels reaching up to 203.5 \$/MWh for time periods $t16 - t18$. In addition to the entry of more expensive producers into the market, as already mentioned, a price premium is applied in the RT market. Thus, the upward reserve activation of power producers is provided at higher bids compared to their day-ahead electricity dispatch.

The right vertical axis of *Figure 3.10* provides the real-time natural gas prices (lines with markers) for both high and low wind generation scenarios, ranging from 3.15 \$/kcf to 4.53 \$/kcf and 3.15 \$/kcf to 4.62 \$/kcf, respectively. The figure also presents the amount of electricity (columns) that the diabatic CAES system provides to the RT market, by activating charging downward reserves (positive values) and discharging upward reserves (negative values). It is also important to note that the diabatic CAES operates in

discharging mode in the real-time market at the same time periods as in the day-ahead market. The natural gas pricing scheme appears to follow the same basic principles as the electricity one, since a price premium policy is also preserved and gas prices correspond to the wind power production stochasticity. In particular, when wind power production is low (scenario $\omega 2$), the D-CAES system is required to supply additional electricity into the real-time electricity market (discharging upward reserves), and therefore engage higher quantities of natural gas as fuel. This, of course leads to an increase in gas prices, as shown in *Figure 3.10*. In particular, the D-CAES system throughout the 24-hours horizon consumes a total amount of natural gas corresponding to 900 MWh, in order to provide upward discharging balancing services in electricity market. The exact opposite scenery occurs in the case of scenario $\omega 1$, where the high production of wind farms results in a decrease in natural gas demand and subsequently in its price. In fact, in scenario $\omega 1$, the diabatic system purchases a quantity of gas equivalent to only 60 MWh in total, since the requirements for electricity in the real-time market are limited.

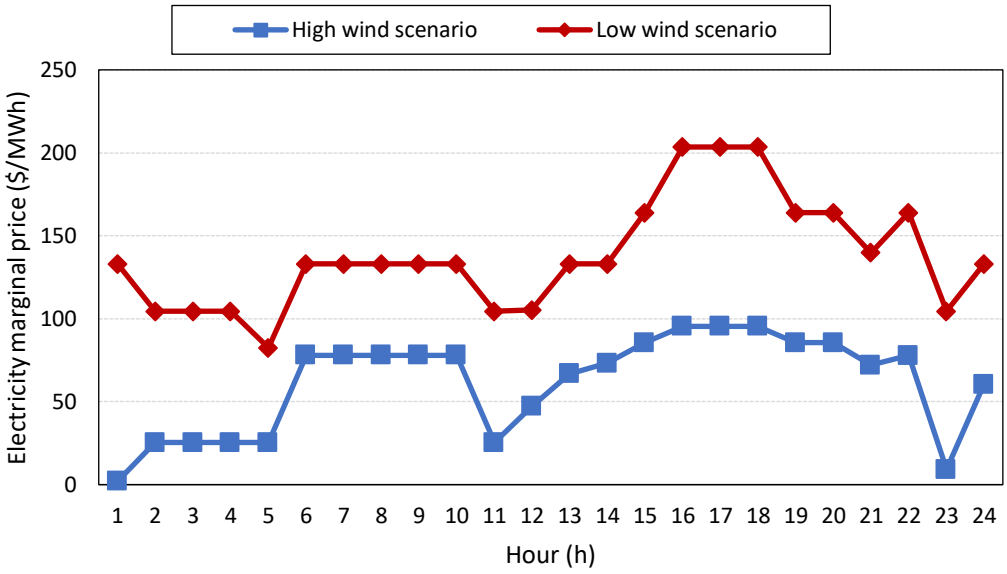

Figure 3.9: Real-time electricity market clearing prices.

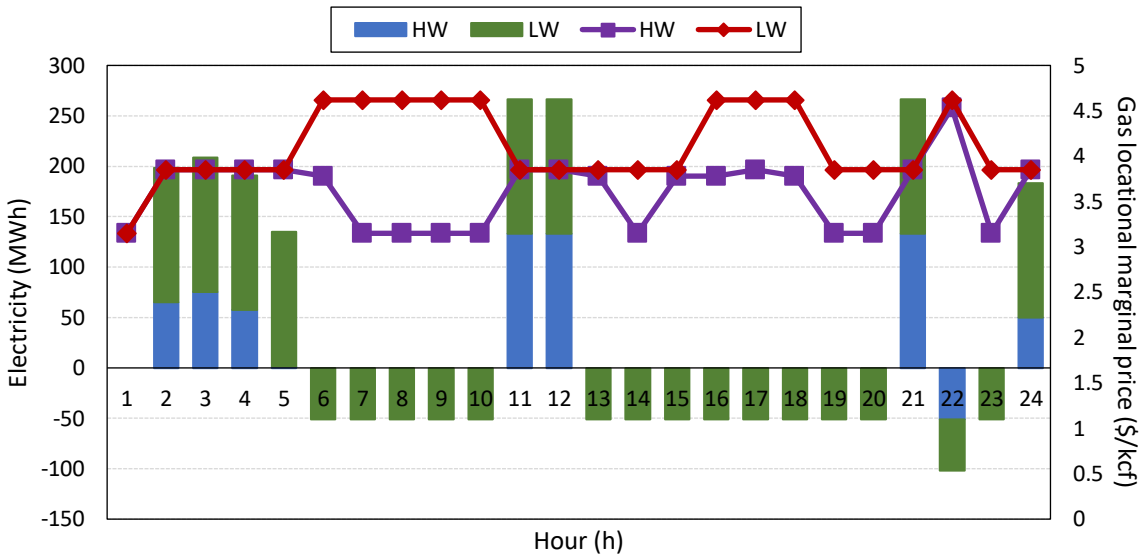

Figure 3.10: Real-time gas market clearing prices and D-CAES dispatch.

Figure 3.11 depicts electricity storage systems' day-ahead and overall profits over a daily time horizon. More specifically, the D-CAES system earns 80,056.9 $ in the day-ahead market, making it the most profitable among storage technologies in the integrated energy system. This is attributed to the fact that the diabatic CAES provides the largest amount of electricity during the 24 hours into the market, through its discharging operation. The market operator, who aims at maximizing social welfare, sets D-CAES to produce the largest amount of energy, since its overall cost is lower compared to the rest of the storage technologies. The primary reason for this low cost is the fact that this energy on a great extent derives from the combustion of natural gas, the price of which is noticeably lower compared to the electricity. The profits of PHS, AA-CAES and Li-ion battery in the DA market are summarized in 67,035.8 $, 23,558.7 $ and 21,935.4 $, respectively.

Regarding the overall profits of the four storage technologies, a particularly significant decrease compared to their day-ahead profits, is noticed. The main reason is the provision of charging downward reserves in the real-time market, in order to preserve energy balance and ensure social welfare maximization. More specifically, the activation of charging/discharging downward reserves is costly for the storage systems, either due to the extra power charged or because the system pays back to the market at

RT price for the energy not produced. In addition to the cost of purchasing the energy, each storage facility is also charged for the operating charging costs.

As shown in *Figure 3.11*, with the exception of PHS system, which provide only discharging reserves, the rest of the storage technologies offer significant amounts of charging downward reserves, which constitute a cost factor. This is also the reason why the DA profits of the PHS system are reduced proportionally less, compared to the other storage systems. However, it is important to highlight that the formulated pricing scheme for the coupled electricity and natural gas market clearing model, ensures cost recovery for each electricity storage technology.

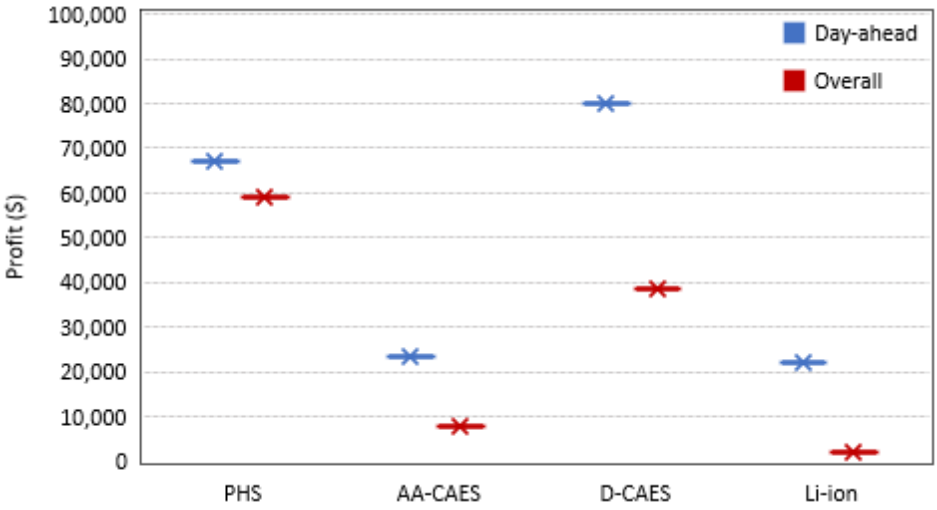

Figure 3.11: Day-ahead and overall profits for electricity storage systems.

3.4.3 Congested power network

As already pointed out in *subsection 3.4.2*, the power grid is further divided into the upper and lower area, due to different levels of electricity generation and consumption. In this case study, this topological feature of the network is utilized, in order to draw useful conclusions for the configuration of electricity prices and the operation of energy storage technologies, under power network congestion. The congestion is a result of the decreased capacity of transmission lines connecting buses $n3$, $n9$, $n10$, $n11$, $n12$ and $n24$, from 1,600 MW to 200 MW.

As shown in *Figure 3.12*, due to the impeded energy transfer among buses, electricity local marginal prices (ELMPs) occur in the day-ahead market, in contrast to

the uncongested network case (*Case 1*), where the price is identical for all nodes. It should be clarified, however, that only the ELMPs of the buses where the storage technologies are installed, are presented, in order to ensure a more coherent depiction of the prices that constitute the main research object of this work. It is evident that the day-ahead ELMPs for all four buses, range at significantly higher levels compared to the DA price in the uncongested network case in *Figure 3.7*. In fact, the greatest increase is observed at time periods $t16 - t18$, when storage facilities operate in discharging mode, providing electricity into the grid. Analyzing *Figure 3.12* further, the ELMPs for buses $n2$ and $n5$, where the PHS and AA-CAES facilities are installed, are noticeably higher than the corresponding prices for buses $n16$ and $n19$, where the Li-ion battery and D-CAES facilities are located. This differentiation is based on the fact that buses $n2$ and $n5$ belong to the lower area of the grid, where electricity demand is higher; thus, producers with higher bids are included in the energy mix, and therefore marginal prices increase. More specifically, the ELMP can reach 164.26 \$/MWh and 163.2 \$/MWh for buses $n2$ and $n5$, while for buses $n16$ and $n19$, 144.8 \$/MWh and 150.5 \$/MWh, respectively.

A different pricing scheme compared to the day-ahead market, is observed in the real-time market for both wind power generation scenarios $\omega 1, \omega 2$, as illustrated in *Figure 3.13*. In particular, in the real-time market the reserve capacities of the power producers are significantly lower compared to the day-ahead ones. Thus, the capacity of 200 MW of the network transmission lines is more than enough to transfer the required amount of electricity without creating congestion. As a result, the RT ELMPs are the same among the four power buses. However, since price premium is applied in the real-time market, the RT clearing prices in the low wind generation scenario are higher compared to the DA prices reaching up to 303.9 \$/MWh at time period $t17$. Equivalently, in the high wind generation scenario, as expected, the marginal prices in the RT market are lower than the DA market.

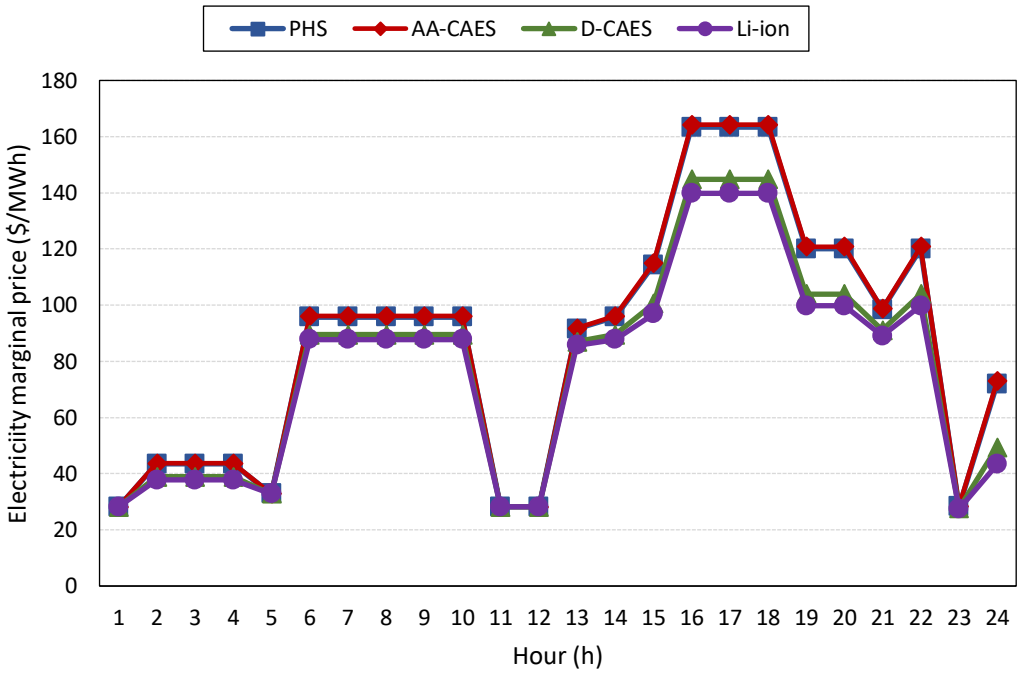

Figure 3.12: Day-ahead electricity market clearing price, under network congestion.

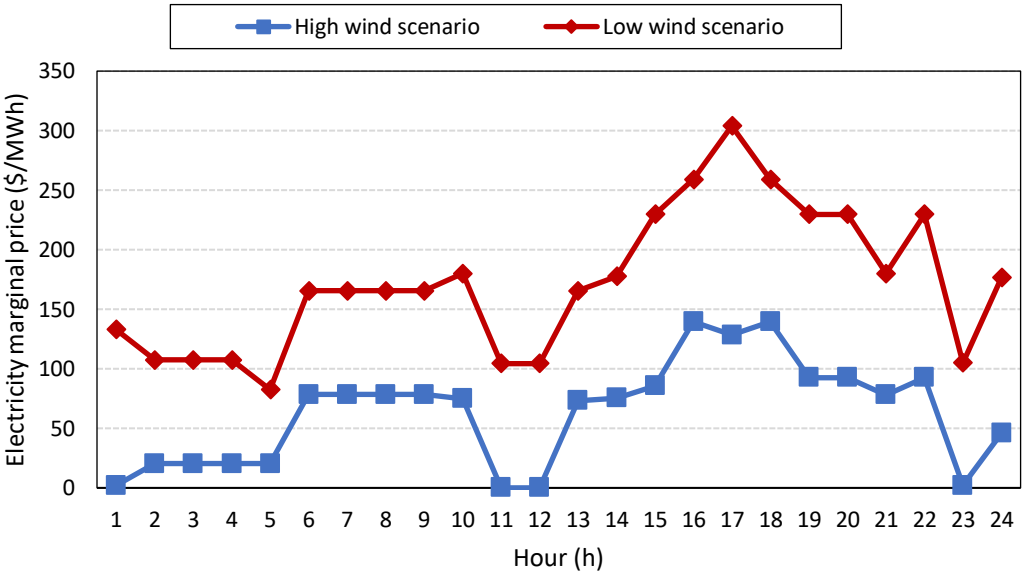

Figure 3.13: Real-time electricity market clearing price, under network congestion.

As in *Case 1*, the storage systems suffer financial losses in the real-time market as they provide high quantities of downward reserves in charging mode, which as already mentioned, constitute a cost factor. However, these losses are reduced for all four storage

technologies in the case of network congestion. *Figure 3.14* illustrates the RT electricity dispatch of D-CAES both in an uncongested and a congested power network. As is the case with all four storage systems, D-CAES provides less charging downward reserves under network congestion and thus their operating cost is significantly decreased. Furthermore, its provision of discharging upward reserves is also decreased. However, the significantly increased RT ELMPs under congestion compensate for the reduced upward reserve activation and even raise the system's income compared to the non-congestion case. In particular, as illustrated by *Figure 3.13* the provision of discharging upward reserves mainly concerns the low wind generation scenario $\omega 2$ and as such the D-CAES is compensated at exceptionally high clearing prices. Comparing *Figure 3.11 and Figure 3.15*, it is evident that the PHS, AA-CAES, D-CAES and Li-ion battery systems benefit from the power network congestion and rising electricity clearing prices. This results in a large increase in their overall expected profits, by 10,699.6 $, 509.4 $, 32,351.3 $ and 3,802.9 $, for each technology respectively.

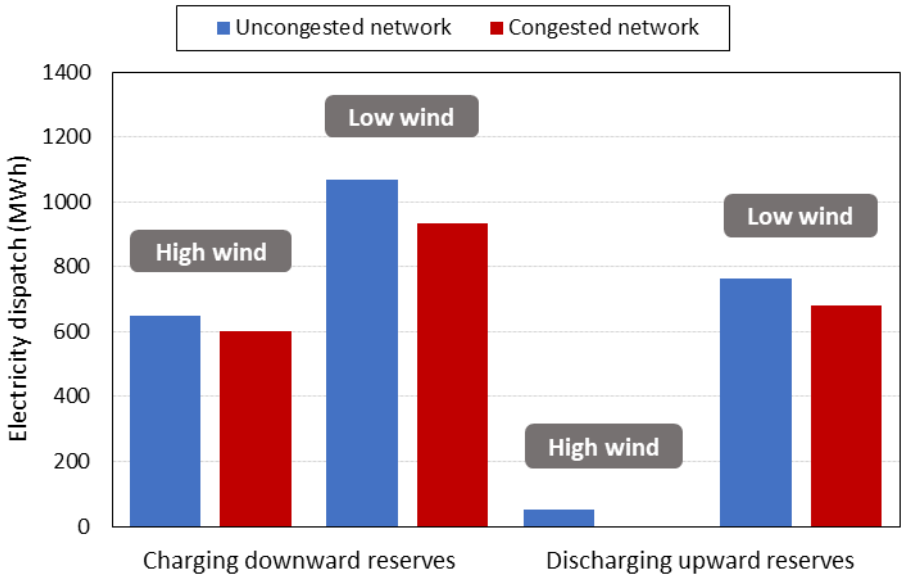

Figure 3.14: D-CAES high and low wind real-time electricity dispatch.

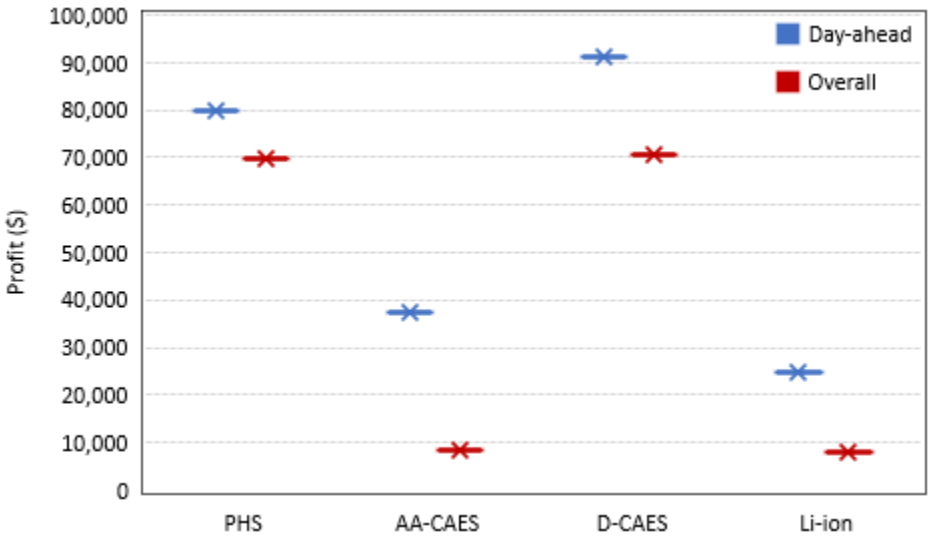

Figure 3.15: Day-ahead and overall profits for electricity storage systems under power network congestion.

3.4.4 Impact of wind power generation volatility

This case study (*Case 3*) investigates how the wind power generation volatility affects the profitability of energy storage systems in a coupled electricity and natural gas market, while the settlement of the uncongested case in *Subsection 3.4.2* is considered. However, in this case, three wind energy scenarios for the real-time market are examined, in order to provide a more detailed analysis. In particular, a high, a medium and a low wind production scenario are considered, with equal probability of realization, 0.33 each. The expected wind power production is 181.5 MW, with three progressively increasing values of expected standard deviation σ estimated at 5.05 %, 35.86 % and 52.24 %, respectively.

The outcomes presented in *Figure 3.16*, show that storage systems seem to benefit on a great extent from the unstable wind production. More specifically, the increment of the standard deviation leads to a significant raise in the requirements for scheduled energy. As a result, the storage technologies provide higher amounts of discharging energy, therefore notably increasing their profitability in the day-ahead market. In fact, the financial gains of the storage systems in the day-ahead trading floor, are able to cover any losses that arise during the activation of their downward reserves in the real-time market and thus the overall profits also show a continuous upward trend. Moreover, as

shown in *Figure 3.16*, the increasing wind power volatility, combined with the raised expected profits of the four electricity storage systems, leads to lower social welfare as the standard deviation escalates, at 8,415,236 $, 8,312,432 $ and 8,241,873 $, respectively.

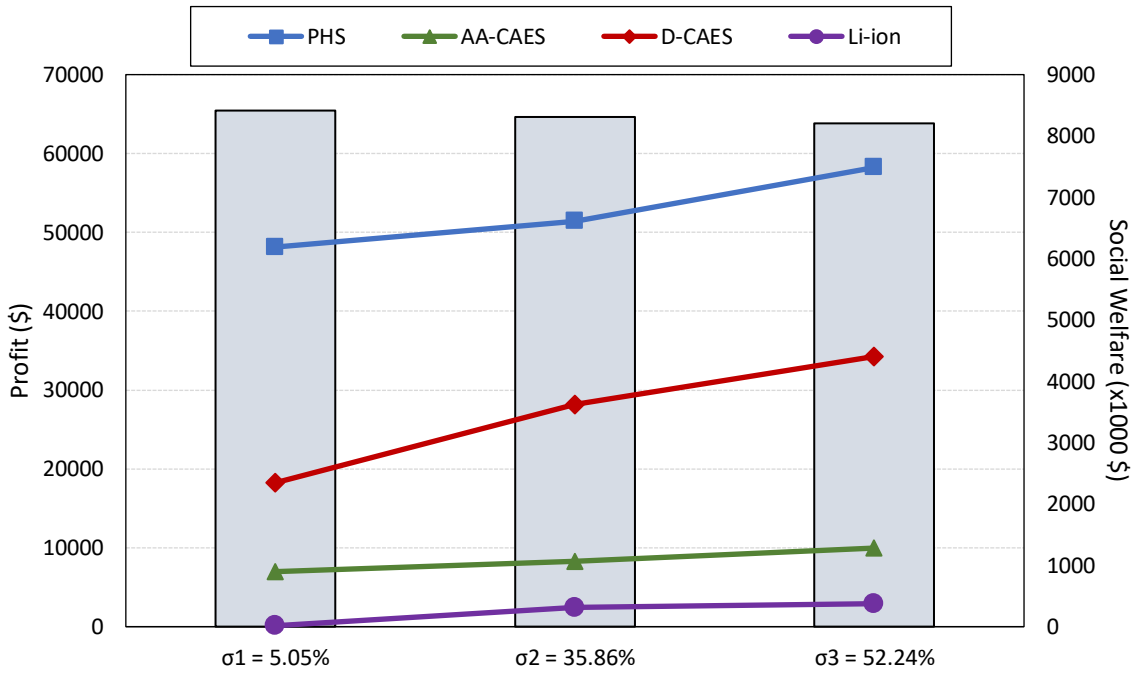

Figure 3.16: Impact of wind generation volatility on storage systems profits and social welfare.

3.5 Computational issues

The proposed MILP has been solved using CPLEX/GAMS 32.1.0 on an Intel Core i7-9700 processor at 3.00 GHz and 32 GB RAM. The computational requirements of the model were considered particularly promising, since despite the increased network sophistication and the substantial number of variables, the algorithm reaches optimal solution in a fairly short time. More specifically, the CPU time required to solve the uncongested power network case is 5.25 seconds, while for *Case 2*, the corresponding time equals 8.5 seconds. However, the increased number of wind generation scenarios in *Case 3*, leads to a CPU time escalation, since the model solution for the three standard deviation values requires 10.5, 10.9 and 10.4 seconds, respectively.

3.6 Conclusions

In this work, a stochastic MILP model is developed to investigate the financial gains and optimal dispatch of various energy storage technologies (PHS, AA-CAES, D-CAES and Li-ion battery) in a coupled electricity and natural gas market, under perfect competition. The model considering energy-only markets, co-optimizes the market clearing procedure of the day-ahead and real-time trading floors, aiming at social welfare maximization, while the stochasticity is introduced into the problem via a set of plausible wind power production scenarios. The proposed optimization framework is applied to an integrated energy system, consisting of a transmission constrained modified 24-bus IEEE Reliability Test System and a single-node natural gas network.

The solution of the problem derives electricity and natural gas marginal prices, optimal (dis)charging dispatch and expected profits for each energy storage technology. A specific analysis is carried out on the operation of the diabatic CAES system, which participates in both systems, either as producer or as a demand load. Furthermore, all four energy storage systems benefit from power transmission line congestions and high wind power volatility thus experiencing significant profit increase compared with the uncongested power network case, as a result of the electricity prices escalation. In particular, the overall profit increases by 18.2 %, 6.5 %, 84.4 % and 89 % for PHS, AA-CAES, D-CAES and Li-ion battery, respectively. Finally, a substantial decrease by 3.1% in social welfare is realized in the congested power network case. Similarly, the social welfare is decreased up to 2.54 % in the high wind power generation volatility scenario.

Nomenclature

A. Indices and sets

i	Index of conventional power plants
j	Index of wind generating units
s	Index of electricity storage units
h	Index of Hydro-pump storage systems ($h \subset s$)
c_a	Index of AA-CAES systems ($c_a \subset s$)
c_d	Index of D-CAES systems ($c_d \subset s$)
li	Index of Li-ion batteries ($li \subset s$)
k	Index of natural gas generating units
d	Index of demands
t, θ	Indices of time periods
n, m	Indices of electricity buses
r	Indices of natural gas nodes
ω	Index of wind generation scenarios
$I\alpha N$	Set of indices of conventional power plants located at bus *n*
JaN	Set of indices of wind generating units located at bus *n*
DaN	Set of indices of electricity demands located at bus *n*
$S\alpha N$	Set of indices of electricity storage units located at bus *n*
NaM	Set of buses *n* connected with bus *m*
$C_d\alpha R$	Set of indices of D-CAES systems located at node *r*
KaR	Set of natural gas generating units located at node *r*
DaR	Set of indices of natural gas demands located at node *r*

B. Acronyms - Superscripts

EL	Electricity
NG	Natural gas
ch	Charging mode of storage system s
dis	Discharging mode of storage system s
inj	Injecting air mode of CAES system
rel	Releasing air mode of CAES system

↑	Upward reserve
↓	Downward reserve

C. Parameters

O_i	Cost offer for conventional power plant *i* ($/MWh)
O_k	Cost offer for natural gas generating unit *k* ($/kcf)
O_s	Cost offer for electricity storage system *s* ($/MWh)
U_d	Utility of demand d ($/MWh)
$\overline{P}_i$	Maximum capacity of conventional power plant *i* (MW)
$\overline{W}_j$	Maximum capacity of wind generating unit *j* (MW)
$\overline{G}_s$	Maximum (dis)charging capacity of storage system *s* (MW)
$\underline{G}_s$	Minimum (dis)charging capacity of storage system *s* (MW)
$\overline{EXP}_{c_d}$	Maximum capacity of electricity produced by natural gas (MW)
$\underline{EXP}_{c_d}$	Minimum capacity of electricity produced by natural gas (MW)
η_s	(Dis)charging efficiency of storage system *s*
$\overline{F}_k$	Maximum capacity of natural gas generating unit *k* (kcf)
$\mathrm{L}_{d,t}^{EL}$	Load of electricity demand *d* at time *t* (MWh)
$\mathrm{L}_{d,t}^{NG}$	Load of natural gas demand *d* at time *t* (kcf)
$\overline{SOC}_s$	Maximum state-of-charge of storage system *s* (MW)
$\underline{SOC}_s$	Minimum state-of-charge of storage system *s* (MW)
SOC_s^{ini}	Initial state-of-charge of storage system *s* (MW)
$\overline{T}_{n,m}$	Transmission capacity of circuit line *n-m* (MW)
$B_{n,m}$	Susceptance of line *n-m*
π_ω	Occurrence probability of scenarios ω
$VOLL_{d,t}^{EL}$	Value of lost load d at time interval *t* ($/MWh)
$VOLL_{d,t}^{NG}$	Value of lost load d at time interval *t* ($/kcf)
$W_{j,\omega,t}^{RT}$	Scenario dependent generation of wind unit *j* at time *t* (MWh)

D. Variables (Day-ahead market)

$p_{i,t}$	Energy dispatch of conventional power plant *i* at time *t* (MWh)

$w_{j,t}$	Energy dispatch of wind generating unit *j* at time *t* (MWh)
$g_{s,t}$	Energy (dis)charged by storage system *s* at time *t* (MWh)
$exp_{c_d,t}$	Electricity produced by natural gas at time *t* (MWh)
$f_{k,t}$	Natural gas production by generating unit *k* at time *t* (kcf)
$\delta_{n,t}$	Voltage angle at bus *n* at time *t*
$soc_{s,t}$	Electricity stored for storage system *s* at time interval *t* (MWh)
$x_{s,t}$	Binary variable for (dis)charging mode of storage system s at time *t*
$\lambda_{n,t}^{EL}$	Electricity locational marginal price in day-ahead market at bus *n* at time *t* ($/MWh)
$\lambda_{r,t}^{NG}$	Natural gas locational marginal price in day-ahead market at node *r* at time *t* ($/kcf)

E. Variables (Real-time market)

$\hat{p}_{i,\omega,t}$	Energy dispatch of conventional power plant *i* under scenario ω at time *t* (MWh)
$\widehat{w}_{j,\omega,t}$	Energy dispatch of wind generating unit *j* under scenario ω at time *t* (MWh)
$\hat{g}_{s,\omega,t}$	Energy (dis)charged by storage system *s* under scenario ω at time *t* (MWh)
$\widehat{exp}_{c_d,\omega,t}$	Electricity produced by natural gas under scenario ω at time *t* (MWh)
$\hat{f}_{k,\omega,t}$	Natural gas production by generating unit *k* under scenario ω at time *t* (kcf)
$\hat{\delta}_{n,\omega,t}$	Voltage angle at bus *n* under scenario ω at time *t*
$w_{j,\omega,t}^{sp}$	Power spillage from wind generating unit *j* under scenario ω at time *t* (MWh)
$l_{d,\omega,t}^{EL,sh}$	Electricity load shedding of demand d^{EL} under scenario ω at time *t* (MWh)
$l_{d,\omega,t}^{NG,sh}$	Natural gas load shedding of demand d^{NG} under scenario ω at time *t* (kcf)

$\hat{x}_{s,\omega,t}$	Binary variable for (dis)charging mode of storage system s under scenario ω at time t
$\frac{\hat{\lambda}^{EL}_{n,\omega,t}}{\pi_\omega}$	Electricity locational marginal price in real-time market at bus n under scenario ω at time t (\$/MWh)
$\frac{\hat{\lambda}^{NG}_{r,\omega,t}}{\pi_\omega}$	Natural gas locational marginal price in real-time market at node r under scenario ω at time t (\$/kcf)

Chapter 4

Strategic bidding of a gas-fired unit in low carbon electricity and natural gas market

This Chapter presents a bi-level optimization framework to determine the optimal bidding strategies for a strategic gas-fired power plant, exerting market power in interdependent pool-based electricity and natural gas markets, under a carbon emission trading scheme (CETS). The objective of the upper-level problem is to maximize the profits of the strategic player. In contrast, the lower-level problem involves the sequential clearing of day-ahead electricity and natural gas markets, taking into account carbon emission allowances for conventional power producers and a high penetration of wind power generation. The bi-level formulation is initially transformed into a Mathematical Program with Equilibrium Constraints (MPEC) using the Karush-Kuhn-Tucker optimality conditions and duality theory. Subsequently, it is further reconfigured into a mixed-integer linear program. The proposed algorithm is implemented in a Pennsylvania-New Jersey-Maryland (PJM) 5-bus power grid, constrained by transmission limitations and a single-node natural gas network. Simulations yield electricity clearing prices embedded with the carbon emission trading prices and optimal bidding decisions for the strategic gas-fired power plant, considering potential power transmission congestions and increments in natural gas prices.

4.1 Introduction

In the midst of continuous political, economic and geostrategic challenges at a global level, the energy markets undoubtedly could not remain unaffected and thus nowadays they are experiencing a new reality, quite different from the one that had been established in recent years. The rapid increase in wholesale prices, the targeting of states

and investors at the decarbonization of the power sector through the profound penetration of renewable energy sources, but also the hopeful prospect of optimizing the coordination between the operation of electricity and natural gas markets, constitute key aspects that each market agent should contemplate and evaluate.

According to the U.S. Energy Information Administration, among the sources of energy for electricity generation, such as coal, petroleum, nuclear and renewables, natural gas holds the largest share accounting for almost the 36% of the total electricity production in USA (U.S. Energy Information Administration, 2022), while in many countries in Europe this percentage exceeds 40%. Moreover, natural gas is considered a clean and efficient fuel, that in the long-term can adequately replace coal, oil and nuclear power (Levitan et al., 2014) encouraging sustainable development without sacrificing the orderly functioning of contemporary energy markets.

Despite the increasing need for sectoral coordination between electricity and natural gas markets, particularly in renewable-based energy systems, as recognized by the Federal Energy Regulatory Commission (FERC) in the U.S (FERC Staff, 2015), in practice the two energy sectors are still cleared separately. More specifically, natural gas market operator (GMO) clears the market (Weigand et al., 2013), based on the gas demand previously determined during the electricity market clearing process, conducted by the national electricity market operator (NEMO). Electricity market agents including gas-fired power plants (GFPPs), submit their offer to the electricity market, based only on an estimation of the gas price, which is not necessarily identical to the cleared gas price.

This Chapter proposes a novel bi-level approach to derive optimal bidding strategies for a price-maker gas-fired power plant, participating in sequentially cleared interdependent electricity and natural gas markets, considering carbon emission trading. It is important to emphasize that the proposed model enables the GFPP, along with its strategic bidding decisions, to optimally manipulate its allocated emission allowances in order to maximize its profit. Furthermore, contrary to the common practice of treating gas prices as fixed values, in the present work, gas prices are endogenously generated, based on the gas suppliers bidding, during the natural gas market clearing procedure. The proposed model also incorporates wind power generation, as one of the most growing sources of renewable energy in the last decade (IRENA, 2019a) and network transmission

constraints, giving the strategic generator the ability to acquire additional financial gains from power network congestions and different electricity clearing prices.
In the above context, the main contributions of this Chapter are fourfold:

- to provide a novel bi-level optimization framework to determine the optimal bidding decisions and emission allowances manipulation of a strategic gas-fired power plant in a pool-based market scheme, acting as a producer in the electricity market and as a consumer in the natural gas market.
- to derive optimal electricity and natural gas dispatch and CETS-embedded electricity locational marginal prices.
- to analyze the impact of power network congestion on electricity locational marginal prices and profitability of the strategic gas-fired power plant.
- to determine the impact of natural gas price increase on the strategic gas-fired power plant's capacity withholding strategies.

4.2 Problem statement

The proposed bi-level programming problem considers the optimal bidding strategies for a GFPP that has dominant position in the market and competes price-takers conventional and wind power producers, in interdependent pool-based electricity and natural gas markets. In the adopted market setup, a carbon emission trading scheme is also integrated, based on a cap-and-trade regulatory program. More specifically, a compulsory cap is set by government on overall emission permitted across the power industry (Rocha et al., 2015). This cap is split into allowances, each of which endorses the emission of one ton of carbon dioxide or related pollutants. Moreover, these allowances are freely allocated to power generation companies and can be traded in the carbon market. Thus, a Genco can either be compensated for surplus emission allowances (if the number of the allocated allowances is greater that its actual carbon emission) or pay for exceeding its corresponding approved emission limit.

The upper-level of the proposed optimization algorithm contains strategic gas-fired unit's expected profit maximization problem and relies on CETS-embedded electricity and natural gas clearing prices. The lower-level problem on the other hand, proposes a low-carbon economic dispatch model to describe the sequential clearing mechanism of

interdependent day-ahead electricity and natural gas markets, conducted by the market operator. The objective functions of the lower-level problems aim at minimizing the total operation costs, including bidding costs of conventional and wind power plants, natural gas suppliers and carbon emission trading costs. It is important to point out that, since the electricity and natural gas demand loads are assumed to be inelastic, social welfare maximization is equivalent to cost minimization for the market operation (Ordoudis et al., 2019).

Considering the satisfaction of the continuity and convexity prerequisites of the lower-level problem, the bi-level model is reformulated to an MPEC by virtue of the KKT optimality conditions' application. Subsequently, by employing the Fortuny-Amat and McCarl linearization methodology (Fortuny-amat et al., 1981) and strong duality theorem, the proposed model is further reduced into a MILP, which imposes rational computational requirements by commercial solvers such as GAMS/CPLEX (Brooke et al., 1998).

The proposed model derives optimal bids for a strategic GFPP co-optimizing scheduled dispatch, carbon emission allowances and estimating the day-ahead electricity and natural gas market prices. The main assumptions made are summarized as follows:

i. All demand loads are inelastic except for GFPP's gas demand.
ii. Wind power generation is considered cost-free and emission-free.
iii. Conversion factor of the GFPP is constant. Thus, the electricity generation of the GFPP has a linear interdependence with its gas consumption (Wang et al., 2018).
iv. The carbon emission trading price is considered as a parameter for the lower-level problem.
v. Gas locational marginal prices (GLMPs) are endogenously generated as dual variables of the natural gas balance equation.

4.3 Mathematical framework

The following bi-level mathematical model presented in *Figure 4.1*, is formulated to determine optimal bidding strategies for a price-maker GFPP in interdependent electricity and gas markets, considering a carbon emission trading scheme that corresponds to the cap-and-trade program. This work assumes that the hourly overall carbon emission allowances Q_t of all the related conventional power generators, varies

over time with the net load (total load minus wind power generation) (R. Zhang et al., 2020), as shown in (4.1). Each conventional power generator receives its corresponding emission allowances $Q_{h,t}^{H}$ as defined by (4.2), depending on its allocated factor of carbon emission allowances α_h, which can be calculated by (4.3):

$$Q_t = \eta \cdot \left(\sum_{d^{EL} \in DaN} L_{d,t}^{E} - \sum_{j \in JaN} w_{j,t} \right) \tag{4.1}$$

$$Q_{h,t}^{H} = \alpha_h \cdot Q_t \tag{4.2}$$

$$\alpha_h = \frac{\zeta_h}{\sum_h \zeta_h} \tag{4.3}$$

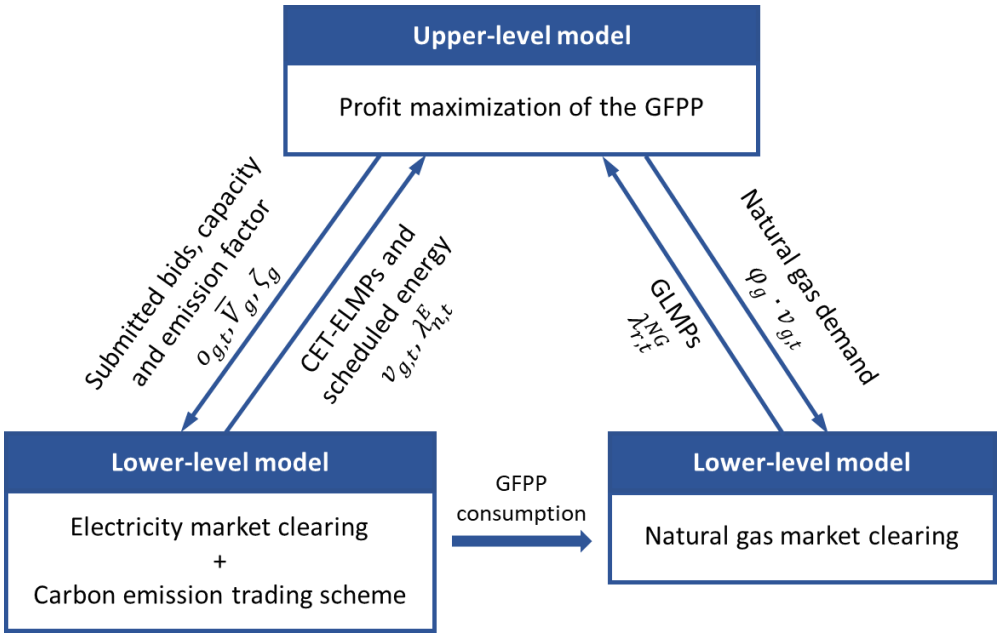

Figure 4.1: Bi-level structure of the proposed strategic bidding framework.

4.3.1 Upper-level problem: GFPP's expected profit maximization

The upper-level problem maximizes the strategic GFPP's expected profits, stemming from its bilateral participation in the energy markets, as electricity supplier and natural gas consumer and also in the cap-and-trade carbon market.

$$\boldsymbol{maximize} \quad \sum_{t}\left\{\sum_{g\in GaN}\lambda^{E}_{n,t}\cdot v_{g,t}-\sum_{g\in GaR}\lambda^{NG}_{r,t}\cdot\varphi_{g}\cdot v_{g,t}-cp\cdot(\zeta_{g}\cdot v_{g,t}-Q^{H}_{g,t})\right\} \tag{4.4}$$

In the objective function (4.4), the first term, $\lambda^{E}_{n,t}\cdot v_{g,t}$ corresponds to the revenue emerged from selling electricity, while the second term, $\lambda^{NG}_{r,t}\cdot\varphi_{g}\cdot v_{g,t}$, represents the cost of purchasing natural gas. The third term, $cp\cdot(\zeta_{g}\cdot v_{g,t}-Q^{H}_{g,t})$ represents the carbon trading cost of the GFPP, which depending on its actual and allocated carbon emissions, can either take positive, or negative values and thus provide financial losses or gains for the strategic GFPP, respectively.

4.3.2 Lower-level problem: Electricity market clearing

The first stage of the lower-level problem represents the low-carbon ED of the day-ahead electricity market, carried out by the MO, and provides optimal electricity dispatch and CETS-embedded electricity locational marginal prices (ELMPs).

$$\boldsymbol{minimize} \quad \sum_{t}\left\{\sum_{g\in GaN}o_{g,t}\cdot v_{g,t}+\sum_{i\in IaN}C_{i}\cdot p_{i,t}+\sum_{g\in GaN}cp\cdot(\zeta_{g}\cdot v_{g,t}-Q^{H}_{g,t})+\sum_{i\in IaN}cp\cdot(\zeta_{i}\cdot p_{i,t}-Q^{H}_{i,t})\right\} \tag{4.5}$$

s.t.

$$-\sum_{i\in IaN}p_{i,t}-\sum_{g\in GaN}v_{g,t}-\sum_{j\in JaN}w_{j,t}+\sum_{d^{EL}\in DaN}L^{E}_{d,t}+\sum_{m\in NaM}B_{n,m}\cdot(\delta_{n,t}-\delta_{m,t})=0 \quad :[\lambda^{E}_{n,t}] \quad \forall n,\forall t \tag{4.6}$$

$$0\le p_{i,t}\le\overline{P_{i}} \quad :\left[\underline{a_{i,t}},\overline{a_{i,t}}\right] \quad \forall i,\forall t \tag{4.7}$$

$$0\le v_{g,t}\le\overline{V_{g}} \quad :\left[\underline{\beta_{g,t}},\overline{\beta_{g,t}}\right] \quad \forall g,\forall t \tag{4.8}$$

$$0\le w_{j,t}\le\overline{W_{j}} \quad :\left[\underline{\gamma_{j,t}},\overline{\gamma_{j,t}}\right] \quad \forall j,\forall t \tag{4.9}$$

$$-Q_{h,t}^{H} + \alpha_h \cdot \eta \cdot \left(\sum_{d^{EL} \in DaN} L_{d,t}^{E} - \sum_{j \in JaN} w_{j,t} \right) = 0 \quad : \left[\rho_{h,t}\right] \qquad \forall h, \forall t \tag{4.10}$$

$$-\overline{T_{n,m}} \leq B_{n,m} \cdot \left(\delta_{n,t} - \delta_{m,t}\right) \leq \overline{T_{n,m}} \quad : \left[\underline{\psi_{n,m,t}}, \overline{\psi_{n,m,t}}\right] \qquad \forall (n,m) \in NaM, \forall t \tag{4.11}$$

$$-3.14 \leq \delta_{n,t} \leq 3.14 \qquad \forall n, \forall t \quad : \left[\underline{\pi_{n,t}}, \overline{\pi_{n,t}}\right] \tag{4.12}$$

$$\delta_{n_1,t} = 0 \quad : \left[\eta_{n,t}^{o}\right] \qquad \forall n = n_1, \forall t \tag{4.13}$$

Objective function (4.5) represents the day-ahead electricity market clearing mechanism, minimizing the overall operation costs, including bidding and carbon emission trading costs of conventional power plants. It is worth mentioning that as is common practice, wind power generation is assumed both cost and carbon emissions free. Constraint (4.6) enforces the power balance at each electric bus and the transmission capacity limits between them. The ELMP for each bus derives as the dual variable of the power balance equation. Constraints (4.7) – (4.9) impose the day-ahead upper and lower limits of the electricity generated by non-gas-fired, gas-fired and wind power plants. Constraint (4.10) determines the allocated carbon emission allowances for each conventional plant, based on the net load. Constraint (4.11) applies capacity limits for transmission lines, while constraints (4.12), (4.13) limit each electric bus's voltage angle range and impose bus A as power grid's slack bus, respectively.

4.3.3 Lower-level problem: Natural gas market clearing

The second stage of the lower-level problem describes the natural gas economic dispatch conducted by the GMO and derives gas locational marginal prices (GLMPs) and optimal gas dispatch.

$$\boldsymbol{minimize} \quad \sum_{\boldsymbol{t}} \left\{ \sum_{k \in KaR} C_k \cdot f_{k,t} \right\} \tag{4.14}$$

s.t.

$$-\sum_{k \in KaR} f_{k,t} + \sum_{g \in GaR} \varphi_g \cdot v_{g,t} + \sum_{d^{NG} \in DaR} L_{d,t}^{NG} = 0 \quad : \left[\lambda_{r,t}^{NG}\right] \qquad \forall r, \forall t \tag{4.15}$$

$$\underline{F_k} \leq f_{k,t} \leq \overline{F_k} \quad : \left[\underline{\varepsilon_{k,t}}, \overline{\varepsilon_{k,t}}\right] \qquad \forall k, \forall t \tag{4.16}$$

Objective function (4.14) portrays the day-ahead natural gas market clearing procedure by minimizing the total operation cost, including the bidding cost by the gas suppliers. Constraint (4.15) constitutes the natural gas balance at each node, while the dual variable corresponding to this equation, constitutes the GLMP of the node. Constraint (4.16) imposes upper and lower limits for the natural gas generation of each gas supplier.

4.3.4 Solution methodology

Considering the satisfaction of the continuity and differentiability requirements by the lower-level optimization problems, the Lagrangian function of each problem can be derived. In addition, it is important to mention that GFPP's bidding decisions $o_{g,t}$, are received as variables in the upper-level problem, while in the objective function (4.5) are treated as parameters by the MO. Thus, the lower-level problems *4.3.2* and *4.3.3* are linear and therefore convex and can be substituted by their respective KKT first order optimality conditions (C.1) – (C.10), recasting the bi-level formulation into a single level MPEC. The resulting non-linear equations (C.11) – (C.22) of the form $0 \leq g(x) \perp \mu \geq 0$, are substituted by equations (C.23) – (C.46), employing the Fortuny-Amat and McCarl linearization technique. To derive the final form of the proposed mathematical model, strong duality theorem is also employed, which suggests that the objective functions of the equivalent primal and dual problems must be equal. All mathematical transformations are analytically presented in Appendix C. Thus, any inherent non-linearities are eradicated and the MPEC model is transformed into the following equal MILP formulation:

$$
\begin{aligned}
\textbf{\textit{maximize}} \quad & -\sum_{i\in IaN} C_i \cdot p_{i,t} + \sum_{g\in GaN} cp \cdot Q^H_{g,t} - \sum_{i\in IaN} cp \cdot (\zeta_i \cdot p_{i,t} - Q^H_{i,t}) \\
& + \sum_{d^E\in DaN} \lambda^E_{n,t} \cdot L^E_{d,t} + \rho_{h,t} \cdot \alpha_h \cdot \eta \cdot \sum_{d^E\in DaN} L^E_{d,t} - \sum_{i\in IaN} \overline{a_{i,t}} \cdot \overline{P}_i \\
& - \sum_{j\in JaN} \overline{\gamma_{j,t}} \cdot \overline{W}_j - \sum_{m\in NaM} \overline{T}_{n,m} \cdot \left(\underline{\psi_{n,m,t}} + \overline{\psi_{n,m,t}}\right) \\
& - \sum_{n\in NaM} 3.14 \cdot \left(\underline{\pi_{n,t}} + \overline{\pi_{n,t}}\right) - \sum_{k\in KaR} C_k \cdot f_{k,t} - \sum_{k\in KaR} \overline{\varepsilon_{k,t}} \cdot \overline{F}_k \\
& + \sum_{d^{NG}\in DaR} \lambda^{NG}_{r,t} \cdot L^{NG}_{d,t} - \sum_{g\in GaN} cp \cdot \left(\zeta_g \cdot v_{g,t} - Q^H_{g,t}\right)
\end{aligned} \tag{4.17}
$$

subjected to (C.1) – (C.10)

(C.23) – (C.46)

4.4 Application study

The proposed mathematical model is applied in a modified Pennsylvania – New Jersey – Maryland (PJM) 5-bus power grid, sketched in *Figure 4.2* and a single-bus gas network. The power grid consists of six non-gas-fired power plants (*I1 – I6*), the strategic gas-fired power plant (*G1*) located at bus *D* and a wind power plant. The electricity load is equally distributed on three load buses. Similarly, the single-node gas network comprises three natural gas suppliers (*K1 – K3*) and three gas demand loads. It is critical to emphasize that since the GFPP consumes gas to generate electricity, it is considered as the fourth gas load, the capacity of which, is not determined a priori, but instead, directly depends on the electricity and natural gas market clearing outcomes.

Technical data regarding the capacity and bidding costs of electricity and natural gas producers are provided in *Table 4.1*. Furthermore, carbon emission factors for each conventional power plant are also presented. The non-gas-fired units are characterized by higher emission factor values, ranging from 0.65 –1.05 tCO_2/MWh, depending on the fossil fuel consumed to generate electricity. However, the emission factor for the gas-fired power plant is noticeably lower at 0.35 tCO_2/MWh, which indicates the eco-friendlier nature of the natural gas. The carbon emission allowance factor is set to be 0.7 tCO_2/MWh, and the carbon emission trading price is constant at 23 $/t. Moreover, *Figure 4.3* depicts

the hourly fluctuation of the total electricity load and the maximum wind power generation forecast, while maximum capacity and susceptance for each power transmission line, measure up to 1000 MW and 9.412, respectively.

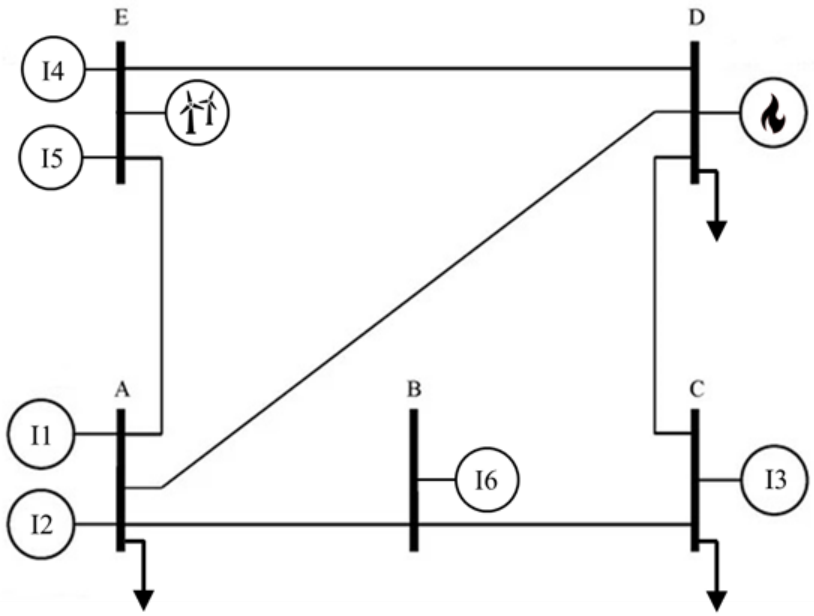

Figure 4.2: PJM 5-bus power grid.

	$\overline{P}_i$ (MW)	$\overline{V}_g(MW)$	$\overline{F}_k(kcf)$	C_i $(\$/MWh)$	C_k $(\$/kcf)$	ζ_h (tCO_2/MWh)
$I1$	100	-	-	15	-	0.65
$I2$	110	-	-	14	-	1.05
$I3$	270	-	-	30	-	1.05
$I4$	350	-	-	35	-	0.65
$I5$	250	-	-	28	-	0.85
$I6$	250	-	-	45	-	0.85
$G1$	-	200	-	-	-	0.35
$K1$	-	-	1900	-	3.5	-
$K2$	-	-	1800	-	4.7	-
$K3$	-	-	780	-	5.3	-

Table 4.1: Data for electricity and natural gas producers.

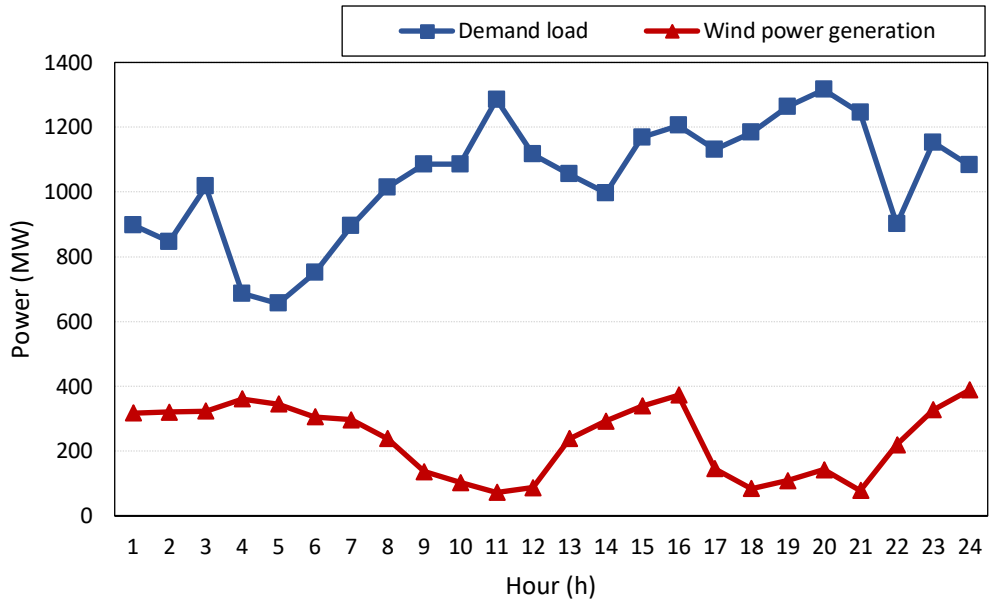

Figure 4.3: Forecasting load and maximum wind power generation.

4.4.1 Uncongested power network

Based on the above details, the proposed optimization framework is solved assuming an uncongested power network, using GAMS/CPLEX. The strategic GFPP exerts market power and manipulates the day-ahead prices to obtain maximum profits. According to *Figure 4.3*, at time period $t5$ the wind power generation forecast ranges in particularly high levels, while the total electricity demand load is the lowest for the entire daily horizon, accounting for only 655.5 MW. Due to its zero marginal cost, wind farm is fully dispatched and generates 345.5 MWh, while the remaining 310 MW are covered by the conventional power generators. More specifically, the non-gas-fired power plants with the lower marginal costs ($I1, I2$) provide a total 210 MWh of electricity, operating at their maximum capacity. Then the strategic GFPP contributes the additional 100 MWh of electricity, bidding at 28 \$/MWh, which is equivalent to the marginal cost of $I5$ and thus it manages to exclude producer $I5$ from the auction and set the ELMP.

An antidiametric scene takes place in time period $t11$, where the total electricity consumption almost doubles to 1285 MW and the wind power plant generates only 72 MWh. The combination of high demand with low wind power production, allows more expensive generators to enter the market, in order to ensure that demand is met, hence the clearing price is settled higher. This also happens in this particular case, where all the

non-gas-fired power plants are fully dispatched to produce the required 1080 MWh, except for the expensive unit $I6$ that is banished by the strategic GFPP, which offers 133 MWh at a price of 45 \$/MWh. ELMPs for the entire daily horizon are analytically presented in *Figure 4.4*. Since the power network is uncongested, there is only one electricity clearing price for each time period, which is common to all buses.

Regarding the GLMP, it is cleared at 3.7 \$/kcf for time period $t5$ and at 4.7 \$/kcf for time period $t11$. The reason behind this increase in natural gas price lies in the increased gas demand for the time period $t11$, resulting in more expensive gas suppliers entering the market. Despite the fact that the increased gas price, could discourage the strategic GFPP from purchasing gas in time period $t11$, it is clear that the high ELMP can completely absorb the production cost increment and incentivize the strategic GFPP to produce additional 33 MWh, compared to when the gas price is low.

The obtained CETS-embedded ELMPs during the 24-hour horizon, also depicted in *Figure 4.4*, are calculated by accounting for the emission cost of the conventional power generators in the carbon market. More specifically, the total bidding cost coefficient for each electricity producer increases by $cp \cdot \zeta_h$, except for the wind power generator, which as previously mentioned is emission-free. Hence, the value of CETS-embedded ELMPs is higher compared to the normal ELMPs. *Figure 4.5* illustrates the electricity dispatch $v_{g,t}$ and strategic bids $o_{g,t}$ for the GFPP. Note that these bids are not CETS-embedded i.e., they do not contain the $cp \cdot \zeta_h$ term, which for the GFPP accounts for 8.05 \$. If this term is added, the strategic bids are equivalent to the CET-ELMPs depicted in *Figure 4.4*, which shows the significant impact of the GFPP in the formation of electricity clearing prices.

It is important to emphasize that along with the reformulation of the electricity generators' cost offers, the priority according to which they are nominated to dispatch energy by the MO, has also changed. In particular, in the normal case, $I2$ is the producer with the lowest cost offer at 14 \$/MWh, while the next closest is $I1$, bidding at 15 \$/MWh. However, since power plant $I2$ is more carbon-intensive with a higher carbon emission factor compared to power plant $I1$, it ends up having a higher CETS-embedded bidding cost (38.15 \$/MWh, while $I1$ bids at 29.95 \$/MWh) and is therefore dispatched after $I1$, according to the merit-order.

The above is coherently confirmed by the market clearing outcomes in the time period $t4$, where the net load is 325.5 MW. According to the merit-order, power plant $I1$ and then $I2$, produce electricity at their maximum capacity, while the GFPP generates

only 115.5 MWh of electricity and sets the CETS-embedded ELMP, by strategically bidding at 47.55 \$/MWh and excluding $I5$ from entering the market. With the aforementioned capacity withholding strategy, the GFPP raises the clearing price by lowering its electricity production and manages to maximize its profit for the specific time period. However, this strategy does not always guarantee financial benefits.

During the time period $t5$ where the net load is 310 MW, $I1$ is fully dispatched, while $I2$ is the marginal producer generating only 41 MWh of electricity and setting the ELMP at its CETS-embedded bidding cost of 38.15 \$/MWh. The strategic GFPP generates 169 MWh and bids at the cost of $I2$. This results in gaining 2655 \$ for time period $t5$. On the contrary, in case the GFPP would withhold its capacity at 100 MWh to act as the marginal producer and raise the price at 47.55 \$/MWh, it would make a lower profit of 2643 \$. This is attributed to the fact that the price increase could not compensate for its substantial electricity production decrease. Therefore, the proposed model provides the optimal bidding strategy for the profit maximization of the GFPP, depending on the circumstances that arise.

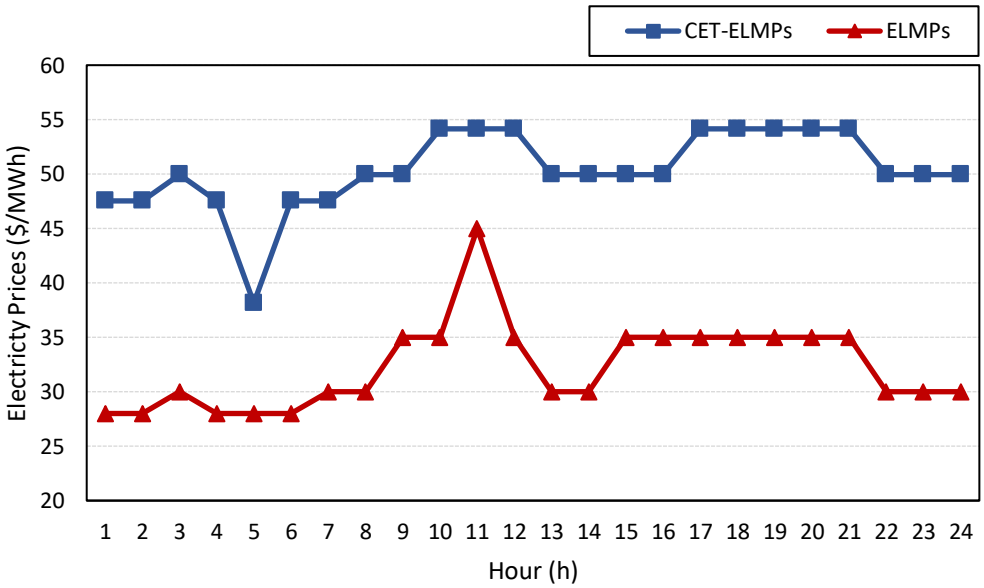

Figure 4.4: Comparison of CETS-embedded ELMPs and ELMPs.

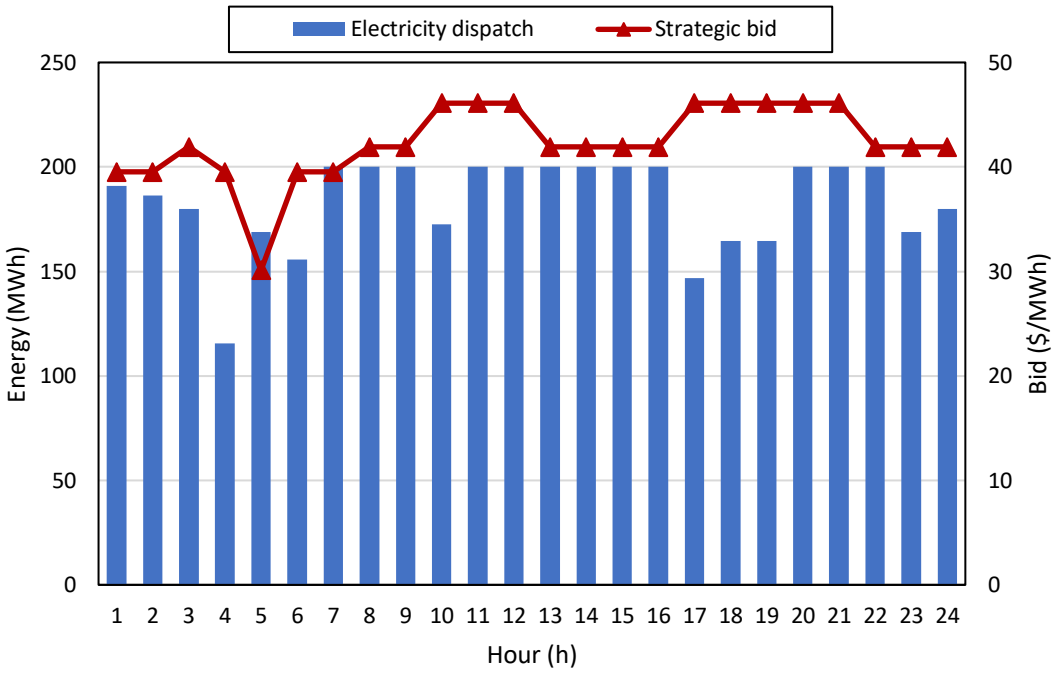

Figure 4.5: Electricity dispatch and strategic bids for the GFPP.

In the calculation of the profits for the conventional power plants, carbon emission allowances trading, which is directly linked to the amount of electricity production, also plays a key role. *Figure 4.6* illustrates the difference (in tons of CO_2) between the cost-free carbon allowances provided to the strategic GFPP by the government and the actual amount of carbon emissions it emits, based on its electricity production. Positive values indicate the amount of carbon allowances (in CO_2 tons) granted to the producer, but not employed. These allowances constitute a source of income for the electricity producer, who trades them at a price of 23 $ each.

On the other hand, the negative values denote the extra carbon allowances that the GFPP decides it is worth paying for, in order to generate the desired amount of electricity. As depicted in *Figure 4.6*, the GFPP strategically decides to pay the extra emission allowances cost, for every hour of the daily horizon, since the CETS-embedded ELMPs are significantly higher, compared to the carbon trading price. Furthermore, the hourly fluctuation of the difference between allocated and actual emissions follows the equivalent fluctuation of the overall net load. Thus, for the time periods $t17 - t19$, where electricity demand is high and wind power generation is low (corresponding to high net load), the strategic GFPP receives a higher number of allocated emission allowances, that almost cover the carbon emissions generated due to its electricity provision.

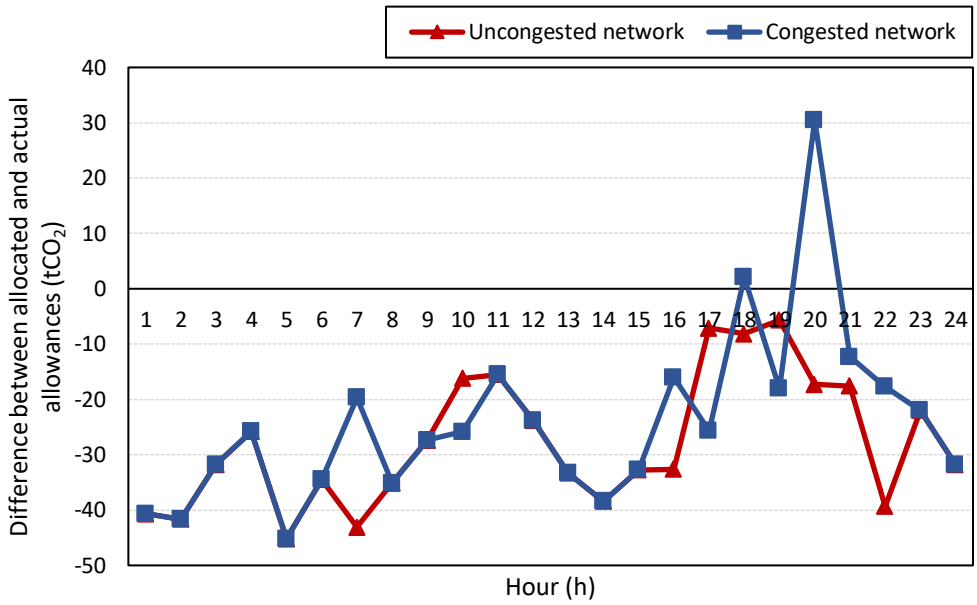

Figure 4.6: Hourly difference between allocated and actual carbon emission allowances for the strategic GFPP.

4.4.2 Congested power network

In the previous uncongested network case, the maximum power flow through each line is 2000 MW. If the capacity of lines A – B and D – E is reduced to 400 and 300 MW respectively, the power network becomes congested, resulting in different CETS-embedded ELMPs, as shown in *Figure 4.7*. It is observed that in the first four nodes the strategic GFPP manages to obtain significant economic benefits, by exerting market power and manipulating the electricity clearing prices. In particular, during periods of the day when electricity demand is high and wind power generation is low ($t11, t16, t20$), the strategic GFPP acts as a marginal producer at all four nodes, setting the price at particularly high levels. Especially in bus D, where the strategic producer is installed, a price cap at 158.05 $ needs to be applied, so as to restrict the bids of the GFPP and prevent excessive speculation. Bus E is the only bus that is not affected by the GFPP's bidding strategy. Zero-cost wind power generation seems to be the reason for the existence of low CETS-embedded ELMPs, since the wind farm, which is located at this bus, generates electricity at its maximum capacity and covers the largest percentage of the required demand load, while the ELMP is determined by the bids of the marginal producers $I4, I5$.

Furthermore, for the first time, the non-gas-fired power plant $I6$ also enters the market during the high net load periods $t11, t20$, generating 274.2 MWh of electricity in total.

It is significant to point out that under the congested power network case, due to the reduced transmission lines' capacity, the GFPP for the entire daily horizon generates 241 MWh less, compared to the uncongested network case, as shown in *Table 4.2*. This reduction in the GFPP's electricity production though, has a direct impact on the management of its allocated carbon emissions allowances. As comprehensively depicted in *Figure 4.6*, the strategic GFPP at time period $t20$, chooses to exchange its unexploited 30.5 carbon emission allowances (in tons of CO_2). It produces only 63.5 MWh of electricity and gain additional 701 $ from carbon emission trading. So, despite its electricity production decrease and the imposition of a cap on the clearing price, the strategic GFPP, by manipulating electricity prices and optimally handling the allocated emission allowances, manages to arbitrage under conditions of congestion and increase its daily expected profits by 26,338.43 $, as illustrated by *Table 4.2*.

	***Electricity generation* (*MWh*)**	***Profit* ($)**
Uncongested power network	4,394	122,005.53
Congested power network	4,153	148,343.96

Table 4.2: Strategic GFPP's electricity generation and expected profits.

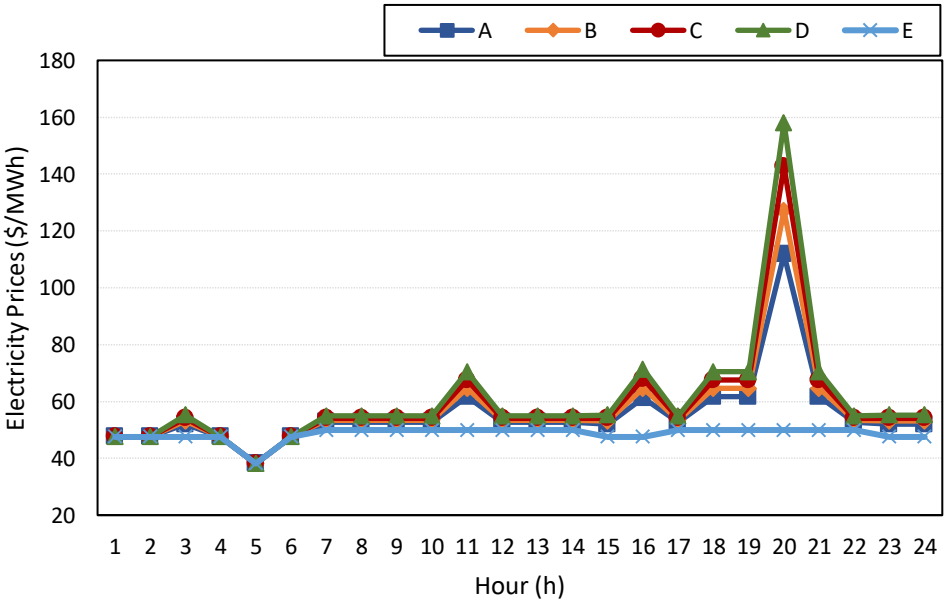

Figure 4.7: CETS-embedded ELMPs for the congested network.

4.4.3 Natural gas price increase

In this case, the influence of natural gas price increase on the electricity market outcomes and the optimal bidding and dispatching decisions of the strategic GFPP, is investigated. More specifically, four extra cases considering the increment of gas suppliers' bidding costs in the natural gas market by 50%, 100%, 150% and 200% respectively, are studied. As suppliers' bidding costs rise, given the gas market clearing mechanism already described, it is natural that the GLMPs increase as well (*Table 4.3*), thus the strategic GFPP chooses to withhold its production in order not to face financial deficits. As shown in *Figure 4.8*, this becomes particularly evident in Case 4, where the GFPP generates only 353 MWh throughout the 24-hour period.

Figure 4.9 indicates the hourly CETS-embedded ELMPs for each case scenario. The GFPP exerts market power and acts as the marginal electricity producer for the majority of the 24 time periods, in all four cases. However, in order to offset its augmented production costs resulting from the gas price increase, the GFPP strategically bids at higher prices. In particular, for the time period $t11$, instead of offering its electricity at 54.15 $/MWh as in the base case scenario, the increased GLMPs force the GFPP to bid at 64.55 $/MWh, which is the marginal cost of the expensive producer $i6$. This is also its ceiling bid in conditions of an uncongested network, since if the GFPP offers its electricity at a higher price, it will not be dispatched by the MO.

Furthermore, it should be noted that for time periods such as $t13, t15, t16, t23$, where, as shown in *Figure 4.9*, an increase in the ELMP is observed only for Case 4. For these specific periods, in Cases 1-3, the GFPP consistently provides some amount of electricity, albeit decreasing, at a price of 49.95 $/MWh, which is also the cost offer of the marginal producer $i4$. In Case 4, the GFPP strategically decides to withhold its production, due to the fact that the GLMP rises at such extent (10.5 $/kcf) that it is no longer profitable for it to generate electricity. Hence, in order for the supply to meet the required electricity demand, producer $i3$ enters the market, bidding at its marginal cost and thus setting the price at 54.15 $/MWh. *Figure 4.8* illustrates the significant profit losses that the gas-fired power plant experiences with the increase in the natural gas prices, which, considering the dramatic decrease of its electricity production, is judged to be perfectly reasonable.

	Increase	***Natural gas price*** ($/kcf$)
Base Case	**0**%	3.5 – 4.7
***Case* 1**	50%	5.3 – 7
***Case* 2**	100%	7
***Case* 3**	150%	8.8
***Case* 4**	200%	10.5

Table 4.3: GLMPs under a gas price increase.

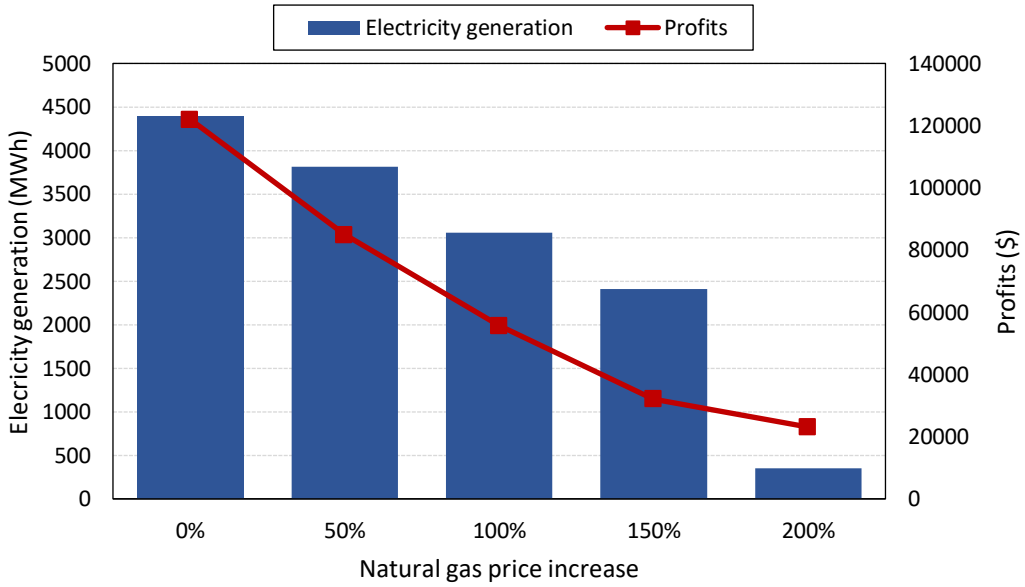

Figure 4.8: Electricity generation and profits for strategic GFPP under a gas price increase.

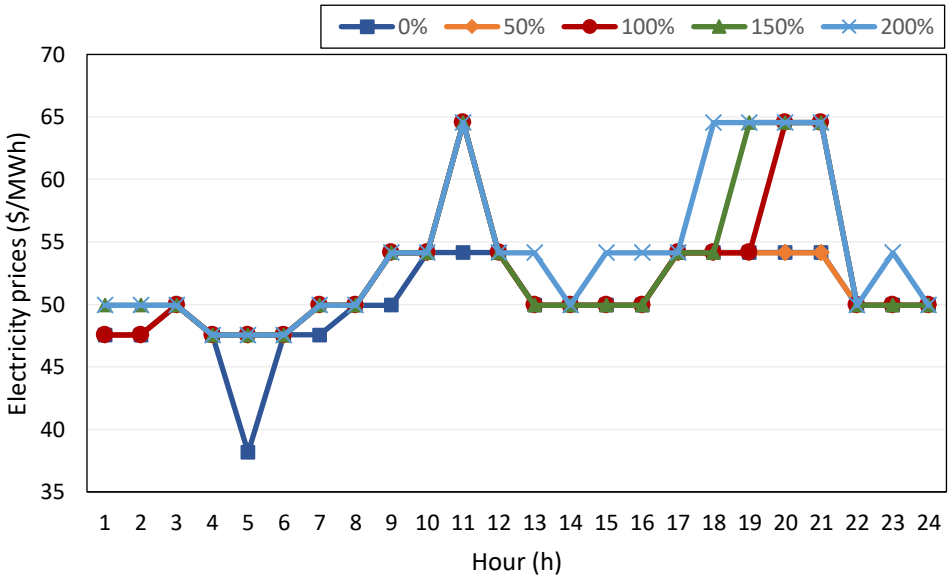

Figure 4.9: CETS-embedded ELMPs under a gas price increase.

4.5 Computational issues

The resulting MILP is solved using GAMS/CPLEX 39.3.0, on an Intel Core i7-7700 processor at 3.60 GHz, with 16 GB RAM. The computational time depends on the sophistication of the power and natural gas networks, as well as the number of market participants. The average CPU time for the uncongested power network case is 3.5 s, while for the congested power network case, 5 s. The determination of big-Ms' value is also firmly associated with the efficiency of the computational process, since the under- or overestimation of their value can lead to a numerically inadequate or an unrestricted problem, respectively. In this work, after implementing a series of trials, the value of Ms was established at 10^4.

4.6 Conclusions

This work proposes a bi-level mathematical approach to derive optimal bidding strategies for a strategic GFPP participating in interdependent pool-based electricity and natural gas markets, under a carbon emission trading scheme. The model considers a sequential clearing mechanism, conducted by the MO to minimize total cost under high wind power penetration and is applied to a PJM 5-bus transmission constrained power grid and a single node gas network.

The problem solution derives CETS-embedded ELMPs and GLMPs as dual variables of the lower-level problems and strategic bidding decisions for the GFPP in the day-ahead market. Furthermore, the model provides information on the optimal correlation of the carbon emission allowances nominated to the GFPP with its electricity/natural gas generation/consumption, in order to maximize its expected profits. The effects of power network congestion on the electricity clearing prices and the profitability of the gas-fired power plant are also investigated. The raised CETS-ELMPs, compared to the uncongested network case, create more arbitrage opportunities for the strategic GFPP, thereby acquiring significant economic benefits. Finally, the ever-increasing natural gas prices lead the gas-fired power plant to a strategic gradual withholding of its power generation since the resulting electricity prices do not seem capable of counterbalancing its increased production costs.

Nomenclature

A. Indices and sets

i	Index for non-gas-fired power plants
g	Index for strategic gas-fired power plants
h	Index for conventional power plants $i \cup g$
j	Index for wind power plant
k	Index for natural gas suppliers
d	Index for demand loads
t	Index for time periods
n, m	Indices for power buses
r	Index of natural gas node
$I\alpha N$	Set of indices for non-gas fired power plants located at bus n
$J\alpha N$	Set of indices for wind power plants located at bus n
$G\alpha N$	Set of indices for strategic gas-fired power plants located at bus n
$D\alpha N$	Set of indices for electricity demands located at bus n
$N\alpha M$	Set of buses n connected with bus m
$G\alpha R$	Set of indices for strategic gas-fired power plants located at node r
$K\alpha R$	Set of indices for natural gas suppliers located at node r
$D\alpha R$	Set of indices for natural gas demands located at node r

B. Acronyms - Superscripts

E	Electricity
NG	Natural gas

C. Parameters

C_i	Cost offer of non-gas-fired power plant i (\$/MWh)
C_k	Cost offer of natural gas supplier k (\$/kcf)
$\overline{P}_i$	Maximum capacity of non-gas-fired power plant i (MW)
$\overline{V}_g$	Maximum capacity of strategic gas-fired power plant g (MW)

W_j	Maximum capacity of wind generating unit *j* (MW)
$\overline{F}_k$	Maximum capacity of natural gas supplier *k* (kcf)
$L_{d,t}^{E}$	Load of electricity demand *d* at time *t* (MWh)
$L_{d,t}^{NG}$	Load of natural gas demand *d* at time *t* (kcf)
$\overline{T}_{n,m}$	Transmission capacity of circuit line *n-m* (MW)
$B_{n,m}$	Susceptance of line *n-m*
φ_g	Gas-electricity conversion factor of strategic GFPP *g* (kcf/MWh)
η	Carbon emission allowance factor (tCO_2/MW)
ζ_h	Carbon emission factor for conventional power plant *h* (tCO_2/MW)
α_h	Allocated factor for carbon emission allowances for conventional power plant *h*
cp	Carbon emission trading price (\$/tCO_2)

D. Primal Variables

$p_{i,t}$	Electricity generation of non-gas-fired power plant *i* at time *t* (MWh)
$v_{g,t}$	Electricity generation of strategic gas-fired power plant *g* at time *t* (MWh)
$o_{g,t}$	Strategic electricity offers for gas-fired power plant *g* (\$/MWh)
$f_{k,t}$	Natural gas production by supplier *k* at time *t* (kcf)
$\delta_{n,t}$	Voltage angle at bus *n* at time *t*
Q_t	Overall allocated carbon emission allowances
$Q_{h,t}^{H}$	Allocated carbon emission allowances for conventional power plant *h*

E. Dual Variables

$\lambda_{n,t}^{E}$	Electricity locational marginal price at bus *n* at time *t* (\$/MWh)
$\lambda_{r,t}^{NG}$	Natural gas locational marginal price at node *r* at time *t* (\$/kcf)
$a_{i,t}$	Upper and lower electricity output of non-gas-fired power plant *i* at time *t*
$\beta_{g,t}$	Upper and lower electricity output of gas-fired power plant *g* at time *t*
$\gamma_{j,t}$	Upper and lower electricity output of wind power plant *j* at time *t*

$\varepsilon_{k,t}$	Upper and lower gas output of natural gas supplier k at time t
$\rho_{h,t}$	Carbon emission allowances
$\psi_{n,m,t}$	Transmission capacity of line n-m at time t
$\pi_{n,t}$	Upper and lower bound of the voltage angle $\delta_{n,t}$ at bus n
$\eta_{n,t}^{o}$	Voltage angle at bus A

Chapter 5

Trading strategy of a renewable energy aggregator in electricity and green certificates markets

5.1 Introduction

Climate change and the security of energy supply are becoming increasingly crucial challenges that impact markets, regulations, policies, and investments on a global scale (Olabi & Abdelkareem, 2022). Renewable energy (RE) plays a pivotal role in the shift toward a low-carbon economy, contributing to greenhouse gas emission mitigation, reducing reliance on fossil fuels, fostering industrial development, diversifying the generation portfolio, and alleviating poverty (Gielen et al., 2019). Global trends indicate a substantial growth in renewables, constituting 40% of the global installed power capacity, as reported by the International Renewable Energy Agency (IRENA, 2021). Projections suggest that by 2050, renewable sources will account for approximately two-thirds of the total energy supply (Larsson, 2009). Consequently, the examination of the involvement and functioning of renewable assets in contemporary energy and derivatives markets emerges as a fundamental area of research.

This Chapter proposes a novel bi-level modelling approach to determine the optimal trading strategy for a price-maker renewable aggregator, participating in sequentially cleared interconnected electricity and green certificates markets. Contrary to the mathematical methodology adopted by reference (Guo et al., 2020), which endorses the estimation of the certificates clearing price based on two parameters of the inverse price function, the proposed model considers an hourly pool-based green certificates market clearing mechanism. This mechanism is perfectly aligned to the electricity market clearing procedure and endogenously generates realistic green certificates prices as dual variables of the problem. It is also important to emphasize, that

a single Market Operator is considered for both markets, thus enhancing their synchronization and information exchange. Furthermore, to the best of authors' knowledge it is the first time that the concept of available green certificates, also named as "state of available certificates" (SOAC) is introduced. This concept allows for the renewable aggregators to optimally decide either to store their available for issuance certificates or to sell them, depending on the market conditions and possible arbitrage opportunities. Finally, this work considers wind and solar energy, as they are the two most popular renewable energy sources worldwide and the ones with the highest capacity expansion, according to IRENA (International Renewable Energy Agency, 2023). Considering the above context, the main contributions of this work are fourfold:

i. to develop a novel bi-level optimization model to derive the optimal trading decisions for a strategic renewable aggregator in a joint pool-based electricity and green certificates market scheme.
ii. to successfully link and coordinate the operation of electricity and green certificates markets.
iii. to analyze the impact of power network congestion on electricity and green certificates prices and the strategic renewable aggregator's profitability.
iv. to assess the applicability of the proposed methodology to a real-life 24-bus power system.

5.2 Problem statement

The proposed bi-level optimization framework analyzes the optimal trading strategies for a renewable aggregator that has dominant position and exerts market power in pool-based electricity and green certificates markets. Following the example of the majority of the US states and other environmentally aware countries, this work adopts an RPS policy. More specifically, the regulatory authority of each state sets a specific RPS target which declares the fraction of the load serving entities' retail electricity that is obligatory to derive exclusively from renewable energy sources. It is important to emphasize that the LSE is not obligated to possess its own RES assets to cover its required electricity demand fraction. Instead, the LSE can purchase electricity from a single or several qualified renewable energy producers, until the overall quantity

of the purchased energy meets the RPS threshold. If the LSE is not able to meet the requirements of this policy, a non-compliance penalty, called Alternative Compliance Penalty (ACP) is imposed.

The upper-level of the proposed modelling approach contains renewable aggregator's expected profit maximization problem and relies on electricity and green certificates dispatch and clearing prices which comprise lower-level decisions. On the other hand, in the lower-level problem an economic dispatch model is considered, where a single entity, called Market Operator (MO), administers the sequential clearing mechanism of day-ahead electricity and green certificates markets. The lower-level objective functions aim at minimizing the overall operation costs, including electricity offering costs of conventional and renewable power plants and green certificates trading costs. It is significant to emphasize that, since the electricity demand loads are assumed to be inelastic, social welfare maximization is equal to cost minimization for the market operation (Ordoudis et al., 2019).

Considering the continuity and convexity of the lower-level problems, they can be replaced by their respective KKT first order optimality conditions, recasting the bi-level model into a single level MPEC. Subsequently, by employing the Fortuny-Amat and McCarl linearization technique, strong duality theory and binary expansion the model is further transformed into a MILP with reduced computational requirements, that can be handled by commercial solvers such as GAMS/CPLEX (Brooke et al., 1998).

This work determines optimal bids for a strategic renewable aggregator with mixed wind and solar portfolio, co-optimizing scheduled energy dispatch, green certificates trading and estimating the day-ahead electricity and certificates market prices. The main assumptions made are summarized as follows:

i. Electricity demand loads are inelastic, thus social welfare maximization is equivalent to market operation cost minimization.
ii. Network losses and reactive power are excluded (Tsimopoulos & Georgiadis, 2019a).
iii. Renewable power generation is considered cost-free.
iv. Tradable green certificates market is assumed to be cleared by the electricity Market Operator (Guo et al., 2020).
v. A uniform price clearing auction mechanism is adopted for both electricity and green certificates markets.

vi. Electricity and green certificates marginal prices are endogenously generated as dual variables of the lower-level problems.

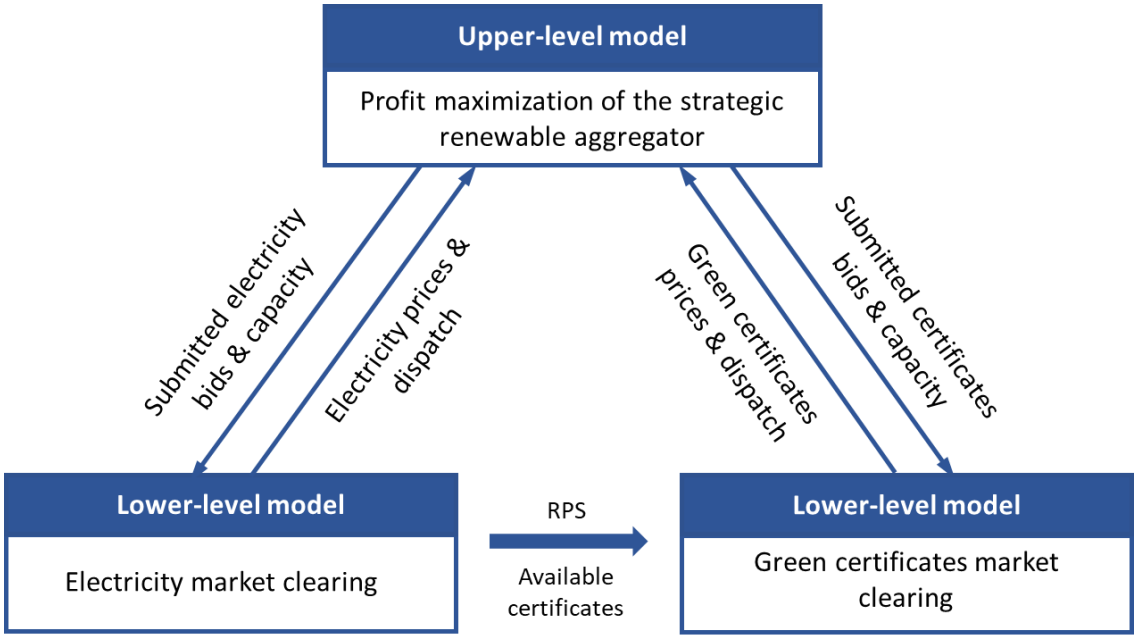

Figure 5.1: Bi-level structure of the proposed strategic bidding framework.

5.3 Bi-level model formulation

The following bi-level algorithm presented in ***Figure 5.1*****,** is formulated to derive the optimal trading strategies for a price-maker renewable energy aggregator in interdependent electricity and green certificates markets. This work assumes that the clearing of the electricity and green certificates market is performed sequentially by the same market entity on an hourly basis, while a uniform pricing scheme is also adopted. Each MWh of energy produced by RESs in the electricity market corresponds to a single certificate, thus the interconnection of the two markets is deeply enhanced and the slightest change in the electricity market can have a significant impact on the green certificates market as well. Based on the above framework and operation of the markets, the strategic renewable aggregator determines its optimal strategy, by submitting the appropriate sell prices and quantities in order to maximize its profits.

5.3.1 Upper-level problem: GFPP's expected profit maximization

The upper-level problem aims at maximizing the strategic renewable aggregator's expected profits, originating from its participation in the electricity and green certificates markets.

$$\boldsymbol{maximize} \quad \sum_{\boldsymbol{t}} \left\{ \sum_{s \in SaN} \lambda_{n,t}^{EL} \cdot f_{s,t} + \sum_{s \in SaN} \lambda_{t}^{GC} \cdot q_{s,t}^{\uparrow} \right\} \tag{5.1}$$

$$SOAC_{s,t} = \sum_{\theta}^{t} f_{s,t} - \sum_{\theta}^{t-1} q_{s,t}^{\uparrow} \qquad \forall s, \forall t \tag{5.2}$$

$$SOAC_{ns,t} = \sum_{\theta}^{t} w_{ns,t} - \sum_{\theta}^{t-1} r_{ns,t}^{\uparrow} \qquad \forall ns, \forall t \tag{5.3}$$

In the objective function (5.1), the term, $\lambda_{n,t}^{EL} \cdot f_{s,t}$ corresponds to the revenue obtained by selling its power production, while the second term, $\lambda_{t}^{GC} \cdot q_{s,t}^{\uparrow}$ represents the revenue from providing green certificates to the load serving entities. Since the marginal cost of renewable power generation, as already mentioned in the Assumptions section, is considered almost zero, the issuance of tradable green certificates is also cost-free and no cost terms are added to the objective function. Constraints (5.2) and (5.3) represent the state of available certificates for the strategic and non-strategic renewable energy assets of the market. This is the first that such a constraint is introduced and enables the aggregators to "store" their available certificates to subsequent time periods and optimally "activate" them in the right time, that will bring the highest possible profits.

5.3.2 Lower-level problem: Electricity market clearing

The first stage of the lower-level problem represents the clearing procedure of the day-ahead electricity market, performed by the MO, and determines optimal energy dispatch and electricity locational marginal prices (ELMPs).

$$\textbf{\textit{minimize}} \quad \sum_{t}\left\{\sum_{s\in SaN} O_{s,t}^{EL}\cdot f_{s,t}+\sum_{i\in IaN} C_i\cdot p_{i,t}\right\} \tag{5.4}$$

s.t.

$$-\sum_{i\in IaN} p_{i,t}-\sum_{s\in SaN} f_{s,t}-\sum_{ns\in NSaN} w_{ns,t}+\sum_{d^{EL}\in DaN} L_{d,t}^{EL} + \sum_{m\in NaM} B_{n,m}\cdot\left(\delta_{n,t}-\delta_{m,t}\right)=0 \quad :\left[\lambda_{n,t}^{EL}\right] \quad \forall n,\forall t \tag{5.5}$$

$$0\le p_{i,t}\le \overline{P_i} \quad :\left[\underline{a_{i,t}},\overline{a_{i,t}}\right] \quad \forall i,\forall t \tag{5.6}$$

$$0\le f_{s,t}\le \overline{F_s} \quad :\left[\underline{\gamma_{s,t}},\overline{\gamma_{s,t}}\right] \quad \forall s,\forall t \tag{5.7}$$

$$0\le w_{ns,t}\le \overline{W_{ns}} \quad :\left[\underline{\theta_{ns,t}},\overline{\theta_{ns,t}}\right] \quad \forall ns,\forall t \tag{5.8}$$

$$-\overline{T_{n,m}}\le B_{n,m}\cdot\left(\delta_{n,t}-\delta_{m,t}\right)\le \overline{T_{n,m}} \quad :\left[\underline{\psi_{n,m,t}},\overline{\psi_{n,m,t}}\right] \quad \forall (n,m)\in NaM,\forall t \tag{5.9}$$

$$-3.14\le \delta_{n,t}\le 3.14 \quad :\left[\underline{\pi_{n,t}},\overline{\pi_{n,t}}\right] \quad \forall n,\forall t \tag{5.10}$$

$$\delta_{n_1,t}=0 \quad :\left[\eta_{n,t}^{o}\right] \quad \forall n=n_1,\forall t \tag{5.11}$$

Objective function (5.4) represents the economic dispatch of the day-ahead electricity market, minimizing the total market operational costs i.e., the bidding strategy of the price-maker renewable aggregator and the cost offers of the conventional producers. The term for the price-taker renewable aggregator is not included in the objective function, since its marginal cost is almost zero. It is worth mentioning that the bid for the strategic aggregator is a decision variable that will be optimally determined to maximize its expected profits. Constraint (5.5) enforces the energy balance at each power bus and the transmission capacity bounds among them. The electricity clearing price for each power bus derives as the dual variable of the equivalent energy balance equation. Constraints (5.6) – (5.8) impose the day-ahead upper and lower boundaries for the power generated by conventional, strategic and non-strategic renewable producers, respectively. Constraint (5.9) imposes capacity limits for the electricity transmission lines, while constraints (5.10) and (5.11) limit power buses' voltage angle range and establish bus A as the slack bus of the power network, respectively.

5.3.3 Lower-level problem: Green certificates market clearing

In the second stage of the lower-level problem, the MO conducts the clearing of the green certificates market and determines the prices and the optimal management of the certificates.

$$\boldsymbol{minimize} \quad \sum_{t}\left\{\sum_{s\in SaN} O_{s,t}^{GC}\cdot q_{s,t}^{\uparrow}+\sum_{ns\in NSaN} C_{ns,t}^{GC}\cdot r_{ns,t}^{\uparrow}+\sum_{d^{EL}\in DaN}\lambda^{ACP}\cdot ACP_{d,t}\right\} \tag{5.12}$$

s.t.

$$-\sum_{s\in SaN} q_{s,t}^{\uparrow}-\sum_{ns\in NSaN} r_{ns,t}^{\uparrow}-\sum_{d^{EL}\in DaN} ACP_{d,t}+\sum_{d^{EL}\in DaN} RPS\cdot L_{d,t}^{EL}=0 \quad : [\lambda_t^{GC}] \quad \forall t \tag{5.13}$$

$$0\le q_{s,t}^{\uparrow}\le SOAC_{s,t} \quad : \left[\underline{\varepsilon_{s,t}},\overline{\varepsilon_{s,t}}\right] \quad \forall s,\forall t \tag{5.14}$$

$$0\le r_{ns,t}^{\uparrow}\le SOAC_{ns,t} \quad : \left[\underline{\kappa_{ns,t}},\overline{\kappa_{ns,t}}\right] \quad \forall ns,\forall t \tag{5.15}$$

$$0\le ACP_{d,t}\le RPS\cdot L_{d,t}^{EL} \quad : \left[\underline{\zeta_{d,t}},\overline{\zeta_{d,t}}\right] \quad \forall d,\forall t \tag{5.16}$$

Objective function (5.12) portrays the day-ahead green certificates market clearing mechanism by minimizing the total operation cost. The first two terms represent the bids by the strategic and non-strategic renewable asset, respectively, while the third term corresponds to the possible penalty to the LSEs, in case of not complying with the RPS requirements. Constraint (5.13) describes the green certificates balance, which applied universally for the whole power system, contrary to the electricity balance equation that applies for each bus individually. It is important to emphasize that the dual variable corresponding to this equation constitutes the universal certificates clearing price. Constraints (5.14), (5.15) ensure that the number of green certificates the strategic and non-strategic renewable aggregators can provide each time period, cannot exceed the number of available certificates they already own. Finally, constraint (5.16) imposes upper and lower limits for the green certificates mismatch of each LSE.

5.3.4 Solution methodology

Considering the fact that the continuity and differentiability standards of the lower-level optimization problems are satisfied, their equivalent Lagrangian functions can be employed to recast them into unconstrained problems. In addition, it is important to mention that while the strategic aggregator's bidding decisions $O_{s,t}^{EL}$, $O_{s,t}^{GC}$ in electricity and certificates markets are considered prime variables, they are encountered as parameters by the MO, rendering the lower-level objective functions (5.4), (5.12) linear and therefore convex. Thus, the lower-level problems *5.3.2* and *5.3.3* can be replaced by their respective KKT first order optimality conditions (D.1) – (D.6), (D.11) – (D.20) and (D.7) – (D.10), (D.21) – (D.26) transforming the bi-level model into the following single level non-linear MPEC.

The resulting non-linear equations (D.11) – (D.26) of the form $0 \leq g(x) \perp \mu \geq 0$, are substituted by equations (D.27) – (D.58), implementing the Fortuny-Amat and McCarl linearization technique (Fortuny-amat et al., 1981). Furthermore, the remaining non-linearities are eradicated by applying strong duality theory to the lower-level problems and binary expansion method. The analytical development of all the mathematical transformations is presented in Appendix D. Hence, the non-linear MPEC formulation is recast into the following equivalent MILP model:

$$
\begin{aligned}
\textbf{\textit{maximize}} \quad & \sum_{t} \Bigg\{ - \sum_{ns \in NSaN} C_{ns}^{EL} \cdot w_{ns,t} - \sum_{i \in IaN} C_i \cdot p_{i,t} + \sum_{d^{EL} \in DaN} \lambda_{n,t}^{EL} \cdot L_{d,t}^{EL} \\
& - \sum_{i \in IaN} \overline{a_{i,t}} \cdot \overline{P}_i - \sum_{s \in SaN} \overline{\gamma_{s,t}} \cdot \overline{F}_{s,t} - \sum_{ns \in NSaN} \overline{\theta_{ns,t}} \cdot \overline{W}_{ns,t} \\
& - \sum_{m \in NaM} \overline{T_{n,m}} \cdot \left(\underline{\psi_{n,m,t}} + \overline{\psi_{n,m,t}} \right) - \sum_{n \in NaM} 3.14 \cdot \left(\underline{\pi_{n,t}} + \overline{\pi_{n,t}} \right) \\
& - \sum_{ns \in NSaN} C_{ns,t}^{GC} \cdot r_{ns,t}^{\uparrow} - \sum_{d^{EL} \in DaN} \lambda^{ACP} \cdot ACP_{d,t} \\
& + \sum_{d^{EL} \in DaN} \lambda_t^{GC} \cdot RPS \cdot L_{d,t}^{EL} - \sum_{ns \in NSaN} \overline{\kappa_{ns,t}} \cdot w_{ns,t} \\
& - \sum_{d \in DaN} \overline{\zeta_{d,t}} \cdot RPS \cdot L_{d,t}^{EL} \Bigg\}
\end{aligned}
\tag{D.72}
$$

subject to: (2) – (3)

(D.1) – (D.10)

(D.27) – (D.58)

(D.73) – (A.78)

5.4 Application study

The proposed optimization framework is applied in a modified Pennsylvania – New Jersey – Maryland (PJM) 5-bus power network, sketched in *Figure 5.2*. The power network consists of six conventional power plants (*I1 – I6*), the strategic renewables aggregator's wind *S1* and solar *S2* power plants, the non-strategic renewables aggregator's wind and solar power plants *NS1* and *NS2* and three Load Serving Entities at buses *A, C, D*. The electricity demand load is equally distributed on the three LSEs.

Technical data considering the capacity and bidding costs of power producers and the issuance/costs of green certificates by the renewable energy plants, are provided in *Table 5.1*. It is significant to point out that the capacities/costs of the corresponding renewable energy assets are equal, both for the strategic and the non-strategic aggregators in order to conduct a balanced comparison regarding their overall operation and expected profits. Furthermore, the marginal cost of the power production for all the renewable plants is assumed to be almost zero and the bidding decisions of the strategic renewable aggregator are considered decision variables both for electricity ($O_{s,t}^{EL}$) and green certificates ($O_{s,t}^{GC}$) markets. The overall electricity demand across the power network is depicted by the green line with the triangle markers in *Figure 5.3*. The ACP rate applied on green certificates mismatches of the LSEs is determined at 25 $, while the hourly RPS compliance imposed to the LSEs by the state regulator is set at 45%. Finally, the maximum capacity and susceptance for each power transmission line measure up to 1,000 MW and 9.412, respectively.

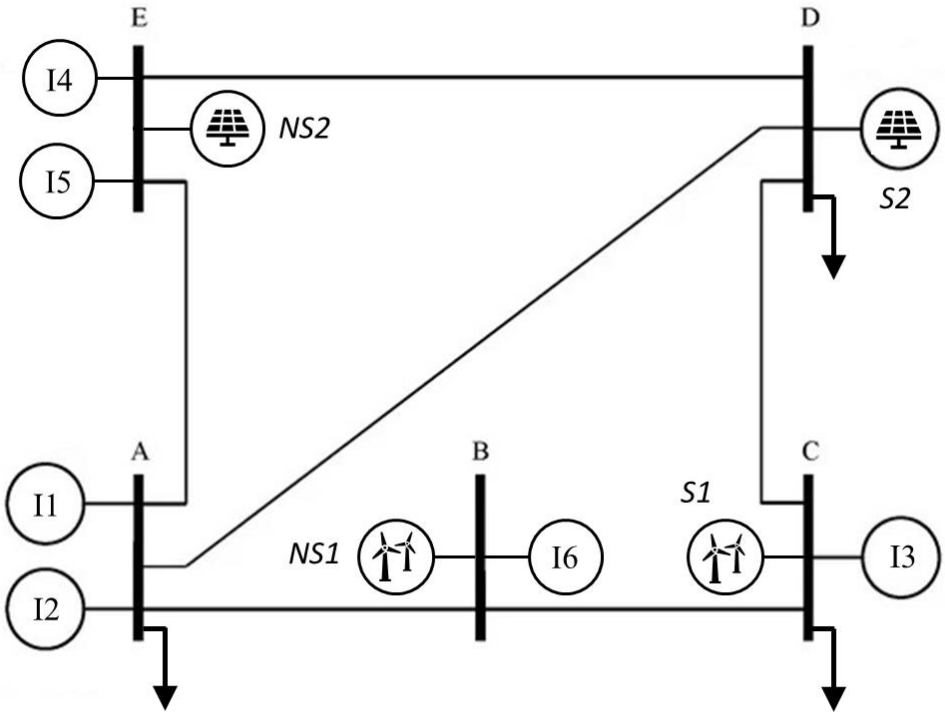

Figure 5.2: PJM 5-bus power network.

	$\overline{P}_i$ (MW)	$\overline{F}_s(MW)$	$\overline{W}_{ns}(MW)$	C $(\$/MWh)$	C $(\$/certificate)$
$I1$	310	-	-	160	-
$I2$	280	-	-	150	-
$I3$	110	-	-	95	-
$I4$	185	-	-	80	-
$I5$	150	-	-	108	-
$I6$	200	-	-	135	-
$S1$	-	150	-	decision variable	decision variable
$S2$	-	20-130	-	decision variable	decision variable
$NS1$	-	-	150	≈ 0	18
$NS2$	-	-	20-130	≈ 0	20

Table 5.1: Data for power producers.

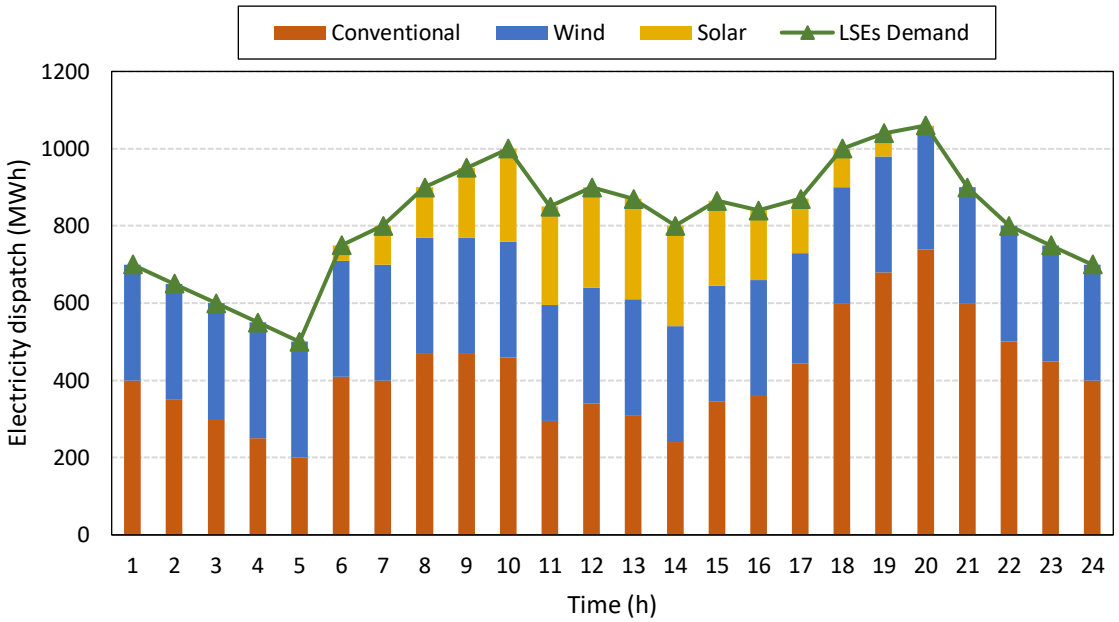

Figure 5.3: Power producers' dispatch and LSEs' power demand.

5.4.1 Uncongested power network

Based on the above framework, the proposed optimization algorithm is solved considering an uncongested power network, using GAMS/CPLEX. The strategic renewable aggregator exerts market power and manipulates the electricity and green certificates prices to maximize its profits. *Figure 5.3* shows the energy mix for the whole 24-hour horizon. Due to their zero marginal cost, wind farms are fully dispatched and generate 300 MWh combined, on an hourly basis. On the other side, solar parks generate electricity only between 7 a.m. and 7 p.m., reaching their maximum capacity during the midday hours when solar radiation is more intense. The remaining energy required to meet the overall electricity demand is covered by conventional producers which burn fossil fuels, such as fuel and natural gas to produce electricity. According to the merit order, the producer I1 which has the highest marginal cost does not participate to the mix in any time of the day, while producer I2 with the second highest cost dispatches electricity only at 7 p.m. and 8 p.m. when the demand is high and the availability of solar energy is significantly limited. As for the comparison between the strategic and the non-strategic aggregators, their overall electricity dispatch is almost equal, providing 4,800 and 4,830 MWhs daily, respectively.

The fluctuation of electricity and green certificates clearing prices across the time horizon is illustrated in *Figure 5.4*. By placing *Figures 5.3* and *5.4* side by side, it is obvious that high electricity prices are strongly correlated to the levels of power demand and RES production. In particular, between 8 p.m. and 9 p.m., when domestic power consumption is increased and no solar energy production is available, more expensive conventional producers enter the market and set the prices at a daily high of 150 $/MWh. In contrast to the non-strategic aggregator that bids at its zero marginal cost, the strategic one determines its own bidding strategies ($O_{s,t}^{EL}$) and operates as a price-maker, since these bids coincide with the electricity clearing prices. In particular, at 5 p.m., instead of operating its wind farm at maximum capacity and providing 150 MWh, the strategic player withholds its production at 135 MWh. This way the conventional producer I5 is fully dispatched, generating 150 MWh and the strategic aggregator can elevate its bid to 135 $/MWh outplacing producer I6, instead of bidding at 108 $/MWh in case of not having withheld its production. Hence, by adopting the proposed mathematical approach, the strategic aggregator can manipulate the prices and earn additional 2,025 $ (18,225 $ instead of 16,200 $) solely from one hour's transactions. Another great example of the strategic behavior of the aggregator is illustrated at time period 11. This time the aggregator withholds the production of its solar park, at 125 MWh instead of 130 MWh, so that the conventional producer I4 can be fully dispatched by providing these extra 5 MWh. This way the strategic aggregator can set the price at 108 $/MWh instead of 95 $/MWh. In other words, the price-maker aggregator sacrifices 5 MWh of its potential production in order to raise the price by 13 $/MWh and gain extra 1,150 $.

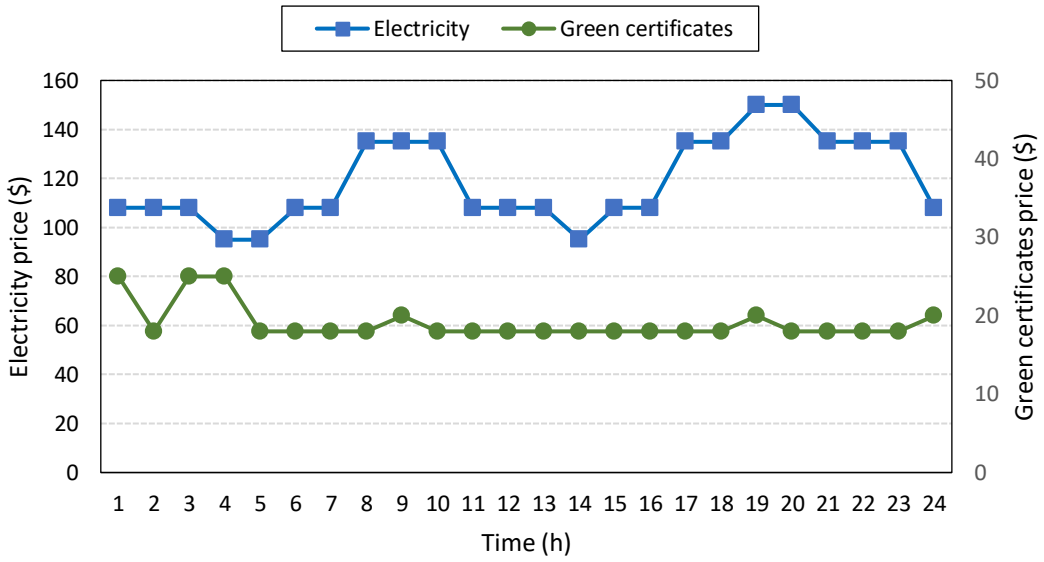

Figure 5.4: Electricity and green certificates clearing prices.

Figure 5.4 also depicts green certificates clearing prices, which are equal to the price-maker aggregator's optimal bids. As shown in this figure, at 9 a.m. the strategic aggregator offers only 86 certificates issued from the operation of its wind farm and solar park combined, at just under 20 $, in order to deter the provision of certificates by the non-strategic solar park. At 1 a.m. and 3 a.m. – 4 a.m. the highest certificates clearing prices are observed, equal to 25 $ which corresponds to the ACP rate. During these hours one or more LSEs decide that it is more beneficial to be charged with the ACP rate at 25 $ for a fraction of their certificates' demand, instead of buying them from the RES producers, as illustrated by *Figure 5.5* and *Figure 5.6*. The reason behind this phenomenon lies in the lack of solar energy production during these hours. Since the non-strategic wind park provides almost all of its available certificates, the strategic aggregator is the only available certificates provider left and can excessively speculate, offering its certificates at the price of 30 $, which is the cap set by the regulatory authority. Faced with this prospect, the LSEs prefer to pay the compliance penalty forcing the strategic aggregator to lower its bids also at 25 $ in order to be competitive.

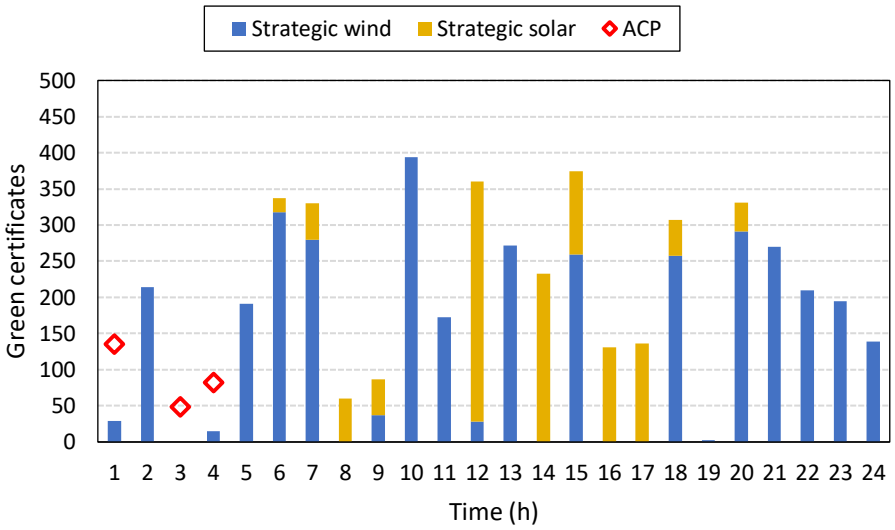

Figure 5.5: Green certificates trading by strategic renewable aggregator.

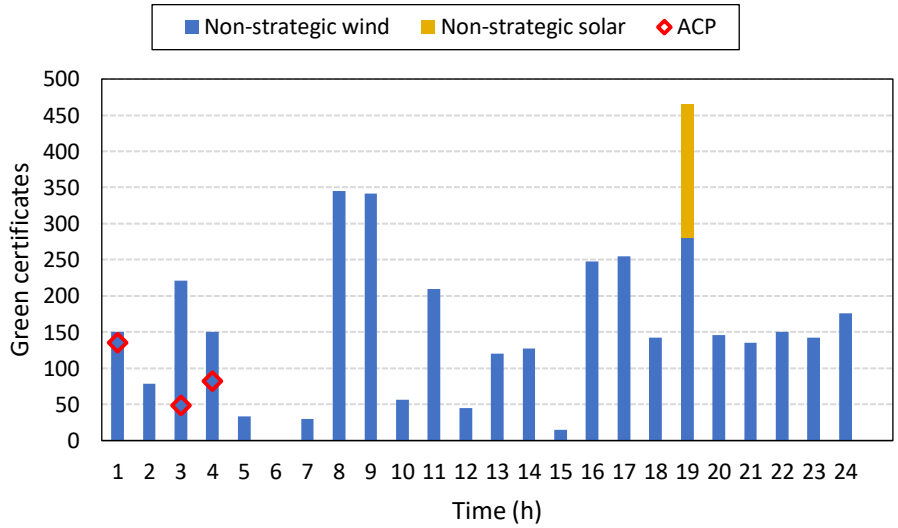

Figure 5.6: Green certificates trading by non-strategic renewable aggregator.

Figure 5.5 and *Figure 5.6* depict the green certificates provision for the strategic and non-strategic renewable aggregators, respectively. The strategic player offers certificates derived both from its wind and solar assets and almost completely outplaces the non-strategic player's solar park participation in the certificates market. Only at 7 p.m. the non-strategic aggregator manages to offer a quota of its certificates originating from solar energy, mostly due to the high electricity load at this hour which also leads to high demand for certificates, according to the RPS policy. Overall, the strategic player undertakes to provide a daily amount of 4,788 certificates, while the non-strategic one

only 3,784. This noteworthy divergence constitutes the key reason behind the considerable difference between the overall profits of the two players, as shown in *Table 5.2*. While. the non-strategic aggregator has slightly higher profits from its participation to the electricity market, the strategic aggregator exerting power in the markets by strategically submitting its bids, manages to obtain significantly higher daily overall profits. Based on the above results, it is confirmed that the proposed algorithm can be characterized as completely effective, as among players with identical assets, it ensures significant financial benefits to the strategic one that will adopt it.

Profits ($)	**Strategic aggregator**	**Non-strategic aggregator**
Electricity	567,665	571,580
Green certificates	86,961	73,736
Overall	**654,626**	**645,316**

Table 5.2: Profits of strategic and non-strategic renewable aggregators.

As already mentioned, this work introduces for the first time the mechanism of the state of available certificates, that indicates the number of certificates that each aggregator could potentially issue each hour of the day. *Figure 5.7* and *Figure 5.8* illustrate the SOAC for the strategic and non-strategic aggregator, respectively. From these two figures, it is obvious that the basic difference between the strategies of the two players lies in the fact that the price-maker aggregator chooses to sell the vast majority of its available certificates by the end of the time horizon of the application study. On the other hand, the trading strategy of the price-taker aggregator results in almost all the solar energy certificates remaining unsold. Selling the majority of the certificates until the end of the time horizon instead of keeping them for the next day, brings higher profits to the RES aggregator, since there is no certain forecast of the next day's price. Although the proposed algorithm does not include a special mathematical constraint that ensures the above strategy, in the general framework of providing the optimal trading plan for the price-maker aggregator, the algorithm automatically suggests this strategy.

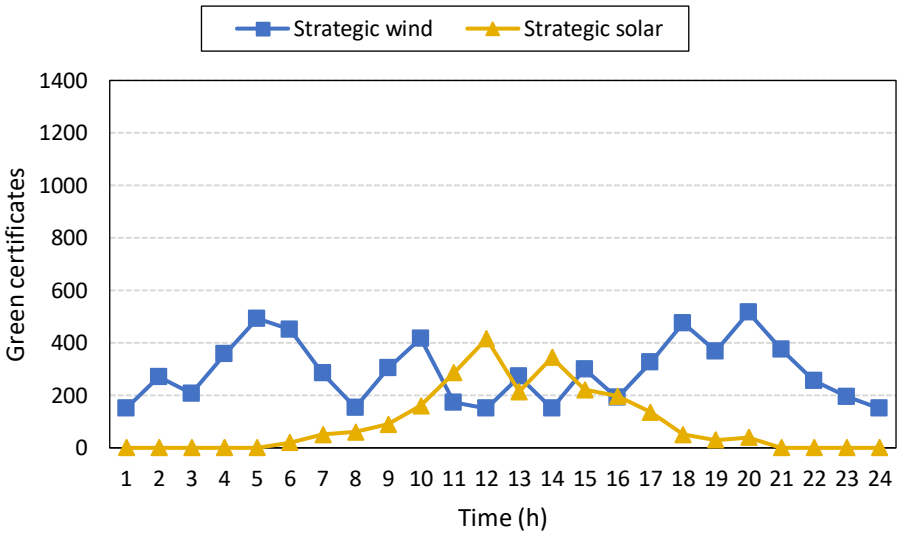

Figure 5.7: Hourly available tradable green certificates of the strategic renewable aggregator.

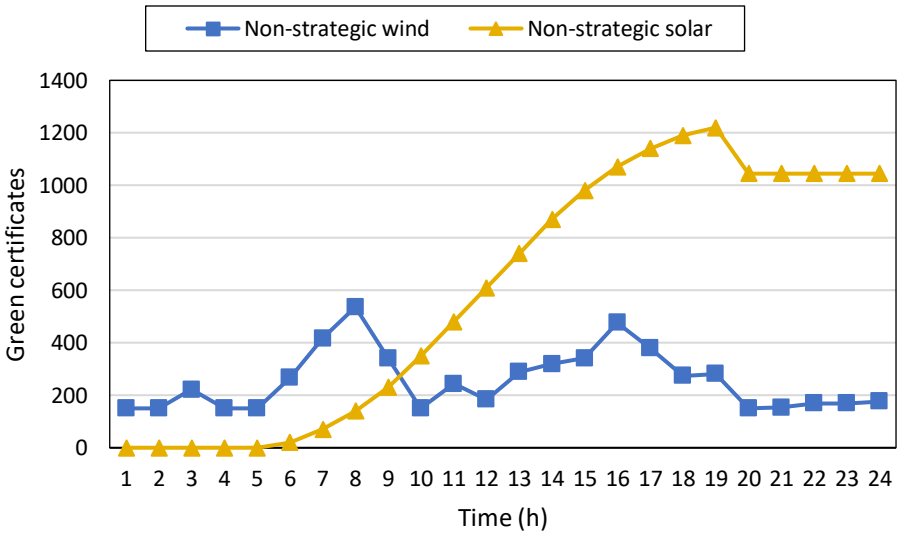

Figure 5.8: Hourly available tradable green certificates of the non-strategic renewable aggregator.

5.4.2 Congested power network

In the former uncongested power network case, the maximum electricity flow through each transmission line is 800 MW. If the capacity of lines A – D, B – C and D – E is reduced to 150 MW respectively, the power network becomes congested and is separated into two distinct sub-areas. The first sub-area includes buses A, B, E, where the assets of non-strategic aggregator are located and the second sub-area contains the renewable assets of the strategic aggregator at buses C, D. Power network congestion leads to different electricity LMPs for the most hours of the day, as shown in *Figure 5.9*. The strategic aggregator manages to exert market power and manipulate the electricity clearing prices. In particular, during the hours of the day when electricity demand is high and solar power generation is low (7 p.m. – 8 p.m.), the strategic player acts as a marginal producer in the second sub-area, setting the price at extremely high levels. Specifically in bus C, where the wind farm of the strategic aggregator is installed, a price cap of 290 $/MWh needs to be applied by the regulatory authority, in order to restrict the bids of the RES aggregator and limit the excessive speculation. Bus E is the least affected bus by the strategic aggregator's participation, since the two conventional units as well as the non-strategic aggregator's zero-cost wind farm that are installed, provide considerable amounts of low-cost power. Moreover, for the first time, the expensive conventional power plant $I1$ enters the market during the high net load hours 7 p.m. – 8 p.m., generating 140 MWh of electricity overall.

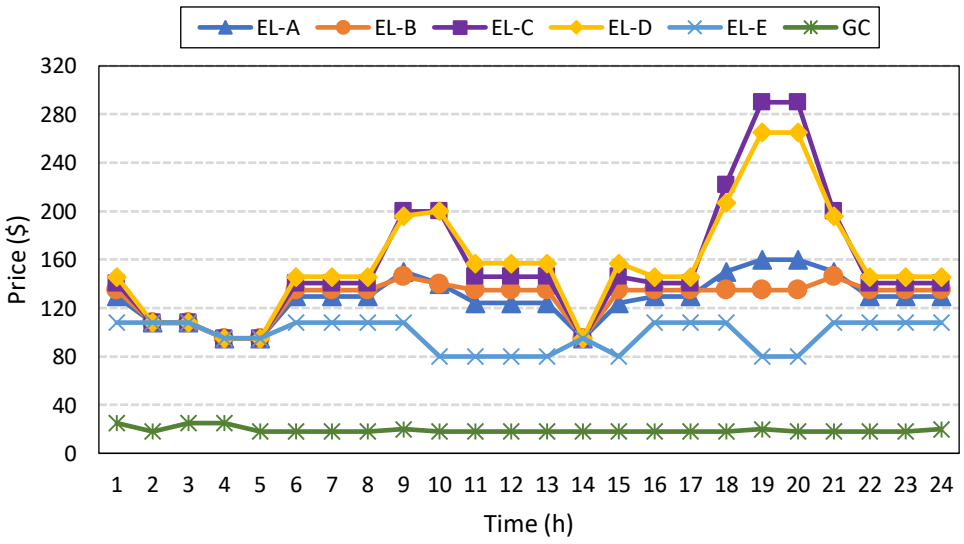

Figure 5.9: Electricity and green certificates clearing prices under power network congestion.

Comparing *Figure 5.4* to *Figure 5.9* it can be seen that the green certificates clearing prices are the same in both the uncongested and congested power network cases and are not directly affected by the changes that occur in the electricity market. However, as shown in *Table 5.3*, the provision of green certificates for the strategic aggregator differs between the two cases. In particular, the aggregator issues 96 certificates less under network congestion, a fact that is undoubtedly related to the lower production of electricity compared to the uncongested case. The non-strategic RES aggregator on the other hand, provides the exact same amount of power and certificates in both cases.

However, despite its slightly limited participation in electricity and green certificates markets under network congestion, the strategic player manages to vastly increase its overall expected profits by 168,000 $ compared to the uncongested case, as comprehensively illustrated by *Table 5.4*. This significant rise is solely due to the inflated electricity prices mentioned earlier, since the profits of strategic aggregator from issuing green certificates remain almost the same. An antidiametric scenario takes place regarding the non-strategic aggregator, who barely manages to benefit from network congestion by augmenting its profitability by almost 4,000 $ on a daily basis. Similar to the previous case study, under power network congestion, the strategic aggregator who has adopted the proposed mathematical approach manages to reap undeniably greater financial benefits compared to the non-strategic player.

Aggregator	***Uncongested power network***		***Congested power network***	
	Electricity (MWh)	*Certificates*	*Electricity (MWh)*	*Certificates*
Strategic	4,800	4,788	4,704	4,692
Non-strategic	4,830	3,784	4,830	3,784

Table 5.3: Renewable aggregators' overall electricity generation and certificates trading.

Profits ($)	**Strategic aggregator**	**Non-strategic aggregator**
Electricity	737,246	576,620
Green certificates	85,323	72,978
Overall	**822,569**	**649,598**

Table 5.4: Profits of strategic and non-strategic renewable aggregators under power network congestion.

5.4.3 Modified IEEE-24 bus power network

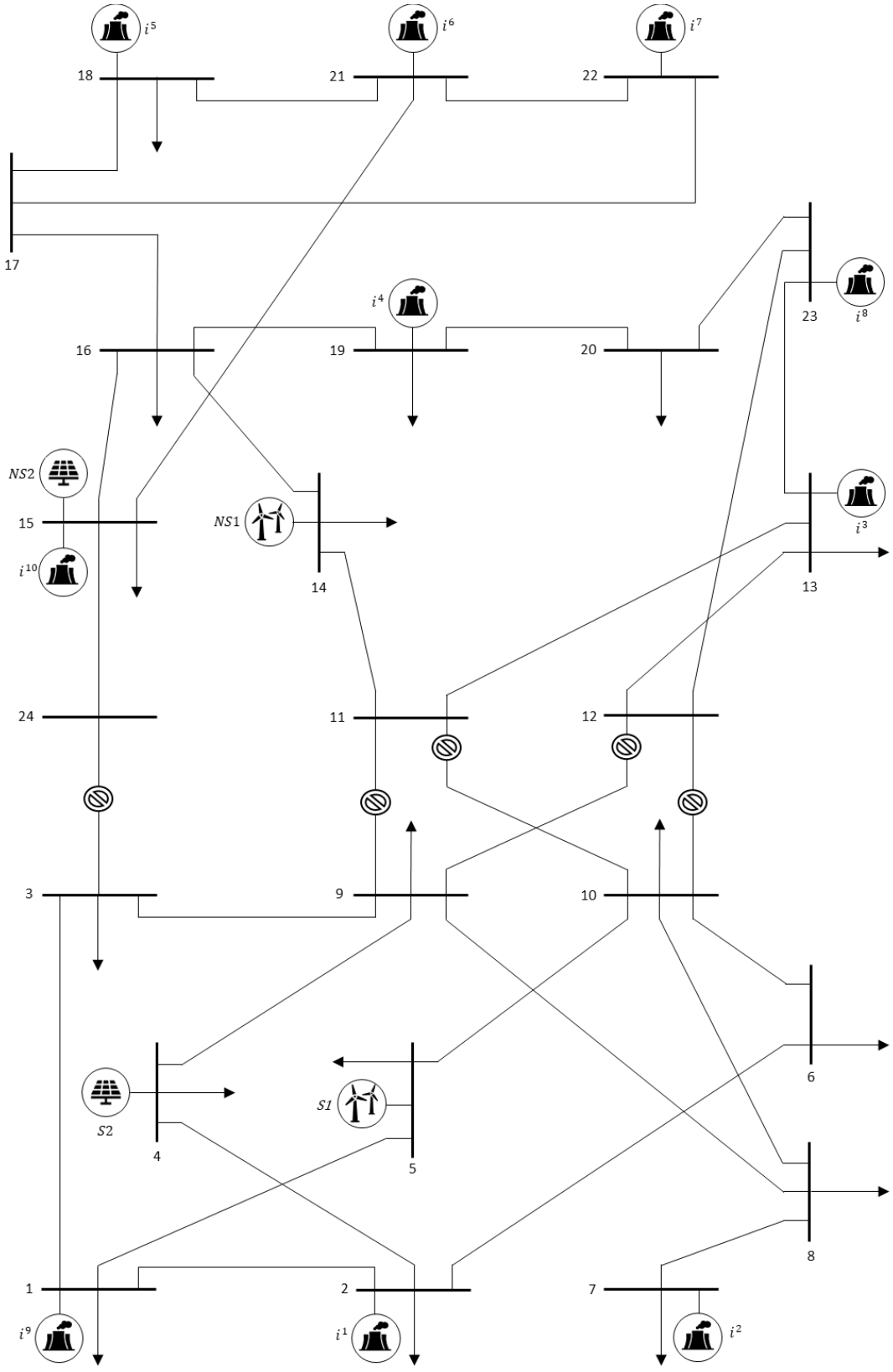

Figure 5.10: Modified IEEE 24-bus power network.

The proposed model is applied to a modified IEEE 24-bus reliability test system (RTS) (*Figure 5.10*). The total electricity demand depicted with the green line in *Figure 5.11* is shared among seventeen LSEs with different loads. The power network is conceivably divided into two sub-areas which are connected by the transmission lines 3 – 24, 9 – 11, 9 – 12, 10 – 11, 10 – 12. As with the PJM 5-bus case, the lower sub-area contains the renewable assets *S1* and *S2* of the strategic aggregator, while in the upper sub-area the assets *NS1* and *NS2* of the non-strategic player are installed. The capacities of the renewable power plants are higher compared to the base case study; however, both the strategic and non-strategic players own identical assets so that the comparison between them remains valid. In addition, there are now ten conventional producers across the power network.

As shown in *Figure 5.11*, the zero-cost wind farms and solar parks operate at their maximum capacity according to the merit order and the remaining required energy is provided by the conventional power producers. Due to their high marginal cost, producers I1 and I2 do not participate in the energy mix for any time of the day. The electricity and green certificates clearing price for the uncongested and congested power networks are depicted in *Figure 5.12* and *Figure 5.13*, respectively. Under power network congestion, it is observed that at the power buses where the renewable assets of the strategic aggregator are installed, the electricity LMPs are the highest across the whole grid. As in the 5-bus case, the strategic aggregator manages to arbitrage and sells its power output at much higher prices compared to the non-strategic player, within the framework of course set by the regulatory authority. Especially, for high electricity demand hours 4 p.m. – 8 p.m. the prices reach up to 161 $/MWh for the power bus where its solar park is installed.

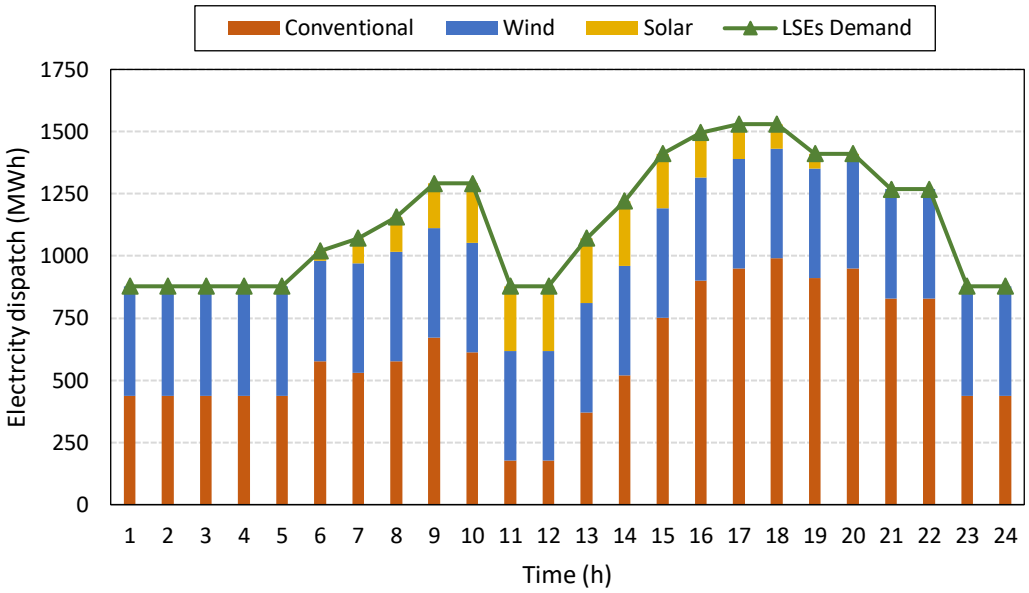

Figure 5.11: Power producers' dispatch and LSEs' power demand in the IEEE 24-bus power network.

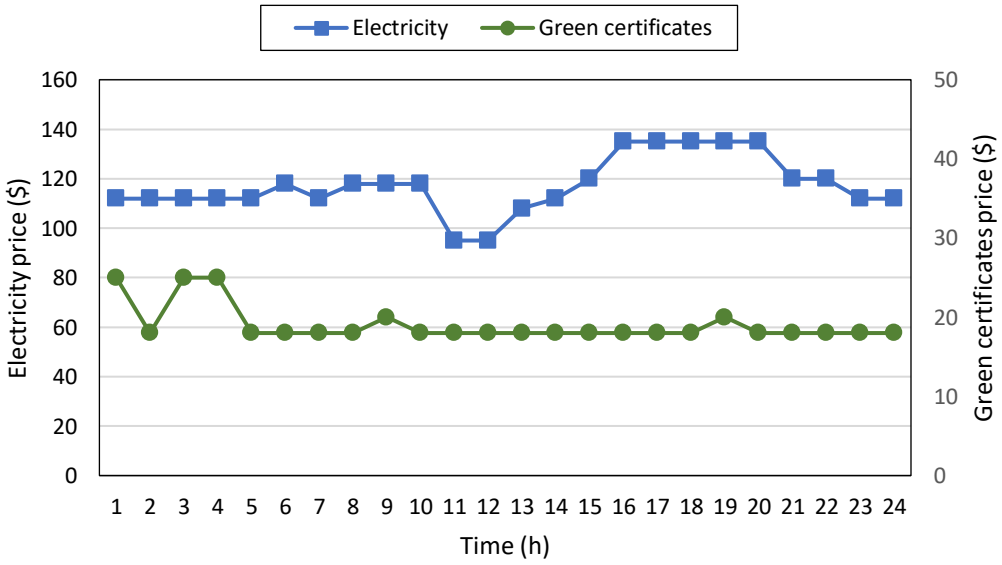

Figure 5.12: Electricity and green certificates clearing prices in the uncongested IEEE 24-bus power network.

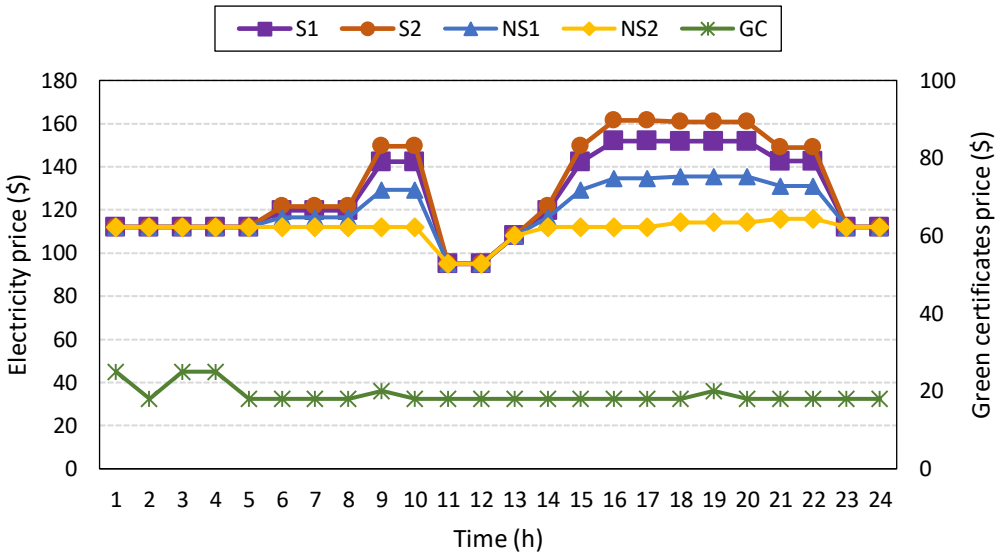

Figure 5.13: Electricity and green certificates clearing prices in the congested IEEE 24-bus power network.

Comparing the profitability of the two aggregators, for the uncongested power network case the strategic aggregator earnings have a slight lead, as shown by *Table 5.5.* While its electricity dispatch is less than the non-strategic player's, the strategic player manages to issue almost 1000 green certificates more (*Table 5.6*) by placing strategic bids and completely displacing the non-strategic player's solar certificates. The same pattern in green certificates market is repeated also in the case of network congestion. In fact, the power output of the strategic player is almost 70 MWh less. However, due to the significant high clearing prices that the strategic player achieves by exerting market power, manages to dramatically increase its profits by almost 70,000 $ (*Table 5.7*) over its rival player.

Profits ($)	**Strategic aggregator**	**Non-strategic aggregator**
Electricity	752,740	760,110
Green certificates	116,778	102,760
Overall	**869,518**	**862,870**

Table 5.5: Profits of strategic and non-strategic renewable aggregators in the uncongested IEEE 24-bus power network.

Aggregator	*Uncongested power network*		*Congested power network*	
	Electricity (MWh)	*Certificates*	*Electricity (MWh)*	*Certificates*
Strategic	4,800	4,788	4,704	4,692
Non-strategic	4,830	3,784	4,830	3,784

Table 5.6: Renewable aggregators' overall electricity generation and certificates trading in the IEEE 24-bus power network.

Profits ($)	Strategic aggregator	Non-strategic aggregator
Electricity	819,264	765,013
Green certificates	117,823	102,683
Overall	**937,087**	**867,696**

Table 5.7: Profits of strategic and non-strategic renewable aggregators in the congested IEEE 24-bus power network.

5.5 Computational issues

The resulting MILP is solved using GAMS/CPLEX 39.3.0, on an Intel Core i7-7700 processor at 3.60 GHz, with 16 GB RAM. The computational time highly depends on the power network sophistication and the number of market players. The average CPU time for the uncongested power network case is 3 seconds, while for the congested power network case, 297 seconds are required in order to reach the problem's optimal solution. For the IEEE 24-bus case, the CPU time is estimated at 37 and 315 seconds for the uncongested and congested power network cases, respectively. The selection of the appropriate big-Ms' value is firmly associated with the efficacy of the computational procedure, since the over- or underestimation of their value, can result either in an unrestricted or in a numerically sparce problem. After executing a series of trials, the value of big-Ms was determined at 10^4.

5.6 Conclusions

This chapter proposes a bi-level mathematical approach to determine the optimal trading scheme for a strategic renewable aggregator owning a wind farm and a solar park in interdependent pool-based electricity and green certificates markets. The algorithmic procedure included the upper-level model that aims at maximizing the profits of the strategic player and the lower-level problems that describe the sequential clearing mechanism, managed by the same MO in to minimize total operating market costs. The proposed model is first applied to a PJM 5-bus transmission constrained power grid and then to a modified IEEE 24-bus in order to illustrate its efficiency in a realistic energy market framework.

The problem solution determines the electricity and green certificates clearing prices as the dual variables of the two lower-level problems and the optimal trading plan for the strategic renewable aggregator in the day-ahead market. In addition, the proposed approach provides valuable information on the optimal management of the green certificates that each RES aggregator issues, in correlation with its power output, in order to maximize its expected profits. The impact of power network congestion on the clearing prices and the profitability of the strategic aggregator are also investigated. The raised prices, compared to the uncongested power network case, create additional arbitrage prospects for the strategic player, therefore acquiring considerably higher financial benefits. Finally, the proposed co-optimized approach for the participation of the strategic renewable aggregator in both energy and derivative markets brings increased revenues by at least 10%, compared to its participation only in the energy market.

Nomenclature

F. Indices and sets

i	Index for conventional power plants
s	Index for strategic renewable units
ns	Index for non-strategic renewable units
d	Index for LSEs
t	Index for time periods
n, m	Indices for power buses
$I\alpha N$	Set of indices for conventional power plants located at bus n
SaN	Set of indices for strategic renewable units located at bus n
$NSaN$	Set of indices for non-strategic renewable units located at bus n
DaN	Set of indices for LSE d located at bus n
NaM	Set of buses n connected with bus m

G. Acronyms – Superscripts

EL	Electricity
GC	Green certificate
ACP	Alternative compliance penalty
LSE	Load serving entity
RPS	Renewable energy portfolio standard

H. Parameters

C_i	Offering price of conventional power plant i ($/MWh)
C_{ns}	Offering price of non-strategic renewable units ($/MWh)
λ^{ACP}	ACP rate applied on green certificates mismatch of LSE d
RPS	RPS compliance imposed of LSE d by state regulator
$\overline{P}_i$	Maximum capacity of conventional power plant i (MW)
$\overline{F}_s$	Maximum capacity of strategic renewable unit s (MW)
$\overline{W}_{ns}$	Maximum capacity of non-strategic renewable unit ns (MW)

$L_{d,t}^{EL}$	Demand load of LSE *d* at time *t* (MWh)
$\overline{T}_{n,m}$	Transmission capacity of circuit line *n*-*m* (MW)
$B_{n,m}$	Susceptance of line *n*-*m*

I. Primal Variables

$O_{s,t}^{EL}$	Strategic electricity offering price of renewable unit *s* ($/MWh)
$O_{s,t}^{GC}$	Green certificate offering price of renewable unit *s* ($/certificate)
$p_{i,t}$	Electricity generation of conventional power plant *i* at time *t* (MWh)
$f_{s,t}$	Electricity generation of strategic renewable unit *s* at time *t* (MWh)
$w_{ns,t}$	Electricity generation of non-strategic renewable unit *ns* at time *t* (MWh)
$q_{s,t}^{\uparrow}$	Green certificates supplied to the market by strategic renewable unit *s* at time *t*
$r_{ns,t}^{\uparrow}$	Green certificates supplied to the market by non-strategic renewable unit *ns* at time *t*
$SOAC_{s,t}$	State of available green certificates for the strategic renewable unit *s* at time *t*
$SOAC_{ns,t}$	State of available green certificates for the non-strategic renewable unit *ns* at time *t*
$ACP_{d,t}$	Green certificates mismatch of LSE *d* at time *t*
$\delta_{n,t}$	Voltage angle at bus *n* at time *t*

J. Dual Variables

$\lambda_{n,t}^{EL}$	Electricity locational marginal price at bus *n* at time *t* ($/MWh)
λ_{t}^{GC}	Green certificates clearing price at time *t* ($/certificate)
$a_{i,t}$	Upper and lower electricity output of conventional power plant *i* at time *t*
$\gamma_{s,t}$	Upper and lower electricity output of strategic renewable unit *s* at time *t*
$\theta_{ns,t}$	Upper and lower electricity output of non-strategic renewable unit *ns* at time *t*

$\varepsilon_{s,t}$	Upper and lower green certificates issuance of strategic renewable unit *s* at time *t*
$\kappa_{ns,t}$	Upper and lower green certificates issuance of non-strategic renewable unit *ns* at time *t*
$\zeta_{d,t}$	Upper and lower green certificates demand for LSE *d* at time *t*
$\psi_{n,m,t}$	Transmission capacity of line *n*-*m* at time *t*
$\pi_{n,t}$	Upper and lower bound of the voltage angle $\delta_{n,t}$ at bus *n*
$\eta^{o}_{n,t}$	Voltage angle at bus *A*

Chapter 6

Conclusions and Future Research

6.1 Conclusions

The objective of this thesis has been to develop optimization-based techniques to investigate the strategic participation of various types of power producers and incorporate sustainability policies such as carbon emission allowances and green certificates trading in contemporary energy markets. Applying the research output of this thesis in real-life cases is expected to have a significant economic and environmental impact.

Chapter 2 presents a game based on the leader-follower Stackelberg hypothesis and proposed a bi-level mathematical framework aiming at deriving optimal strategies for offering/bidding by a strategic Energy Storage System (ESS) agent in a pool-based joint energy and reserves market. The model takes into account a sequential clearing process involving a day-ahead market for joint energy and reserve, as well as a real-time market for energy, both overseen by the Market Operator (MO). Uncertainty is introduced during the balancing stage through plausible wind power generation scenarios. Applying this model to a 6-bus transmission-constrained network, local marginal prices are derived as dual variables for the lower-level problems, determining optimal energy dispatch (charging/discharging) and reserve provisions for the ESS agent. The algorithm results in higher clearing prices compared to cost optimization. Additionally, the impact of potential network transmission congestions on ESS operation and expected profit is examined. Specifically, the ESS agent benefits from line congestions, experiencing a significant profit increase compared to uncongested scenarios. In conclusion, the model offers valuable insights for formulating policies that energy storage agents should adopt to leverage potential increases in wind generation capacity and achieve a lucrative profit boost.

In Chapter 3, a probabilistic Mixed-Integer Linear Programming (MILP) model is created to examine the financial benefits and optimal utilization of different energy storage technologies (Pumped Hydro Storage - PHS, Adiabatic Air-Compressed Energy

Storage - AA-CAES, Diabatic Compressed Air Energy Storage - D-CAES, and Lithium-Ion Battery) within an interconnected electricity and natural gas market operating under conditions of perfect competition. The model, designed for energy-only markets, simultaneously optimizes the market clearing process for both day-ahead and real-time trading platforms with the goal of maximizing social welfare. Stochasticity is introduced through a set of plausible scenarios for wind power production. The optimization framework is applied to an integrated energy system, comprising a transmission-constrained modified 24-bus IEEE Reliability Test System and a single-node natural gas network. The solution to the problem provides marginal prices for electricity and natural gas, optimal dispatch for (discharging) charging, and expected profits for each energy storage technology. A specific analysis is conducted on the operation of the diabatic CAES system, which participates in both systems as either a producer or a demand load. Additionally, all four energy storage systems benefit from power transmission line congestion and high wind power volatility, leading to a significant increase in profits compared to the case of an uncongested power network due to escalating electricity prices.

The next Chapter introduces a bi-level mathematical framework aiming at formulating optimal bidding strategies for a strategically positioned Gas-Fired Power Plant (GFPP) involved in interconnected markets for electricity and natural gas, operating within the context of a carbon emission trading scheme (CETS). The proposed model takes into account a sequential clearing process overseen by the Market Operator (MO), which seeks to minimize overall costs amidst high wind power integration. The application of this model is demonstrated on a PJM 5-bus transmission-constrained power grid and a singular-node gas network. The solution to the problem involves the derivation of CETS-embedded Electricity Locational Marginal Prices (ELMPs) and Gas Locational Marginal Prices (GLMPs) as dual variables for the lower-level problems. Additionally, strategic bidding decisions for the GFPP in the day-ahead market are obtained. The model furnishes insights into the optimal alignment of carbon emission allowances allocated to the GFPP with its electricity and natural gas generation/consumption, with the goal of maximizing expected profits. An examination of the impact of power network congestion on electricity clearing prices and the profitability of the gas-fired power plant is also conducted. In comparison to the scenario with an uncongested network, the increased CETS-ELMPs create more opportunities for

arbitrage for the strategic GFPP, resulting in substantial economic advantages. Lastly, the continual rise in natural gas prices prompts the gas-fired power plant to strategically curtail its power generation, as the ensuing electricity prices do not adequately offset the increased production costs.

The final Chapter 5 introduces a bi-level mathematical strategy to identify the most effective trading plan for a strategic renewable aggregator that owns both a wind farm and a solar park, operating within interconnected pool-based electricity and green certificates markets. The algorithmic process encompasses an upper-level model focused on maximizing the strategic player's profits, along with lower-level problems detailing the sequential clearing mechanism. These lower-level problems are managed by the same multi-objective optimization (MO) to minimize overall operating market costs. To showcase its effectiveness in a practical energy market context, the proposed model is initially applied to a PJM 5-bus transmission-constrained power grid and subsequently to a modified IEEE 24-bus. The solution to the problem determines the clearing prices for electricity and green certificates as the dual variables of the two lower-level problems, along with the optimal trading strategy for the strategic renewable aggregator in the day-ahead market. Furthermore, the proposed approach furnishes valuable insights into the optimal management of green certificates issued by each Renewable Energy Source (RES) aggregator, correlating with its power output to maximize expected profits. The study also explores the impact of power network congestion on clearing prices and the profitability of the strategic aggregator. Elevated prices resulting from network congestion, compared to an uncongested power network scenario, create additional arbitrage opportunities for the strategic player, leading to significantly higher financial gains. Ultimately, the co-optimized approach for the strategic renewable aggregator's participation in both energy and derivative markets is shown to yield increased revenues of at least 10% compared to its exclusive participation in the energy market.

6.2 Main Contributions of this work

In summary, the main contributions of this thesis have been:

- A novel bi-level complementarity model to analyse the inter-relationships between the ESS's optimal bidding and offering strategies, participating in a jointly cleared energy and reserve day-ahead pool, as well as in real-time pool, under network transmission constraints. Numerical simulations provide the market outcomes of transmission lines congestions and variable levels of wind power generation insertion and the measure of their influence on ESS agent's (dis)charging decision strategies.
- The development of a stochastic MILP market-clearing model to determine optimal dispatch and analyze expected profits of PHS, AA-CAES, D-CAES and Li-ion battery systems in a coupled electricity and natural gas market, under perfect competition. The proposed modelling for the diabatic CAES system's operation in both markets is of great interest, since it acts bilaterally as power producers and gas consumer.
- A bi-level optimization framework to determine the optimal bidding decisions and emission allowances manipulation of a strategic gas-fired power plant in a pool-based market scheme, acting as a producer in the electricity market and as a consumer in the natural gas market. This model derives the optimal electricity and natural gas dispatch and CETS-embedded electricity locational marginal prices and analyzes the impact of power network congestion on electricity locational marginal prices and profitability of the strategic gas-fired power plant.
- A novel bi-level mathematical model to derive the optimal trading decisions for a strategic renewable aggregator in a joint pool-based electricity and green certificates market scheme and to successfully link and coordinate the operation of the two markets. The proposed approach also analyzes the impact of power network congestion on electricity and green certificates prices and the strategic renewable aggregator's profitability in a real-life 24-bus power system.

6.3 Recommendations for future research

A range of subjects requiring further investigation has been revealed in the course of this work. More specifically, future research directions could focus on:

- The development of an algorithm studying the strategic behavior of an agent with a mixed generation portfolio (i.e., conventional, wind and electricity storage) in a joint energy and reserve market. Extensions could also integrate detailed technical parameters of storage and electricity generators or other types of renewables with a representative and realistic set of scenarios. In that case, due to the increased complexity of the optimization problem, special solution techniques (decomposition algorithms) should be investigated.
- A bi-level optimization algorithm in the form of equilibrium problem with equilibrium constraints (EPEC) to investigate the optimal bidding strategies for the above storage systems that act strategically in an imperfect coupled electricity and natural gas market. A possible future extension of the model may also incorporate a carbon emission trading scheme, to compare the diabatic CAES system which emits carbon pollutants when burning natural gas, with the rest carbon-free storage technologies.
- An optimization framework, investigating the strategic behaviour of a market agent with a mixed generation portfolio (gas-fired power plant combined with wind farm), in a CETS-embedded joint electricity and natural gas market scheme. Extensions could also incorporate the natural gas network expansion, in order to study GFPP's demeanour, acting as strategic gas consumer in multiple nodes.
- An equilibrium problem with equilibrium constraints (EPEC) that will investigate the arbitrage opportunities of two or more strategic aggregators in electricity and green certificates market. A possible future extension of the model may also incorporate the examination of significant investment opportunities for the strategic aggregator and the possible expansion of its assets and activity in the market.

Bibliography

Aburub, H., Basnet, S., & Jewell, W. T. (2019). On the use of adjustable-speed pumped hydro storage operation in the U.S electricity market. *Journal of Energy Storage*, *23*(April), 495–503. https://doi.org/10.1016/j.est.2019.04.011

Afshar, K., Ghiasvand, F. S., & Bigdeli, N. (2018). Optimal bidding strategy of wind power producers in pay-as-bid power markets. *Renewable Energy*, *127*, 575–586. https://doi.org/10.1016/j.renene.2018.05.015

Ahmad, F., Iqbal, A., Ashraf, I., Marzband, M., & khan, I. (2022). Optimal location of electric vehicle charging station and its impact on distribution network: A review. *Energy Reports*, *8*, 2314–2333. https://doi.org/10.1016/j.egyr.2022.01.180

Akbari-Dibavar, A., Mohammadi-Ivatloo, B., & Zare, K. (2020). Optimal stochastic bilevel scheduling of pumped hydro storage systems in a pay-as-bid energy market environment. *Journal of Energy Storage*, *31*(May), 101608. https://doi.org/10.1016/j.est.2020.101608

Akbari-Dibavar, A., Mohammadi-Ivatloo, B., Zare, K., Khalili, T., & Bidram, A. (2021). Economic-Emission Dispatch Problem in Power Systems with Carbon Capture Power Plants. *IEEE Transactions on Industry Applications*, *57*(4), 3341–3351. https://doi.org/10.1109/TIA.2021.3079329

Akhavan-Hejazi, H., Asghari, B., & Sharma, R. K. (2015). A joint bidding and operation strategy for battery storage in multi-temporal energy markets. *2015 IEEE Power and Energy Society Innovative Smart Grid Technologies Conference, ISGT 2015*. https://doi.org/10.1109/ISGT.2015.7131830

An, X., Zhang, S., Li, X., & Du, D. (2019). Two-stage joint equilibrium model of electricity market with tradable green certificates. *Transactions of the Institute of Measurement and Control*, *41*(6), 1615–1626. https://doi.org/10.1177/0142331217718619

Arabkoohsar, A., & Namib, H. (2021). Pumped hydropower storage. *Mechanical Energy Storage Technologies*, *September*, 73–100. https://doi.org/10.1016/b978-0-12-820023-0.00004-3

Arabkoohsar, A., Rahrabi, H. R., Alsagri, A. S., & Alrobaian, A. A. (2020). Impact of Off-design operation on the effectiveness of a low-temperature compressed air energy storage system. *Energy*, *197*, 117176. https://doi.org/10.1016/j.energy.2020.117176

Arteaga, J., & Zareipour, H. (2019). A Price-Maker/Price-Taker Model for the Operation of Battery Storage Systems in Electricity Markets. *IEEE Transactions on Smart Grid*. https://doi.org/10.1109/TSG.2019.2913818

Babaei, S. M., Nabat, M. H., Lashgari, F., Pedram, M. Z., & Arabkoohsar, A. (2021). Thermodynamic analysis and optimization of an innovative hybrid multi-generating liquid air energy storage system. *Journal of Energy Storage*, *43*(July), 103262. https://doi.org/10.1016/j.est.2021.103262

Bafrani, H. A., Sedighizadeh, M., Dowlatshahi, M., Ershadi, M. H., & Rezaei, M. M. (2021). Reliability and reserve in day ahead joint energy and reserve market stochastic scheduling in presence of compressed air energy storage. *Journal of Energy Storage*, *43*(September), 103194. https://doi.org/10.1016/j.est.2021.103194

Baherifard, M. A., Kazemzadeh, R., Yazdankhah, A. S., & Marzband, M. (2022). Intelligent charging planning for electric vehicle commercial parking lots and its impact on distribution network's imbalance indices. *Sustainable Energy, Grids and Networks*, *30*, 100620. https://doi.org/10.1016/j.segan.2022.100620

Baringo, L., & Conejo, A. J. (2011). Wind power investment within a market environment. *Applied Energy*. https://doi.org/10.1016/j.apenergy.2011.03.023

Baringo, L., & Conejo, A. J. (2013). Strategic offering for a wind power producer. *IEEE Transactions on Power Systems*. https://doi.org/10.1109/TPWRS.2013.2273276

Baziar, A. A., Niknam, T., & Simab, M. (2021). Strategic offering of producers in the day-ahead coupled gas and electricity market including energy and reserve models. *Electric Power Systems Research*, *199*(June), 107376. https://doi.org/10.1016/j.epsr.2021.107376

Borenstein, S. (2000). Understanding Competitive Pricing and Market Power in Wholesale Electricity Markets. *The Electricity Journal*, *13*(6), 49–57. https://doi.org/10.1016/s1040-6190(00)00124-x

Brook, A., Kendrick, D., & Meeraus, A. (1988). GAMS, a user's guide. *ACM SIGNUM Newsletter*. https://doi.org/10.1145/58859.58863

Brooke, A., Kendrick, D., Meeraus, A., Raman, R., & Rosenthal, R. E. (1998). GAMS: A User's Guide, GAMS Development Corporation. *Washington, DC*, *20007*.

Budt, M., Wolf, D., Span, R., & Yan, J. (2016). A review on compressed air energy storage: Basic principles, past milestones and recent developments. *Applied Energy*, *170*, 250–268. https://doi.org/https://doi.org/10.1016/j.apenergy.2016.02.108

California Public Utility Commission. (n.d.). *Energy Storage Decision D.13-10-040*. Oct.2013 [Online]. Available: https://www.cpuc.ca.gov/

Cavallo, A. (2007). Controllable and affordable utility-scale electricity from intermittent wind resources and compressed air energy storage (CAES). *Energy*, *32*, 120–127. https://doi.org/10.1016/j.energy.2006.03.018

Chen, R., Wang, J., & Sun, H. (2018). Clearing and Pricing for Coordinated Gas and Electricity Day-Ahead Markets Considering Wind Power Uncertainty. *IEEE Transactions on Power Systems*, *33*(3), 2496–2508. https://doi.org/10.1109/TPWRS.2017.2756984

Chen, S., Rahbari, H. R., Arabkoohsar, A., & Zhu, T. (2020). Impacts of partial-load service on energy, exergy, environmental and economic performances of low-temperature compressed air energy storage system. *Journal of Energy Storage*, *32*(July), 101900. https://doi.org/10.1016/j.est.2020.101900

Chen, Y., Hobbs, B. F., Leyffer, S., & Munson, T. S. (2006). Leader-follower equilibria for electric power and NOx allowances markets. *Computational Management Science*, *3*(4), 307–330. https://doi.org/10.1007/s10287-006-0020-1

Chen, Z., Umar, M., Su, C.-W., & Mirza, N. (2023). Renewable energy, credit portfolios and intermediation spread: Evidence from the banking sector in BRICS. *Renewable Energy*, *208*(March), 561–566. https://doi.org/10.1016/j.renene.2023.03.003

Conejo, A. J., Carrión, M., & Morales, J. M. (2010). *Decision Making Under Uncertainty in Electricity Markets* (Issues 978-1-4419-7421–1). Springer. https://doi.org/10.1007/978-1-4419-7421-1

Corchero, C., Heredia, F. J., & Cifuentes, J. (2012). Optimal electricity market bidding strategies considering emission allowances. *9th International Conference on the European Energy Market, EEM 12*. https://doi.org/10.1109/EEM.2012.6254676

Coulon, M., Khazaei, J., & Powell, W. B. (2015). SMART-SREC: A stochastic model of the New Jersey solar renewable energy certificate market. *Journal of Environmental Economics and Management*, *73*, 13–31. https://doi.org/10.1016/j.jeem.2015.05.004

Dai, T., & Qiao, W. (2015). Optimal bidding strategy of a strategic wind power producer in the short-term market. *IEEE Transactions on Sustainable Energy*, *6*(3), 707–719. https://doi.org/10.1109/TSTE.2015.2406322

De La Nieta, A. A. S., Contreras, J., & Muñoz, J. I. (2013). Optimal coordinated wind-hydro bidding strategies in day-ahead markets. *IEEE Transactions on Power Systems*, *28*(2), 798–809. https://doi.org/10.1109/TPWRS.2012.2225852

Delikaraoglou, S., Papakonstantinou, A., Ordoudis, C., & Pinson, P. (2015). Price-maker wind power producer participating in a joint day-ahead and real-time market. *International Conference on the European Energy Market, EEM*, *2015-Augus*. https://doi.org/10.1109/EEM.2015.7216701

Denholm, P., Ela, E., Kirby, B., & Milligan, M. (2011). The role of energy storage with renewable electricity generation. In *Energy Storage: Issues and Applications*.

Drury, E., Denholm, P., & Sioshansi, R. (2011). The value of compressed air energy storage in energy and reserve markets. *Energy*, *36*(8), 4959–4973. https://doi.org/10.1016/j.energy.2011.05.041

Dueñas, P., Leung, T., Gil, M., & Reneses, J. (2015). Gas-electricity coordination in competitive markets under renewable energy uncertainty. *IEEE Transactions on Power Systems*, *30*(1), 123–131. https://doi.org/10.1109/TPWRS.2014.2319588

EnergyTag. (2021). *EnergyTag and granular energy certificates: Accelerating the transition to 24/7 clean power*.

Exizidis, L., Kazempour, J., Pinson, P., De Greve, Z., & Vallee, F. (2016). Strategic wind power trading considering rival wind power production. *IEEE PES Innovative Smart*

Grid Technologies Conference Europe, 873–878. https://doi.org/10.1109/ISGT-Asia.2016.7796500

Fang, Y., & Zhao, S. (2020). Look-ahead bidding strategy for concentrating solar power plants with wind farms. *Energy*, *203*, 117895. https://doi.org/10.1016/j.energy.2020.117895

Feng, Q., Wu, Z., & Zhang, W. (2020). Carbon emissions market adjustment in the electricity supply sector: A government perspective. *Journal of Cleaner Production*, *275*, 123132. https://doi.org/10.1016/j.jclepro.2020.123132

FERC Staff. (2015). FERC Order 809: Coordination of the Scheduling Processes of Interstate Natural Gas Pipelines and Public Utilities. *Federal Energy Regulatory Commission (FERC)*, *809*. https://www.ferc.gov/whats-new/comm-meet/2015/041615/M-1.pdf

Fortuny-amat, A. J., Mccarl, B., Fortuny-amat, J., & Mccarl, B. (1981). Linked references are available on JSTOR for this article : A Representation and Economic Interpretation of a Two-Level Programming Problem. *Thejournal of the Operational Research Society*, *32*(9), 783–792.

Fortuny-Amat, J., & McCarl, B. (1981). A Representation and Economic Interpretation of a Two-Level Programming Problem. *The Journal of the Operational Research Society*. https://doi.org/10.2307/2581394

Gabriel, S. A., & Leuthold, F. U. (2010). Solving discretely-constrained MPEC problems with applications in electric power markets. *Energy Economics*, *32*(1), 3–14. https://doi.org/10.1016/j.eneco.2009.03.008

Gan, D., Feng, D., & Xie, J. (2013). Electricity Markets and Power System Economics. In *Electricity Markets and Power System Economics*. https://doi.org/10.1201/b15550

Gielen, D., Boshell, F., Saygin, D., Bazilian, M. D., Wagner, N., & Gorini, R. (2019). The role of renewable energy in the global energy transformation. *Energy Strategy Reviews*, *24*(June 2018), 38–50. https://doi.org/10.1016/j.esr.2019.01.006

Gil, M., Duenas, P., & Reneses, J. (2016). Electricity and natural gas interdependency: Comparison of two methodologies for coupling large market models within the

european regulatory framework. *IEEE Transactions on Power Systems*, *31*(1), 361–369. https://doi.org/10.1109/TPWRS.2015.2395872

Graça Gomes, J., Jiang, J., Chong, C. T., Telhada, J., Zhang, X., Sammarchi, S., Wang, S., Lin, Y., & Li, J. (2023). Hybrid solar PV-wind-battery system bidding optimisation: A case study for the Iberian and Italian liberalised electricity markets. *Energy*, *263*(November 2022). https://doi.org/10.1016/j.energy.2022.126043

Green, R., & Vasilakos, N. (2010). Market behaviour with large amounts of intermittent generation. *Energy Policy*. https://doi.org/10.1016/j.enpol.2009.07.038

Greenblatt, J. B., Succar, S., Denkenberger, D. C., Williams, R. H., & Socolow, R. H. (2007). Baseload wind energy: modeling the competition between gas turbines and compressed air energy storage for supplemental generation. *Energy Policy*, *35*(3), 1474–1492. https://doi.org/10.1016/j.enpol.2006.03.023

Grigg, C., & Wong, P. (1999). The IEEE reliability test system -1996 a report prepared by the reliability test system task force of the application of probability methods subcommittee. *IEEE Transactions on Power Systems*, *14*(3), 1010–1020. https://doi.org/10.1109/59.780914

Guo, H., Chen, Q., Xia, Q., & Kang, C. (2020). Modeling Strategic Behaviors of Renewable Energy with Joint Consideration on Energy and Tradable Green Certificate Markets. *IEEE Transactions on Power Systems*, *35*(3), 1898–1910. https://doi.org/10.1109/TPWRS.2019.2953114

Gupta, S. K., & Purohit, P. (2013). Renewable energy certificate mechanism in India: A preliminary assessment. *Renewable and Sustainable Energy Reviews*, *22*, 380–392. https://doi.org/10.1016/j.rser.2013.01.044

Hansen, J.-P., & Percebois, J. (2019). *Énergie: Économie et politiques*. De Boeck Supérieur.

He, G., Chen, Q., Kang, C., Pinson, P., & Xia, Q. (2016). Optimal Bidding Strategy of Battery Storage in Power Markets Considering Performance-Based Regulation and Battery Cycle Life. *IEEE Transactions on Smart Grid*, *7*(5), 2359–2367. https://doi.org/10.1109/TSG.2015.2424314

Helgesen, P. I., & Tomasgard, A. (2018). An equilibrium market power model for power

markets and tradable green certificates, including Kirchhoff's Laws and Nash-Cournot competition. *Energy Economics*, *70*, 270–288. https://doi.org/10.1016/j.eneco.2018.01.013

Hosseini, S. A., Toubeau, J. F., De Grève, Z., & Vallée, F. (2020). An advanced day-ahead bidding strategy for wind power producers considering confidence level on the real-time reserve provision. *Applied Energy*, *280*(September). https://doi.org/10.1016/j.apenergy.2020.115973

Hui, W., Xin-gang, Z., Ling-zhi, R., & Fan, L. (2021). An agent-based modeling approach for analyzing the influence of market participants' strategic behavior on green certificate trading. *Energy*, *218*, 119463. https://doi.org/10.1016/j.energy.2020.119463

Hulshof, D., Jepma, C., & Mulder, M. (2019). Performance of markets for European renewable energy certificates. *Energy Policy*, *128*(February), 697–710. https://doi.org/10.1016/j.enpol.2019.01.051

Hustveit, M., Frogner, J. S., & Fleten, S. E. (2017). Tradable green certificates for renewable support: The role of expectations and uncertainty. *Energy*, *141*, 1717–1727. https://doi.org/10.1016/j.energy.2017.11.013

International Renewable Energy Agency. (2023). Renewable Capacity Highlights 2023. *Irena*, *April*, 1–3.

International Renewable Energy Agency (IRENA). (2017). Electricity storage and renewables: Costs and markets to 2030. In *Electricity-storage-and-renewables-costs-and-markets*.

IRENA. (2019a). Renewable capacity statistics 2019, International Renewable Energy Agency (IRENA), Abu Dhabi. In *International Renewable Energy Agency (IRENA), Abu Dhabi*. https://www.irena.org/publications/2019/Mar/Renewable-Capacity-Statistics-2019

IRENA. (2019b). Utility-Scale Batteries Innovation Landscape Brief. *International Renewable Energy Agency*, 7.

IRENA. (2021). *Renewable Capacity Statistiques De Capacité Estadísticas De Capacidad*.

www. irena.org

Irfan, M. (2021). Integration between electricity and renewable energy certificate (REC) markets: Factors influencing the solar and non-solar REC in India. *Renewable Energy*, *179*, 65–74. https://doi.org/10.1016/j.renene.2021.07.020

Joshi, J. (2021). Do renewable portfolio standards increase renewable energy capacity? Evidence from the United States. *Journal of Environmental Management*, *287*(February), 112261. https://doi.org/10.1016/j.jenvman.2021.112261

Jülch, V. (2016). Comparison of electricity storage options using levelized cost of storage (LCOS) method. *Applied Energy*, *183*, 1594–1606. https://doi.org/10.1016/j.apenergy.2016.08.165

Kanakasabapathy, P., & Shanti Swarup, K. (2010). Bidding strategy for pumped-storage plant in pool-based electricity market. *Energy Conversion and Management*, *51*(3), 572–579. https://doi.org/10.1016/j.enconman.2009.11.001

Kardakos, E. G., Simoglou, C. K., & Bakirtzis, A. G. (2014). Optimal bidding strategy in transmission-constrained electricity markets. *Electric Power Systems Research*, *109*, 141–149. https://doi.org/10.1016/j.epsr.2013.12.014

Kardakos, E. G., Simoglou, C. K., & Bakirtzis, A. G. (2016). Optimal Offering Strategy of a Virtual Power Plant: A Stochastic Bi-Level Approach. *IEEE Transactions on Smart Grid*, *7*(2), 794–806. https://doi.org/10.1109/TSG.2015.2419714

Kazempour, S. J., Yousefi, A., Zare, K., Moghaddam, M. P., Haghifam, M. R., & Tarbiat, G. R. Y. (2008). A MIP-Based optimal operation scheduling of pumped-storage plant in the energy and regulation markets. *Proceedings of the Universities Power Engineering Conference*, 1–5. https://doi.org/10.1109/UPEC.2008.4651465

Khaloie, H., Abdollahi, A., Shafie-khah, M., Anvari-Moghaddam, A., Nojavan, S., Siano, P., & Catalão, J. P. S. (2020). Coordinated wind-thermal-energy storage offering strategy in energy and spinning reserve markets using a multi-stage model. *Applied Energy*, *259*(June 2019), 114168. https://doi.org/10.1016/j.apenergy.2019.114168

Khaloie, H., Abdollahi, A., Shafie-Khah, M., Siano, P., Nojavan, S., Anvari-Moghaddam, A., & Catalão, J. P. S. (2020). Co-optimized bidding strategy of an integrated wind-thermal-

photovoltaic system in deregulated electricity market under uncertainties. *Journal of Cleaner Production*, *242*. https://doi.org/10.1016/j.jclepro.2019.118434

Khatami, R., Oikonomou, K., & Parvania, M. (2020). Look-ahead optimal participation of compressed air energy storage in day-ahead and real-time markets. *IEEE Transactions on Sustainable Energy*, *11*(2), 682–692. https://doi.org/10.1109/TSTE.2019.2903783

Khojasteh, M., Faria, P., & Vale, Z. (2022). Scheduling of battery energy storages in the joint energy and reserve markets based on the static frequency of power system. *Journal of Energy Storage*, *49*, 104115. https://doi.org/10.1016/j.est.2022.104115

Kirschen, D., & Strbac, G. (2005). Fundamentals of Power System Economics. In *Fundamentals of Power System Economics*. https://doi.org/10.1002/0470020598

Koohi-Fayegh, S., & Rosen, M. A. (2020). A review of energy storage types, applications and recent developments. *Journal of Energy Storage*, *27*(July 2019), 101047. https://doi.org/10.1016/j.est.2019.101047

Labay, V. Y., Savchenko, O. O., Zhelykh, V. M., & Kozak, K. R. (2019). Mathematical modeling of the heating process in a vortex tube at the gas distribution stations. *Mathematical Modeling and Computing*, *6*(2), 311–319. https://doi.org/10.23939/mmc2019.02.311

Laia, R., Pousinho, H. M. I., Melíco, R., & Mendes, V. M. F. (2016). Bidding strategy of wind-thermal energy producers. *Renewable Energy*, *99*, 673–681. https://doi.org/10.1016/j.renene.2016.07.049

Larsson, M. (2009). Global energy transformation: Four necessary steps to make clean energy the next success story. In *Global Energy Transformation: Four Necessary Steps to Make Clean Energy the Next Success Story*. https://doi.org/10.1057/9780230244092

Levitan, R., Wilmer, S., & Carlson, R. (2014). Pipeline to reliability: Unraveling gas and electric interdependencies across the eastern interconnection. *IEEE Power and Energy Magazine*, *12*(6), 78–88. https://doi.org/10.1109/MPE.2014.2347632

Li, X., Liu, P., Cheng, L., Cheng, Q., Zhang, W., Xu, S., & Zheng, Y. (2023). Strategic bidding

for a hydro-wind-photovoltaic hybrid system considering the profit beyond forecast time. *Renewable Energy*, *204*(September 2022), 277–289. https://doi.org/10.1016/j.renene.2022.12.098

Lu, N., Chow, J. H., & Desrochers, A. A. (2004). Pumped-storage hydro-turbine bidding strategies in a competitive electricity market. *IEEE Transactions on Power Systems*, *19*(2), 834–841. https://doi.org/10.1109/TPWRS.2004.825911

Lu, Z., Liu, M., Lu, W., & Lin, S. (2022). Shared-constraint approach for multi-leader multi-follower game of generation companies participating in electricity markets with carbon emission trading mechanism. *Journal of Cleaner Production*, *350*(February), 131424. https://doi.org/10.1016/j.jclepro.2022.131424

Madlener, R., & Latz, J. (2013). Economics of centralized and decentralized compressed air energy storage for enhanced grid integration of wind power. *Applied Energy*, *101*, 299–309. https://doi.org/10.1016/j.apenergy.2011.09.033

Mazzi, N., Kazempour, J., & Pinson, P. (2018). Price-Taker Offering Strategy in Electricity Pay-as-Bid Markets. *IEEE Transactions on Power Systems*, *33*(2), 2175–2183. https://doi.org/10.1109/TPWRS.2017.2737322

McConnell, D., Forcey, T., & Sandiford, M. (2015). Estimating the value of electricity storage in an energy-only wholesale market. *Applied Energy*. https://doi.org/10.1016/j.apenergy.2015.09.006

Moazeni, F., & Khazaei, J. (2020). Optimal operation of water-energy microgrids; a mixed integer linear programming formulation. *Journal of Cleaner Production*, *275*, 122776. https://doi.org/10.1016/j.jclepro.2020.122776

Mohsenian-Rad, H. (2016). Coordinated Price-Maker Operation of Large Energy Storage Units in Nodal Energy Markets. *IEEE Transactions on Power Systems*, *31*(1), 786–797. https://doi.org/10.1109/TPWRS.2015.2411556

Morales, J. M., Conejo, A. J., Liu, K., & Zhong, J. (2012). Pricing electricity in pools with wind producers. *IEEE Transactions on Power Systems*. https://doi.org/10.1109/TPWRS.2011.2182622

Morales, J. M., Conejo, A. J., Madsen, H., Pinson, P., & Zugno, M. (2014). Integrating

renewables in electricity markets - Operational problems. In *Springer*. https://doi.org/10.1007/978-1-4614-9411-9

Morales, J. M., Conejo, A. J., & Pérez-Ruiz, J. (2010). Short-term trading for a wind power producer. *IEEE Transactions on Power Systems*, *25*(1), 554–564. https://doi.org/10.1109/TPWRS.2009.2036810

Morales, J. M., Zugno, M., Pineda, S., & Pinson, P. (2014). Electricity market clearing with improved scheduling of stochastic production. *Eur. J. Oper. Res.*, *235*, 765–774.

Narula, K. (2013). Renewable Energy Certificates (RECs) in India - A performance analysis and future outlook. *Renewable and Sustainable Energy Reviews*, *27*, 654–663. https://doi.org/10.1016/j.rser.2013.07.040

Nasiri, N., Sadeghi Yazdankhah, A., Mirzaei, M. A., Loni, A., Mohammadi-Ivatloo, B., Zare, K., & Marzband, M. (2020). A bi-level market-clearing for coordinated regional-local multi-carrier systems in presence of energy storage technologies. *Sustainable Cities and Society*, *63*, 102439. https://doi.org/https://doi.org/10.1016/j.scs.2020.102439

Nasiri, N., Zeynali, S., Ravadanegh, S. N., & Marzband, M. (2021). A hybrid robust-stochastic approach for strategic scheduling of a multi-energy system as a price-maker player in day-ahead wholesale market. *Energy*, *235*. https://doi.org/10.1016/j.energy.2021.121398

Nasrolahpour, E., Kazempour, J., Zareipour, H., & Rosehart, W. D. (2018). A Bilevel Model for Participation of a Storage System in Energy and Reserve Markets. *IEEE Transactions on Sustainable Energy*. https://doi.org/10.1109/TSTE.2017.2749434

Nguyen, H. T., & Felder, F. A. (2020). Generation expansion planning with renewable energy credit markets: A bilevel programming approach. *Applied Energy*, *276*(June), 115472. https://doi.org/10.1016/j.apenergy.2020.115472

Olabi, A. G., & Abdelkareem, M. A. (2022). Renewable energy and climate change. *Renewable and Sustainable Energy Reviews*, *158*(November 2020), 112111. https://doi.org/10.1016/j.rser.2022.112111

Ordoudis, C., Delikaraoglou, S., Kazempour, J., & Pinson, P. (2020). Market-based

coordination of integrated electricity and natural gas systems under uncertain supply. *European Journal of Operational Research*, *287*(3), 1105–1119. https://doi.org/10.1016/j.ejor.2020.05.007

Ordoudis, C., Delikaraoglou, S., Pinson, P., & Kazempour, J. (2017). Exploiting flexibility in coupled electricity and natural gas markets: A price-based approach. *2017 IEEE Manchester PowerTech, Powertech 2017*. https://doi.org/10.1109/PTC.2017.7981047

Ordoudis, C., Pinson, P., & Morales, J. M. (2019). An Integrated Market for Electricity and Natural Gas Systems with Stochastic Power Producers. *European Journal of Operational Research*, *272*(2), 642–654. https://doi.org/10.1016/j.ejor.2018.06.036

PandŽić, H., Morales, J. M., Conejo, A. J., & Kuzle, I. (2013). Offering model for a virtual power plant based on stochastic programming. *Applied Energy*, *105*, 282–292. https://doi.org/10.1016/j.apenergy.2012.12.077

Pereira, M. V., Granville, S., Fampa, M. H. C., Dix, R., & Barroso, L. A. (2005). Strategic bidding under uncertainty: A binary expansion approach. *IEEE Transactions on Power Systems*. https://doi.org/10.1109/TPWRS.2004.840397

Pineda, S., & Bock, A. (2016). Renewable-based generation expansion under a green certificate market. *Renewable Energy*, *91*, 53–63. https://doi.org/10.1016/j.renene.2015.12.061

Porras-Ortiz, F., Añó, O., Rubio-Barros, R., & Weber, C. (2020). Energy and reserve strategic offers in regional electricity markets: A complementarity approach. *International Journal of Electrical Power and Energy Systems*, *119*(November 2019), 105860. https://doi.org/10.1016/j.ijepes.2020.105860

Rahimi, M., Ardakani, F. J., Olatujoye, O., & Ardakani, A. J. (2022). Two-stage interval scheduling of virtual power plant in day-ahead and real-time markets considering compressed air energy storage wind turbine. *Journal of Energy Storage*, *45*(December 2021), 103599. https://doi.org/10.1016/j.est.2021.103599

Reddy, S. S., Bijwe, P. R., & Abhyankar, A. R. (2013). Multi-objective market clearing of electrical energy, spinning reserves and emission for wind-thermal power system. *International Journal of Electrical Power and Energy Systems*, *53*, 782–794.

https://doi.org/10.1016/j.ijepes.2013.05.050

Reddy, S. S., Bijwe, P. R., & Abhyankar, A. R. (2015). Optimum day-ahead clearing of energy and reserve markets with wind power generation using anticipated real-time adjustment costs. *International Journal of Electrical Power and Energy Systems*. https://doi.org/10.1016/j.ijepes.2015.03.002

Rintamäki, T., Siddiqui, A. S., & Salo, A. (2020). Strategic offering of a flexible producer in day-ahead and intraday power markets. *European Journal of Operational Research*, *284*(3), 1136–1153. https://doi.org/10.1016/j.ejor.2020.01.044

Rocha, P., Das, T. K., Nanduri, V., & Botterud, A. (2015). Impact of CO2 cap-and-trade programs on restructured power markets with generation capacity investments. *International Journal of Electrical Power and Energy Systems*, *71*, 195–208. https://doi.org/10.1016/j.ijepes.2015.02.031

Ruiz, C., & Conejo, A. J. (2009). Pool strategy of a producer with endogenous formation of locational marginal prices. *IEEE Transactions on Power Systems*. https://doi.org/10.1109/TPWRS.2009.2030378

Ruiz, C., Conejo, A. J., & Bertsimas, D. J. (2013). Prices Via Inverse Optimization. *IEEE On Power Systems*, *28*, *No. 3*(August), 3056–3064.

Ruiz, C., Conejo, A. J., & Gabriel, S. A. (2012). Pricing non-convexities in an electricity pool. *IEEE Transactions on Power Systems*, *27*(3), 1334–1342. https://doi.org/10.1109/TPWRS.2012.2184562

Safarzadeh, S., Hafezalkotob, A., & Jafari, H. (2022). Energy supply chain empowerment through tradable green and white certificates: A pathway to sustainable energy generation. *Applied Energy*, *323*(July), 119601. https://doi.org/10.1016/j.apenergy.2022.119601

Shafiee, S., Zamani-Dehkordi, P., Zareipour, H., & Knight, A. M. (2016). Economic assessment of a price-maker energy storage facility in the Alberta electricity market. *Energy*. https://doi.org/10.1016/j.energy.2016.05.086

Sheikhahmadi, P., & Bahramara, S. (2020). The participation of a renewable energy-based aggregator in real-time market: A Bi-level approach. *Journal of Cleaner Production*,

276, 123149. https://doi.org/10.1016/j.jclepro.2020.123149

Sioshansi, F. P. (2008). Competitive Electricity Markets: Questions Remain about Design, Implementation, Performance. *Electricity Journal*. https://doi.org/10.1016/j.tej.2008.02.001

Sioshansi, R., Denholm, P., Jenkin, T., & Weiss, J. (2009). Estimating the value of electricity storage in PJM: Arbitrage and some welfare effects. *Energy Economics*. https://doi.org/10.1016/j.eneco.2008.10.005

Soares, T., Jensen, T. V., Mazzi, N., Pinson, P., & Morais, H. (2017). Optimal offering and allocation policies for wind power in energy and reserve markets. *Wind Energy*, *20*(11), 1851–1870. https://doi.org/10.1002/we.2125

Steven A. Gabriel, Antonio J. Conejo, J. David Fuller, Benjamin F. Hobbs, Carlos Ruiz, Gabriel, S. A., Conejo, A. J., Fuller, J. D., Hobbs, B. F., & Ruiz, C. (2013). Complementarity Modeling in Energy Markets. *Media*. https://doi.org/10.1007/978-1-4419-6123-5

Stoft, S. (2003). Power System Economics: Designing Markets for Electricity. In *IEEE Power and Energy Magazine* (Vol. 99, Issue 1). https://doi.org/10.1109/MPAE.2003.1180363

Sun, G., Shen, S., Chen, S., Zhou, Y., & Wei, Z. (2022). Bidding strategy for a prosumer aggregator with stochastic renewable energy production in energy and reserve markets. *Renewable Energy*, *191*, 278–290. https://doi.org/10.1016/j.renene.2022.04.066

Tanaka, M., & Chen, Y. (2012). Market power in emissions trading: Strategically manipulating permit price through fringe firms. *Applied Energy*, *96*, 203–211. https://doi.org/10.1016/j.apenergy.2011.08.049

Tang, L., Wang, H., Li, L., Yang, K., & Mi, Z. (2020). Quantitative models in emission trading system research: A literature review. *Renewable and Sustainable Energy Reviews*, *132*(May), 110052. https://doi.org/10.1016/j.rser.2020.110052

Tierney, S., Ph, D., Schatzki, T., Ph, D., & Mukerji, R. (2007). *An abbreviated version of this paper is published in the March 2008 edition of*. *April*, 1–24.

Tsimopoulos, E. G., & Georgiadis, M. C. (2019a). Optimal strategic offerings for a conventional producer in jointly cleared energy and balancing markets under high penetration of wind power production. *Applied Energy*. https://doi.org/10.1016/j.apenergy.2019.03.161

Tsimopoulos, E. G., & Georgiadis, M. C. (2019b). Strategic offers in day-ahead market co-optimizing energy and reserve under high penetration of wind power production: An MPEC approach. *AIChE Journal*, *65*(7), 1–11. https://doi.org/10.1002/aic.16495

Tsimopoulos, E. G., & Georgiadis, M. C. (2020). Withholding strategies for a conventional and wind generation portfolio in a joint energy and reserve pool market: A gaming-based approach. *Computers and Chemical Engineering*, *134*, 106692. https://doi.org/10.1016/j.compchemeng.2019.106692

Twomey, P., Green, R., Neuhoff, K., & Newbery, D. (2005). Cambridge Working Papers in Economics CWPE 0504: A Review of the Monitoring of Market Power. *CMI Working Paper*, *December 2013*.

U.S. Energy Information Administration. (2022). *Electricity in the United States*. https://www.eia.gov/energyexplained/electricity/electricity-in-the-us.php

Uria-Martinez, R., Johnson, M., & Rui, S. (2021). 2021 Hydropower Market Report. *Office of Energy Efficiency & Renewable Energy*, *January*. https://www.energy.gov/sites/prod/files/2018/04/f51/Hydropower Market Report.pdf

Vega-Redondo, F. (2003). Economics and the theory of games. In *Economics and the Theory of Games*. https://doi.org/10.1017/CBO9780511753954

Wang, C., Wei, W., Wang, J., Bai, L., Liang, Y., & Bi, T. (2018). Convex Optimization Based Distributed Optimal Gas-Power Flow Calculation. *IEEE Transactions on Sustainable Energy*, *9*(3), 1145–1156. https://doi.org/10.1109/TSTE.2017.2771954

Wei, Y., Liang, X., Xu, L., Kou, G., & Chevallier, J. (2022). Trading, Storage, or Penalty? Uncovering Firms' Decision-Making Behavior in the Shanghai Emissions Trading Scheme: Insights from Agent-Based Modeling. *SSRN Electronic Journal*, *117*(December 2022), 106463. https://doi.org/10.2139/ssrn.4086414

Weigand, P., Lander, G., & Malme, R. (2013). Synchronizing natural gas & power market: A series of proposed solutions. *Skipping Stone Energy Market Consultants, Tech. Rep*.

Yan, Y., Lin, Z., Wen, F., Palu, I., Chen, X., Zheng, W., & Zhang, L. (2019). Optimal Operation Strategy for an Integrated Low-Carbon Energy System in Coupled Electricity and Natural Gas Markets. *2019 IEEE PES Innovative Smart Grid Technologies Asia, ISGT 2019*, 3696–3701. https://doi.org/10.1109/ISGT-Asia.2019.8881228

Zhang, Q., Wu, X., Deng, X., Huang, Y., Li, C., & Wu, J. (2023). Bidding strategy for wind power and Large-scale electric vehicles participating in Day-ahead energy and frequency regulation market. *Applied Energy*, *341*(January), 121063. https://doi.org/10.1016/j.apenergy.2023.121063

Zhang, R., Jiang, T., Li, F., Li, G., Chen, H., & Li, X. (2021). International Journal of Electrical Power and Energy Systems Bi-level strategic bidding model for P2G facilities considering a carbon emission trading scheme-embedded LMP and wind power uncertainty. *International Journal of Electrical Power and Energy Systems*, *128*(January), 106740. https://doi.org/10.1016/j.ijepes.2020.106740

Zhang, R., Yan, K., Li, G., Jiang, T., Li, X., & Chen, H. (2020). Privacy-preserving decentralized power system economic dispatch considering carbon capture power plants and carbon emission trading scheme via over-relaxed ADMM. *International Journal of Electrical Power and Energy Systems*, *121*(January), 106094. https://doi.org/10.1016/j.ijepes.2020.106094

Zhang, X., Guo, X., & Zhang, X. (2023). Bidding modes for renewable energy considering electricity-carbon integrated market mechanism based on multi-agent hybrid game. *Energy*, *263*(PA), 125616. https://doi.org/10.1016/j.energy.2022.125616

Zhao, B., Zlotnik, A., Conejo, A. J., Sioshansi, R., & Rudkevich, A. M. (2019). Shadow price-based co-ordination of natural gas and electric power systems. *IEEE Transactions on Power Systems*, *34*(3), 1942–1954. https://doi.org/10.1109/TPWRS.2018.2879801

Zou, P., Chen, Q., Xia, Q., He, G., Kang, C., & Conejo, A. J. (2016). Pool equilibria including strategic storage. *Applied Energy*. https://doi.org/10.1016/j.apenergy.2016.05.105

Zugno, M., Morales, J. M., Pinson, P., & Madsen, H. (2013). Pool strategy of a price-maker wind power producer. *IEEE Transactions on Power Systems*, *28*(3), 3440–3450.

https://doi.org/10.1109/TPWRS.2013.2252633

Research Outputs

Herein, an overview of the research outputs of this dissertation is provided.

Peer-reviewed journal publications

1. Christos N. Dimitriadis, Evangelos G. Tsimopoulos, Michael C. Georgiadis (2022). "Strategic bidding of an energy storage agent in a joint energy and reserve market under stochastic generation.", *Energy*, vol. 242, p. 123026, https://doi.org/10.1016/j.energy.2021.123026.

2. Christos N. Dimitriadis, Evangelos G. Tsimopoulos, Michael C. Georgiadis (2021). "A Review on the Complementarity Modelling in Competitive Electricity Markets.", *Energies*, vol. 14, p. 7133, https://doi.org/10.3390/en14217133.

3. Christos N. Dimitriadis, Evangelos G. Tsimopoulos, Michael C. Georgiadis (2023). "Optimization-based economic analysis of energy storage technologies in a coupled electricity and natural gas market.", *Journal of Energy Storage*, vol. 58, p. 106332, https://doi.org/10.1016/j.est.2022.106332.

4. Christos N. Dimitriadis, Evangelos G. Tsimopoulos, Michael C. Georgiadis (2023). "Optimal bidding strategy of a gas-fired power plant in interdependent low-carbon electricity and natural gas markets.", *Energy*, vol. 277, p. 127710, https://doi.org/10.1016/j.energy.2023.127710.

5. Christos N. Dimitriadis, Evangelos G. Tsimopoulos, Michael C. Georgiadis (2024). "Co-optimized trading strategy of a renewable aggregator in electricity and green certificates markets.", *Submitted for publication in Renewable Energy journal (November 2023).*

Other peer-reviewed journal publications due to collaborations with members of Prof. Georgiadis' group

1. Evangelos G. Tsimopoulos, Christos N. Dimitriadis, Michael C. Georgiadis (2024). "Financial arbitrage in electricity markets via virtual bidding." *Computers & Chemical Engineering*, vol. 181, p. 108550, https://doi.org/10.1016/j.compchemeng.2023.108550.

2. Maria Kanta, Evangelos G. Tsimopoulos, Christos N. Dimitriadis, Michael C. Georgiadis (2024). "Strategic investments and portfolio management in interdependent low-carbon electricity and natural gas markets.", *Submitted for publication in Energy journal (February 2024).*

International conference proceedings

1. Christos N. Dimitriadis, Evangelos G. Tsimopoulos and Michael C. Georgiadis (2023). "Strategic participation of a gas-fired power plant in interdependent electricity and natural gas markets under carbon emission trading schemes.", *European Symposium on Computer-Aided Process Engineering-33*, Athens, June 2023, (published in Computer-Aided Chemical Engineering, 52, pp. 2763-2768).

2. Maria Kanta, Evangelos G. Tsimopoulos, Christos N. Dimitriadis, Michael C. Georgiadis (2023). "Optimal Investment Strategies in a Joint Natural Gas and Carbon Emission-Embedded Electricity Market.", *26th Conference on Process Integration, Modelling and Optimization for Energy Saving and Pollution Reduction*, Thessaloniki, October 2023.

Appendices

Appendix A

Mathematical Transformations for Chapter 2

The KKT optimality conditions of the lower-level day-ahead problem *2.2.2* are described by equations (A.1)-(A.50):

$$O_{s,t}^{dis} - \lambda_{n,t}^{DA} + \gamma_{s,t}^{dis,max} - \gamma_{s,t}^{dis,min} - \gamma_{s,t}^{dis,\downarrow} = 0 \quad \forall s, \forall t \tag{A.1}$$

$$-O_{s,t}^{ch} + \lambda_{n,t}^{DA} + \gamma_{s,t}^{ch,max} - \gamma_{s,t}^{ch,min} - \gamma_{s,t}^{ch,\uparrow} = 0 \quad \forall s, \forall t \tag{A.2}$$

$$c_{i,t} - \lambda_{n,t}^{DA} + a_{i,t}^{max} - a_{i,t}^{min} + a_{i,t}^{\uparrow} - a_{i,t}^{\downarrow} = 0 \quad \forall i, \forall t \tag{A.3}$$

$$-u_{d,t} + \lambda_{n,t}^{DA} + \beta_{d,t}^{max} - \beta_{d,t}^{min} + \beta_{d,t}^{\downarrow} - \beta_{d,t}^{\uparrow} = 0 \quad \forall d, \forall t \tag{A.4}$$

$$O_{s,t}^{dis,\uparrow} - \lambda_{t}^{\uparrow} + \gamma_{s,t}^{dis,\uparrow,max} - \gamma_{s,t}^{dis,\uparrow,min} = 0 \quad \forall s, \forall t \tag{A.5}$$

$$O_{s,t}^{dis,\downarrow} - \lambda_{t}^{\downarrow} + \gamma_{s,t}^{dis,\downarrow,max} - \gamma_{s,t}^{dis,\downarrow,min} + \gamma_{s,t}^{dis,\downarrow} = 0 \quad \forall s, \forall t \tag{A.6}$$

$$O_{s,t}^{ch,\uparrow} - \lambda_{t}^{\uparrow} + \gamma_{s,t}^{ch,\uparrow,max} - \gamma_{s,t}^{ch,\uparrow,min} + \gamma_{s,t}^{ch,\uparrow} = 0 \quad \forall s, \forall t \tag{A.7}$$

$$O_{s,t}^{ch,\downarrow} - \lambda_{t}^{\downarrow} + \gamma_{s,t}^{ch,\downarrow,max} - \gamma_{s,t}^{ch,\downarrow,min} = 0 \quad \forall s, \forall t \tag{A.8}$$

$$c_{i,t}^{res} - \lambda_{t}^{\uparrow} + \alpha_{i,t}^{\uparrow,max} - \alpha_{i,t}^{\uparrow,min} + \alpha_{i,t}^{\uparrow} = 0 \quad \forall i, \forall t \tag{A.9}$$

$$c_{i,t}^{res} - \lambda_{t}^{\downarrow} + \alpha_{i,t}^{\downarrow,max} - \alpha_{i,t}^{\downarrow,min} + \alpha_{i,t}^{\downarrow} = 0 \quad \forall i, \forall t \tag{A.10}$$

$$u_{d,t}^{res} - \lambda_{t}^{\uparrow} + \beta_{d,t}^{\uparrow,max} - \beta_{d,t}^{\uparrow,min} + \beta_{d,t}^{\uparrow} = 0 \quad \forall d, \forall t \tag{A.11}$$

$$u_{d,t}^{res} - \lambda_{t}^{\downarrow} + \beta_{d,t}^{\downarrow,max} - \beta_{d,t}^{\downarrow,min} + \beta_{d,t}^{\downarrow} = 0 \quad \forall d, \forall t \tag{A.12}$$

$$-\lambda_{n,t}^{DA} + \varepsilon_{j,t}^{max} - \varepsilon_{j,t}^{min} = 0 \quad \forall j, \forall t \tag{A.13}$$

$$\sum_{m \in NaM} B_{n,m} \cdot \left(\lambda_{n,t}^{DA} - \lambda_{m,t}^{DA}\right) + \sum_{m \in NaM} B_{n,m} \cdot \left(\zeta_{n,m,t}^{max} - \zeta_{m,n,t}^{max}\right) - \sum_{m \in NaM} B_{n,m} \cdot \left(\zeta_{n,m,t}^{min} - \zeta_{m,n,t}^{min}\right) + \tilde{\zeta}_{n,t}^{max} - \tilde{\zeta}_{n,t}^{min} + \zeta_{n_1,t}^{\circ} = 0 \quad \forall n, \forall t \tag{A.14}$$

$$0 \le P_{i,t}^{DA} \perp a_{i,t}^{min} \ge 0 \quad \forall i, \forall t \tag{A.15}$$

$$0 \le (P_{i}^{max} - P_{i,t}^{DA}) \perp a_{i,t}^{max} \ge 0 \quad \forall i, \forall t \tag{A.16}$$

$$0 \le L_{d,t}^{DA} \perp \beta_{d,t}^{min} \ge 0 \quad \forall d, \forall t \tag{A.17}$$

$$0 \le (L_{d,t}^{max} - L_{d,t}^{DA}) \perp \beta_{d,t}^{max} \ge 0 \quad \forall d, \forall t \tag{A.18}$$

$$0 \le G_{s,t}^{DA,ch} \perp \gamma_{s,t}^{ch,min} \ge 0 \quad \forall s, \forall t \tag{A.19}$$

$$0 \le (\bar{G}_{s,t}^{ch} - G_{s,t}^{DA,ch}) \perp \gamma_{s,t}^{ch,max} \ge 0 \quad \forall s, \forall t \tag{A.20}$$

$$0 \leq G_{s,t}^{DA,dis} \perp \gamma_{s,t}^{dis,min} \geq 0 \quad \forall s, \forall t \tag{A.21}$$

$$0 \leq (\bar{G}_{s,t}^{dis} - G_{s,t}^{DA,dis}) \perp \gamma_{s,t}^{dis,max} \geq 0 \quad \forall s, \forall t \tag{A.22}$$

$$0 \leq rp_{s,t}^{ch,\uparrow} \perp \gamma_{s,t}^{ch,\uparrow,min} \geq 0 \quad \forall s, \forall t \tag{A.23}$$

$$0 \leq (\bar{rc}_{s,t}^{ch,\uparrow} - rp_{s,t}^{ch,\uparrow}) \perp \gamma_{s,t}^{ch,\uparrow,max} \geq 0 \quad \forall s, \forall t \tag{A.24}$$

$$0 \leq rp_{s,t}^{ch,\downarrow} \perp \gamma_{s,t}^{ch,\downarrow,min} \geq 0 \quad \forall s, \forall t \tag{A.25}$$

$$0 \leq (\bar{rc}_{s,t}^{ch,\downarrow} - rp_{s,t}^{ch,\downarrow}) \perp \gamma_{s,t}^{ch,\downarrow,max} \geq 0 \quad \forall s, \forall t \tag{A.26}$$

$$0 \leq rp_{s,t}^{dis,\uparrow} \perp \gamma_{s,t}^{dis,\uparrow,min} \geq 0 \quad \forall s, \forall t \tag{A.27}$$

$$0 \leq (\bar{rc}_{s,t}^{dis,\uparrow} - rp_{s,t}^{dis,\uparrow}) \perp \gamma_{s,t}^{dis,\uparrow,max} \geq 0 \quad \forall s, \forall t \tag{A.28}$$

$$0 \leq rp_{s,t}^{dis,\downarrow} \perp \gamma_{s,t}^{dis,\downarrow,min} \geq 0 \quad \forall s, \forall t \tag{A.29}$$

$$0 \leq (\bar{rc}_{s,t}^{dis,\downarrow} - rp_{s,t}^{dis,\downarrow}) \perp \gamma_{s,t}^{dis,\downarrow,max} \geq 0 \quad \forall s, \forall t \tag{A.30}$$

$$0 \leq (G_{s,t}^{DA,ch} - rp_{s,t}^{ch,\uparrow}) \perp \gamma_{s,t}^{ch,\uparrow} \geq 0 \quad \forall s, \forall t \tag{A.31}$$

$$0 \leq (G_{s,t}^{DA,dis} - rp_{s,t}^{dis,\downarrow}) \perp \gamma_{s,t}^{dis,\downarrow} \geq 0 \quad \forall s, \forall t \tag{A.32}$$

$$0 \leq rpc_{i,t}^{\uparrow} \perp \alpha_{i,t}^{\uparrow,min} \geq 0 \quad \forall i, \forall t \tag{A.33}$$

$$0 \leq (RCc_{i}^{\uparrow,max} - rpc_{i,t}^{\uparrow}) \perp \alpha_{i,t}^{\uparrow,max} \geq 0 \quad \forall i, \forall t \tag{A.34}$$

$$0 \leq rpc_{i,t}^{\downarrow} \perp \alpha_{i,t}^{\downarrow,min} \geq 0 \quad \forall i, \forall t \tag{A.35}$$

$$0 \leq (RCc_{i}^{\downarrow,max} - rpc_{i,t}^{\downarrow}) \perp \alpha_{i,t}^{\downarrow,max} \geq 0 \quad \forall i, \forall t \tag{A.36}$$

$$0 \leq (P_{i}^{max} - P_{i,t}^{DA} - rpc_{i,t}^{\uparrow}) \perp \alpha_{i,t}^{\uparrow} \geq 0 \quad \forall i, \forall t \tag{A.37}$$

$$0 \leq (P_{i,t}^{DA} - rpc_{i,t}^{\downarrow}) \perp \alpha_{i,t}^{\downarrow} \geq 0 \quad \forall i, \forall t \tag{A.38}$$

$$0 \leq rpd_{d,t}^{\uparrow} \perp \beta_{d,t}^{\uparrow,min} \geq 0 \quad \forall d, \forall t \tag{A.39}$$

$$0 \leq (RCd_{d,t}^{\uparrow,max} - rpd_{d,t}^{\uparrow}) \perp \beta_{d,t}^{\uparrow,max} \geq 0 \quad \forall d, \forall t \tag{A.40}$$

$$0 \leq rpd_{d,t}^{\downarrow} \perp \beta_{d,t}^{\downarrow,min} \geq 0 \quad \forall d, \forall t \tag{A.41}$$

$$0 \leq (RCd_{d,t}^{\downarrow,max} - rpd_{d,t}^{\downarrow}) \perp \beta_{d,t}^{\downarrow,max} \geq 0 \quad \forall i, \forall t \tag{A.42}$$

$$0 \leq (L_{d,t}^{max} - L_{d,t}^{DA} - rpd_{d,t}^{\downarrow}) \perp \beta_{d,t}^{\downarrow} \geq 0 \quad \forall d, \forall t \tag{A.43}$$

$$0 \leq (L_{d,t}^{DA} - rpd_{d,t}^{\uparrow}) \perp \beta_{d,t}^{\uparrow} \geq 0 \quad \forall d, \forall t \tag{A.44}$$

$$0 \leq W_{j,t}^{DA} \perp \varepsilon_{j,t}^{min} \geq 0 \quad \forall i, \forall t \tag{A.45}$$

$$0 \leq (W_{j,t}^{max} - W_{j,t}^{DA}) \perp \varepsilon_{j,t}^{max} \geq 0 \quad \forall i, \forall \tag{A.46}$$

$$0 \leq \left(B_{n,m} \cdot \left(\delta_{n,t}^{\circ} - \delta_{m,t}^{\circ}\right) + T_{n,m}^{max}\right) \perp \zeta_{n,m,t}^{min} \geq 0 \quad \forall n, \forall m \in NaM, \forall t \tag{A.47}$$

$$0 \le \left(T_{n,m}^{max} - B_{n,m} \cdot \left(\delta_{n,t}^{\circ} - \delta_{m,t}^{\circ}\right)\right) \perp \zeta_{n,m,t}^{max} \ge 0 \quad \forall n, \forall m \in NaM, \forall t \tag{A.48}$$

$$0 \le (\delta_{n,t}^{\circ} + \pi) \perp \tilde{\zeta}_{n,t}^{min} \ge 0 \quad \forall n, \forall t \tag{A.49}$$

$$0 \le (\pi - \delta_{n,t}^{\circ}) \perp \tilde{\zeta}_{n,t}^{max} \ge 0 \quad \forall n, \forall t \tag{A.50}$$

The KKT optimality conditions of the lower-level real-time problem *2.2.3* are described by equations (A.51)-(A.85):

$$O_{s,t}^{dis} - \lambda_{n,t,\omega}^{RT} + \nu_{s,t,\omega}^{dis,\uparrow,max} - \nu_{s,t,\omega}^{dis,\uparrow,min} = 0 \quad \forall s, \forall t, \forall \omega \tag{A.51}$$

$$-O_{s,t}^{dis} + \lambda_{n,t,\omega}^{RT} + \nu_{s,t,\omega}^{dis,\downarrow,max} - \nu_{s,t,\omega}^{dis,\downarrow,min} = 0 \quad \forall s, \forall t, \forall \omega \tag{A.52}$$

$$O_{s,t}^{ch} - \lambda_{n,t,\omega}^{RT} + \nu_{s,t,\omega}^{ch,\uparrow,max} - \nu_{s,t,\omega}^{ch,\uparrow,min} = 0 \quad \forall s, \forall t, \forall \omega \tag{A.53}$$

$$-O_{s,t}^{ch} + \lambda_{n,t,\omega}^{RT} + \nu_{s,t,\omega}^{ch,\downarrow,max} - \nu_{s,t,\omega}^{ch,\downarrow,min} = 0 \quad \forall s, \forall t, \forall \omega \tag{A.54}$$

$$c_{i,t} - \lambda_{n,t,\omega}^{RT} + \theta_{i,t,\omega}^{\uparrow,max} - \theta_{i,t,\omega}^{\uparrow,min} = 0 \quad \forall i, \forall t, \forall \omega \tag{A.55}$$

$$-c_{i,t} + \lambda_{n,t,\omega}^{RT} + \theta_{i,t,\omega}^{\downarrow,max} - \theta_{i,t,\omega}^{\downarrow,min} = 0 \quad \forall i, \forall t, \forall \omega \tag{A.56}$$

$$u_{d,t} - \lambda_{n,t,\omega}^{RT} + \mu_{d,t,\omega}^{\uparrow,max} - \mu_{d,t,\omega}^{\uparrow,min} = 0 \quad \forall d, \forall t, \forall \omega \tag{A.57}$$

$$-u_{d,t} + \lambda_{n,t,\omega}^{RT} + \mu_{d,t,\omega}^{\downarrow,max} - \mu_{d,t,\omega}^{\downarrow,min} = 0 \quad \forall d, \forall t, \forall \omega \tag{A.58}$$

$$VOLL_{d,t} + \lambda_{n,t,\omega}^{RT} + \mu_{d,t,\omega}^{max} - \mu_{d,t,\omega}^{min} = 0 \quad \forall d, \forall t, \forall \omega \tag{A.59}$$

$$\lambda_{n,t,\omega}^{RT} + \xi_{j,t,\omega}^{max} - \xi_{j,t,\omega}^{min} = 0 \quad \forall j, \forall t, \forall \omega \tag{A.60}$$

$$\begin{aligned} &- \sum_{m \in NaM} B_{n,m} \cdot \left(\lambda_{n,t,\omega}^{RT} - \lambda_{m,t,\omega}^{RT}\right) + \sum_{m \in NaM} B_{n,m} \cdot \left(\varphi_{n,m,t,\omega}^{max} - \varphi_{m,n,t,\omega}^{max}\right) - \sum_{m \in NaM} B_{n,m} \\ &\cdot \left(\varphi_{n,m,t,\omega}^{min} - \varphi_{m,n,t,\omega}^{min}\right) + \tilde{\varphi}_{n,t,\omega}^{max} - \tilde{\varphi}_{n,t,\omega}^{min} + \varphi_{n_1,t,\omega}^{\circ} = 0 \quad \forall n, \forall t, \forall \omega \end{aligned} \tag{A.61}$$

$$0 \le rac_{i,t,\omega}^{\uparrow} \perp \theta_{i,t,\omega}^{\uparrow,min} \ge 0 \quad \forall i, \forall t, \forall \omega \tag{A.62}$$

$$0 \le (rpc_{i,t}^{\uparrow} - rac_{i,t,\omega}^{\uparrow}) \perp \theta_{i,t,\omega}^{\uparrow,max} \ge 0 \quad \forall i, \forall t, \forall \omega \tag{A.63}$$

$$0 \le rac_{i,t,\omega}^{\downarrow} \perp \theta_{i,t,\omega}^{\downarrow,min} \ge 0 \quad \forall i, \forall t, \forall \omega \tag{A.64}$$

$$0 \le (rpc_{i,t}^{\downarrow} - rac_{i,t,\omega}^{\downarrow}) \perp \theta_{i,t,\omega}^{\downarrow,max} \ge 0 \quad \forall i, \forall t, \forall \omega \tag{A.65}$$

$$0 \le rad_{d,t,\omega}^{\uparrow} \perp \mu_{d,t,\omega}^{\uparrow,min} \ge 0 \quad \forall d, \forall t, \forall \omega \tag{A.66}$$

$$0 \le (rpd_{d,t}^{\uparrow} - rad_{d,t,\omega}^{\uparrow}) \perp \mu_{d,t,\omega}^{\uparrow,max} \ge 0 \quad \forall d, \forall t, \forall \omega \tag{A.67}$$

$$0 \le rad_{d,t,\omega}^{\downarrow} \perp \mu_{d,t,\omega}^{\downarrow,min} \ge 0 \quad \forall d, \forall t, \forall \omega \tag{A.68}$$

$$0 \le (rpd_{d,t}^{\downarrow} - rad_{d,t,\omega}^{\downarrow}) \perp \mu_{d,t,\omega}^{\downarrow,max} \ge 0 \quad \forall d, \forall t, \forall \omega \tag{A.69}$$

$$0 \le ra_{s,t,\omega}^{dis,\uparrow} \perp \nu_{s,t,\omega}^{dis,\uparrow,min} \ge 0 \quad \forall s, \forall t, \forall \omega \tag{A.70}$$

$$0 \le (rp_{s,t}^{dis,\uparrow} - ra_{s,t,\omega}^{dis,\uparrow}) \perp \nu_{s,t,\omega}^{dis,\uparrow,max} \ge 0 \quad \forall s, \forall t, \forall \omega \tag{A.71}$$

$$0 \le ra_{s,t,\omega}^{dis,\downarrow} \perp v_{s,t,\omega}^{dis,\downarrow,min} \ge 0 \quad \forall s, \forall t, \forall \omega \tag{A.72}$$

$$0 \le (rp_{s,t}^{dis,\downarrow} - ra_{s,t,\omega}^{dis,\downarrow}) \perp v_{s,t,\omega}^{dis,\downarrow,max} \ge 0 \quad \forall s, \forall t, \forall \omega \tag{A.73}$$

$$0 \le ra_{s,t,\omega}^{ch,\uparrow} \perp v_{s,t,\omega}^{ch,\uparrow,min} \ge 0 \quad \forall s, \forall t, \forall \omega \tag{A.74}$$

$$0 \le (rp_{s,t}^{ch,\uparrow} - ra_{s,t,\omega}^{ch,\uparrow}) \perp v_{s,t,\omega}^{ch,\uparrow,max} \ge 0 \quad \forall s, \forall t, \forall \omega \tag{A.75}$$

$$0 \le ra_{s,t,\omega}^{ch,\downarrow} \perp v_{s,t,\omega}^{ch,\downarrow,min} \ge 0 \quad \forall s, \forall t, \forall \omega \tag{A.76}$$

$$0 \le (rp_{s,t}^{ch,\downarrow} - ra_{s,t,\omega}^{ch,\downarrow}) \perp v_{s,t,\omega}^{ch,\downarrow,max} \ge 0 \quad \forall s, \forall t, \forall \omega \tag{A.77}$$

$$0 \le L_{d,t,\omega}^{sh} \perp \mu_{d,t,\omega}^{min} \ge 0 \quad \forall d, \forall t, \forall \omega \tag{A.78}$$

$$0 \le (L_{d,t}^{DA} - L_{d,t,\omega}^{sh}) \perp \mu_{d,t,\omega}^{max} \ge 0 \quad \forall d, \forall t, \forall \omega \tag{A.79}$$

$$0 \le W_{j,t,\omega}^{sp} \perp \xi_{j,t,\omega}^{min} \ge 0 \quad \forall j, \forall t, \forall \omega \tag{A.80}$$

$$0 \le (W_{j,t,\omega}^{RT} - W_{j,t,\omega}^{sp}) \perp \xi_{j,t,\omega}^{max} \ge 0 \quad \forall j, \forall t, \forall \omega \tag{A.81}$$

$$0 \le \left(B_{n,m} \cdot \left(\delta_{n,t,\omega} - \delta_{m,t,\omega}\right) + T_{n,m}^{max}\right) \perp \varphi_{n,m,t,\omega}^{min} \ge 0 \quad \forall n, \forall m \in NaM, \forall t, \forall \omega \tag{A.82}$$

$$0 \le \left(T_{n,m}^{max} - B_{n,m} \cdot \left(\delta_{n,t,\omega} - \delta_{m,t,\omega}\right)\right) \perp \varphi_{n,m,t,\omega}^{max} \ge 0 \quad \forall n, \forall m \in NaM, \forall t, \forall \omega \tag{A.83}$$

$$0 \le (\delta_{n,t,\omega} + \pi) \perp \tilde{\varphi}_{n,t,\omega}^{min} \ge 0 \quad \forall n, \forall t, \forall \omega \tag{A.84}$$

$$0 \le \left(\pi - \delta_{n,t,\omega}\right) \perp \tilde{\varphi}_{n,t,\omega}^{max} \ge 0 \quad \forall n, \forall t, \forall \omega \tag{A.85}$$

The nonlinearities arisen in the above KKT complementarity conditions are eradicated using the Fortuny-Amat and McCarl big-M linearization approach, which entails the introduction of a set of binary variables σ.

Linearization of complementarity conditions (A.15)-(A.50) is established through their reformulation into the equations (A.86)-(A.158):

$$0 \le P_{i,t}^{DA} \le M^{P1} \cdot \sigma_{i,t}^{1} \quad \forall i, \forall t \tag{A.86}$$

$$0 \le \alpha_{i,t}^{min} \le M^{M1} \cdot (1 - \sigma_{i,t}^{1}) \quad \forall i, \forall t \tag{A.87}$$

$$0 \le P_{i}^{max} - P_{i,t}^{DA} \le M^{P2} \cdot \sigma_{i,t}^{2} \quad \forall i, \forall t \tag{A.88}$$

$$0 \le \alpha_{i,t}^{max} \le M^{M2} \cdot (1 - \sigma_{i,t}^{2}) \quad \forall i, \forall t \tag{A.89}$$

$$0 \le L_{d,t}^{DA} \le M^{P3} \cdot \sigma_{d,t}^{3} \quad \forall d, \forall t \tag{A.90}$$

$$0 \le \beta_{d,t}^{min} \le M^{M3} \cdot (1 - \sigma_{d,t}^{3}) \quad \forall d, \forall t \tag{A.91}$$

$$0 \le L_{d,t}^{max} - L_{d,t}^{DA} \le M^{P4} \cdot \sigma_{d,t}^{4} \quad \forall d, \forall t \tag{A.92}$$

$$0 \le \beta_{d,t}^{max} \le M^{M4} \cdot (1 - \sigma_{d,t}^{4}) \quad \forall d, \forall t \tag{A.93}$$

$$0 \leq G_{s,t}^{DA,ch} \leq M^{P5} \cdot \sigma_{s,t}^{5} \quad \forall s, \forall t \tag{A.94}$$

$$0 \leq \gamma_{s,t}^{ch,min} \leq M^{M5} \cdot (1 - \sigma_{s,t}^{5}) \quad \forall s, \forall t \tag{A.95}$$

$$0 \leq \bar{G}_{s,t}^{ch} - G_{s,t}^{DA,ch} \leq M^{P6} \cdot \sigma_{s,t}^{6} \quad \forall s, \forall t \tag{A.96}$$

$$0 \leq \gamma_{s,t}^{ch,max} \leq M^{M6} \cdot (1 - \sigma_{s,t}^{6}) \quad \forall s, \forall t \tag{A.97}$$

$$0 \leq G_{s,t}^{DA,dis} \leq M^{P7} \cdot \sigma_{s,t}^{7} \quad \forall s, \forall t \tag{A.98}$$

$$0 \leq \gamma_{s,t}^{dis,min} \leq M^{M7} \cdot (1 - \sigma_{s,t}^{7}) \quad \forall s, \forall t \tag{A.99}$$

$$0 \leq \bar{G}_{s,t}^{dis} - G_{s,t}^{DA,dis} \leq M^{P8} \cdot \sigma_{s,t}^{8} \quad \forall s, \forall t \tag{A.100}$$

$$0 \leq \gamma_{s,t}^{dis,max} \leq M^{M8} \cdot (1 - \sigma_{s,t}^{8}) \quad \forall s, \forall t \tag{A.101}$$

$$0 \leq rp_{s,t}^{ch,\uparrow} \leq M^{P9} \cdot \sigma_{s,t}^{9} \quad \forall s, \forall t \tag{A.102}$$

$$0 \leq \gamma_{s,t}^{ch,\uparrow,min} \leq M^{M9} \cdot (1 - \sigma_{s,t}^{9}) \quad \forall s, \forall t \tag{A.103}$$

$$0 \leq \bar{rc}_{s,t}^{ch,\uparrow} - rp_{s,t}^{ch,\uparrow} \leq M^{P10} \cdot \sigma_{s,t}^{10} \quad \forall s, \forall t \tag{A.104}$$

$$0 \leq \gamma_{s,t}^{ch,\uparrow,max} \leq M^{M10} \cdot (1 - \sigma_{s,t}^{10}) \quad \forall s, \forall t \tag{A.105}$$

$$0 \leq rp_{s,t}^{ch,\downarrow} \leq M^{P11} \cdot \sigma_{s,t}^{11} \quad \forall s, \forall t \tag{A.106}$$

$$0 \leq \gamma_{s,t}^{ch,\downarrow,min} \leq M^{M11} \cdot (1 - \sigma_{s,t}^{11}) \quad \forall s, \forall t \tag{A.107}$$

$$0 \leq \bar{rc}_{s,t}^{ch,\downarrow} - rp_{s,t}^{ch,\downarrow} \leq M^{P12} \cdot \sigma_{s,t}^{12} \quad \forall s, \forall t \tag{A.108}$$

$$0 \leq \gamma_{s,t}^{ch,\downarrow,max} \leq M^{M12} \cdot (1 - \sigma_{s,t}^{12}) \quad \forall s, \forall t \tag{A.109}$$

$$0 \leq rp_{s,t}^{dis,\uparrow} \leq M^{P13} \cdot \sigma_{s,t}^{13} \quad \forall s, \forall t \tag{A.110}$$

$$0 \leq \gamma_{s,t}^{dis,\uparrow,min} \leq M^{M13} \cdot (1 - \sigma_{s,t}^{13}) \quad \forall s, \forall t \tag{A.111}$$

$$0 \leq \bar{rc}_{s,t}^{dis,\uparrow} - rp_{s,t}^{dis,\uparrow} \leq M^{P14} \cdot \sigma_{s,t}^{14} \quad \forall s, \forall t \tag{A.112}$$

$$0 \leq \gamma_{s,t}^{dis,\uparrow,max} \leq M^{M14} \cdot (1 - \sigma_{s,t}^{14}) \quad \forall s, \forall t \tag{A.113}$$

$$0 \leq rp_{s,t}^{dis,\downarrow} \leq M^{P15} \cdot \sigma_{s,t}^{15} \quad \forall s, \forall t \tag{A.114}$$

$$0 \leq \gamma_{s,t}^{dis,\downarrow,min} \leq M^{M15} \cdot (1 - \sigma_{s,t}^{15}) \quad \forall s, \forall t \tag{A.115}$$

$$0 \leq \bar{rc}_{s,t}^{dis,\downarrow} - rp_{s,t}^{dis,\downarrow} \leq M^{P16} \cdot \sigma_{s,t}^{16} \quad \forall s, \forall t \tag{A.116}$$

$$0 \leq \gamma_{s,t}^{dis,\downarrow,max} \leq M^{M16} \cdot (1 - \sigma_{s,t}^{16}) \quad \forall s, \forall t \tag{A.117}$$

$$0 \leq G_{s,t}^{DA,ch} - rp_{s,t}^{ch,\uparrow} \leq M^{P17} \cdot \sigma_{s,t}^{17} \quad \forall s, \forall t \tag{A.118}$$

$$0 \leq \gamma_{s,t}^{ch,\uparrow} \leq M^{M17} \cdot (1 - \sigma_{s,t}^{17}) \quad \forall s, \forall t \tag{A.119}$$

$$0 \leq G_{s,t}^{DA,dis} - rp_{s,t}^{dis,\downarrow} \leq M^{P18} \cdot \sigma_{s,t}^{18} \quad \forall s, \forall t \tag{A.120}$$

$$0 \leq \gamma_{s,t}^{dis,\downarrow} \leq M^{M18} \cdot (1 - \sigma_{s,t}^{18}) \quad \forall s, \forall t \tag{A.121}$$

$$0 \leq rpc_{i,t}^{\uparrow} \leq M^{P19} \cdot \sigma_{i,t}^{19} \quad \forall i, \forall t \tag{A.122}$$

$$0 \leq \alpha_{i,t}^{\uparrow,min} \leq M^{M19} \cdot (1 - \sigma_{i,t}^{19}) \quad \forall i, \forall t \tag{A.123}$$

$$0 \leq RCc_{i}^{\uparrow,max} - rpc_{i,t}^{\uparrow} \leq M^{P20} \cdot \sigma_{i,t}^{20} \quad \forall i, \forall t \tag{A.124}$$

$$0 \leq \alpha_{i,t}^{\uparrow,max} \leq M^{M20} \cdot (1 - \sigma_{i,t}^{20}) \quad \forall i, \forall t \tag{A.125}$$

$$0 \leq rpc_{i,t}^{\downarrow} \leq M^{P21} \cdot \sigma_{i,t}^{21} \quad \forall i, \forall t \tag{A.126}$$

$$0 \leq \alpha_{i,t}^{\downarrow,min} \leq M^{M21} \cdot (1 - \sigma_{i,t}^{21}) \quad \forall i, \forall t \tag{A.127}$$

$$0 \leq RCc_{i}^{\downarrow,max} - rpc_{i,t}^{\downarrow} \leq M^{P22} \cdot \sigma_{i,t}^{22} \quad \forall i, \forall t \tag{A.128}$$

$$0 \leq \alpha_{i,t}^{\downarrow,max} \leq M^{M22} \cdot (1 - \sigma_{i,t}^{22}) \quad \forall i, \forall t \tag{A.129}$$

$$0 \leq P_{i}^{max} - P_{i,t}^{DA} - rpc_{i,t}^{\uparrow} \leq M^{P23} \cdot \sigma_{i,t}^{23} \quad \forall i, \forall t \tag{A.130}$$

$$0 \leq \alpha_{i,t}^{\uparrow} \leq M^{M23} \cdot (1 - \sigma_{i,t}^{23}) \quad \forall i, \forall t \tag{A.131}$$

$$0 \leq P_{i,t}^{DA} - rpc_{i,t}^{\uparrow} \leq M^{P24} \cdot \sigma_{i,t}^{24} \quad \forall i, \forall t \tag{A.132}$$

$$0 \leq \alpha_{i,t}^{\downarrow} \leq M^{M24} \cdot (1 - \sigma_{i,t}^{24}) \quad \forall i, \forall t \tag{A.134}$$

$$0 \leq rpd_{d,t}^{\uparrow} \leq M^{P25} \cdot \sigma_{d,t}^{25} \quad \forall d, \forall t \tag{A.135}$$

$$0 \leq \beta_{d,t}^{\uparrow,min} \leq M^{M25} \cdot (1 - \sigma_{d,t}^{25}) \quad \forall d, \forall t \tag{A.136}$$

$$0 \leq RCd_{d,t}^{\uparrow,max} - rpd_{d,t}^{\uparrow} \leq M^{P26} \cdot \sigma_{d,t}^{26} \quad \forall d, \forall t \tag{A.137}$$

$$0 \leq \beta_{d,t}^{\downarrow,min} \leq M^{M26} \cdot (1 - \sigma_{d,t}^{26}) \quad \forall d, \forall t \tag{A.138}$$

$$0 \leq rpd_{d,t}^{\downarrow} \leq M^{P27} \cdot \sigma_{d,t}^{27} \quad \forall d, \forall t \tag{A.139}$$

$$0 \leq \beta_{d,t}^{\downarrow,min} \leq M^{M27} \cdot (1 - \sigma_{d,t}^{27}) \quad \forall d, \forall t \tag{A.140}$$

$$0 \leq RCd_{d,t}^{\downarrow,max} - rpd_{d,t}^{\downarrow} \leq M^{P28} \cdot \sigma_{d,t}^{28} \quad \forall d, \forall t \tag{A.141}$$

$$0 \leq \beta_{d,t}^{\downarrow,max} \leq M^{M28} \cdot (1 - \sigma_{d,t}^{28}) \quad \forall d, \forall t \tag{A.142}$$

$$0 \leq L_{d,t}^{max} - L_{d,t}^{DA} - rpd_{d,t}^{\downarrow} \leq M^{P29} \cdot \sigma_{d,t}^{29} \quad \forall d, \forall t \tag{A.143}$$

$$0 \leq \beta_{d,t}^{\downarrow} \leq M^{M29} \cdot (1 - \sigma_{d,t}^{29}) \quad \forall d, \forall t \tag{A.144}$$

$$0 \leq L_{d,t}^{DA} - rpd_{d,t}^{\uparrow} \leq M^{P30} \cdot \sigma_{d,t}^{30} \quad \forall d, \forall t \tag{A.145}$$

$$0 \leq \beta_{d,t}^{\uparrow} \leq M^{M30} \cdot (1 - \sigma_{d,t}^{30}) \quad \forall d, \forall t \tag{A.146}$$

$$0 \leq W_{j,t}^{DA} \leq M^{P31} \cdot \sigma_{j,t}^{31} \quad \forall j, \forall t \tag{A.147}$$

$$0 \leq \varepsilon_{j,t}^{min} \leq M^{M31} \cdot (1 - \sigma_{j,t}^{31}) \quad \forall j, \forall t \tag{A.148}$$

$$0 \leq W_{j,t}^{max} - W_{j,t}^{DA} \leq M^{P32} \cdot \sigma_{j,t}^{32} \quad \forall j, \forall t \tag{A.149}$$

$$0 \leq \varepsilon_{j,t}^{max} \leq M^{M32} \cdot (1 - \sigma_{j,t}^{32}) \quad \forall j, \forall t \tag{A.150}$$

$$0 \leq B_{n,m} \cdot (\delta_{n,t}^{\circ} - \delta_{m,t}^{\circ}) + T_{n,m}^{max} \leq M^{P33} \cdot \sigma_{n,m,t}^{33} \quad \forall n, \forall m, \forall t \tag{A.151}$$

$$0 \leq \zeta_{n,m,t}^{min} \leq M^{M33} \cdot (1 - \sigma_{n,m,t}^{33}) \quad \forall n, \forall m, \forall t \tag{A.152}$$

$$0 \leq T_{n,m}^{max} - B_{n,m} \cdot (\delta_{n,t}^{\circ} - \delta_{m,t}^{\circ}) \leq M^{P34} \cdot \sigma_{n,m,t}^{34} \quad \forall n, \forall m, \forall t \tag{A.153}$$

$$0 \leq \zeta_{n,m,t}^{max} \leq M^{M34} \cdot (1 - \sigma_{n,m,t}^{34}) \quad \forall n, \forall m, \forall t \tag{A.154}$$

$$0 \leq \delta_{n,t}^{\circ} + \pi \leq M^{P35} \cdot \sigma_{n,t}^{35} \quad \forall n, \forall t \tag{A.155}$$

$$0 \leq \tilde{\zeta}_{n,t}^{min} \leq M^{M35} \cdot (1 - \sigma_{n,t}^{35}) \quad \forall n, \forall t \tag{A.156}$$

$$0 \leq \pi - \delta_{n,t}^{\circ} \leq M^{P36} \cdot \sigma_{n,t}^{36} \quad \forall n, \forall t \tag{A.157}$$

$$0 \leq \tilde{\zeta}_{n,t}^{max} \leq M^{M36} \cdot (1 - \sigma_{n,t}^{36}) \quad \forall n, \forall t \tag{A.158}$$

Linearization of complementarity conditions (A.62)-(A.85) is established through their reformulation into the equations (A.159)-(A.206):

$$0 \leq rac_{i,t,\omega}^{\uparrow} \leq M^{P37} \cdot \sigma_{i,t,\omega}^{37} \quad \forall i, \forall t, \forall \omega \tag{A.159}$$

$$0 \leq \theta_{i,t,\omega}^{\uparrow,min} \leq M^{M37} \cdot (1 - \sigma_{i,t,\omega}^{37}) \quad \forall i, \forall t, \forall \omega \tag{A.160}$$

$$0 \leq rpc_{i,t}^{\uparrow} - rac_{i,t,\omega}^{\uparrow} \leq M^{P38} \cdot \sigma_{i,t,\omega}^{38} \quad \forall i, \forall t, \forall \omega \tag{A.161}$$

$$0 \leq \theta_{i,t,\omega}^{\uparrow,max} \leq M^{M38} \cdot (1 - \sigma_{i,t,\omega}^{38}) \quad \forall i, \forall t, \forall \omega \tag{A.162}$$

$$0 \leq rac_{i,t,\omega}^{\downarrow} \leq M^{P39} \cdot \sigma_{i,t,\omega}^{39} \quad \forall i, \forall t, \forall \omega \tag{A.163}$$

$$0 \leq \theta_{i,t,\omega}^{\downarrow,min} \leq M^{M39} \cdot (1 - \sigma_{i,t,\omega}^{39}) \quad \forall i, \forall t, \forall \omega \tag{A.164}$$

$$0 \leq rpc_{i,t}^{\downarrow} - rac_{i,t,\omega}^{\downarrow} \leq M^{P40} \cdot \sigma_{i,t,\omega}^{40} \quad \forall i, \forall t, \forall \omega \tag{A.165}$$

$$0 \leq \theta_{i,t,\omega}^{\downarrow,max} \leq M^{M40} \cdot (1 - \sigma_{i,t,\omega}^{40}) \quad \forall i, \forall t, \forall \omega \tag{A.166}$$

$$0 \leq rad_{d,t,\omega}^{\uparrow} \leq M^{P41} \cdot \sigma_{d,t,\omega}^{41} \quad \forall d, \forall t, \forall \omega \tag{A.167}$$

$$0 \leq \mu_{d,t,\omega}^{\uparrow,min} \leq M^{M41} \cdot (1 - \sigma_{d,t,\omega}^{41}) \quad \forall d, \forall t, \forall \omega \tag{A.168}$$

$$0 \leq rpd_{d,t}^{\uparrow} - rad_{d,t,\omega}^{\uparrow} \leq M^{P42} \cdot \sigma_{d,t,\omega}^{42} \quad \forall d, \forall t, \forall \omega \tag{A.169}$$

$$0 \leq \mu_{d,t,\omega}^{\uparrow,max} \leq M^{M42} \cdot (1 - \sigma_{d,t,\omega}^{42}) \quad \forall d, \forall t, \forall \omega \tag{A.170}$$

$$0 \leq rad_{d,t,\omega}^{\downarrow} \leq M^{P43} \cdot \sigma_{d,t,\omega}^{43} \quad \forall d, \forall t, \forall \omega \tag{A.171}$$

$$0 \leq \mu_{d,t,\omega}^{\downarrow,min} \leq M^{M43} \cdot (1 - \sigma_{d,t,\omega}^{43}) \quad \forall d, \forall t, \forall \omega \tag{A.172}$$

$$0 \leq rpd_{d,t}^{\downarrow} - rad_{d,t,\omega}^{\downarrow} \leq M^{P44} \cdot \sigma_{d,t,\omega}^{44} \quad \forall d, \forall t, \forall \omega \tag{A.173}$$

$$0 \leq \mu_{d,t,\omega}^{\downarrow,max} \leq M^{M44} \cdot (1 - \sigma_{d,t,\omega}^{44}) \quad \forall d, \forall t, \forall \omega \tag{A.174}$$

$$0 \leq ra_{s,t,\omega}^{dis,\uparrow} \leq M^{P45} \cdot \sigma_{s,t,\omega}^{45} \quad \forall s, \forall t, \forall \omega \tag{A.175}$$

$$0 \leq \nu_{s,t,\omega}^{dis,\uparrow,min} \leq M^{M45} \cdot (1 - \sigma_{s,t,\omega}^{45}) \quad \forall s, \forall t, \forall \omega \tag{A.176}$$

$$0 \leq rp_{s,t}^{dis,\uparrow} - ra_{s,t,\omega}^{dis,\uparrow} \leq M^{P46} \cdot \sigma_{s,t,\omega}^{46} \quad \forall s, \forall t, \forall \omega \tag{A.177}$$

$$0 \leq \nu_{s,t,\omega}^{dis,\uparrow,max} \leq M^{M46} \cdot (1 - \sigma_{s,t,\omega}^{46}) \quad \forall s, \forall t, \forall \omega \tag{A.178}$$

$$0 \leq ra_{s,t,\omega}^{dis,\downarrow} \leq M^{P47} \cdot \sigma_{s,t,\omega}^{47} \quad \forall s, \forall t, \forall \omega \tag{A.179}$$

$$0 \leq \nu_{s,t,\omega}^{dis,\downarrow,min} \leq M^{M47} \cdot (1 - \sigma_{s,t,\omega}^{47}) \quad \forall s, \forall t, \forall \omega \tag{A.180}$$

$$0 \leq rp_{s,t}^{dis,\downarrow} - ra_{s,t,\omega}^{dis,\downarrow} \leq M^{P48} \cdot \sigma_{s,t,\omega}^{48} \quad \forall s, \forall t, \forall \omega \tag{A.181}$$

$$0 \leq \nu_{s,t,\omega}^{dis,\downarrow,max} \leq M^{M48} \cdot (1 - \sigma_{s,t,\omega}^{48}) \quad \forall s, \forall t, \forall \omega \tag{A.182}$$

$$0 \leq ra_{s,t,\omega}^{ch,\uparrow} \leq M^{P49} \cdot \sigma_{s,t,\omega}^{49} \quad \forall s, \forall t, \forall \omega \tag{A.183}$$

$$0 \leq \nu_{s,t,\omega}^{ch,\uparrow,min} \leq M^{M49} \cdot (1 - \sigma_{s,t,\omega}^{49}) \quad \forall s, \forall t, \forall \omega \tag{A.184}$$

$$0 \leq rp_{s,t}^{ch,\uparrow} - ra_{s,t,\omega}^{ch,\uparrow} \leq M^{P50} \cdot \sigma_{s,t,\omega}^{50} \quad \forall s, \forall t, \forall \omega \tag{A.185}$$

$$0 \leq \nu_{s,t,\omega}^{ch,\uparrow,max} \leq M^{M50} \cdot (1 - \sigma_{s,t,\omega}^{50}) \quad \forall s, \forall t, \forall \omega \tag{A.186}$$

$$0 \leq ra_{s,t,\omega}^{ch,\downarrow} \leq M^{P51} \cdot \sigma_{s,t,\omega}^{51} \quad \forall s, \forall t, \forall \omega \tag{A.187}$$

$$0 \leq \nu_{s,t,\omega}^{ch,\downarrow,min} \leq M^{M51} \cdot (1 - \sigma_{s,t,\omega}^{51}) \quad \forall s, \forall t, \forall \omega \tag{A.188}$$

$$0 \leq rp_{s,t}^{ch,\downarrow} - ra_{s,t,\omega}^{ch,\downarrow} \leq M^{P52} \cdot \sigma_{s,t,\omega}^{52} \quad \forall s, \forall t, \forall \omega \tag{A.189}$$

$$0 \leq \nu_{s,t,\omega}^{ch,\downarrow,max} \leq M^{M52} \cdot (1 - \sigma_{s,t,\omega}^{52}) \quad \forall s, \forall t, \forall \omega \tag{A.190}$$

$$0 \leq L_{d,t,\omega}^{sh} \leq M^{P53} \cdot \sigma_{d,t,\omega}^{53} \quad \forall d, \forall t, \forall \omega \tag{A.191}$$

$$0 \leq \mu_{d,t,\omega}^{min} \leq M^{M53} \cdot (1 - \sigma_{d,t,\omega}^{53}) \quad \forall d, \forall t, \forall \omega \tag{A.192}$$

$$0 \leq L_{d,t}^{DA} - L_{d,t,\omega}^{sh} \leq M^{P54} \cdot \sigma_{d,t,\omega}^{54} \quad \forall d, \forall t, \forall \omega \tag{A.193}$$

$$0 \leq \mu_{d,t,\omega}^{max} \leq M^{M54} \cdot (1 - \sigma_{d,t,\omega}^{54}) \quad \forall d, \forall t, \forall \omega \tag{A.194}$$

$$0 \leq W_{j,t,\omega}^{sp} \leq M^{P55} \cdot \sigma_{j,t,\omega}^{55} \quad \forall j, \forall t, \forall \omega \tag{A.195}$$

$$0 \leq \xi_{j,t,\omega}^{min} \leq M^{P55} \cdot (1 - \sigma_{j,t,\omega}^{55}) \quad \forall j, \forall t, \forall \omega \tag{A.196}$$

$$0 \leq W_{j,t,\omega}^{RT} - W_{j,t,\omega}^{sp} \leq M^{P56} \cdot \sigma_{j,t,\omega}^{56} \quad \forall j, \forall t, \forall \omega \tag{A.197}$$

$$0 \leq \xi_{j,t,\omega}^{max} \leq M^{P56} \cdot (1 - \sigma_{j,t,\omega}^{56}) \quad \forall j, \forall t, \forall \omega \tag{A.198}$$

$$0 \leq B_{n,m} \cdot \left(\delta_{n,t,\omega} - \delta_{m,t,\omega}\right) + T_{n,m}^{max} \leq M^{P57} \cdot \sigma_{n,m,t,\omega}^{33} \quad \forall n, \forall m, \forall t, \forall \omega \tag{A.199}$$

$$0 \le \varphi_{n,m,t,\omega}^{min} \le M^{M57} \cdot (1 - \sigma_{n,m,t,\omega}^{57}) \quad \forall n, \forall m, \forall t, \forall \omega \tag{A.200}$$

$$0 \le T_{n,m}^{max} - B_{n,m}\left(\delta_{n,t,\omega} - \delta_{m,t,\omega}\right) \le M^{P58} \cdot \sigma_{n,m,t,\omega}^{58} \quad \forall n, \forall m, \forall t, \forall \omega \tag{A.201}$$

$$0 \le \varphi_{n,m,t,\omega}^{max} \le M^{M58} \cdot (1 - \sigma_{n,m,t,\omega}^{58}) \quad \forall n, \forall m, \forall t, \forall \omega \tag{A.202}$$

$$0 \le \delta_{n,t,\omega} + \pi \le M^{P59} \cdot \sigma_{n,t,\omega}^{59} \quad \forall n, \forall t, \forall \omega \tag{A.203}$$

$$0 \le \tilde{\varphi}_{n,t,\omega}^{min} \le M^{M59} \cdot (1 - \sigma_{n,t,\omega}^{59}) \quad \forall n, \forall t, \forall \omega \tag{A.204}$$

$$0 \le \pi - \delta_{n,t,\omega} \le M^{P60} \cdot \sigma_{n,t,\omega}^{60} \quad \forall n, \forall t, \forall \omega \tag{A.205}$$

$$0 \le \tilde{\varphi}_{n,t,\omega}^{max} \le M^{M60} \cdot (1 - \sigma_{n,t,\omega}^{60}) \quad \forall n, \forall t, \forall \omega \tag{A.206}$$

In this section, strong duality theorem is applied to the day-ahead ISO's optimization problem, which practically guarantees the equality of objective function's value to the corresponding value of its dual problem's objective function:

$$\begin{aligned}
&-\sum_{s}\left(O_{s,t}^{ch} \cdot G_{s,t}^{DA,ch} - O_{s,t}^{dis} \cdot G_{s,t}^{DA,dis}\right) - \sum_{d} u_{d,t} \cdot L_{d,t}^{DA} + \sum_{i} c_{i,t} \cdot P_{i,t}^{DA} \\
&\quad + \sum_{s}\left(O_{s,t}^{ch,\uparrow} \cdot rp_{s,t}^{ch,\uparrow} + O_{s,t}^{ch,\downarrow} \cdot rp_{s,t}^{ch,\downarrow} + O_{s,t}^{dis,\uparrow} \cdot rp_{s,t}^{dis,\uparrow} + O_{s,t}^{dis,\downarrow}\right. \\
&\quad \left. \cdot rp_{s,t}^{dis,\downarrow}\right) + \sum_{i} c_{i,t}^{res} \cdot \left(rpc_{i,t}^{\uparrow} + rpc_{i,t}^{\downarrow}\right) \\
&\quad + \sum_{d} u_{d,t}^{res} \cdot \left(rpd_{d,t}^{\uparrow} + rpd_{d,t}^{\downarrow}\right) \\
&\quad = -\sum_{s}\left(\gamma_{s,t}^{ch,max} \cdot \bar{G}_{s,t}^{ch} + \gamma_{s,t}^{dis,max} \cdot \bar{G}_{s,t}^{dis} + \gamma_{s,t}^{ch,\uparrow,max} \cdot \bar{rc}_{s,t}^{ch,\uparrow}\right. \\
&\quad \left. + \gamma_{s,t}^{ch,\downarrow,max} \cdot \bar{rc}_{s,t}^{ch,\downarrow} + \gamma_{s,t}^{dis,\uparrow,max} \cdot \bar{rc}_{s,t}^{dis,\uparrow} + \gamma_{s,t}^{dis,\downarrow,max} \cdot \bar{rc}_{s,t}^{dis,\downarrow}\right) \\
&\quad + \Omega_{t}^{DA} \quad \forall
\end{aligned} \tag{A.207}$$

$$\begin{aligned}
\Omega_{t}^{DA} = &-\sum_{d} \beta_{d,t}^{max} \cdot L_{d,t}^{max} - \sum_{i} a_{i,t}^{max} \cdot P_{i}^{max} - \sum_{d} \beta_{d,t}^{\uparrow,max} \cdot RCd_{d,t}^{\uparrow,max} \\
&- \sum_{d} \beta_{d,t}^{\downarrow,max} \cdot RCd_{d,t}^{\downarrow,max} - \sum_{i} \alpha_{i,t}^{\uparrow,max} \cdot RCc_{i}^{\uparrow,max} \\
&- \sum_{i} \alpha_{i,t}^{\downarrow,max} \cdot RCc_{i}^{\downarrow,max} - \sum_{d} \beta_{d,t}^{\downarrow} \cdot L_{d,t}^{max} - \sum_{i} a_{i,t}^{\uparrow} \cdot P_{i}^{max} \\
&- \sum_{j} \varepsilon_{j,t}^{max} \cdot W_{j,t}^{max} - \sum_{n,m \in NaM} T_{n,m}^{max} \cdot \left(\zeta_{n,m,t}^{min} + \zeta_{n,m,t}^{max}\right) \\
&- \sum_{n} \pi \cdot \left(\tilde{\zeta}_{n,t}^{min} + \tilde{\zeta}_{n,t}^{max}\right) + \lambda_{t}^{\uparrow} \cdot R_{t}^{\uparrow} + \lambda_{t}^{\downarrow} \cdot R_{t}^{\downarrow} \quad \forall t
\end{aligned} \tag{A.208}$$

Using (A.20), (A.22), (A.24), (A.26), (A.28), (A.30) the following equations emerge:

$$\gamma_{s,t}^{ch,max} \cdot \bar{G}_{s,t}^{ch} = \gamma_{s,t}^{ch,max} \cdot G_{s,t}^{DA,ch} \quad \forall s, \forall t \tag{A.209}$$

$$\gamma_{s,t}^{dis,max} \cdot \bar{G}_{s,t}^{dis} = \gamma_{s,t}^{dis,max} \cdot G_{s,t}^{DA,dis} \quad \forall s, \forall t \tag{A.210}$$

$$\gamma_{s,t}^{ch,\uparrow,max} \cdot \overline{rc}_{s,t}^{ch,\uparrow} = \gamma_{s,t}^{ch,\uparrow,max} \cdot rp_{s,t}^{ch,\uparrow} \quad \forall s, \forall t \tag{A.211}$$

$$\gamma_{s,t}^{ch,\downarrow,max} \cdot \overline{rc}_{s,t}^{ch,\downarrow} = \gamma_{s,t}^{ch,\downarrow,max} \cdot rp_{s,t}^{ch,\downarrow} \quad \forall s, \forall t \tag{A.212}$$

$$\gamma_{s,t}^{dis,\uparrow,max} \cdot \overline{rc}_{s,t}^{dis,\uparrow} = \gamma_{s,t}^{dis,\uparrow,max} \cdot rp_{s,t}^{dis,\uparrow} \quad \forall s, \forall t \tag{A.213}$$

$$\gamma_{s,t}^{dis,\downarrow,max} \cdot \overline{rc}_{s,t}^{dis,\downarrow} = \gamma_{s,t}^{dis,\downarrow,max} \cdot rp_{s,t}^{dis,\downarrow} \quad \forall s, \forall t \tag{A.214}$$

Introducing (A.209)-(A.214) to (A.207) results in:

$$\begin{aligned}\sum_{s}\Big[&\left(-O_{s,t}^{ch} + \gamma_{s,t}^{ch,max}\right) \cdot G_{s,t}^{DA,ch} + \left(O_{s,t}^{dis} + \gamma_{s,t}^{dis,max}\right) \cdot G_{s,t}^{DA,dis} \\ &+ \left(O_{s,t}^{ch,\uparrow} + \gamma_{s,t}^{ch,\uparrow,max}\right) \cdot rp_{s,t}^{ch,\uparrow} + \left(O_{s,t}^{ch,\downarrow} + \gamma_{s,t}^{ch,\downarrow,max}\right) \cdot rp_{s,t}^{ch,\downarrow} \\ &+ \left(O_{s,t}^{dis,\uparrow} + \gamma_{s,t}^{dis,\uparrow,max}\right) \cdot rp_{s,t}^{dis,\uparrow} + \left(O_{s,t}^{dis,\downarrow} + \gamma_{s,t}^{dis,\downarrow,max}\right) \cdot rp_{s,t}^{dis,\downarrow}\Big] \\ &= \sum_{d} u_{d,t} \cdot L_{d,t}^{DA} - \sum_{d} c_{i,t} \cdot P_{i,t}^{DA} - \sum_{d} c_{i,t}^{res} \cdot \left(rpc_{i,t}^{\uparrow} + rpc_{i,t}^{\downarrow}\right) \\ &- \sum_{d} u_{d,t}^{res} \cdot \left(rpd_{d,t}^{\uparrow} + rpd_{d,t}^{\downarrow}\right) + \Omega_{t}^{DA} \quad \forall t\end{aligned} \tag{A.215}$$

Using (A.1), (A.2), (A.5)-(A.8) and implementing the appropriate adaptations the following equations occur:

$$\begin{aligned}\lambda_{n,t}^{DA} \cdot G_{s,t}^{DA,dis} = {} & O_{s,t}^{dis} \cdot G_{s,t}^{DA,dis} + \gamma_{s,t}^{dis,max} \cdot G_{s,t}^{DA,dis} - \gamma_{s,t}^{dis,min} \cdot G_{s,t}^{DA,dis} - \gamma_{s,t}^{dis,\downarrow} \\ & \cdot G_{s,t}^{DA,dis} \quad \forall s, \forall t\end{aligned} \tag{A.216}$$

$$\begin{aligned}\lambda_{n,t}^{DA} \cdot G_{s,t}^{DA,ch} = {} & O_{s,t}^{ch} \cdot G_{s,t}^{DA,ch} - \gamma_{s,t}^{ch,max} \cdot G_{s,t}^{DA,ch} + \gamma_{s,t}^{ch,min} \cdot G_{s,t}^{DA,ch} + \gamma_{s,t}^{ch,\uparrow} \\ & \cdot G_{s,t}^{DA,ch} \quad \forall s, \forall t\end{aligned} \tag{A.217}$$

$$\lambda_{t}^{\uparrow} \cdot rp_{s,t}^{dis,\uparrow} = O_{s,t}^{dis,\uparrow} \cdot rp_{s,t}^{dis,\uparrow} + \gamma_{s,t}^{dis,\uparrow,max} \cdot rp_{s,t}^{dis,\uparrow} - \gamma_{s,t}^{dis,\uparrow,min} \cdot rp_{s,t}^{dis,\uparrow} \quad \forall s, \forall t \tag{A.218}$$

$$\begin{aligned}\lambda_{t}^{\downarrow} \cdot rp_{s,t}^{dis,\downarrow} = {} & O_{s,t}^{dis,\downarrow} \cdot rp_{s,t}^{dis,\downarrow} + \gamma_{s,t}^{dis,\downarrow,max} \cdot rp_{s,t}^{dis,\downarrow} - \gamma_{s,t}^{dis,\downarrow,min} \cdot rp_{s,t}^{dis,\downarrow} + \gamma_{s,t}^{dis,\downarrow} \\ & \cdot rp_{s,t}^{dis,\downarrow} \quad \forall s, \forall t\end{aligned} \tag{A.219}$$

$$\begin{aligned}\lambda_{t}^{\uparrow} \cdot rp_{s,t}^{ch,\uparrow} = {} & O_{s,t}^{ch,\uparrow} \cdot rp_{s,t}^{ch,\uparrow} + \gamma_{s,t}^{ch,\uparrow,max} \cdot rp_{s,t}^{ch,\uparrow} - \gamma_{s,t}^{ch,\uparrow,min} \cdot rp_{s,t}^{ch,\uparrow} + \gamma_{s,t}^{ch,\uparrow} \\ & \cdot rp_{s,t}^{ch,\uparrow} \quad \forall s, \forall t\end{aligned} \tag{A.220}$$

$$\lambda_{t}^{\downarrow} \cdot rp_{s,t}^{ch,\downarrow} = O_{s,t}^{ch,\downarrow} \cdot rp_{s,t}^{ch,\downarrow} + \gamma_{s,t}^{ch,\downarrow,max} \cdot rp_{s,t}^{ch,\downarrow} - \gamma_{s,t}^{ch,\downarrow,min} \cdot rp_{s,t}^{ch,\downarrow} \quad \forall s, \forall t \tag{A.221}$$

From (A.19), (A.21), (A.23), (A.25), (A.27), (A.29), (A.31), (A.32):

$$\gamma_{s,t}^{ch,min} \cdot G_{s,t}^{DA,ch} = 0 \quad \forall s, \forall t \tag{A.222}$$

$$\gamma_{s,t}^{dis,min} \cdot G_{s,t}^{DA,dis} = 0 \quad \forall s, \forall t \tag{A.223}$$

$$\gamma_{s,t}^{dis,\uparrow,min} \cdot rp_{s,t}^{dis,\uparrow} = 0 \quad \forall s, \forall t \tag{A.224}$$

$$\gamma_{s,t}^{dis,\downarrow,min} \cdot rp_{s,t}^{dis,\downarrow} = 0 \quad \forall s, \forall t \tag{A.225}$$

$$\gamma_{s,t}^{ch,\uparrow,min} \cdot rp_{s,t}^{ch,\uparrow} = 0 \quad \forall s, \forall t \tag{A.226}$$

$$\gamma_{s,t}^{ch,\downarrow,min} \cdot rp_{s,t}^{ch,\downarrow} = 0 \quad \forall s, \forall t \tag{A.227}$$

$$\gamma_{s,t}^{dis,\downarrow} \cdot G_{s,t}^{DA,dis} = \gamma_{s,t}^{dis,\downarrow} \cdot rp_{s,t}^{dis,\downarrow} \quad \forall s, \forall t \tag{A.228}$$

$$\gamma_{s,t}^{ch,\uparrow} \cdot G_{s,t}^{DA,ch} = \gamma_{s,t}^{ch,\uparrow} \cdot rp_{s,t}^{ch,\uparrow} \quad \forall s, \forall t \tag{A.229}$$

Substituting (A.216)-(A.229) to (A.215) yields:

$$\begin{aligned} -\sum_{s}\big(&\lambda_{n,t}^{DA} \cdot G_{s,t}^{DA,ch} - \lambda_{n,t}^{DA} \cdot G_{s,t}^{DA,dis} - \lambda_{t}^{\uparrow} \cdot rp_{s,t}^{ch,\uparrow} - \lambda_{t}^{\downarrow} \cdot rp_{s,t}^{ch,\downarrow} - \lambda_{t}^{\uparrow} \cdot rp_{s,t}^{dis,\uparrow} - \lambda_{t}^{\downarrow} \\ &\cdot rp_{s,t}^{dis,\downarrow}\big) \\ &= +\sum_{d} u_{d,t} \cdot L_{d,t}^{DA} - \sum_{i} c_{i,t} \cdot P_{i,t}^{DA} - \sum_{i} c_{i,t}^{res} \cdot \left(rpc_{i,t}^{\uparrow} + rpc_{i,t}^{\downarrow}\right) \\ &- \sum_{d} u_{d,t}^{res} \cdot \left(rpd_{d,t}^{\uparrow} + rpd_{d,t}^{\downarrow}\right) + \Omega_{t}^{DA} \quad \forall t \end{aligned} \tag{A.230}$$

Strong duality theorem is also applied to the real-time ISO's optimization problem, for the same purposes as above i.e., generate a linear equivalent for the nonlinear balancing variables of the objective function (1). Therefore, the strong duality theorem for equation (45) is presented below:

$$\begin{aligned} &\sum_{d} VOLL_{d,t} \cdot L_{d,t,\omega}^{sh} + \sum_{i} c_{i,t} \cdot \left(rac_{i,t,\omega}^{\uparrow} + rac_{i,t,\omega}^{\downarrow}\right) + \sum_{s} O_{s,t}^{dis} \cdot \left(ra_{s,t,\omega}^{dis,\uparrow} + ra_{s,t,\omega}^{dis,\downarrow}\right) \\ &\quad + \sum_{s} O_{s,t}^{ch} \cdot \left(ra_{s,t,\omega}^{ch,\uparrow} + ra_{s,t,\omega}^{ch,\downarrow}\right) + \sum_{d} u_{d,t} \cdot \left(rad_{d,t,\omega}^{\uparrow} + rad_{d,t,\omega}^{\downarrow}\right) \\ &\quad = -\sum_{s}\big(\nu_{s,t,\omega}^{dis,\uparrow,max} \cdot rp_{s,t}^{dis,\uparrow} + \nu_{s,t,\omega}^{dis,\downarrow,max} \cdot rp_{s,t}^{dis,\downarrow} + \nu_{s,t,\omega}^{ch,\uparrow,max} \cdot rp_{s,t}^{ch,\uparrow} \\ &\quad + \nu_{s,t,\omega}^{ch,\downarrow,max} \cdot rp_{s,t}^{ch,\downarrow}\big) + \Omega_{t,\omega}^{RT} \quad \forall t, \forall \omega \end{aligned} \tag{A.231}$$

$$\begin{aligned}\Omega_{t,\omega}^{RT} = &-\sum_{i}\left(\theta_{i,t,\omega}^{\uparrow,max}\cdot rpc_{i,t}^{\uparrow}+\theta_{i,t,\omega}^{\downarrow,max}\cdot rpc_{i,t}^{\downarrow}\right)\\ &-\sum_{d}\left(\mu_{d,t,\omega}^{\uparrow,max}\cdot rpd_{d,t}^{\uparrow}+\mu_{d,t,\omega}^{\downarrow,max}\cdot rpd_{d,t}^{\downarrow}+\mu_{d,t,\omega}^{max}\cdot L_{d,t}^{DA}\right)\\ &-\sum_{j\in JaN,n}\lambda_{n,t,\omega}^{RT}\cdot\left(W_{j,t,\omega}^{RT}-W_{j,t}^{DA}\right)\\ &+\sum_{n,m\in NaM}\lambda_{n,t,\omega}^{RT}\cdot B_{n,m}\cdot\left(-\delta_{n,t}^{\circ}+\delta_{m,t}^{\circ}\right)-\sum_{j}\xi_{j,t,\omega}^{max}\cdot W_{j,t,\omega}^{RT}\\ &-\sum_{n,m\in NaM,\omega}T_{n,m}^{max}\cdot\left(\varphi_{n,m,t,\omega}^{min}+\varphi_{n,m,t,\omega}^{max}\right)\\ &-\sum_{n,\omega}\pi\cdot\left(\tilde{\varphi}_{n,t,\omega}^{min}+\tilde{\varphi}_{n,t,\omega}^{max}\right)\quad\forall t,\forall\omega\end{aligned}\tag{A.232}$$

Using (A.71), (A.73), (A.75), (A.77) the following equations emerge:

$$\nu_{s,t,\omega}^{dis,\uparrow,max}\cdot rp_{s,t}^{dis,\uparrow}=\nu_{s,t,\omega}^{dis,\uparrow,max}\cdot ra_{s,t,\omega}^{dis,\uparrow}\quad\forall s,\forall t,\forall\omega\tag{A.233}$$

$$\nu_{s,t,\omega}^{dis,\downarrow,max}\cdot rp_{s,t}^{dis,\downarrow}=\nu_{s,t,\omega}^{dis,\downarrow,max}\cdot ra_{s,t,\omega}^{dis,\downarrow}\quad\forall s,\forall t,\forall\omega\tag{A.234}$$

$$\nu_{s,t,\omega}^{ch,\uparrow,max}\cdot rp_{s,t}^{ch,\uparrow}=\nu_{s,t,\omega}^{ch,\uparrow,max}\cdot ra_{s,t,\omega}^{ch,\uparrow}\quad\forall s,\forall t,\forall\omega\tag{A.235}$$

$$\nu_{s,t,\omega}^{ch,\downarrow,max}\cdot rp_{s,t}^{ch,\downarrow}=\nu_{s,t,\omega}^{ch,\downarrow,max}\cdot ra_{s,t,\omega}^{ch,\downarrow}\quad\forall s,\forall t,\forall\omega\tag{A.236}$$

Introducing (A.233)-(A.236) to (A.231) results in:

$$\begin{aligned}\sum_{s}\Big[&\left(O_{s,t}^{dis}+\nu_{s,t,\omega}^{dis,\uparrow,max}\right)\cdot ra_{s,t,\omega}^{dis,\uparrow}-\left(O_{s,t}^{dis}-\nu_{s,t,\omega}^{dis,\downarrow,max}\right)\cdot ra_{s,t,\omega}^{dis,\downarrow}\\ &+\left(O_{s,t}^{ch}+\nu_{s,t,\omega}^{ch,\uparrow,max}\right)\cdot ra_{s,t,\omega}^{ch,\uparrow}-\left(O_{s,t}^{ch}-\nu_{s,t,\omega}^{ch,\downarrow,max}\right)\cdot ra_{s,t,\omega}^{ch,\downarrow}\Big]\\ &=-\sum_{d}VOLL_{d,t}\cdot L_{d,t,\omega}^{sh}-\sum_{i}c_{i,t}\cdot\left(rac_{i,t,\omega}^{\uparrow}-rac_{i,t,\omega}^{\downarrow}\right)\\ &-\sum_{d}u_{d,t}\cdot\left(rad_{d,t,\omega}^{\uparrow}-rad_{d,t,\omega}^{\downarrow}\right)+\Omega_{t,\omega}^{RT}\quad\forall t,\forall\omega\end{aligned}\tag{A.237}$$

Using (A.51)-(A.54) and implementing the appropriate adaptations the following equations occur:

$$\begin{aligned}\lambda_{n,t,\omega}^{RT}\cdot ra_{s,t,\omega}^{dis,\uparrow}=&\,O_{s,t}^{dis}\cdot ra_{s,t,\omega}^{dis,\uparrow}+\nu_{s,t,\omega}^{dis,\uparrow,max}\cdot ra_{s,t,\omega}^{dis,\uparrow}-\nu_{s,t,\omega}^{dis,\uparrow,min}\\ &\cdot ra_{s,t,\omega}^{dis,\uparrow}\quad\forall s,\forall t,\forall\omega\end{aligned}\tag{A.238}$$

$$\begin{aligned}\lambda_{n,t,\omega}^{RT}\cdot ra_{s,t,\omega}^{dis,\downarrow}=&\,O_{s,t}^{dis}\cdot ra_{s,t,\omega}^{dis,\downarrow}-\nu_{s,t,\omega}^{dis,\downarrow,max}\cdot ra_{s,t,\omega}^{dis,\downarrow}+\nu_{s,t,\omega}^{dis,\downarrow,min}\\ &\cdot ra_{s,t,\omega}^{dis,\downarrow}\quad\forall s,\forall t,\forall\omega\end{aligned}\tag{A.239}$$

$$\lambda_{n,t,\omega}^{RT} \cdot ra_{s,t,\omega}^{ch,\uparrow} = O_{s,t}^{ch} \cdot ra_{s,t,\omega}^{ch,\uparrow} + v_{s,t,\omega}^{ch,\uparrow,max} \cdot ra_{s,t,\omega}^{ch,\uparrow} - v_{s,t,\omega}^{ch,\uparrow,min} \cdot ra_{s,t,\omega}^{ch,\uparrow} \quad \forall s, \forall t, \forall \omega \qquad \text{(A.240)}$$

$$\lambda_{n,t,\omega}^{RT} \cdot ra_{s,t,\omega}^{ch,\downarrow} = O_{s,t}^{ch} \cdot ra_{s,t,\omega}^{ch,\downarrow} - v_{s,t,\omega}^{ch,\downarrow,max} \cdot ra_{s,t,\omega}^{ch,\downarrow} + v_{s,t,\omega}^{ch,\downarrow,min} \cdot ra_{s,t,\omega}^{ch,\downarrow} \quad \forall s, \forall t, \forall \omega \qquad \text{(A.241)}$$

Furthermore from (A.70), (A.72), (A.74) and (A.76):

$$v_{s,t,\omega}^{dis,\uparrow,min} \cdot ra_{s,t,\omega}^{dis,\uparrow} = 0 \quad \forall s, \forall t, \forall \omega \qquad \text{(A.242)}$$

$$v_{s,t,\omega}^{dis,\downarrow,min} \cdot ra_{s,t,\omega}^{dis,\downarrow} = 0 \quad \forall s, \forall t, \forall \omega \qquad \text{(A.243)}$$

$$v_{s,t,\omega}^{ch,\uparrow,min} \cdot ra_{s,t,\omega}^{ch,\uparrow} = 0 \quad \forall s, \forall t, \forall \omega \qquad \text{(A.244)}$$

$$v_{s,t,\omega}^{ch,\downarrow,min} \cdot ra_{s,t,\omega}^{ch,\downarrow} = 0 \quad \forall s, \forall t, \forall \omega \qquad \text{(A.245)}$$

Using equations (A.238)-(A.245) to simplify equation (A.237):

$$\begin{aligned} \sum_{s} \left(\lambda_{n,t,\omega}^{RT} \cdot ra_{s,t,\omega}^{dis,\uparrow} - \lambda_{n,t,\omega}^{RT} \cdot ra_{s,t,\omega}^{dis,\downarrow} + \lambda_{n,t,\omega}^{RT} \cdot ra_{s,t,\omega}^{ch,\uparrow} - \lambda_{n,t,\omega}^{RT} \cdot ra_{s,t,\omega}^{ch,\downarrow} \right) \\ = -\sum_{d} VOLL_{d,t} \cdot L_{d,t,\omega}^{sh} - \sum_{i} c_{i,t} \cdot \left(rac_{i,t,\omega}^{\uparrow} - rac_{i,t,\omega}^{\downarrow} \right) \\ - \sum_{d} u_{d,t} \cdot \left(rad_{d,t,\omega}^{\uparrow} - rad_{d,t,\omega}^{\downarrow} \right) + \Omega_{t,\omega}^{RT} \quad \forall t, \forall \omega \end{aligned} \qquad \text{(A.246)}$$

The nonlinear objective function (1) can now be reformulated into the equivalent form, through the application of equations (A.230) and (A.246) as follows:

$$\begin{aligned} \textbf{\textit{Minimize}} \quad & \sum_{t} \sum_{s} \Bigg[\left(c_s^{ch} \cdot G_{s,t}^{DA,ch} + c_s^{dis} \cdot G_{s,t}^{DA,dis} \right) - \sum_{d} u_{d,t} \cdot L_{d,t}^{DA} \\ & + \sum_{i} c_{i,t} \cdot P_{i,t}^{DA} + \sum_{i} c_{i,t}^{res} \cdot \left(rpc_{i,t}^{\uparrow} + rpc_{i,t}^{\downarrow} \right) \\ & + \sum_{d} u_{d,t}^{res} \cdot \left(rpd_{d,t}^{\uparrow} + rpd_{d,t}^{\downarrow} \right) - \Omega_{t}^{DA} \\ & + \sum_{\omega} \pi_{\omega} \\ & \cdot \Bigg[-c_s^{ch} \cdot \left(ra_{s,t,\omega}^{ch,\uparrow} - ra_{s,t,\omega}^{ch,\downarrow} \right) + c_s^{dis} \cdot \left(ra_{s,t,\omega}^{dis,\uparrow} - ra_{s,t,\omega}^{dis,\downarrow} \right) \\ & + \sum_{d} VOLL_{d,t} \cdot L_{d,t,\omega}^{sh} + \sum_{i} c_{i,t} \cdot \left(rac_{i,t,\omega}^{\uparrow} - rac_{i,t,\omega}^{\downarrow} \right) \\ & + \sum_{d} u_{d,t} \cdot \left(rad_{d,t,\omega}^{\uparrow} - rad_{d,t,\omega}^{\downarrow} \right) - \Omega_{t,\omega}^{RT} \Bigg] \Bigg] \end{aligned} \qquad \text{(A.247)}$$

Despite the fact that, the majority of the nonlinearities is eradicated via the above displayed methodologies, some bilinear terms still remain in the equation (A.232) and consist of primal day-ahead and dual real-time variables, such as:

$$\theta_{i,t,\omega}^{\uparrow,max} \cdot rpc_{i,t}^{\uparrow} \, , \theta_{i,t,\omega}^{\downarrow,max} \cdot rpc_{i,t}^{\downarrow}$$

$$\mu_{d,t,\omega}^{\uparrow,max} \cdot rpd_{d,t}^{\uparrow} \, , \mu_{d,t,\omega}^{\downarrow,max} \cdot rpd_{d,t}^{\downarrow} \, , \mu_{d,t,\omega}^{max} \cdot L_{d,t}^{DA}$$

$$\lambda_{n,t,\omega}^{RT} \cdot W_{j,t}^{DA} \, , \lambda_{n,t,\omega}^{RT} \cdot \delta_{n,t}^{\circ}$$

In order to linearize these terms, a binary expansion method is implemented, which necessitates the introduction of auxiliary variables, such as binary and continuous variables $y_{i,t,\omega,ex}^{\uparrow}$ and $z_{i,t,\omega,ex}^{\uparrow}$ respectively, as well as a set of big-M constants. Next, an application of this method is attempted involving the bilinear term $\theta_{i,t,\omega}^{\uparrow,max} \cdot rpc_{i,t}^{\uparrow}$:

$$\theta_{i,t,\omega}^{\uparrow,max} \cdot rpc_{i,t}^{\uparrow} = \sum_{ex} z_{i,t,\omega,ex}^{\uparrow} \cdot r\ddot{p}c_{i,t,ex}^{\uparrow} \quad \forall i, \forall t, \forall \tag{A.248}$$

Continuous variables $rpc_{i,t}^{\uparrow}$ are approximated through a set of discrete values $\{r\ddot{p}c_{i,t,ex}^{\uparrow}$, $ex = 1 \dots EX\}$, acting as parameters and bounded by the $[0, RCc_{i}^{\uparrow,max}]$ interval.

$$0 \leq \theta_{i,t,\omega}^{\uparrow,max} - z_{i,t,\omega,ex}^{\uparrow} \leq M^{1} \cdot \left(1 - y_{i,t,\omega,ex}^{\uparrow}\right) \quad \forall i, \forall t, \forall \omega, \forall ex \tag{A.249}$$

$$0 \leq z_{i,t,\omega,ex}^{\uparrow} \leq M^{1} \cdot y_{i,t,\omega,ex}^{\uparrow} \quad \forall i, \forall t, \forall \omega, \forall ex \tag{A.250}$$

The following equation identifies the closest discrete value $r\ddot{p}c_{i,t,ex}^{\uparrow}$ to the $rpc_{i,t}^{\uparrow}$ variable:

$$rpc_{i,t}^{\uparrow} - \frac{\Delta_{rp_{i,t}^{\uparrow}}}{2} \leq \sum_{ex} y_{i,t,\omega,ex}^{\uparrow} \cdot r\ddot{p}c_{i,t,ex}^{\uparrow} \leq rpc_{i,t}^{\uparrow} + \frac{\Delta_{rp_{i,t}^{\uparrow}}}{2} \quad \forall i, \forall t, \forall \omega \tag{A.251}$$

Where:

$$\Delta_{rpc_{i,t}^{\uparrow}} = \frac{RCc_{i}^{\uparrow,max}}{EX} \quad \forall i, \forall t \tag{A.252}$$

$$\sum_{ex} y_{i,t,\omega,ex}^{\uparrow} = 1 \quad \forall i, \forall t, \forall \omega \tag{A.253}$$

The aforementioned algorithm is applied to the summation of the remaining nonlinear terms, rendering equation (A.247) linear and computationally viable.

Appendix B

Additional data and results for Chapter 2

In this section, useful data and results of this work are presented, in order to avoid an extended illustration of raw information in the main body, which may hinder manuscript's legibility.

i. Data

Units	$t1$	$t2$	$t3$	$t4$	$t5$	$t6$	$t7$	$t8$	$t9$	$t10$	$t11$	$t12$	$t13$	$t14$	$t15$	$t16$	$t17$	$t18$	$t19$	$t20$	$t21$	$t22$	$t23$	$t24$
$i1$	12	12	12	12	12	12	12	12	16	12	12	12	12	18	12	12	18	12	12	12	16	16	12	12
$i2$	17	17	17	17	17	17	17	17	39	17	17	17	17	48	30	30	48	17	17	17	39	39	17	17
$i3$	15	15	15	15	15	15	15	15	31	15	15	15	15	35	23	23	35	15	15	15	31	31	15	15
$i4$	14	14	14	14	14	14	14	14	27	14	14	14	14	30	20	20	30	14	14	14	27	27	14	14
$i5$	16	16	16	16	16	16	16	16	35	16	16	16	16	41	26	26	41	16	16	16	35	35	16	16
$i6$	13	13	13	13	13	13	13	13	19	13	13	13	13	25	16	16	25	13	13	13	19	19	13	13

Table B.1: Marginal energy cost offers for conventional generators.

Units	$t1$	$t2$	$t3$	$t4$	$t5$	$t6$	$t7$	$t8$	$t9$	$t10$	$t11$	$t12$	$t13$	$t14$	$t15$	$t16$	$t17$	$t18$	$t19$	$t20$	$t21$	$t22$	$t23$	$t24$
$d1$	70	70	70	70	70	70	70	70	70	70	70	70	70	70	70	70	70	70	70	70	70	70	70	70
$d2$	80	80	80	90	80	80	80	80	80	90	80	80	80	80	80	90	80	80	80	80	80	90	80	80
$d3$	80	80	90	75	90	90	80	80	90	75	90	90	80	80	90	75	90	90	80	80	90	75	90	90
$d4$	65	65	65	65	65	65	65	65	65	65	65	65	65	65	65	65	65	65	65	65	65	65	65	65
$d5$	65	65	65	65	65	65	65	65	65	65	65	65	65	65	65	65	65	65	65	65	65	65	65	65

Table B.2: Maximum energy capacity for demand loads.

Units	$t1$	$t2$	$t3$	$t4$	$t5$	$t6$	$t7$	$t8$	$t9$	$t10$	$t11$	$t12$	$t13$	$t14$	$t15$	$t16$	$t17$	$t18$	$t19$	$t20$	$t21$	$t22$	$t23$	$t24$
$d1$	5	5.5	4.5	5	5	5	5	5.5	4.5	5	5	5	5	5.5	4.5	5	5	5	5	5.5	4.5	5	5	5
$d2$	8	7.5	8.5	9	8	8	8	7.5	8.5	9	8	8	8	7.5	8.5	9	8	8	8	7.5	8.5	9	8	8
$d3$	8	7	8.5	7.5	9	7	8	7	8.5	7.5	9	7	8	7	8.5	7.5	9	7	8	7	8.5	7.5	9	7
$d4$	5	4.5	6	5.5	4.5	5.5	5	4.5	6	5.5	4.5	5.5	5	4.5	6	5.5	4.5	5.5	5	4.5	6	5.5	4.5	5.5
$d5$	6.5	6	4.5	5	5.5	4	6.5	6	4.5	5	5.5	4	6.5	6	4.5	5	5.5	4	6.5	6	4.5	5	5.5	4

Table B.3: Maximum upward/downward reserve capacity for demand loads.

ii. Results

- *Uncongested network*

	Day-ahead Market				Reserve Market							
Hr.	$G_{s1,t}^{DA,ch}$ (MWh)	$G_{s1,t}^{DA,dis}$ (MWh)	$O_{s1,t}^{ch}$ $(€/MWh)$	$O_{s1,t}^{dis}$ $(€/MWh)$	$rp_{s1,t}^{ch,\downarrow}$ (MW)	$rp_{s1,t}^{ch,\uparrow}$ (MW)	$O_{s1,t}^{ch,\downarrow}$ $(€/MWh)$	$O_{s1,t}^{ch,\uparrow}$ $(€/MWh)$	$rp_{s1,t}^{dis,\downarrow}$ (MW)	$rp_{s1,t}^{dis,\uparrow}$ (MW)	$O_{s1,t}^{dis,\downarrow}$ $(€/MWh)$	$O_{s1,t}^{dis,\uparrow}$ $(€/MWh)$
1	4.14		200		2.82	4.14	6	5				
2										12		5
3	6.2		200		7	6.2	7	5.5				
4										11.75		5
5										11.75		5
6										11.75		5
7	4.31		200		12	3.83	6	5.5				
8										9.83		5
9		3.31		31					3.31	8.85	5	5
10										11.85		5
11	5.2		200		12	5.2	6	5				
12										11.95		5
13	4.3		200		8.54	1.74	6	5				
14		8.3		35					8.3	3.7	5	5
15		0.7		24					0.7	2.63	5	5
16		9.62		24					9.62	0.75	5.5	5.5
17		5.36		35					5.36		5	
18	7.69		200		6.75	7.69	6	5				
19	4.3		200		8.3	4	6	5				
20	4.3		200		9	2.04	6	5.5				
21		2.9		31					2.9	11.75	5	5
22		12		31					12	12	5	5
23	6.2		200		11	6.2	6	5				
24	6.2		200		12	6.2	6	5				

Table B.4: Results for storage system $s1$, in the joint energy and reserve day-ahead market.

	Balancing Market									
Hr.	$ra_{s1,t,\omega1}^{ch,\downarrow}$ (MWh)	$ra_{s1,t,\omega2}^{ch,\downarrow}$ (MWh)	$ra_{s1,t,\omega1}^{ch,\uparrow}$ (MWh)	$ra_{s1,t,\omega2}^{ch,\uparrow}$ (MWh)	$ra_{s1,t,\omega1}^{dis,\downarrow}$ (MWh)	$ra_{s1,t,\omega2}^{dis,\downarrow}$ (MWh)	$ra_{s1,t,\omega1}^{dis,\uparrow}$ (MWh)	$ra_{s1,t,\omega2}^{dis,\uparrow}$ (MWh)	$\lambda_{n,t,\omega1}^{RT}$ $(€/MWh)$	$\lambda_{n,t,\omega2}^{RT}$ $(€/MWh)$
1	2.82			4.14					16	200
2								12	16	200
3	7			6.2					16	200
4								11.55	16	200
5								11.75	16	200
6								11.75	16	200
7	12			3.83					16	200
8								9.83	16	200
9					3.31			8.85	35	35
10								9.52	16	200
11	5.12			5.2					16	200
12								11.95	16	200
13	8.54			1.74					16	200
14					8.3			3.7	41	41
15					0.7			2.63	20	20
16					9			0.75	26	26
17					5.36				41	41
18			7.69	7.69					14	200
19	8.3			4					16	200
20	9			2.04					16	200
21					2.25			11.75	35	35
22					2.22			12	35	35
23			6.2	6.2					16	200
24			6.2	6.2					16	200

Table B.5: Results for storage system $s1$ in the balancing market.

	Day-Ahead Market				Reserve Market							
Hr.	$G_{s2,t}^{DA,ch}$ (MWh)	$G_{s2,t}^{DA,dis}$ (MWh)	$O_{s2,t}^{ch}$ $(€/MWh)$	$O_{s2,t}^{dis}$ $(€/MWh)$	$rp_{s2,t}^{ch,\downarrow}$ (MW)	$rp_{s2,t}^{ch,\uparrow}$ (MW)	$O_{s2,t}^{ch,\downarrow}$ $(€/MWh)$	$O_{s2,t}^{ch,\uparrow}$ $(€/MWh)$	$rp_{s2,t}^{dis,\downarrow}$ (MW)	$rp_{s2,t}^{dis,\uparrow}$ (MW)	$O_{s2,t}^{dis,\downarrow}$ $(€/MWh)$	$O_{s2,t}^{dis,\uparrow}$ $(€/MWh)$
1	-9.1		200		8.18	9.1	5	5				
2	-9.55		200		10	9.55	6	5				
3										10		5
4	-10		200		10	10	6	5				
5		4.25		15					4.25	10	5	5
6		0.5		15					0.5	10	5	5
7	-9.72		200		4	9.72	6	5.5				
8	-9.72		200		10	9.72	6	5.5				
9										10		5
10	-10		200		10	10	6	5				
11				15						10		5
12		6.55							6.55	10	5	5
13	-9.72		200		2.46	9.72	6	5				
14		3.52		35					3.52	10	5	5
15	-7.72		200		10	7.72	7	5.5				
16		0.03		24					0.03	10	5	5.5
17		9.4		35					9.4	9	5	7
18	-7.56		200		0	7.56	6	5				
19	-9.72		200		4.72	9.72	6	5				
20	-9.72		200		7.5	9.72	6	5.5				
21										10		5
22		2		31					2	9.75	5	5
23										9.75		5
24										9.75		5

Table B.6: Results for storage system $s2$, in the joint energy and reserve day-ahead market.

	Balancing Market							
Hr.	$ra_{s2,t,\omega1}^{ch,\downarrow}$ (MWh)	$ra_{s2,t,\omega2}^{ch,\downarrow}$ (MWh)	$ra_{s2,t,\omega1}^{ch,\uparrow}$ (MWh)	$ra_{s2,t,\omega2}^{ch,\uparrow}$ (MWh)	$ra_{s2,t,\omega1}^{dis,\downarrow}$ (MWh)	$ra_{s2,t,\omega2}^{dis,\downarrow}$ (MWh)	$ra_{s2,t,\omega1}^{dis,\uparrow}$ (MWh)	$ra_{s2,t,\omega2}^{dis,\uparrow}$ (MWh)
1				9.1				
2				9.55				
3								10
4				10				
5					2.25			10
6					0.44			10
7				9.72				
8				9.72				
9					3.31			10
10	9.52			10				
11								10
12					3.64			10
13				9.72				
14								10
15				7.72				
16								10
17								9
18				7.76				
19				9.72				
20				9.72				
21								10
22					0.03			9.75
23								9.75
24								9.75

Table B.7: Results for storage system $s2$ in the balancing market.

	$P_{i,t}^{DA}$ (MWh)						$rpc_{i,t}^{\downarrow}, rpc_{i,t}^{\uparrow}$ (MW)					
Hr	**i1**	**i2**	**i3**	**i4**	**i5**	**i6**	**i1**	**i2**	**i3**	**i4**	**i5**	**i6**
1	80	0	39.25	75	9	100	0, 0	0, 0	0, 0	0, 0	9, 6.75	0, 0
2	80	0	39.81	75	4.74	100	0, 0	0, 0	0, 0	7.26, 0	4.74, 0.45	0, 0
3	80	0	42.2	75	9	100	0, 0	0, 0.8	0, 0	10, 0	9, 9	0, 0
4	80	0	42.5	75	7.5	100	0, 0	0, 0	0, 0	4.5, 0	7.5, 0.45	0, 0
5	80	0	31.75	75	9	100	0, 0	0, 0	0.3, 0	10, 0	9, 2.25	0.45, 0
6	80	0	35.5	75	9	100	0, 0	0, 0	4.5, 0	10, 0	9, 2.25	0, 0
7	80	0	40	75	9	100	0, 0	0, 2.45	0, 0	0, 0	9, 9	0, 0
8	80	0	40	75	4.7	100	0, 0	0, 0	0, 0	5.3, 0	4.7, 0.45	0, 0
9	80	0	41.7	75	0	100	8, 0	0, 0	0.3, 0	10, 0	0, 3.15	0.39, 0
10	80	0	42.5	75	7.5	100	0, 0	0, 0	0, 0	7.5, 0	7.5, 3.15	0, 0
11	80	0	42.2	75	8	100	0, 0	0, 0	0, 0	0, 0	8, 4.8	0, 0
12	80	0	29.45	75	9	100	0, 0	0, 0	0, 0	10, 0	9, 4.05	0.45, 0
13	80	0	40	75	9	100	0, 0	0, 0	0, 0	0, 0	9, 8.54	0, 0
14	80	0	23.2	75	0	100	0, 0	0, 0	0, 0	10, 0	0, 8.3	0.18, 0
15	80	0	52	75	0	100	0.06, 0	0, 6.65	0.3, 0	10, 0	0, 9	4.95, 0
16	80	0	30.35	75	0	100	0.4, 0	0, 5.25	4.5, 0	10, 0	0, 9	0.45, 0
17	80	0	30.25	75	0	100	0.23, 0	0, 7	0, 0	10, 0	0, 9	0, 0
18	80	0	51.7	75	8.55	100	0, 0	0, 0	0, 0	6.7, 0	8.55, 6.75	0, 0
19	80	0	40	75	9	100	0, 0	0, 0	0, 0	0, 0	9, 8.28	0, 0
20	80	0	40	75	9	100	0, 0	0, 5.25	0, 0	0.5, 0	9, 9	0, 0
21	80	0	42.1	75	0	100	6, 0	0, 0	5.1, 0	10, 0	0, 2.25	0, 0
22	80	0	26	75	0	100	0, 0	0, 0	0, 0	10, 0	0, 2.25	0, 0
23	80	0	42.2	75	9	100	0, 0	0, 0	0, 0	0, 0	9, 4.05	0, 0
24	80	0	42.2	75	9	100	0, 0	0, 0	0, 0	3, 0	9, 8.55	0, 0

Table B.8: Results for conventional generators in the joint energy and reserve day-ahead market.

$rac^{\downarrow}_{i,t,\omega}, rac^{\uparrow}_{i,t,\omega}$ (MWh)						
Hr	**i1**	**i2**	**i3**	**i4**	**i5**	**i6**
1	0, 0	0, 0	0, 0	0, 0	-3.9, 6.75	0, 0
2	0, 0	0, 0	0, 0	0, 0	0, 0.45	0, 0
3	0, 0	0, 0.8	0, 0	0, 0	-2, 9	0, 0
4	0, 0	0, 0	0, 0	0, 0	-0.92, 0.45	0, 0
5	0, 0	0, 0	0, 0	0, 0	2.25, 2.25	0, 0
6	0, 0	0, 0	0, 0	0, 0	0.44, 2.25	0, 0
7	0, 0	0, 2.45	0, 0	0, 0	9, 9	0, 0
8	0, 0	0, 0	0, 0	0, 0	0, 0.45	0, 0
9	0, 0	0, 0	0, 0	0, 0	2.9, 3.15	0, 0
10	0, 0	0, 0	0, 0	0, 0	-0.48, 3.15	0, 0
11	0, 0	0, 0	0, 0	0, 0	-4.88, 4.8	0, 0
12	0, 0	0, 0	0, 0	0, 0	-0.4, 4.05	0, 0
13	0, 0	0, 0	0, 0	0, 0	8.54, 8.54	0, 0
14	0, 0	0, 0	0, 0	0, 0	8.3, 8.3	0, 0
15	0, 0	0, 6.65	0, 0	-6.72, 0	0, 9	0, 0
16	0, 0	0, 5.25	0, 0	0, 0	9, 9	0, 0
17	0, 0	0, 7	0, 0	0, 0	5.36, 9	0, 0
18	0, 0	0, 0	0, 0	-6.7, 0	-8.55, 6.75	0, 0
19	0, 0	0, 0	0, 0	0, 0	8.3, 8.3	0, 0
20	0, 0	0, 5.25	0, 0	0, 0	9, 9	0, 0
21	0, 0	0, 0	0, 0	0, 0	2.25, 2.25	0, 0
22	0, 0	0, 0	0, 0	0, 0	2.25, 2.25	0, 0
23	0, 0	0, 0	0, 0	0, 0	-9, 4.05	0, 0
24	0, 0	0, 0	0, 0	0, 0	-9, 8.55	0, 0

Table B.9: Results for conventional generators in the balancing market.

- *Congested network*

	Day-Ahead Market				Reserve Market							
Hr.	$G_{s1,t}^{DA,ch}$ (MWh)	$G_{s1,t}^{DA,dis}$ (MWh)	$O_{s1,t}^{ch}$ $(€/MWh)$	$O_{s1,t}^{dis}$ $(€/MWh)$	$rp_{s1,t}^{ch,\downarrow}$ (MW)	$rp_{s1,t}^{ch,\uparrow}$ (MW)	$O_{s1,t}^{ch,\downarrow}$ $(€/MWh)$	$O_{s1,t}^{ch,\uparrow}$ $(€/MWh)$	$rp_{s1,t}^{dis,\downarrow}$ (MW)	$rp_{s1,t}^{dis,\uparrow}$ (MW)	$O_{s1,t}^{dis,\downarrow}$ $(€/MWh)$	$O_{s1,t}^{dis,\uparrow}$ $(€/MWh)$
1	9.55		200		11	9.55	5.5	5				
2	11.5				12	11.55	5.5	5				
3	12		200		10	12	6	5				
4	12				5.2	12	5.5	5				
5		6.7		16					6.7	12	5	5
6	12				10.2	12	5.5	5				
7	12		200		9.35	12	5.5	5				
8	12				12	12	5	5				
9		12		33.7					12	11.55	5	5
10	12				9.35	12	5.5	5				
11	9.55		200		11	9.55	5.5	5				
12	11.05				9.2	11.05	5.5	5				
13	9.55		200		9.55	9.55	5	5				
14		13.9		37					12	12	6	5
15	11.05		200		12	11.05	5	5				
16	43.12		200		6	11.2	5.5	5.5				
17		7.4		37					7.4	12	6	5
18	12		200		6	12	6	5				
19			200							12		5
20	9.25		200		12	9.25	5.5	5				
21		19.855		33.7					12	12	6	5
22		5		33.7					5	12	7	5
23	12		200		9.95	12	5.5	5				
24		6.94		16					6.94	12	6	

Table B.10: Results for storage system $s1$, in the joint energy and reserve day-ahead market.

	Balancing Market							
Hr.	$ra_{s1,t,\omega1}^{ch,\downarrow}$ (MWh)	$ra_{s1,t,\omega2}^{ch,\downarrow}$ (MWh)	$ra_{s1,t,\omega1}^{ch,\uparrow}$ (MWh)	$ra_{s1,t,\omega2}^{ch,\uparrow}$ (MWh)	$ra_{s1,t,\omega1}^{dis,\downarrow}$ (MWh)	$ra_{s1,t,\omega2}^{dis,\downarrow}$ (MWh)	$ra_{s1,t,\omega1}^{dis,\uparrow}$ (MWh)	$ra_{s1,t,\omega2}^{dis,\uparrow}$ (MWh)
1			9	9.55				
2			9.29	11.55				
3			12	12				
4	5.2			12				
5					6.7			12
6			12	12				
7			2.36	12				
8				12				
9					12			11.55
10	9.35			12				
11			9	9.55				
12			9.88	11.05				
13	0.45			9.55				
14							1.61	12
15			9	11.05				
16	6			11.2				
17								12
18			12	12				
19								12
20			2.25	9.25				
21					11.3			12
22					5			12
23			9.88	12				
24					3.15			12

Table B.11: Results for storage system $s1$ in the balancing market.

	Day-Ahead Market				Reserve Market							
Hr.	$G_{s2,t}^{DA,ch}$ (MWh)	$G_{s2,t}^{DA,dis}$ (MWh)	$O_{s2,t}^{ch}$ $(€/MWh)$	$O_{s2,t}^{dis}$ $(€/MWh)$	$rp_{s2,t}^{ch,\downarrow}$ (MW)	$rp_{s2,t}^{ch,\uparrow}$ (MW)	$O_{s2,t}^{ch,\downarrow}$ $(€/MWh)$	$O_{s2,t}^{ch,\uparrow}$ $(€/MWh)$	$rp_{s2,t}^{dis,\downarrow}$ (MW)	$rp_{s2,t}^{dis,\uparrow}$ (MW)	$O_{s2,t}^{dis,\downarrow}$ $(€/MWh)$	$O_{s2,t}^{dis,\uparrow}$ $(€/MWh)$
1	10.5		200			10		5				
2		0.65		22					0.65	10	5.5	5
3										9.95		5
4					7.79		5.5					
5	9.75		200		8.29	9.75	5.5	5				
6		0.25		24					0.25	9.75	5.5	5
7										9.85		5
8	15.4		200		8	8	5	5				
9		10		50					10	10	6	5
10										9.85		5
11	25.75		200			10		5				
12		6.75		24					6.75	10	5.5	5
13	14.7		200		10	10	5	5				
14		5.16		50					5.16	10	5	5
15		11.15		44					5	10	5	5
16					10		5.5					
17	8.95		200			8.95		5				
18										10		5
19	21.97		200		6	10	6	5				
20		5		22					5	10	5.5	5
21		11.45		50					10	3.45	6	5
22	4.18		200			3.45		5				
23										1.25		5
24										8.85		5

Table B.12: Results for storage system $s2$, in the joint energy and reserve day-ahead market.

	Balancing Market							
Hr.	$ra_{s2,t,\omega1}^{ch,\downarrow}$ (MWh)	$ra_{s2,t,\omega2}^{ch,\downarrow}$ (MWh)	$ra_{s2,t,\omega1}^{ch,\uparrow}$ (MWh)	$ra_{s2,t,\omega2}^{ch,\uparrow}$ (MWh)	$ra_{s2,t,\omega1}^{dis,\downarrow}$ (MWh)	$ra_{s2,t,\omega2}^{dis,\downarrow}$ (MWh)	$ra_{s2,t,\omega1}^{dis,\uparrow}$ (MWh)	$ra_{s2,t,\omega2}^{dis,\uparrow}$ (MWh)
1				10				
2							0.06	10
3							1.17	9.95
4								
5			4.46	9.75				
6							0.76	9.75
7								
8				8				
9								10
10								
11				10				
12							0.18	10
13	10			10				
14							3.23	10
15								10
16								
17				8.95				
18							1.17	10
19				10				
20								10
21							1.33	3.45
22				3.45				
23							0.18	1.25
24								8.85

Table B.13: Results for storage system $s2$ in the balancing market.

	$P_{i,t}^{DA}$ (MWh)						$rpc_{i,t}^{\downarrow}, rpc_{i,t}^{\uparrow}$ (MW)					
Hr	**i1**	**i2**	**i3**	**i4**	**i5**	**i6**	**i1**	**i2**	**i3**	**i4**	**i5**	**i6**
1	80	18.65	3.65	75	22.25	100	0, 0	0, 0	0, 0	0, 0	-9, 0.45	0, 0
2	80	17.05	5.95	75	22.9	100	0, 0	-0.35,	0, 0	0, 0	-9, 0.45	0, 0
3	80	10.63	15.63	75	20.74	100	0, 0	-7, 0	0, 0	0, 0	-9, 0.45	0, 0
4	80	4.95	19.95	75	27.09	100	0, 0	0, 1	0, 0	0, 0	-9, 9	0, 0
5	80	5.31	10.31	75	12.67	100	0, 0	0, 0	0, 0	0, 0	-9, 2.25	0, 0
6	80	8.28	13.28	75	25.43	100	0, 0	-4.55, 0	0, 0	0, 0	-9, 2.25	0, 0
7	80	18.33	3.33	75	25.33	100	0, 0	-6.65, 0	0, 0	0, 0	-9, 3.15	0, 0
8	80	18.65	3.65	75	24.7	100	0, 0	0, 0	0, 0	0, 0	0, 0	0, 0
9	80	0	20.43	75	0	100	0, 0	0, 0	0, 0	0, 0	0, 0.45	0, 0
10	80	8.78	23.78	75	19.44	100	0, 0	-6.65, 0	0, 0	0, 0	-9, 3.15	0, 0
11	80	5.31	10.31	75	28.92	100	0, 0	0, 0	0, 0	0, 0	-9, 0.45	0, 0
12	80	8.28	13.28	75	24.5	100	0, 0	-1.05, 0	0, 0	0, 0	-9, 4.95	0, 0
13	80	18.65	3.65	75	22.25	100	0, 0	0, 0	0, 0	0, 0	-0.45, 0.45	0, 0
14	80	0	15.94	75	0	100	0, 0	0, 0	0, 0	-4.84, 0	0, 0	0, 0
15	80	0	11.92	75	32.97	100	0, 0	0, 0	0, 0	0, 0	-9, 4.95	0, 0
16	80	3.33	18.33	75	61.45	100	0, 0	0, 5.25	0, 0	0, 0	-9, 8.55	0, 0
17	80	0	24.37	75	0	100	-7.6, 0	0, 0	0, 0	-10, 0	0, 4.05	0, 0
18	80	10.63	15.63	75	20.74	100	0, 0	-7, 0	0, 0	0, 0	-9, 0	0, 0
19	80	18.33	3.33	75	13.33	100	0, 0	-7, 0	0, 0	0, 0	-9, 0	0, 0
20	80	0	15	75	24.25	100	0, 0	0, 0	0, 0	0, 0	-9, 6.75	0, 0
21	80	0	13.7	75	0	100	0, 0	0, 0	0, 0	-2, 0	0, 8.55	0, 0
22	80	0	24.43	75	9	100	0, 0	0, 0	0, 0	-10, 0	-9, 8.55	0, 0
23	80	5.31	10.31	75	31.37	100	0, 0	-1.05, 0	0, 0	0, 0	-9, 6.75	0, 0
24	80	7	12	75	9.06	100	0, 0	-7, 0	0, 0	-1.06, 0	-9, 3.15	0, 0

Table B.14: Results for conventional generators in the joint energy and reserve day-ahead market.

- *Wind power generation increment scenarios*

Wind Percentage	$\sum_{i,t} P_{i,t}^{DA}$	$\sum_{i,t} rpc_{i,t}^{\downarrow}$	$\sum_{i,t} rpc_{i,t}^{\uparrow}$	$\sum_{i,t} rac_{i,t,\omega 1}^{\downarrow}$	$\sum_{i,t} rac_{i,t,\omega 2}^{\downarrow}$	$\sum_{i,t} rac_{i,t,\omega 1}^{\uparrow}$	$\sum_{i,t} rac_{i,t,\omega 2}^{\uparrow}$
12.17%	7186.9	321.3	158.2	52.9	-	98.2	158.2
16.53%	6644.8	528.2	143.8	171.3	-	0.5	71.9
19.2%	6183.6	373.8	68.1	196	-	-	68.1

Table B.15: Energy dispatch (MWh) and reserve provisions (MW) for conventional generators, under wind generation increment *Cases 1,2,3.*

	$G_{s1,t1}^{DA,ch}$ (MWh)	$rp_{s1,t1}^{ch,\downarrow}$ (MW)	$rp_{s1,t1}^{ch,\uparrow}$ (MW)	$ra_{s1,t1,\omega 1}^{ch,\downarrow}$ (MWh)	$ra_{s1,t1,\omega 2}^{ch,\downarrow}$ (MWh)	$ra_{s1,t1,\omega 1}^{ch,\uparrow}$ (MWh)	$ra_{s1,t1,\omega 2}^{ch,\uparrow}$ (MWh)	$\lambda_{n,t1}^{DA}$ $(€/MWh)$	$\lambda_{n,t1,\omega 1}^{RT}$ $(€/MWh)$	$\lambda_{n,t1,\omega 2}^{RT}$ $(€/MWh)$
Wind 12.17%	4.14	2.82	4.14	2.82	-	-	4.14	15	16	200
Wind 16.53%	12	10.5	12	-	-	9.5	12	15	14	200
Wind 19.2%	12.65	4.15	12.65	-	-	8.3	12.65	14	14	200

Table B.16: Energy dispatch and reserve procurements of storage system $s1$, during time period 1, under three wind generation cases.

Appendix C

Mathematical Transformations for Chapter 4

KKT equality conditions of the lower-level problem (4.5) – (4.13):

$$o_{g,t} + cp \cdot \zeta_g - \lambda^E_{n,t} + \overline{\beta_{g,t}} - \underline{\beta_{g,t}} = 0 \qquad \forall g, \forall t \tag{C.1}$$

$$C_i + cp \cdot \zeta_i - \lambda^E_{n,t} + \overline{\alpha_{i,t}} - \underline{\alpha_{i,t}} = 0 \qquad \forall i, \forall t \tag{C.2}$$

$$-\lambda^E_{n,t} - \sum_h \alpha_h \cdot \eta \cdot \rho_{h,t} + \overline{\gamma_{j,t}} - \underline{\gamma_{j,t}} = 0 \qquad \forall j, \forall t \tag{C.3}$$

$$cp + \rho_{h,t} = 0 \qquad \forall h, \forall t \tag{C.4}$$

$$\sum_{m \in NaM} B_{n,m} \cdot \left(\lambda^E_{n,t} - \lambda^E_{m,t}\right) + \sum_{m \in NaM} B_{n,m} \cdot \left(\overline{\psi_{n,m,t}} - \overline{\psi_{m,n,t}}\right) - \sum_{m \in NaM} B_{n,m} \cdot \left(\underline{\psi_{n,m,t}} - \underline{\psi_{m,n,t}}\right) + \overline{\pi_{n,t}} - \underline{\pi_{n,t}} + \eta^o_{n,t} = 0 \qquad \forall n, \forall t \tag{C.5}$$

$$-\sum_{i \in IaN} p_{i,t} - \sum_{g \in GaN} v_{g,t} - \sum_{j \in JaN} w_{j,t} + \sum_{d^{EL} \in DaN} L^E_{d,t} + \sum_{m \in NaM} B_{n,m} \cdot \left(\delta_{n,t} - \delta_{m,t}\right) = 0 \quad : \left[\lambda^E_{n,t}\right] \quad \forall n, \forall t \tag{C.6}$$

$$Q^H_{h,t} = \alpha_h \cdot \eta \cdot \left(\sum_{d^{EL} \in DaN} L^E_{d,t} - \sum_{j \in JaN} w_{j,t}\right) \quad : \left[\rho_{h,t}\right] \quad \forall h, \forall t \tag{C.7}$$

$$\delta_{n_1,t} = 0 \quad : \left[\eta^o_{n,t}\right] \qquad \forall n = n_1, \forall t \tag{C.8}$$

KKT equality conditions of the lower-level problem (4.14) – (4.16):

$$C_k - \lambda^{NG}_{r,t} + \overline{\varepsilon_{k,t}} - \underline{\varepsilon_{k,t}} = 0 \qquad \forall k, \forall t \tag{C.9}$$

$$-\sum_{k \in KaR} f_{k,t} + \sum_{g \in GaR} \varphi_g \cdot v_{g,t} + \sum_{d^{NG} \in DaR} L^{NG}_{d,t} = 0 \quad : \left[\lambda^{NG}_{r,t}\right] \quad \forall r, \forall t \tag{C.10}$$

KKT complementarity conditions of the lower-level problems:

$$0 \le p_{i,t} \perp \underline{a_{i,t}} \ge 0 \qquad \forall i, \forall t \tag{C.11}$$

$$0 \le \overline{P}_i - p_{i,t} \perp \overline{a_{i,t}} \ge 0 \qquad \forall i, \forall t \tag{C.12}$$

$$0 \le v_{g,t} \perp \underline{\beta_{g,t}} \ge 0 \qquad \forall g, \forall t \tag{C.13}$$

$$0 \le \overline{V_g} - v_{g,t} \perp \overline{\beta_{g,t}} \ge 0 \qquad \forall i, \forall t \tag{C.14}$$

$$0 \le w_{j,t} \perp \underline{\gamma_{j,t}} \ge 0 \qquad \forall j, \forall t \tag{C.15}$$

$$0 \le \overline{W_j} - w_{j,t} \perp \overline{\gamma_{j,t}} \ge 0 \qquad \forall j, \forall t \tag{C.16}$$

$$0 \le f_{k,t} \perp \underline{\varepsilon_{k,t}} \ge 0 \qquad \forall k, \forall t \tag{C.17}$$

$$0 \le \overline{F}_k - f_{k,t} \perp \overline{\varepsilon_{k,t}} \ge 0 \qquad \forall k, \forall t \tag{C.18}$$

$$0 \le B_{n,m} \cdot \left(\delta_{n,t} - \delta_{m,t}\right) + \overline{T}_{n,m} \perp \underline{\psi_{n,m,t}} \ge 0 \qquad \forall n, \forall m, \forall t \tag{C.19}$$

$$0 \le \overline{T}_{n,m} - B_{n,m} \cdot \left(\delta_{n,t} - \delta_{m,t}\right) \perp \overline{\psi_{n,m,t}} \ge 0 \qquad \forall n, \forall m, \forall t \tag{C.20}$$

$$0 \le \delta_{n,t} + 3.14 \perp \underline{\pi_{n,t}} \ge 0 \qquad \forall n, \forall t \tag{C.21}$$

$$0 \le 3.14 - \delta_{n,t} \perp \overline{\pi_{n,t}} \ge 0 \qquad \forall n, \forall t \tag{C.22}$$

The nonlinearities appearing in the above complementarity conditions are eliminated by employing the Fortuny-Amat and McCarl linearization process:

$$0 \le p_{i,t} \le M^{pP} \cdot z^1_{i,t} \qquad \forall i, \forall t \tag{C.23}$$

$$0 \le \underline{a_{i,t}} \le M^{cP} \cdot (1 - z^1_{i,t}) \qquad \forall i, \forall t \tag{C.24}$$

$$0 \le \overline{P}_i - p_{i,t} \le M^{pP} \cdot z^2_{i,t} \qquad \forall i, \forall t \tag{C.25}$$

$$0 \le \overline{a_{i,t}} \le M^{cP} \cdot (1 - z^2_{i,t}) \qquad \forall i, \forall t \tag{C.26}$$

$$0 \le v_{g,t} \le M^{pP} \cdot z^3_{g,t} \qquad \forall g, \forall t \tag{C.27}$$

$$0 \le \underline{\beta_{g,t}} \le M^{cP} \cdot (1 - z^3_{g,t}) \qquad \forall g, \forall t \tag{C.28}$$

$$0 \le \overline{V}_g - v_{g,t} \le M^{pP} \cdot z^4_{g,t} \qquad \forall i, \forall t \tag{C.29}$$

$$0 \le \overline{\beta_{g,t}} \le M^{cP} \cdot (1 - z^4_{g,t}) \qquad \forall i, \forall t \tag{C.30}$$

$$0 \le w_{j,t} \le M^{pP} \cdot z^7_{j,t} \qquad \forall j, \forall t \tag{C.31}$$

$$0 \le \underline{\gamma_{j,t}} \le M^{cP} \cdot (1 - z^7_{j,t}) \qquad \forall j, \forall t \tag{C.32}$$

$$0 \le \overline{W}_{j,t} - w_{j,t} \le M^{pP} \cdot z^8_{j,t} \qquad \forall j, \forall t \tag{C.33}$$

$$0 \le \overline{\gamma_{j,t}} \le M^{cP} \cdot (1 - z^8_{j,t}) \qquad \forall j, \forall t \tag{C.34}$$

$$0 \le f_{k,t} \le M^{pP} \cdot z^9_{k,t} \qquad \forall k, \forall t \tag{C.35}$$

$$0 \le \underline{\varepsilon_{k,t}} \le M^{cP} \cdot (1 - z^9_{k,t}) \qquad \forall k, \forall t \tag{C.36}$$

$$0 \le \overline{F}_k - f_{k,t} \le M^{pP} \cdot z^{10}_{k,t} \qquad \forall k, \forall t \tag{C.37}$$

$$0 \le \overline{\varepsilon_{k,t}} \le M^{cP} \cdot (1 - z^{10}_{k,t}) \qquad \forall k, \forall t \tag{C.38}$$

$$0 \le B_{n,m} \cdot \left(\delta_{n,t} - \delta_{m,t}\right) + \overline{T}_{n,m} \le M^{pX} \cdot z^{41}_{n,m,t} \qquad \forall n, \forall m, \forall t \tag{C.39}$$

$$0 \le \underline{\psi_{n,m,t}} \le M^{cX} \cdot (1 - z^{41}_{n,m,t}) \qquad \forall n, \forall m, \forall t \tag{C.40}$$

$$0 \le \overline{T}_{n,m} - B_{n,m} \cdot \left(\delta_{n,t} - \delta_{m,t}\right) \le M^{pX} \cdot z^{42}_{n,m,t} \qquad \forall n, \forall m, \forall t \tag{C.41}$$

$$0 \le \overline{\psi_{n,m,t}} \le M^{cX} \cdot (1 - z^{42}_{n,m,t}) \qquad \forall n, \forall m, \forall t \tag{C.42}$$

$$0 \le \delta_{n,t} + 3.14 \le M^{pX} \cdot z^{45}_{n,t} \qquad \forall n, \forall t \tag{C.43}$$

$$0 \le \underline{\pi_{n,t}} \le M^{cX} \cdot (1 - z^{45}_{n,t}) \qquad \forall n, \forall t \tag{C.44}$$

$$0 \le 3.14 - \delta_{n,t} \le M^{pX} \cdot z^{46}_{n,t} \qquad \forall n, \forall t \tag{C.45}$$

$$0 \le \overline{\pi_{n,t}} \le M^{cX} \cdot (1 - z^{46}_{n,t}) \qquad \forall n, \forall t \tag{C.46}$$

To eliminate the nonlinearities of the objective function (4.4), the below process is followed:

The KKT equality (C.1) results in:

$$\lambda^{E}_{n,t} = o_{g,t} + cp \cdot \zeta_g + \overline{\beta_{g,t}} - \underline{\beta_{g,t}} \qquad \forall g, \forall t \tag{C.47}$$

Multiplying by $v_{g,t}$ gives:

$$\begin{aligned} \sum_{g \in GaN} \lambda^{E}_{n,t} \cdot v_{g,t} \\ = \sum_{g \in GaN} o_{g,t} \cdot v_{g,t} + \sum_{g \in GaN} cp \cdot \zeta_g \cdot v_{g,t} + \sum_{g \in GaN} \overline{\beta_{g,t}} \cdot v_{g,t} \\ - \sum_{g \in GaN} \underline{\beta_{g,t}} \cdot v_{g,t} \end{aligned} \tag{C.48}$$

From the KKT complementarity conditions (C.13), (C.14):

$$\underline{\beta_{g,t}} \cdot v_{g,t} = 0 \quad \forall g, \forall t \quad \Rightarrow \quad \sum_{g \in GaN} \underline{\beta_{g,t}} \cdot v_{g,t} = 0 \tag{C.49}$$

$$\overline{\beta_{g,t}} \cdot v_{g,t} = \overline{\beta_{g,t}} \cdot \overline{V}_g \quad \forall g, \forall t \quad \Rightarrow \quad \sum_{g \in GaN} \overline{\beta_{g,t}} \cdot v_{g,t} = \sum_{g \in GaN} \overline{\beta_{g,t}} \cdot \overline{V}_g \tag{C.50}$$

Hence (C.48) becomes:

$$\sum_{g\in GaN} \lambda^{E}_{n,t}\cdot v_{g,t} = \sum_{g\in GaN} o_{g,t}\cdot v_{g,t} + \sum_{g\in GaN} cp\cdot \zeta_g \cdot v_{g,t} + \sum_{g\in GaN} \overline{\beta_{g,t}}\cdot \overline{V}_g \tag{C.51}$$

By applying the strong duality theorem for the electricity market clearing objective function (4.5) :

$$\begin{aligned}\sum_{g\in GaN} o_{g,t}\cdot v_{g,t} + \sum_{i\in IaN} C_i\cdot p_{i,t} + \sum_{g\in GaN} cp\cdot(\zeta_g\cdot v_{g,t} - Q^{H}_{g,t}) \\ + \sum_{i\in IaN} cp\cdot(\zeta_i\cdot p_{i,t} - Q^{H}_{i,t}) \\ = \sum_{d^E\in DaN} \lambda^{E}_{n,t}\cdot L^{E}_{d,t} + \rho_{h,t}\cdot\alpha_h\cdot\eta\cdot \sum_{d^{EL}\in DaN} L^{E}_{d,t} - \sum_{i\in IaN}\overline{a_{i,t}}\cdot\overline{P}_i \\ - \sum_{g\in GaN}\overline{\beta_{g,t}}\cdot\overline{V}_g - \sum_{j\in JaN}\overline{\gamma_{j,t}}\cdot\overline{W}_j \\ - \sum_{m\in NaM}\overline{T}_{n,m}\cdot\left(\underline{\psi_{n,m,t}} + \overline{\psi_{n,m,t}}\right) - \sum_{n\in NaM} 3.14\cdot\left(\underline{\pi_{n,t}} + \overline{\pi_{n,t}}\right)\end{aligned} \tag{C.52}$$

By applying the strong duality theorem for natural gas market clearing objective function (4.14):

$$\sum_{k\in KaR} C_k\cdot f_{k,t} = \sum_{d^{NG}\in DaR} \lambda^{NG}_{r,t}\cdot L^{NG}_{d,t} + \sum_{g\in GaR}\lambda^{NG}_{r,t}\cdot\varphi_g\cdot v_{g,t} - \sum_{k\in KaR}\overline{\varepsilon_{k,t}}\cdot\overline{F}_k \tag{C.53}$$

Keeping the non-linear terms of the equation (C.52) on the left part:

$$\begin{aligned}\sum_{g\in GaN} o_{g,t}\cdot v_{g,t} \\ = -\sum_{i\in IaN} C_i\cdot p_{i,t} - \sum_{g\in GaN} cp\cdot\left(\zeta_g\cdot v_{g,t} - Q^{H}_{g,t}\right) \\ - \sum_{i\in IaN} cp\cdot\left(\zeta_i\cdot p_{i,t} - Q^{H}_{i,t}\right) + \sum_{d^E\in DaN}\lambda^{E}_{n,t}\cdot L^{E}_{d,t} + \rho_{h,t}\cdot\alpha_h\cdot\eta \\ \cdot \sum_{d^{EL}\in DaN} L^{E}_{d,t} - \sum_{i\in IaN}\overline{a_{i,t}}\cdot\overline{P}_i - \sum_{g\in GaN}\overline{\beta_{g,t}}\cdot\overline{V}_g - \sum_{j\in JaN}\overline{\gamma_{j,t}}\cdot\overline{W}_j \\ - \sum_{m\in NaM}\overline{T}_{n,m}\cdot\left(\underline{\psi_{n,m,t}} + \overline{\psi_{n,m,t}}\right) - \sum_{n\in NaM} 3.14\cdot\left(\underline{\pi_{n,t}} + \overline{\pi_{n,t}}\right)\end{aligned} \tag{C.54}$$

Combining equations (C.51) and (C.54):

$$\sum_{g \in GaN} \lambda^{E}_{n,t} \cdot v_{g,t} = -\sum_{i \in IaN} C_i \cdot p_{i,t} + \sum_{g \in GaN} cp \cdot Q^{H}_{g,t} - \sum_{i \in IaN} cp \cdot \left(\zeta_i \cdot p_{i,t} - Q^{H}_{\iota,t}\right) + \sum_{d^E \in DaN} \lambda^{E}_{n,t} \cdot L^{E}_{d,t} + \rho_{h,t} \cdot \alpha_h \cdot \eta \cdot \sum_{d^E L \in DaN} L^{E}_{d,t} - \sum_{i \in IaN} \overline{a_{i,t}} \cdot \overline{P}_i - \sum_{j \in JaN} \overline{\gamma_{j,t}} \cdot \overline{W}_j - \sum_{m \in NaM} \overline{T}_{n,m} \cdot \left(\underline{\psi_{n,m,t}} + \overline{\psi_{n,m,t}}\right) - \sum_{n \in NaM} 3.14 \cdot \left(\underline{\pi_{n,t}} + \overline{\pi_{n,t}}\right) \tag{C.55}$$

Keeping the non-linear terms of the equation (C.53) on the left part:

$$\sum_{g \in GaR} \lambda^{NG}_{r,t} \cdot \varphi_g \cdot v_{g,t} = \sum_{k \in KaR} C_k \cdot f_{k,t} + \sum_{k \in KaR} \overline{\varepsilon_{k,t}} \cdot \overline{F}_k - \sum_{d^{NG} \in DaR} \lambda^{NG}_{r,t} \cdot L^{NG}_{d,t} \qquad \forall r, \forall t \tag{C.56}$$

Substituting the non-linear terms of the equation (4.4) for the right part of the equations (C.55) and (C.56), the non-linear objective function (4.4) is reduced to the equivalent linear expression:

$$\boldsymbol{maximize} \; -\sum_{i \in IaN} C_i \cdot p_{i,t} + \sum_{g \in GaN} cp \cdot Q^{H}_{g,t} - \sum_{i \in IaN} cp \cdot (\zeta_i \cdot p_{i,t} - Q^{H}_{\iota,t}) + \sum_{d^E \in DaN} \lambda^{E}_{n,t} \cdot L^{E}_{d,t} + \rho_{h,t} \cdot \alpha_h \cdot \eta \cdot \sum_{d^E L \in DaN} L^{E}_{d,t} - \sum_{i \in IaN} \overline{a_{i,t}} \cdot \overline{P}_i - \sum_{j \in JaN} \overline{\gamma_{j,t}} \cdot \overline{W}_j - \sum_{m \in NaM} \overline{T}_{n,m} \cdot \left(\underline{\psi_{n,m,t}} + \overline{\psi_{n,m,t}}\right) - \sum_{n \in NaM} 3.14 \cdot \left(\underline{\pi_{n,t}} + \overline{\pi_{n,t}}\right) - \sum_{k \in KaR} C_k \cdot f_{k,t} - \sum_{k \in KaR} \overline{\varepsilon_{k,t}} \cdot \overline{F}_k + \sum_{d^{NG} \in DaR} \lambda^{NG}_{r,t} \cdot L^{NG}_{d,t} - \sum_{g \in GaN} cp \cdot \left(\zeta_g \cdot v_{g,t} - Q^{H}_{g,t}\right) \tag{C.57}$$

Appendix D

Mathematical Transformations for Chapter 5

KKT equality conditions:

$$O_{s,t}^{EL} - \lambda_{n,t}^{EL} + \overline{\gamma_{s,t}} - \underline{\gamma_{s,t}} = 0 \qquad \forall s, \forall t \tag{D.1}$$

$$-\lambda_{n,t}^{EL} + \overline{\theta_{ns,t}} - \underline{\theta_{ns,t}} = 0 \qquad \forall ns, \forall t \tag{D.2}$$

$$C_i - \lambda_{n,t}^{EL} + \overline{a_{i,t}} - \underline{a_{i,t}} = 0 \qquad \forall i, \forall t \tag{D.3}$$

$$\begin{aligned} &\sum_{m \in NaM} B_{n,m} \cdot \left(\lambda_{n,t}^{EL} - \lambda_{m,t}^{EL}\right) + \sum_{m \in NaM} B_{n,m} \cdot \left(\overline{\psi_{n,m,t}} - \overline{\psi_{m,n,t}}\right) \\ &\quad - \sum_{m \in NaM} B_{n,m} \cdot \left(\underline{\psi_{n,m,t}} - \underline{\psi_{m,n,t}}\right) + \overline{\pi_{n,t}} - \underline{\pi_{n,t}} + \eta_{n,t}^{o} \\ &\quad = 0 \qquad \forall n, \forall t \end{aligned} \tag{D.4}$$

$$\begin{aligned} &-\sum_{i \in IaN} p_{i,t} - \sum_{s \in SaN} f_{s,t} - \sum_{ns \in NSaN} w_{ns,t} + \sum_{d^{EL} \in DaN} L_{d,t}^{EL} \\ &\quad + \sum_{m \in NaM} B_{n,m} \cdot \left(\delta_{n,t} - \delta_{m,t}\right) = 0 \qquad : \left[\lambda_{n,t}^{EL}\right] \qquad \forall n, \forall t \end{aligned} \tag{D.5}$$

$$\delta_{n_1,t} = 0 \qquad \forall n = n_1, \forall t \tag{D.6}$$

$$O_{s,t}^{GC} - \lambda_{t}^{GC} + \overline{\varepsilon_{s,t}} - \underline{\varepsilon_{s,t}} = 0 \qquad \forall s, \forall t \tag{D.7}$$

$$C_{ns}^{GC} - \lambda_{t}^{GC} + \overline{\kappa_{ns,t}} - \underline{\kappa_{ns,t}} = 0 \qquad \forall ns, \forall t \tag{D.8}$$

$$\lambda^{ACP} - \lambda_{t}^{GC} + \overline{\zeta_{d,t}} - \underline{\zeta_{d,t}} = 0 \qquad \forall d, \forall t \tag{D.9}$$

$$\begin{aligned} &-\sum_{s \in SaN} q_{s,t}^{\uparrow} - \sum_{ns \in NSaN} r_{ns,t}^{\uparrow} - \sum_{d^{EL} \in DaN} ACP_{d,t} + \sum_{d^{EL} \in DaN} RPS \cdot L_{d,t}^{EL} = 0 \\ &\quad : \left[\lambda_{t}^{GC}\right] \qquad \forall t \end{aligned} \tag{D.10}$$

KKT complementarity conditions:

$$0 \leq p_{i,t} \perp \underline{a_{i,t}} \geq 0 \qquad \forall i, \forall t \tag{D.11}$$

$$0 \leq \overline{P}_i - p_{i,t} \perp \overline{a_{i,t}} \geq 0 \qquad \forall i, \forall t \tag{D.12}$$

$$0 \leq f_{s,t} \perp \underline{\gamma_{s,t}} \geq 0 \qquad \forall s, \forall t \tag{D.13}$$

$$0 \leq \overline{F}_s - f_{s,t} \perp \overline{\gamma_{s,t}} \geq 0 \qquad \forall s, \forall t \tag{D.14}$$

$$0 \leq w_{ns,t} \perp \underline{\theta_{ns,t}} \geq 0 \qquad \forall ns, \forall t \tag{D.15}$$

$$0 \leq \overline{W}_{ns} - w_{ns,t} \perp \overline{\theta_{ns,t}} \geq 0 \qquad \forall ns, \forall t \tag{D.16}$$

$$0 \leq B_{n,m} \cdot (\delta_{n,t} - \delta_{m,t}) + \overline{T}_{n,m} \perp \underline{\psi_{n,m,t}} \geq 0 \qquad \forall n, \forall m, \forall t \tag{D.17}$$

$$0 \leq \overline{T}_{n,m} - B_{n,m} \cdot (\delta_{n,t} - \delta_{m,t}) \perp \overline{\psi_{n,m,t}} \geq 0 \qquad \forall n, \forall m, \forall t \tag{D.18}$$

$$0 \leq \delta_{n,t} + 3.14 \perp \underline{\pi_{n,t}} \geq 0 \qquad \forall n, \forall t \tag{D.19}$$

$$0 \leq 3.14 - \delta_{n,t} \perp \overline{\pi_{n,t}} \geq 0 \qquad \forall n, \forall t \tag{D.20}$$

$$0 \leq q_{s,t}^{\uparrow} \perp \underline{\varepsilon_{s,t}} \geq 0 \qquad \forall s, \forall t \tag{D.21}$$

$$0 \leq SOAC_{s,t} - q_{s,t}^{\uparrow} \perp \overline{\varepsilon_{s,t}} \geq 0 \qquad \forall s, \forall t \tag{D.22}$$

$$0 \leq r_{ns,t}^{\uparrow} \perp \underline{\kappa_{ns,t}} \geq 0 \qquad \forall ns, \forall t \tag{D.23}$$

$$0 \leq SOAC_{ns,t} - r_{ns,t}^{\uparrow} \perp \overline{\kappa_{ns,t}} \geq 0 \qquad \forall ns, \forall t \tag{D.24}$$

$$0 \leq ACP_{d,t} \perp \underline{\zeta_{d,t}} \geq 0 \qquad \forall d, \forall t \tag{D.25}$$

$$0 \leq RPS \cdot L_{d,t}^{EL} - ACP_{d,t} \perp \overline{\zeta_{d,t}} \geq 0 \qquad \forall d, \forall t \tag{D.26}$$

The nonlinearities appearing in the KKT complementarity conditions are eliminated by employing the Fortuny-Amat and McCarl linearization process:

$$0 \leq p_{i,t} \leq M^{pP} \cdot z_{i,t}^{1} \qquad \forall i, \forall t \tag{D.27}$$

$$0 \leq \underline{a_{i,t}} \leq M^{cP} \cdot (1 - z_{i,t}^{1}) \qquad \forall i, \forall t \tag{D.28}$$

$$0 \leq \overline{P}_i - p_{i,t} \leq M^{pP} \cdot z_{i,t}^{2} \qquad \forall i, \forall t \tag{D.29}$$

$$0 \leq \overline{a_{i,t}} \leq M^{cP} \cdot (1 - z_{i,t}^{2}) \qquad \forall i, \forall t \tag{D.30}$$

$$0 \leq f_{s,t} \leq M^{pP} \cdot z_{s,t}^{5} \qquad \forall s, \forall t \tag{D.31}$$

$$0 \leq \underline{\gamma_{s,t}} \leq M^{cP} \cdot (1 - z_{s,t}^{5}) \qquad \forall s, \forall t \tag{D.32}$$

$$0 \leq \overline{F}_s - f_{s,t} \leq M^{pP} \cdot z_{s,t}^{6} \qquad \forall s, \forall t \tag{D.33}$$

$$0 \leq \overline{\gamma_{s,t}} \leq M^{cP} \cdot (1 - z_{s,t}^{6}) \qquad \forall s, \forall t \tag{D.34}$$

$$0 \leq w_{ns,t} \leq M^{pP} \cdot z_{ns,t}^{7} \qquad \forall ns, \forall t \tag{D.35}$$

$$0 \leq \underline{\theta_{ns,t}} \leq M^{cP} \cdot (1 - z_{ns,t}^{7}) \qquad \forall ns, \forall t \tag{D.36}$$

$$0 \leq \overline{W}_{ns} - w_{ns,t} \leq M^{pP} \cdot z_{ns,t}^{8} \qquad \forall ns, \forall t \tag{D.37}$$

$$0 \leq \overline{\theta_{ns,t}} \leq M^{cP} \cdot (1 - z_{ns,t}^{8}) \qquad \forall ns, \forall t \tag{D.38}$$

$$0 \leq q_{s,t}^{\uparrow} \leq M^{pP} \cdot z_{s,t}^{9} \qquad \forall s, \forall t \tag{D.39}$$

$$0 \leq \underline{\varepsilon_{s,t}} \leq M^{cP} \cdot (1 - z_{s,t}^{9}) \qquad \forall s, \forall t \tag{D.40}$$

$$0 \leq SOAC_{s,t} - q_{s,t}^{\uparrow} \leq M^{pP} \cdot z_{s,t}^{10} \qquad \forall s, \forall t \tag{D.41}$$

$$0 \leq \overline{\varepsilon_{s,t}} \leq M^{cP} \cdot (1 - z_{s,t}^{10}) \qquad \forall s, \forall t \tag{D.42}$$

$$0 \leq r_{ns,t}^{\uparrow} \leq M^{pP} \cdot z_{ns,t}^{11} \qquad \forall ns, \forall t \tag{D.43}$$

$$0 \leq \underline{\kappa_{ns,t}} \leq M^{cP} \cdot (1 - z_{ns,t}^{11}) \qquad \forall ns, \forall t \tag{D.44}$$

$$0 \leq SOAC_{ns,t} - r_{ns,t}^{\uparrow} \leq M^{pP} \cdot z_{ns,t}^{12} \qquad \forall ns, \forall t \tag{D.45}$$

$$0 \leq \overline{\kappa_{ns,t}} \leq M^{cP} \cdot (1 - z_{ns,t}^{12}) \qquad \forall ns, \forall t \tag{D.46}$$

$$0 \leq ACP_{d,t} \leq M^{pP} \cdot z_{d,t}^{13} \qquad \forall d, \forall t \tag{D.47}$$

$$0 \leq \underline{\zeta_{d,t}} \leq M^{cP} \cdot (1 - z_{d,t}^{13}) \qquad \forall d, \forall t \tag{D.48}$$

$$0 \leq RPS \cdot L_{d,t}^{EL} - ACP_{d,t} \leq M^{pP} \cdot z_{d,t}^{14} \qquad \forall d, \forall t \tag{D.49}$$

$$0 \leq \overline{\zeta_{d,t}} \leq M^{cP} \cdot (1 - z_{d,t}^{14}) \qquad \forall d, \forall t \tag{D.50}$$

$$0 \leq B_{n,m} \cdot \left(\delta_{n,t} - \delta_{m,t}\right) + \overline{T}_{n,m} \leq M^{pX} \cdot z_{n,m,t}^{15} \qquad \forall n, \forall m, \forall t \tag{D.51}$$

$$0 \leq \underline{\psi_{n,m,t}} \leq M^{cX} \cdot (1 - z_{n,m,t}^{15}) \qquad \forall n, \forall m, \forall t \tag{D.52}$$

$$0 \leq \overline{T}_{n,m} - B_{n,m} \cdot \left(\delta_{n,t} - \delta_{m,t}\right) \leq M^{pX} \cdot z_{n,m,t}^{16} \qquad \forall n, \forall m, \forall t \tag{D.53}$$

$$0 \leq \overline{\psi_{n,m,t}} \leq M^{cX} \cdot (1 - z_{n,m,t}^{16}) \qquad \forall n, \forall m, \forall t \tag{D.54}$$

$$0 \leq \delta_{n,t} + 3.14 \leq M^{pX} \cdot z_{n,t}^{17} \qquad \forall n, \forall t \tag{D.55}$$

$$0 \leq \underline{\pi_{n,t}} \leq M^{cX} \cdot (1 - z_{n,t}^{17}) \qquad \forall n, \forall t \tag{D.56}$$

$$0 \leq 3.14 - \delta_{n,t} \leq M^{pX} \cdot z_{n,t}^{18} \qquad \forall n, \forall t \tag{D.57}$$

$$0 \leq \overline{\pi_{n,t}} \leq M^{cX} \cdot (1 - z_{n,t}^{18}) \qquad \forall n, \forall t \tag{D.58}$$

The KKT equality condition (D.1) results in:

$$\lambda_{n,t}^{EL} = O_{s,t}^{EL} + \overline{\gamma_{s,t}} - \underline{\gamma_{s,t}} \qquad \forall s, \forall t \tag{D.59}$$

Multiplying by $f_{s,t}$ gives:

$$\sum_{s \in SaN} \lambda_{n,t}^{EL} \cdot f_{s,t} = \sum_{s \in SaN} O_{s,t}^{EL} \cdot f_{s,t} + \sum_{s \in SaN} \overline{\gamma_{s,t}} \cdot f_{s,t} - \sum_{s \in SaN} \underline{\gamma_{s,t}} \cdot f_{s,t} \tag{D.60}$$

From the KKT complementarity conditions (D.13), (D.14):

$$\underline{\gamma_{s,t}} \cdot f_{s,t} = 0 \quad \forall s, \forall t \quad \Rightarrow \quad \sum_{s \in SaN} \underline{\gamma_{s,t}} \cdot f_{s,t} = 0 \tag{D.61}$$

$$\overline{\gamma_{s,t}} \cdot f_{s,t} = \overline{\gamma_{s,t}} \cdot \overline{F}_s \quad \forall s, \forall t \quad \Rightarrow \quad \sum_{s \in SaN} \overline{\gamma_{s,t}} \cdot f_{s,t} = \sum_{s \in SaN} \overline{\gamma_{s,t}} \cdot \overline{F}_s \tag{D.62}$$

Hence (D.59) becomes:

$$\sum_{s\in SaN} \lambda_{n,t}^{EL} \cdot f_{s,t} = \sum_{s\in SaN} O_{s,t}^{EL} \cdot f_{s,t} + \sum_{s\in SaN} \overline{\gamma_{s,t}} \cdot \overline{F}_s \tag{D.63}$$

The KKT equality (D.7) results in:

$$\lambda_t^{GC} = O_{s,t}^{GC} + \overline{\varepsilon_{s,t}} - \underline{\varepsilon_{s,t}} \qquad \forall s, \forall t \tag{D.64}$$

Multiplying by $q_{s,t}^{\uparrow}$ gives:

$$\sum_{s\in SaN} \lambda_t^{GC} \cdot q_{s,t}^{\uparrow} = \sum_{s\in SaN} O_{s,t}^{GC} \cdot q_{s,t}^{\uparrow} + \sum_{s\in SaN} \overline{\varepsilon_{s,t}} \cdot q_{s,t}^{\uparrow} - \sum_{s\in SaN} \underline{\varepsilon_{s,t}} \cdot q_{s,t}^{\uparrow} \tag{D.65}$$

From the KKT complementarity conditions (D.21), (D.22):

$$\underline{\varepsilon_{s,t}} \cdot q_{s,t}^{\uparrow} = 0 \quad \forall s, \forall t \quad \Rightarrow \quad \sum_{s\in SaN} \underline{\varepsilon_{s,t}} \cdot q_{s,t}^{\uparrow} = 0 \tag{D.66}$$

$$\overline{\varepsilon_{s,t}} \cdot q_{s,t}^{\uparrow} = \overline{\varepsilon_{s,t}} \cdot SOAC_{s,t} \quad \forall s, \forall t \quad \Rightarrow \quad \sum_{s\in SaN} \overline{\varepsilon_{s,t}} \cdot q_{s,t}^{\uparrow} = \sum_{s\in SaN} \overline{\varepsilon_{s,t}} \cdot SOAC_{s,t} \tag{D.67}$$

Hence (D.64) becomes:

$$\sum_{s\in SaN} \lambda_t^{GC} \cdot q_{s,t}^{\uparrow} = \sum_{s\in SaN} O_{s,t}^{GC} \cdot q_{s,t}^{\uparrow} + \sum_{s\in SaN} \overline{\varepsilon_{s,t}} \cdot SOAC_{s,t} \tag{D.68}$$

By applying the strong duality theorem for the electricity market clearing objective function (5.4):

$$\begin{aligned} \sum_{s\in SaN} O_{s,t}^{EL} \cdot f_{s,t} + \sum_{i\in IaN} C_i \cdot p_{i,t} \\ = \sum_{d^E\in DaN} \lambda_{n,t}^{EL} \cdot L_{d,t}^{EL} - \sum_{i\in IaN} \overline{a_{i,t}} \cdot \overline{P}_i - \sum_{s\in SaN} \overline{\gamma_{s,t}} \cdot \overline{F}_s \\ - \sum_{ns\in NSaN} \overline{\theta_{ns,t}} \cdot \overline{W}_{ns} - \sum_{m\in NaM} \overline{T_{n,m}} \cdot \left(\underline{\psi_{n,m,t}} + \overline{\psi_{n,m,t}}\right) \\ - \sum_{n\in NaM} 3.14 \cdot \left(\underline{\pi_{n,t}} + \overline{\pi_{n,t}}\right) \end{aligned} \tag{D.69}$$

By applying the strong duality theorem for green certificates market clearing objective function (5.12):

$$\begin{aligned}\sum_{s\in SaN} O^{GC}_{s,t}\cdot q^{\uparrow}_{s,t} + \sum_{ns\in NSaN} C^{GC}_{ns,t}\cdot r^{\uparrow}_{ns,t} + \sum_{d^{EL}\in DaN} \lambda^{ACP}\cdot ACP_{d,t} \\ = \sum_{d^{EL}\in DaN} \lambda^{GC}_{t}\cdot RPS\cdot L^{EL}_{d,t} - \sum_{s\in SaN} \overline{\varepsilon_{s,t}}\cdot SOAC_{s,t} \\ - \sum_{ns\in NSaN} \overline{\kappa_{ns,t}}\cdot SOAC_{ns,t} - \sum_{d\in DaN} \overline{\zeta_{d,t}}\cdot RPS\cdot L^{EL}_{d,t}\end{aligned} \tag{D.70}$$

Objective function (5.1) becomes:

$$\begin{aligned}\boldsymbol{maximize}\quad \sum_{\boldsymbol{t}}\Bigg\{\sum_{s\in SaN} O^{EL}_{s,t}\cdot f_{s,t} + \sum_{s\in SaN} \overline{\gamma_{s,t}}\cdot \overline{F}_{s} + \sum_{s\in SaN} O^{GC}_{s,t}\cdot q^{\uparrow}_{s,t} \\ + \sum_{s\in SaN} \overline{\varepsilon_{s,t}}\cdot SOAC_{s,t}\Bigg\}\end{aligned} \tag{D.71}$$

Combining the above equations, the objective function takes the following final form:

$$\begin{aligned}\boldsymbol{maximize}\quad \sum_{\boldsymbol{t}}\Bigg\{-\sum_{i\in IaN} C_{i}\cdot p_{i,t} + \sum_{d^{E}\in DaN} \lambda^{EL}_{n,t}\cdot L^{EL}_{d,t} - \sum_{i\in IaN} \overline{a_{i,t}}\cdot \overline{P}_{i} \\ - \sum_{ns\in NSaN} \overline{\theta_{ns,t}}\cdot \overline{W}_{ns,t} - \sum_{m\in NaM} \overline{T_{n,m}}\cdot \left(\underline{\psi_{n,m,t}} + \overline{\psi_{n,m,t}}\right) \\ - \sum_{n\in NaM} 3.14\cdot \left(\underline{\pi_{n,t}} + \overline{\pi_{n,t}}\right) - \sum_{ns\in NSaN} C^{GC}_{ns,t}\cdot r^{\uparrow}_{ns,t} \\ - \sum_{d^{EL}\in DaN} \lambda^{ACP}\cdot ACP_{d,t} + \sum_{d^{EL}\in DaN} \lambda^{GC}_{t}\cdot RPS\cdot L^{EL}_{d,t} \\ - \sum_{ns\in NSaN} \overline{\kappa_{ns,t}}\cdot SOAC_{ns,t} - \sum_{d\in DaN} \overline{\zeta_{d,t}}\cdot RPS\cdot L^{EL}_{d,t}\Bigg\}\end{aligned} \tag{D.72}$$

Even though, the majority of the nonlinearities is eradicated via the above displayed methodologies, a bilinear term still remains and consists of a primal energy and a dual green certificates variable, such as:

$$\overline{\kappa_{ns,t}}\cdot SOAC_{ns,t}$$

To linearize these terms, a binary expansion method is implemented, which necessitates the introduction of auxiliary variables, such as binary and continuous variables $y^{\uparrow}_{ns,t,ex}$ and $x^{\uparrow}_{ns,t,ex}$ respectively, as well as a set of big-M constants. Next, an application of this method is attempted involving the bilinear term $\overline{\kappa_{ns,t}} \cdot SOAC_{ns,t}$:

$$\overline{\kappa_{ns,t}} \cdot SOAC_{ns,t} = \sum_{ex} x^{\uparrow}_{ns,t,ex} \cdot \ddot{SOAC}_{ns,t,ex} \quad \forall ns, \forall t \tag{D.73}$$

Continuous variables $SOAC_{ns,t}$ are approximated through a set of discrete values $\{\ddot{SOAC}_{ns,t,ex}\ ,\ ex = 1 \dots EX\}$, acting as parameters and bounded by the $[0, \overline{SOAC_{ns}}]$ interval.

$$0 \leq \overline{\kappa_{ns,t}} - x^{\uparrow}_{ns,t,ex} \leq M^1 \cdot \left(1 - y^{\uparrow}_{ns,t,ex}\right) \quad \forall ns, \forall t, \forall ex \tag{D.74}$$

$$0 \leq x^{\uparrow}_{ns,t,ex} \leq M^1 \cdot y^{\uparrow}_{ns,t,ex} \quad \forall ns, \forall t, \forall ex \tag{D.75}$$

The following equation identifies the closest discrete value $\ddot{w}_{ns,t,ex}$ to the $w_{ns,t}$ variable:

$$SOAC_{ns,t} - \frac{\Delta_{SOAC_{ns,t}}}{2} \leq \sum_{ex} y^{\uparrow}_{ns,t,ex} \cdot \ddot{SOAC}_{ns,t,ex} \leq SOAC_{ns,t} + \frac{\Delta_{SOAC_{ns,t}}}{2} \quad \forall ns, \forall t \tag{D.76}$$

Where:

$$\Delta_{SOAC_{ns,t}} = \frac{\overline{SOAC_{ns}}}{EX} \quad \forall ns, \forall t \tag{D.77}$$

$$\sum_{ex} y^{\uparrow}_{ns,t,ex} = 1 \quad \forall ns, \forall t \tag{D.78}$$